

**SYNTHETIC SEISMOGRAMS
RELATED TO DETAILED GEOLOGY
IN THE CELTIC FIELD,
SASKATCHEWAN**

MARGARET KATHLEEN LOMAS

1983

SYNTHETIC SEISMOGRAMS RELATED TO DETAILED GEOLOGY
IN THE CELTIC FIELD, SASKATCHEWAN

A THESIS
SUBMITTED TO THE FACULTY OF GRADUATE STUDIES AND RESEARCH
IN PARTIAL FULLFILLMENT OF THE REQUIREMENTS
FOR THE DEGREE OF
MASTERS OF SCIENCE
IN THE
DEPARTMENT OF GEOLOGICAL SCIENCES
UNIVERSITY OF SASKATCHEWAN

by

Margaret Kathleen Lomas

Saskatoon, Saskatchewan

c 1983. M. K. Lomas

The author has agreed that the Library, University of Saskatchewan, may make this thesis freely available for inspection. Moreover, the author has agreed that permission for extensive copying of this thesis for scholarly purposes may be granted by the professor or professors who supervised the thesis work recorded herein or, in their absence, by the Head of the Department or the Dean of the College in which the thesis work was done. It is understood that due recognition will be given to the author of this thesis and to the University of Saskatchewan in any use of the material in this thesis. Copying or publication or any other use of the thesis for financial gain without approval by the University of Saskatchewan and the author's written permission is prohibited.

Requests for permission to copy or to make any other use of material in this thesis in whole or in part should be addressed to:

Head of the Department of Geological Sciences

University of Saskatchewan

SASKATOON, Canada

ABSTRACT

In the Lloydminster area of Saskatchewan, heavy oil commonly occurs in thin, less than five-metre thick, vertically-stacked lenses within the sand beds of the Lower Cretaceous Mannville Group. Seismic mapping of the Mannville section has proved difficult due to the thinness of the beds, the lateral variation of these beds, and the lack of acoustic markers. The comparison of synthetic seismograms to detailed stratigraphic and core-analysis data allowed the interpretation of subtle seismic responses on these computer-simulated seismograms.

Synthetic seismograms, which included the effects of absorption and dispersion, were constructed for seven closely-spaced wells located in and near an enhanced-recovery pilot-project in the Celtic field. Input parameters of an impulse source buried at 29.9 m and a Q curve derived from published Q-values provided the best synthetic-seismic response to the zones of economic importance located within the Mannville Group.

In the Celtic field, the seismic-reflection method could be used for heavy-oil exploration or development if sufficient frequency-content in the 60 to 115 hz range is returned from the Mannville section. However, the dominant frequency imposed by the natural filtering of the earth is only 39 hz in all but one of the wells studied. Data acquisition and processing techniques must, therefore, be chosen to accentuate the 60 to 115 hz range.

ACKNOWLEDGEMENTS

This project was supervised by Dr. Z. Hajnal, whose encouragement and eternal optimism were greatly appreciated. I would also like to thank Drs. B. Pandit, D.J. Gendzwill, and W.G.E. Caldwell for their critical reviews of the manuscript in its early stages. Special thanks go to Dr. J.A. Lorsong, who made his expertise and unpublished data freely available to me. Dr. D.C. Ganley supplied the basic computer code for the synthetic-seismogram program.

Research funds for the project were provided by Petro-Canada Exploration Inc. Data were contributed by Mobil Oil Canada Ltd. and the Saskatchewan Department of Mineral Resources.

The author was supported by scholarships from the Saskatchewan Research Council and the University of Saskatchewan.

TABLE OF CONTENTS

Chapter	Page
1. INTRODUCTION	1
2. GEOLOGY	6
2.1 Stratigraphy	6
2.2 Economic Geology	10
3. GEOPHYSICAL CONSIDERATIONS	14
4. DATA COLLECTION AND PREPARATION	18
4.1 Well Locations	18
4.2 Geophysical Logs	20
4.3 Subsurface Section	30
4.3.1 Core Units	30
4.3.2 Geophysical-Log Marker-Beds	32
4.3.3 Properties of the Surficial Layers	36
4.4 Core Analyses	39
4.5 Q Values	45
5. GEOPHYSICAL PROCESSING AND ANALYSIS	50
5.1 Synthetic Seismograms	50
5.2 Spectral Analysis	54
5.3 Model Parameters	56
5.3.1 Introduction	56
5.3.2 Geologic modelling	57
5.3.3 Q Values	70
5.3.4 Depth of Source Burial	85
5.3.5 Input Source	94
5.4 Variation Among Wells	110

6.	INTERPRETATION	129
6.1	Resolution Limits	129
6.2	Earth Filter	135
6.3	Physical Rock-Properties	147
6.4	Possible Correlation to Real Seismic-Data	156
7.	CONCLUSION	160
	REFERENCES	161
	APPENDIX A: Core-analysis data, as stored in the CA.DAT files	171
	CA4B2.DAT	172
	CA2D2.DAT	172
	CA4D2.DAT	173
	CA2B8.DAT	174
	CA4B8.DAT	175
	CA2D8.DAT	176
	CA411.DAT	177
	APPENDIX B: Listings of computer programs	178
	CELGRF	179
	LOGGRF	203
	SPECAN	212
	SYNCEL	229

LIST OF FIGURES

Figure		Page
1.1	Location map for the Celtic pilot-project	4
2.1	Stratigraphic divisions of the Cretaceous Series	7
4.1	Data locations in the study area	19
4.2	Edited and unedited logs for well 2B8	23
4.3	Velocity and density values for well 2D2	27
4.4	Velocity and density values--Mannville portion, well 2D2	29
4.5	Core and log data--Mannville sections of pilot-project wells	in pocket
4.6	Stratigraphic marker-beds for well 2D2	35
4.7	Core and log data--Mannville section, well 4-11	in pocket
4.8	Location map for the shallow wells	38
4.9	Example sheet of core-analysis results	43
4.10	Q values used in the study area	48
5.1	Well-log zones edited for geologic modelling	58
5.2	Parameters used for geologic modelling	59
5.3	Well logs and seismogram--Waseca oil-zones shaded out	60
5.4	Unmodified well-logs and resulting synthetic-seismogram	61
5.5	Well logs and seismogram--W6 oil-zone shaded out	62
5.6	Well logs and seismogram--W3 oil-zone Shaded out	63
5.7	Amplitude spectrum--unmodified well-logs	66
5.8	Well logs and seismogram--gas effect removed from Colony	68
5.9	Well logs and seismogram--MC coal-bed replaced by shale	69
5.10	Well logs and seismogram--W1 zone edited to appear non-cemented	71
5.11	Seismogram--Q value of 20	72

5.12	Seismogram--Q value of 50	73
5.13	Seismogram--Q value of 100	74
5.14	Amplitude spectrum--Q value of 20	76
5.15	Amplitude spectrum--Q value of 50	77
5.16	Amplitude spectrum--Q value of 100	78
5.17	Seismogram--standard Q function	79
5.18	Amplitude spectrum--standard Q function	80
5.19	Seismogram--Q value of 20; plotted without gain	82
5.20	Seismogram--Q value of 50; plotted without gain	83
5.21	Seismogram--Q value of 100; plotted without gain	84
5.22	Seismogram--impulse source at 0.0 m	86
5.23	Seismogram--impulse source at 9.8 m	87
5.24	Seismogram--impulse source at 29.9 m	88
5.25	Seismogram--impulse source at 46.7 m	89
5.26	Amplitude spectrum--impulse source at 0.0 m	90
5.27	Amplitude spectrum--impulse source at 9.8 m	91
5.28	Amplitude spectrum--impulse source at 29.9 m	92
5.29	Amplitude spectrum--impulse source at 46.7 m	93
5.30	Velocity-type Ricker-wavelet	95
5.31	Phase and amplitude spectra of Ricker wavelet	96
5.32	Seismogram--60 hz Ricker-wavelet source	98
5.33	Seismogram--80 hz Ricker-wavelet source	99
5.34	Seismogram--100 hz Ricker-wavelet source	100
5.35	Seismogram--140 hz Ricker-wavelet source	101
5.36	Seismogram--180 hz Ricker-wavelet source	102
5.37	Seismogram--220 hz Ricker-wavelet source	103
5.38	Amplitude spectrum--60 hz Ricker-wavelet source	104
5.39	Amplitude spectrum--80 hz Ricker-wavelet source	105

5.40	Amplitude spectrum--100 hz Ricker-wavelet source	106
5.41	Amplitude spectrum--140 hz Ricker-wavelet source	107
5.42	Amplitude spectrum--180 hz Ricker-wavelet source	108
5.43	Amplitude spectrum--220 hz Ricker-wavelet source	109
5.44	Well logs and synthetic seismogram for well 4B2	112
5.45	Well logs and synthetic seismogram for well 2D2	113
5.46	Well logs and synthetic seismogram for well 4D2	114
5.47	Well logs and synthetic seismogram for well 2B8	115
5.48	Well logs and synthetic seismogram for well 4B8	116
5.49	Well logs and synthetic seismogram for well 2D8	117
5.50	Well logs and synthetic seismogram for well 4-11	118
5.51	Amplitude spectrum--well 4B2	119
5.52	Amplitude spectrum--well 2D2	120
5.53	Amplitude spectrum--well 4D2	121
5.54	Amplitude spectrum--well 2B8	122
5.55	Amplitude spectrum--well 4B8	123
5.56	Amplitude spectrum--well 2D8	124
5.57	Amplitude spectrum--well 4-11	125
5.58	Synthetic-seismogram cross-section	126
6.1	Time gates through seismogram--impulse source	136
6.2	Amplitude spectrum--impulse source	140
6.3	Amplitude spectrum--time gate from 0.15 to 0.25 s	142
6.4	Amplitude spectrum--time gate from 0.25 to 0.35 s	143
6.5	Amplitude spectrum--time gate from 0.30 to 0.40 s	144
6.6	Porosity values, well logs, and core data	149
6.7	Key to the core-data symbols	150
6.8	Permeability-to-air values, well logs, and core data	152
6.9	Clay-content values, well logs, and core data	154

6.10 Oil saturation, presence of gas, well logs, and core data 157

LIST OF TABLES

Table		Page
1.1	A.P.I. densities of liquids	3
4.1	Summary of acoustic-well-log editing	24
4.2	Summary of density-well-log editing	25
4.3	Surficial-geology data	40
4.4	Stratigraphic marker-bed depths	41
4.5	Summary of <u>in situ</u> measurements of Q	47
5.1	Summary of reflection data from the modelled zones	65
6.1	Theoretical resolution of the modelled zones	132

CHAPTER ONE

INTRODUCTION

"The relationship of borehole data and seismic data should be such that rock properties can be assigned to the seismic trace" (Stone, 1980). An understanding of the detailed relationship between a seismic trace and the geologic section that it represents is essential to the stratigraphic interpretation of seismic sections. Too often, the relationship is not fully appreciated and subtle expressions in the seismic trace are not interpreted correctly, or are not even recognized. The heavy-oil deposits of western Canada are located in a complex geologic environment; the thin beds and lateral variability of these beds make seismic records difficult to interpret. Although the seismic method would be a great aid to exploration and development, it is seldom used with success. A theoretical study of the detailed relationship between a geologic section in the heavy-oil area and its calculated seismic response was undertaken to test the applicability of new, high-resolution, seismic-reflection methods to this difficult environment. The term 'high resolution' is used here to mean the recording of seismic frequencies above the normal exploration range (Sheriff, 1973).

Lower Cretaceous rocks in the Canadian portion of the Western Interior basin contain viscous oil along a broad arcuate belt that extends from the Peace River oil sands of northwestern Alberta into the North Battleford-Lloydminster heavy oil district of west-central Saskatchewan. The deeper reservoirs at the southeast end of the belt contain oil that is more paraffinic, of lower specific gravity (higher A.P.I. gravity), and of lower viscosity than that oil in the shallower

northwestern reservoirs (Vigrass, 1965). A.P.I. gravity is a standard adopted by the American Petroleum Institute for denoting the specific weight of oils (Gary et al., 1974, p 32). Wennekers et al. (1979) distinguished heavy oil as having an A.P.I. gravity of between 10 and 25 degrees and tar-sands oil as having as A.P.I. gravity of less than 10 degrees. These and other A.P.I. values are shown in Table 1.1.

The Lloydminster area is the site of maximum heavy oil accumulation within the viscous-oil belt of western Canada. Its reserves are estimated to be 4.5 billion cubic metres, of which 0.45 billion cubic metres are economically recoverable using tertiary production methods (Wennekers et al., 1979). The Lloydminster heavy oil area is located along the Alberta-Saskatchewan border, approximately 450 to 540 km north of the United States border. The location of this study is the tertiary recovery pilot project in the Celtic heavy-oil field. The pilot project occupies the southeast quarter of Section 10, Township 52, Range 23 west of the Third Meridian (see Figure 1.1) and will hereafter be referred to as the Celtic pilot project. In 1980, the Celtic pilot project was unique within the Lloydminster area because of its large quantity of high quality cores, geophysical logs, and existing geological studies. In addition, the geology of the Celtic field is fairly typical of that of the Lloydminster area (Haidl, personal communication, 1981; Lorsong, 1981)

The goals of this study were to

- 1) Investigate the potential usefulness of the seismic reflection technique in the heavy-oil area.
- 2) Develop a method to evaluate the high-resolution seismic technique in the study area.
- 3) Study the detailed relationship between the subsurface geology of the

TABLE 1.1. A.P.I. DENSITIES OF LIQUIDS

LIQUID	A.P.I. DENSITY	REFERENCE
tar sand oil	less than 10 degrees	Wennekers <u>et al.</u> (1979)
fresh salt-water	10 degrees	Wennekers <u>et al.</u> (1979)
heavy oil	10 to 25 degrees	Wennekers <u>et al.</u> (1979)
conventional oil	25 to 40 degrees	Mossop (1978)

LOCATION OF CELTIC PILOT PROJECT

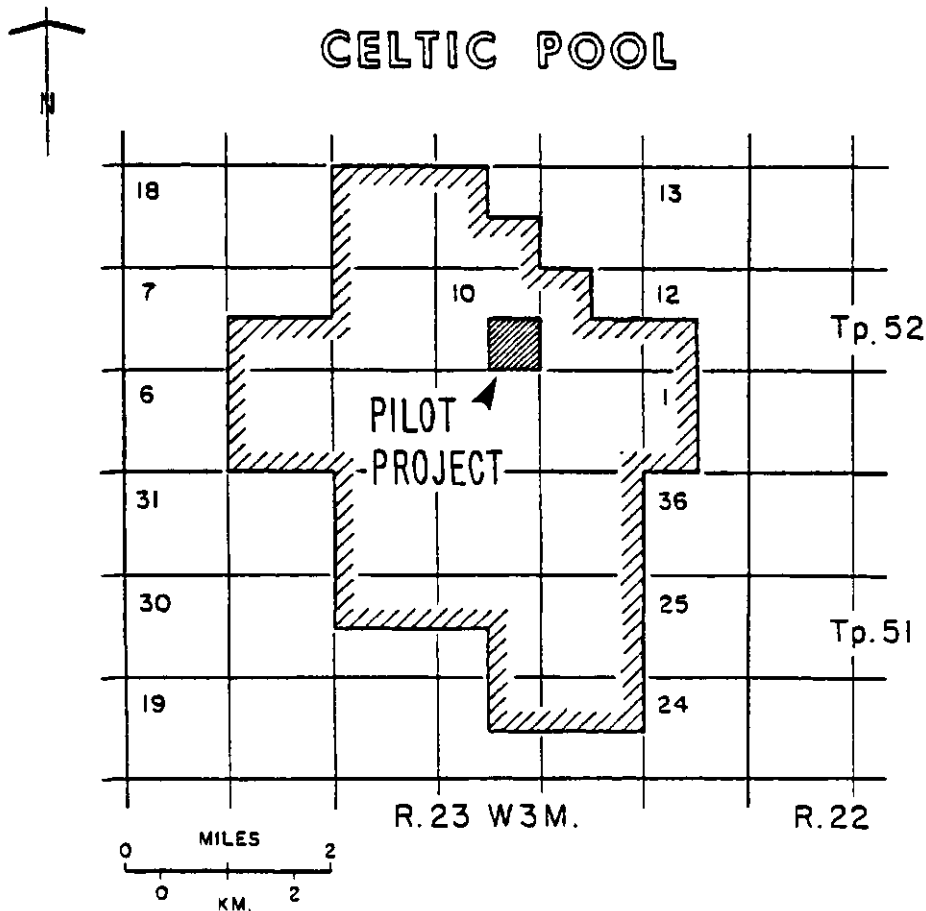
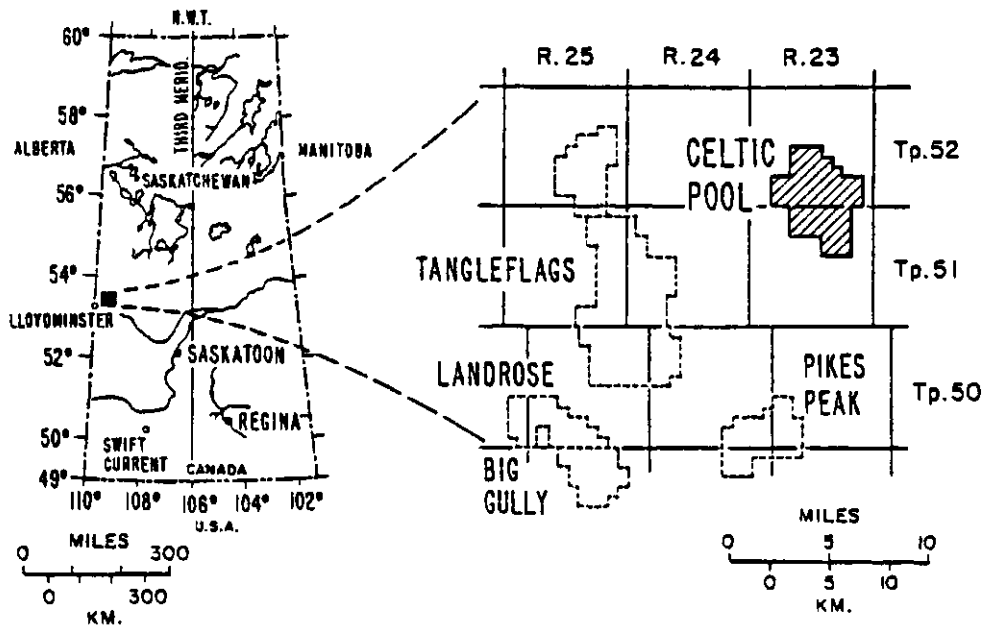


Figure 1.1 - Location map for the Celtic pilot project.

study area and the theoretical seismic trace computed from it.

4) Determine the parameters for synthetic seismogram construction that will best detect the economically important intervals.

5) Evaluate the potential of the seismic method as a tool for exploration and reservoir evaluation in the study area and, if possible, extend the results to other areas.

CHAPTER TWO

GEOLOGY

2.1 Stratigraphy

Attention has been focussed on the Lower Cretaceous sequences of western Canada because of the presence of deposits of conventional oil, heavy oil, tar sands, natural gas, and coal. As a result of extensive drilling, these rocks have been widely studied in the subsurface. In general, Cretaceous strata were deposited in north-south trending facies belts, as successive seas transgressed and regressed. The Cretaceous sequence is, therefore, highly variable across the Western Canada basin, making correlation difficult in an east-west direction (North and Caldwell, 1975). For this reason the stratigraphic section discussed will be restricted to that of the heavy oil area near Lloydminster, where three major Cretaceous units are present: the Mannville Group, the Colorado Group, and the Montana Group. A stratigraphic column for the Cretaceous rocks of the study area is given in Figure 2.1.

The Mannville Group in the Lloydminster area is a sandstone-shale sequence of Late Neocomian to Middle Albian age (Christopher, 1974, p. 49-50; 1980) that lies with a slight angular unconformity on eroded, mainly carbonate strata of Devonian age. Relief on the pre-Cretaceous surface is subdued, with shallow basins and valleys and southwesterly dip. White and von Osinski (1977) described the Mannville as comprising an interbedded sequence of sandstone, shale, and mudstone. These sandstones are actually weakly consolidated to uncemented sands that are fine grained to silty, and quartz rich. Minor feldspar, siderite, glauconite, garnet, tourmaline, zircon, chlorite, pyrite, and limonite may be present. The total thickness of the Mannville Group varies from

CRETACEOUS SERIES	MONTANA GROUP		LEA PARK FORMATION
	COLORADO GROUP	UPPER	UPPER COLORADO SUBGROUP (PART)
			2nd WHITE - SPECKLED SHALE
		LOWER	LOWER COLORADO SUBGROUP (PART)
			ST. WALBURG SANDSTONE
			LOWER COLORADO SUBGROUP (PART)
			LOWER COLORADO SUBGROUP (PART)
	MANNVILLE GROUP	COLONY FM.	
		McLAREN FM.	
		WASECA FM.	
		SPARKY FM.	
		GENERAL PETROLEUMS FM.	
		REX FM.	
LLOYDMINSTER FM.			
CUMMINGS FM.			
DINA FM.			

Figure 2.1 - Stratigraphic divisions of the Cretaceous Series in the Lloydminster area.

80 to 230 m, with regional thinning to the southwest (White and von Osinski, 1977).

Nine stratigraphic units have been informally recognized within the Mannville Group on the basis of electric log characteristics. However, the lateral variation, repetition of similar lithotypes in a vertical sequence, and the absence of marker beds preclude the identification of any unit by a characteristic electric-log response (Haidl, 1980; Gross, 1980). Correlations over long distances are highly speculative (White and von Osinski, 1977). In spite of this limitation, the above authors agree that the stratigraphic scheme is useful in that it provides a framework in which to discuss Mannville geology and to place a segment of rock in relative stratigraphic position. The stratigraphic names used are, from oldest to youngest: Dina, Cummings, Lloydminster, Rex, General Petroleum (G.P.), Sparky, Waseca, McLaren, and Colony formations. The names were adapted by Fuglem (1970) from a well established drillers' terminology that originated near the town of Lloydminster. His descriptions were later modified by Vigrass (1977) and the divisions were raised from member to formational status by Orr et al. (1977).

For part of Early Cretaceous time, the Lloydminster area was situated near the edge of an epicontinental sea (Robson, 1980). This accounts in part for the wide variety of depositional environments and the lateral variability of the facies units throughout the Mannville Group. It is generally agreed that the Dina formation is a fluvial and alluvial-plain deposit, filling topographic depressions (Williams, 1963; Orr et al., 1977; Vigrass, 1977; Gross 1980). The Cummings, Lloydminster, Rex, G.P., and Sparky formations are mainly marine to nearshore marine (Fuglem, 1970; Orr et al., 1977; Vigrass, 1977;

Gross, 1980). In contrast, the Waseca, McLaren, and Colony formations are a subject of controversy with regard to depositional environment; interpretations range from fluvial (Putnam, 1980) through coastal marine (Lorsong, 1979).

The total thickness of Mannville sediments in the Celtic field is approximately 200 m. All nine formations are present, with the Dina resting directly on Devonian carbonates of the Duperow Formation. The strata are draped over a prominent, southeast-trending structural arch, the pilot project area being located on the northeast edge of this arch (White and von Osinski, 1977). A complete description of the lithotypes present in the cored sections of the Celtic pilot project is presented in section 4.3.1.

The Mannville Group is overlain abruptly, and probably disconformably, by the marine silts and shales of the Colorado Group. In Saskatchewan, the division into upper and lower subgroups of the Colorado is made at the base of the Second White-Speckled Shale. The division between the Upper and Lower Cretaceous Series is taken approximately 20 to 30 m below the top of the Lower Colorado Subgroup, at the bottom of the Fish Scale Marker (Simpson, 1975). The Fish Scale Marker was not identified on the logs used in this study. Simpson (1975) places minor unconformities at the base of the Fish Scale Zone and at the base of the Lower Colorado.

The Lower Colorado Subgroup is of Middle Albian to Late Cenomanian age (North and Caldwell, 1975). It is approximately 140 m thick in the study area. The sequence is characterised by mudstones with subordinate silt and sand layers. The St. Walburg Sandstone is the only readily identifiable marker within the Lower Colorado on the geophysical logs recorded in the study area. There the sandstone is approximately 20 m

thick. Simpson (1975) described the St. Walburg Sandstone as being composed of horizontally laminated and micro-cross-laminated, very fine grained sandstones that were deposited as tidal ridges.

The Upper Colorado Subgroup is of Turonian to Late Santonian age (North and Caldwell, 1975). It is only 40 m thick in the area of study, due to its northeasterly thinning. The Upper Colorado in west-central Saskatchewan is composed of two principal calcareous units. The thickest of these is the First White-Speckled Shale, which rests with minor angular unconformity upon the Second White-Speckled Shale (North and Caldwell, 1975). In the area studied the Second White-Speckled Shale is only about 6 m thick but is a reliable marker on the geophysical logs.

Near Lloydminster, the Upper Colorado shaley chinks are directly overlain by the Lea Park Formation of the Montana Group. North and Caldwell (1975) attributed an Early Campanian age to the Lea Park and argued for a minor unconformity at its base. In the Celtic pilot project, the Lea Park is located in the uppermost 230 m of the bedrock section and, based on the geophysical logs, forms an apparently homogeneous sequence of argillaceous rocks.

2.2 Economic Geology

In the Lloydminster area, heavy oil is produced from quartzose Mannville sands with porosities exceeding 30 per cent and with permeabilities greater than one darcy (Fuglem, 1970). Lorsong (1981) studied controls on oil emplacement in a small area believed to be typical of the Lloydminster region. He concluded that oil is trapped laterally and vertically by facies changes and by cemented zones within the less quartz-rich sands. In the cemented zones, porosity is reduced

to virtually nil. On a larger scale, however, the overall distribution of oil is definitely structurally controlled. Strata of the Mannville Group dip gently to the southwest, at approximately 5 m/km (Vigrass, 1977). In general the sites of maximum oil accumulation change updip, from the basal sands (Dina formation) in the southwest, through the Sparky sands (near the Alberta-Saskatchewan border), and to the Colony sands in the northeast. Nevertheless, heavy-oil fields may produce from up to eight major lenses of oil in different sand layers (Wennekers et al., 1979). The Celtic field hosts oil accumulations in the Rex, G.P., Sparky, Waseca, and McLaren formations. The Waseca and Sparky formations of this field were estimated to contain approximately 16,500,000 cubic metres of oil-in-place, of which about 1,000,000 cubic metres was recoverable (Saskatchewan Department of Mineral Resources, 1979, p. c-2).

A broad domal structure supports the Lloydminster region (Christopher et al., 1971) and, as was mentioned in the previous section, the Celtic field is located over a northeasterly trending ridge. White and von Osinski (1977) reviewed the structure of the Mannville Group and concluded that the regional dip is interrupted by local structures resulting mainly from draping and compaction over the pre-Cretaceous unconformity. This is complicated by downwarps related to dissolution of Devonian Prairie Evaporite salt. They also noted that most heavy oil pools are associated with gentle highs and that none occurred in structurally very low sands. Moreover, in pool areas the strata are nearly horizontal.

According to Wennekers et al. (1979) there are thirty major pools in the Lloydminster heavy-oil region. Production from any one well is marginal. Within established pools, where A.P.I gravities usually range

from 13 to 18 degrees, primary production averaged only 5 per cent (White and von Osinski, 1977; Vigrass 1977). These same authors agreed that with presently available methods for secondary recovery, such as waterflooding, the production rises to about 8 per cent. Based on these data, the reserve figures of Wennekers et al. (1979) imply that tertiary-recovery methods, such as steam and fire flooding, could increase production to about 25 per cent. Although recoveries are poor and the oil lenses are thin, the shallow location, the large areal extent, and the vertical stacking of the lenses make the area economically attractive.

Traditionally, most exploration for heavy oil was accomplished drilling. Because the oil-bearing horizons are multiple, shallow, and usually cover a large area, drilling was one of the cheapest and surest ways to assess the resource. It is now recognized that the information produced by drilling alone is not of adequate quality. White and von Osinski (1977), Wennekers et al. (1979), Gross (1980), Haidl (1980), and Lorsong (1980) all agreed that correlations based solely on geophysical logs are unreliable; log signatures do not relate to unique geological sequences. Even when cores are taken, accurate correlation over any distance is made impossible by the absence of marker beds within the Mannville Group and by the extremely variable nature of the geology. Lorsong (1980) and Wennekers et al. (1979) provided examples of two cases where infill drilling between drill holes that were already correlated changed the geological interpretation radically. Based on his work with cored sections in the Celtic pilot project, Lorsong (1980) concluded that "...wells located 140 m apart represent the maximum spacing for confident prediction of sand body geometry." When spacings of 140 m are required, drilling is no longer a quick or cheap method of

exploration and development. A method is required that will provide more continuous coverage of the subsurface. Drill holes could then be selectively placed where they would provide the most useful information.

The seismic reflection-method provides much more detailed lateral resolution of the data-collection sites than does drilling. However, while gaining in lateral resolution, the seismic method loses in vertical resolution. In the last few years some limited success has been obtained by using high-resolution techniques, particularly if the oil bearing horizon is thick. Focht and Baker (1979) and Dunning et al. (1980) described exploration successes using reflection seismology. In both cases, the reservoirs mapped were channel deposits, which are much thicker than the blanket sand reservoirs containing the majority of the heavy oil reserves. Special care and the most up-to-date knowledge of high-resolution, seismic-acquisition and processing methods, coupled with a detailed understanding of the geology and its seismic expression, will be necessary before seismic mapping will succeed in all heavy oil environments.

CHAPTER 3

Geophysical Considerations

Seismic modelling is a method of computer simulation of the seismic response from a set of input values. Synthetic seismograms are one-dimensional seismic models that simulate a single seismic trace from well log data. The primary use of synthetic seismograms is as a tool to correlate between known borehole geology and a seismic response obtained near the borehole.

The preferred input data for synthetic seismogram construction are the velocity log (the measurement of interval transit-time with depth) and the density log. The product of the velocity and density, or the acoustic impedance, of the subsurface layers controls the seismic reflections. The amplitude of the reflection from a boundary separating two media is directly proportional to their contrast in acoustic impedance, and is measured by the reflection coefficient R . For normal incidence on an interface that separates layers of densities ρ_n and ρ_{n+1} and velocities V_n and V_{n+1} ,

$$R = \frac{\rho_{n+1}V_{n+1} - \rho_nV_n}{\rho_{n+1}V_{n+1} + \rho_nV_n} .$$

To construct a simple synthetic-seismogram, velocity values from logs are digitized and integrated to form arrays in travel time. Then, density and velocity values are combined in the above formula and converted into an array of reflection coefficients versus travel time. Finally, the reflectivity series is filtered to simulate a propagating wavelet.

Synthetic seismograms have been used since the late 1950s and in

the early methods of construction many assumptions were made. Assumptions such as a perfectly-elastic earth, constant density, the nonexistence of multiples, plane waves, normal incidence, and noiseless conditions allow easier computation of the synthetic seismogram but are, in general, not valid and therefore make correlation of the synthetic seismogram to the true seismic response difficult. Obviously, a balance must be struck between the ease of synthetic-seismogram construction (and, therefore, the cost), and the degree of sophistication of the model that the target requires. It is important to note that even if the data sets were perfect, and no invalid assumptions were made, the inherent differences in the seismic and log data preclude exact correlations (Sheriff, 1977).

Synthetic seismograms should be as realistic as possible, especially in an area of complicated geology such as Lloydminster. The geology there presents special problems to the seismic method and these must be included in the seismic models or comparisons between the two will not be possible.

The oil-bearing beds in the study area are thin, typically only 4 or 5 m thick. The vertical resolution or detection of these beds necessitates high frequency-content in the propagating wavelet. Widess (1973) defined the ideal limit of resolution as occurring at a bed thickness of one eighth of the predominant wavelength. Beds thicker than this limit may be resolved--that is, the reflections from the upper and lower interfaces of the bed will be separate in time. On the other hand, beds thinner than this limit will not be resolved, but they may be detected, even when their thicknesses are considerably less than one eighth of the predominant wavelength. The limit of detection also depends on the signal to noise ratio.

The lateral variability of Mannville sediments in the area of interest necessitates considerations of lateral resolution. Seismic waves do not reflect from a point, but from an area on the reflecting surface called the Fresnel zone. The size of the Fresnel zone depends on the predominant frequency content of the seismic signal; high frequencies will produce a smaller Fresnel zone than low frequencies.

The unconsolidated nature and shallow occurrence of the Cretaceous sediments in the area of study suggests that absorption of seismic energy will be a problem. Absorption is a specific type of attenuation in which some of the energy of a seismic wave is converted into heat while passing through a medium (Sheriff, 1973). Reported absorption measurements of rocks (Ganley, 1979) show trends of decreased absorption with increasing consolidation and depth of burial. For this reason, weathered surficial-rocks should be particularly absorptive. Absorption preferentially reduces the amplitude of the higher frequency components of the seismic signal; in consequence, the high frequencies required for vertical and lateral resolution of the subsurface may be attenuated before they reach the beds of interest.

The interbedded nature of the Mannville sequence presents another formidable problem--that of attenuation of the seismic wavelet caused by intrabed, or short-path, multiples. In cyclically-bedded sequences in which the reflecting interfaces alternate in sign, O'Doherty and Anstey (1971) recognized that short-path multiple reflections can have the effect of delaying the pulse, broadening the pulse, and magnifying the low frequency portion of the pulse transmitted through the layered sequence. The effect of these multiples is similar to the high-cut effect of absorption and their results may be confused (Anstey, 1977, p. 139). Schoenberger and Levin (1978) measured the contribution of the

attenuation caused by intrabed multiples and concluded that this effect contributed an appreciable portion (15 to 70 per cent) of the total observed attenuation. As in the case of absorption, the important high frequency content of the propagating wavelet is reduced.

To simulate the effects discussed above, the method of synthetic seismogram construction must be relatively complex. The computer program was written by D. Ganley and is described in Ganley (1981). All orders of surface and internal multiple reflections are calculated by this program, and therefore, any attenuation of the waveform due to intrabed multiples will be included. The program allows for the input of both velocity and density data in the calculation of the reflectivity series. Effects of absorption and dispersion are included in the synthetic seismogram by specifying Q , a measure of absorption, for each input interval. As well, the effect of the highly absorptive surficial layers may be investigated by simulating the burial of the seismic source at any desired depth. The above features make the construction of the synthetic seismogram more realistic and, as a result, more easily correlated to real seismic reflection data. The assumption of plane waves and the normal incidence of these waves on flat-lying interfaces is made, but this is a reasonable approximation for comparison with near-source geophones when dips are small. The specifics of this method of synthetic-seismogram construction will be discussed in section 5.1.

CHAPTER FOUR

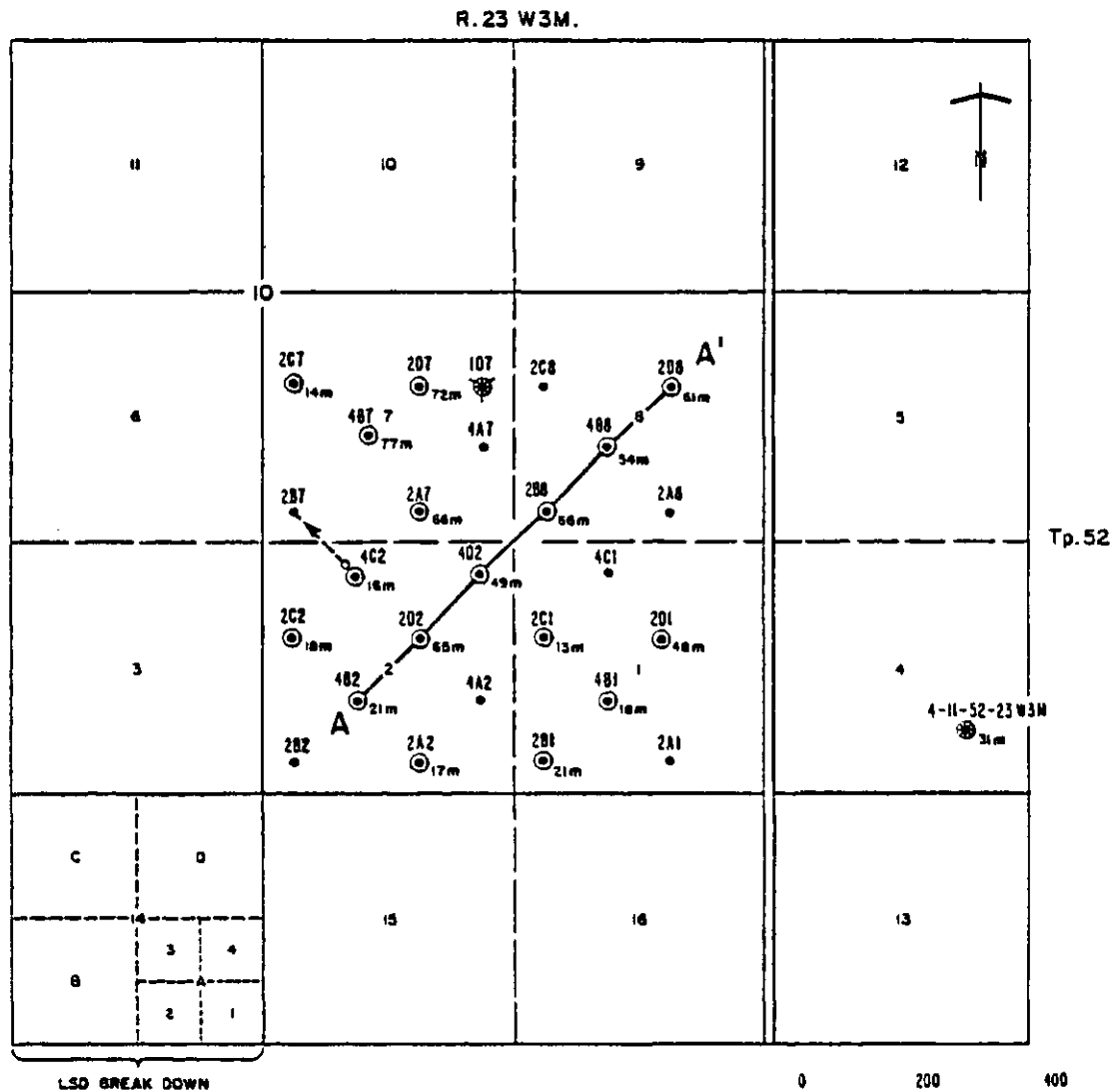
DATA COLLECTION AND PREPARATION

4.1 Well Locations

Six wells within the area of the Celtic pilot project and one well just outside the pilot area were chosen for this study. The six wells from within the pilot project lie 140 m apart along cross-section AA' in Figure 4.1. The seventh well is located at L.S.D. 4, Sec. 11, Tp. 52, R. 23, W3M. At the closest point it is approximately 725 m from the section AA'. The wells within the pilot project are referred to by the first part of their L.S.D. location (for example, 2D2) and the well location outside the pilot project is abbreviated to 4-11.

The six wells along section AA' were chosen for the present study because of their superior log and core data. In addition, these wells form a diagonal cross-section across the pilot project and perpendicular to the local strike of the Mannville strata. All of these six wells produce oil, with pay zones in the G.P., Sparky, McLaren, and Waseca formations. A dry well would have facilitated comparison between the seismic character of producing and non-producing wells. Unfortunately, there were no dry wells with acoustic logs within the boundaries of the Celtic field. The Mannville geology of the seventh well, 4-11, is rather different from the other six wells; the Waseca formation is severely reduced in thickness and the sands of the Sparky formation have been replaced by a thick sequence of shale. Although the status of well 4-11 is that of an oil producer, it now produces only from the McLaren formation (Saskatchewan Department of Mineral Resources, personal communication, 1983) and provides an example of a well in which the important Waseca oil zones are poorly developed.

DATA LOCATIONS IN THE CELTIC PILOT PROJECT



- 202 PRODUCING WELL LOCATION
- ⊕ WATER DISPOSAL WELL LOCATION
- ⊙ WELL LOCATION WITH DIGITIZED ACOUSTIC AND DENSITY LOG
- WELL LOCATION WITH DIGITIZED ACOUSTIC LOG ONLY
- ⊙_{10m} METRES OF CORE RECOVERED FROM WELL
- A-A' WELLS USED IN SYNTHETIC SEISMOGRAM STUDY

NOTE - WELLS ARE REFERENCED BY THE FIRST THREE CHARACTERS OF THE LAND SURVEY DESIGNATION (eg., 288). THE OFFICIAL NAME OF EACH OF THESE WELLS IS MOBIL CELTIC XXX-10-52-23 W3M, WHERE XXX IS THE THREE-CHARACTER DESIGNATION.

Figure 4.1 - Data locations in the study area.

4.2 Geophysical Logs

A large suite of logs, comprising induction-electric logs, a compensated-density log, a compensated-neutron-porosity log, natural gamma-ray logs, caliper logs, a borehole-compensated acoustic-log, and sometimes a spontaneous-potential log is available for each of the six wells from the pilot project. Well 4-11 lacks only the density and neutron logs. Hole conditions for the wells in the pilot project should be similar, since all were drilled within a short period of time (late 1978 and early 1979) and by the same crew, who were using the same equipment (Lorsong, personal communication, 1981). This means that differences between the log suites of the wells are more likely due to geologic changes than to differing hole conditions. All of the wells, with the exception of 2B8, were logged by Schlumberger of Canada. Well 2B8 was logged by Dresser Atlas.

Well-log data must be in digital form in order to construct a synthetic seismogram. The original digital field-recordings of the logs were used for wells 4B2, 2D2, 4D8, and 2D8. The logs for wells 2B8, 4B8, and 4-11 were digitized by Rileys Datashare International Inc. from analogue copies of the logs. A 0.2 m digital interval was used for all six of the pilot-project wells. Well 4-11 was drilled in 1969, and as its logs are non-metric, the digital interval used was one-half foot (.1524 m). A 0.2 m sample interval will allow beds of greater than 0.4 m thickness to be represented.

The next step in preparing the logs was editing. The stratigraphic interpretation of seismic records is based on the ability to correlate seismic character to the subsurface geology. As it is well-log data that provide the in situ physical-properties of the subsurface section, it is extremely important that they provide the most accurate

information possible. Crain and Boyd (1979) felt that most geophysicists underestimate the severity of the editing problem.

Either mechanical log-problems or environmental conditions may cause portions of well logs to contain data that are significantly different from the true, in situ formational properties (Ausburn, 1977). Mechanical problems could include: effects caused by imperfectly calibrated logs, cycle skip caused by gain settings that are too low, and noise spikes caused by instrument or electronic noise. Environmental conditions are generally related to poor hole-conditions, such as erosion of the borehole wall, but could also include gas effects, which can reduce the measured velocity appreciably even when gas is present in concentrations as low as 5 per cent by volume (Domenico, 1974). In addition, almost all formations, particularly the softer, less competent ones, are altered when a borehole is drilled through them (Ausburn, 1977). Shales cave, erode, absorb water, and swell in response to drilling and exposure to mud filtrate. On the other hand, sandstones are less affected but are altered by relaxation, erosion, and invasion of mud filtrate.

There are two major facets of log editing (Ausburn, 1977). The first is to recognize that bad data have been recorded, and the second is to try to determine better values, which can be substituted for the bad ones. The bad data recognized in logs used in this study were mainly as a result of hole conditions, and cycle skip and noise due to gas effects. Density logs are often affected by rough or washed-out hole conditions. Acoustic logs are affected less often than density logs. Bad data were replaced based on empirical observations of trends in other holes where the data were better. In some severely altered zones, published velocity and density values for similar rocks were used

as a guide. Figure 4.2 shows a comparison of the unedited and edited density and velocity curves for well 2B8. The logs are plotted at the same horizontal scales so that the severity of the editing problems may be appreciated.

A series of checks was made on the density- and acoustic-log data in each well. The calibration was examined to ensure that it had not changed during the logging run. The starting depths of the logs were altered to be sure that both logs started at the same subsurface horizon and that no spurious events were included due to the effect of the surface casing. The depths of certain distinct events were compared to be sure that they were the same on both the density and acoustic logs; this was possible because both the density and velocity logs were run with a simultaneous natural gamma log. Lastly, computer plots of the digitized density and velocity values were made and compared. Several wells were found to have discrepancies of up to 0.6 m between the depths of the same events in the acoustic and velocity logs. Most of these cases occurred only over a portion of the log, but well 2B8 was found to have a difference of between 0.2 and 0.4 m over the entire length of the logs. A computer program was written to shift the data. However, when the synthetic seismograms computed using shifted and non-shifted data were compared there was no visible difference, that is, the rock velocities were low enough that there was no visible difference at the 1 ms sampling interval used for the synthetic seismograms. These small differences in log depths were, therefore, ignored.

The caliper logs were checked for hole rugosity and washouts. Four areas of poor borehole conditions were encountered in the wells. These are listed in the summaries of well-log editing presented in Tables 4.1 and 4.2. Bad data due to hole conditions were corrected by replacing

CELTIC 2B8 10 52 23 W3M

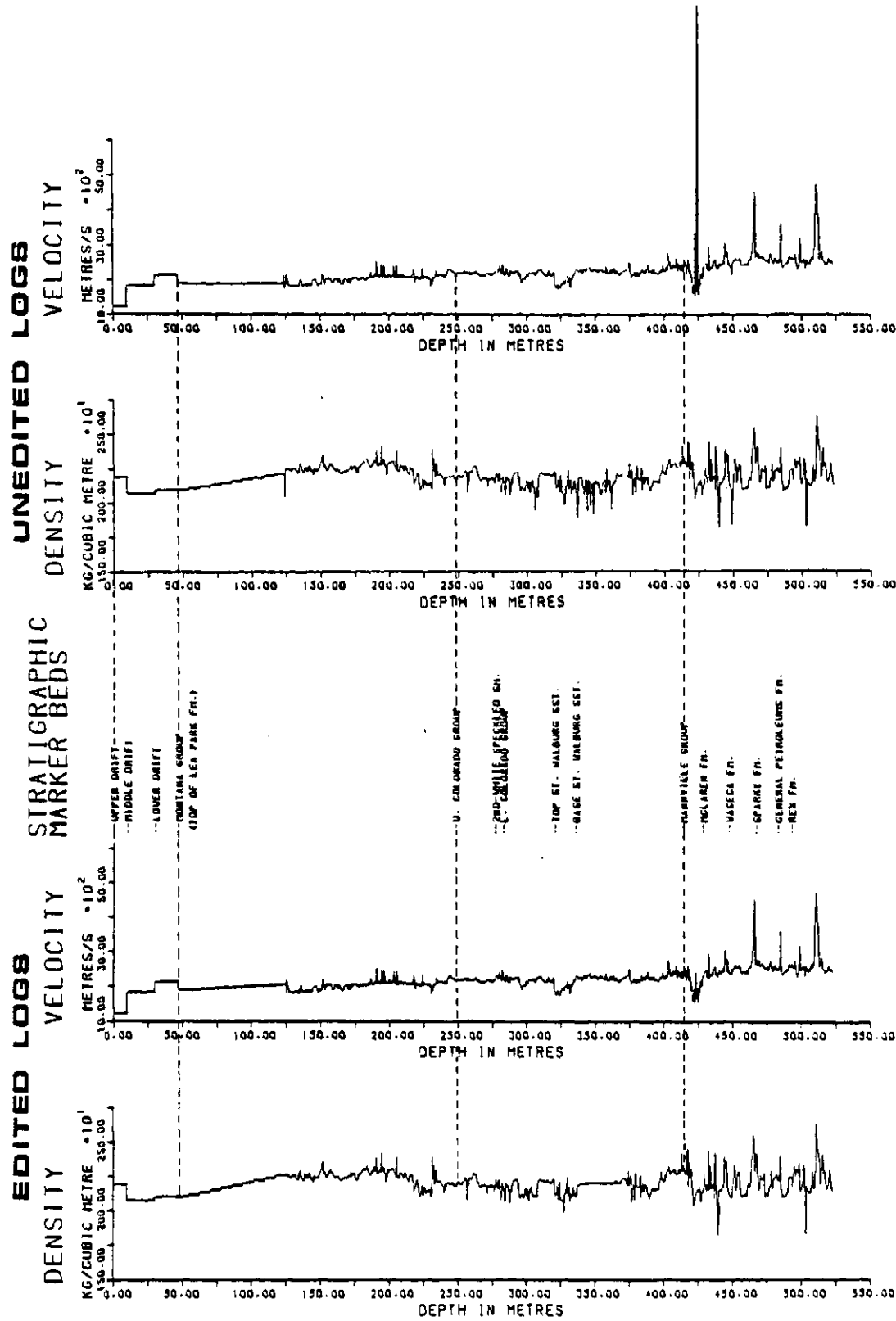


Figure 4.2 - Comparison of edited and unedited logs for well 2B8.

TABLE 4.1. SUMMARY OF ACOUSTIC-WELL-LOG EDITING

	4B2	2D2	4D2	2B8	4B8	2D8	4-11
source of digitized logs	field records	field records	field records	Rileys Datashare	Rileys Datashare	field records	Rileys Datashare
calibration	good	good	good	good	good	good	N/A
starting depth, original (edited)	94.0 m (96.8 m)	96.0 m (97.4 m)	89.0 m (90.4 m)	124.0 m (125.4 m)	98.0 m (98.0 m)	90.0 m (90.0 m)	90.2 m (90.2 m)
match of digitized acoustic to density data	fair	fair	fair	about .4 m too deep	about .3 m too deep	up to .4 m out	N/A
general hole condition	poor	very good	poor	good	good	very good	poor
St. Walburg Sst	fair	fair	good	good	good	fair	good
interval up to 20 m below base of St. Walburg Sst	fair	good	fair	fair	good	fair	fair
interval up to 10 m above top of Mannville Group	fair	good	fair	good	good	good	fair
W6 bed	good	good	good	edited	good	edited	fair
other edits	4	0	0	0	0	0	0
Colony gas zone	edited	edited	fair	edited	fair	fair	fair

TABLE 4.2. SUMMARY OF DENSITY-WELL-LOG EDITING

	482	202	4D2	288	488	2D8	4-11
source of digitized logs	field records	field records	field records	Rileys Database	Rileys Database	field records	Rileys Database
calibration	N/A	good	fair	good	N/A	good	N/A
starting depth, original (edited)	94.0 m (96.8 m)	96.0 m (97.4 m)	89.0 m (90.4 m)	124.0 m (125.4 m)	377.0 m (98.0 m)	90.0 m (90.0 m)	N/A (90.2 m)
match of digitized density to acoustic data	fair	fair	fair	about .4 m too shallow	about .3 m too shallow	up to .4 m out	N/A
general hole condition	poor	very good	poor	good	good	very good	poor
St. Walburg Sst	fair	edited	good	good	N/A	edited	N/A
interval up to 20 m below base of St. Walburg Sst	fair	good	edited	edited	N/A	fair	N/A
interval up to 10 m above top of Mannville Group	fair	good	edited	good	good	good	N/A
W6 bed	good	good	good	edited	good	edited	N/A
other edits	4	0	1	3	0	1	0
Colony gas zone	good	good	good	good	good	good	N/A

the bad values with empirical values that suited the general trend of that log and were similar to values in other wells where hole conditions in the zone were better.

In wells 4B2, 2D2, and 2B8 severe cycle-skipping and noise problems in the Colony formation portion of the velocity logs were attributed to gas effects. Lorsong (1981) shows gas to be present in the Colony formation of the pilot-project wells. The obvious cycle-skips and spikes were replaced by an average of the more reasonable values from within the gas zone. The limits of the gas zone were based on the crossover of density- and neutron-porosity logs.

Two of the seven wells lacked complete density logs. The density log for well 4B8 begins at a depth of 377 m and well 4-11 has no density log. Density logs of constant values were constructed where they were required in these two wells. For well 4B8, a program was written to calculate the average of the first 21 density values from the logged section and then write this value into the interval between 98.0 and 377.0 m, where density values were lacking. In well 4-11 a constant density of 2200 kilograms per cubic metre was used below the cased surface zone. This value was felt to be reasonable, based on the densities in the other wells.

The use of a constant density in the calculation of synthetic seismograms is a valid assumption if the rock density and velocity are approximately related by a general expression of the form $\rho = kv^n$, where the values of k and n are reasonably constant over sections of the well that are at least as long as the longest wavelength of interest (Peterson et al., 1955). Figure 4.3 shows the plotted values of density versus velocity for the logged section of well 2D2. This well was chosen because of its good-quality geophysical-logs (see Tables 4.1 and

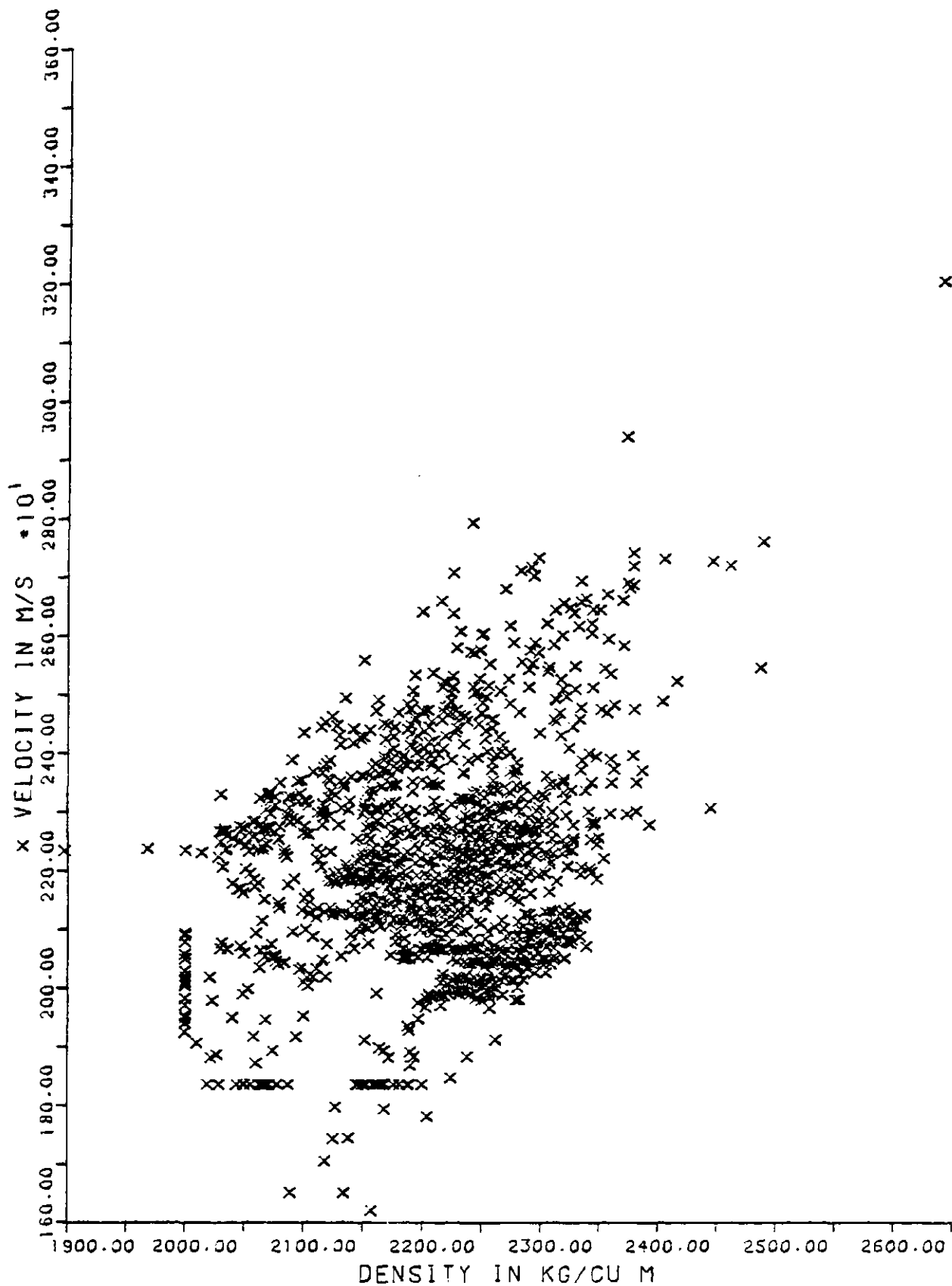


Figure 4.3 - Relationship of velocity and density values for the logged section of well 2D2.

4.2). The lack of a definite trend in the points in Figure 4.3 is probably due to the heterogeneity of the samples; they were taken from the entire logged section of the well. Separate graphs were, therefore, made to study the velocity and density relationships within the three major rock units--the Montana, Colorado, and Mannville Groups. The graph of the Mannville data is shown in Figure 4.4. There is considerable scatter in the data points; nevertheless, Figure 4.4 illustrates that an expression of the form $\rho=100v^4$ fits the Mannville data fairly well. The constant density assumption is, therefore, valid.

Scatter in the data points of Figure 4.4 makes it difficult to choose a curve. The high velocity and density values in the top right-hand corner of the graph are from cemented zones, whereas the low velocity grouping at the bottom of the graph relates to the presence of gas in the Colony formation. The curve in Figure 4.4 was compared to the well-known Nafe and Drake curve (Nafe and Drake, 1963, Figure 4), which relates velocities and densities measured in water-saturated sedimentary-rock of all types, and at all depths. The curve in Figure 4.4 plots below, and is flatter than, the corresponding portion of the Nafe and Drake curve. A possible explanation for this response is that saturation effects (particularly the gas-saturation effect) have decreased the measured velocities in well 2D2 and flattened the curve.

The edited, digitized, density- and acoustic-log values are contained in data files called DEN.DAT (for example, DEN2B8.DAT) and AU.DAT (for example, AU2B8.DAT) respectively. These files are used as input to the synthetic-seismogram program and to plotting routines.

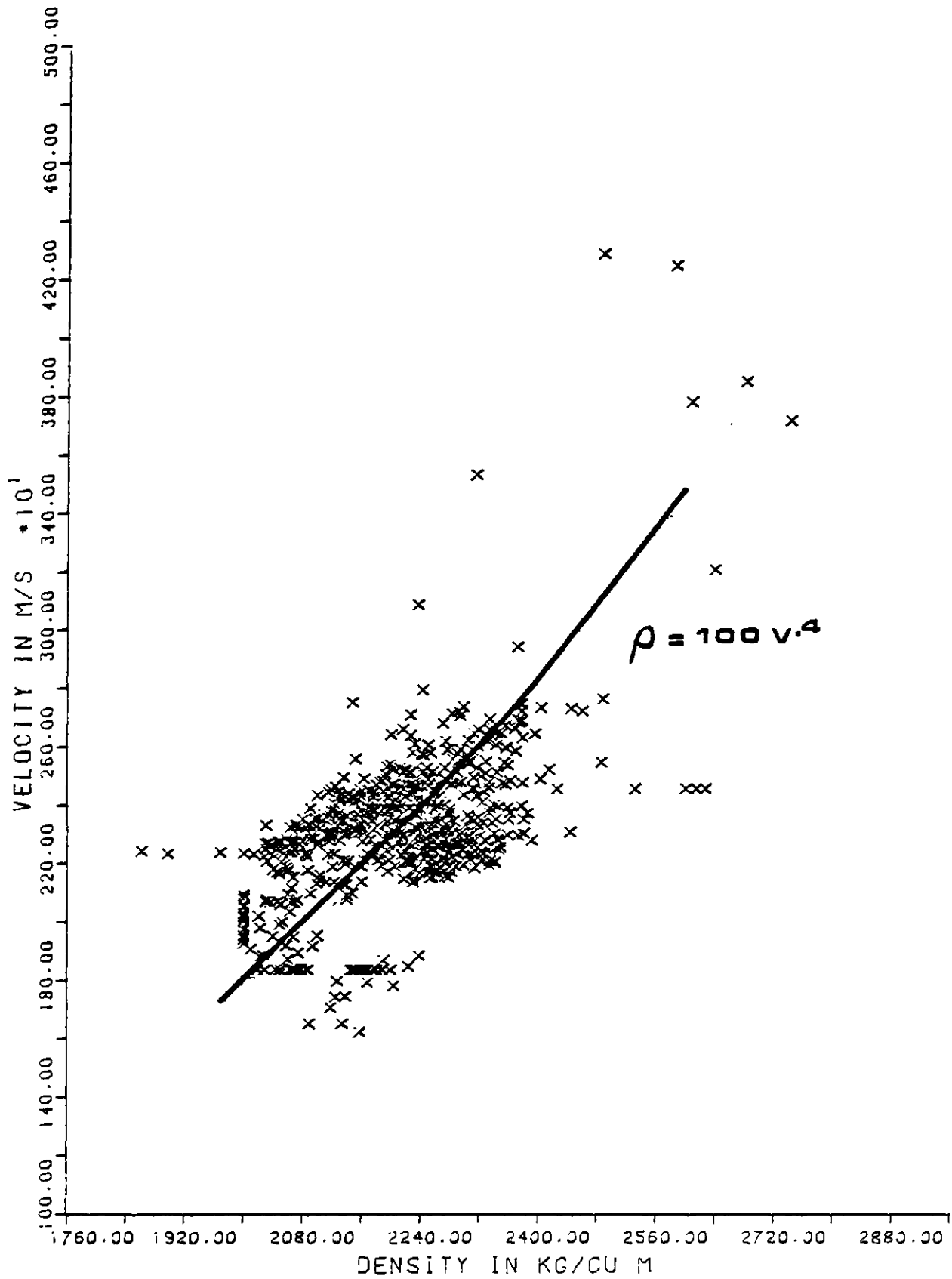


Figure 4.4 - Relationship of velocity and density values for the Mannville section of well 2D2.

4.3 Subsurface Section

4.3.1 Core Units

For the six pilot project wells, a total of 315.7 m of core is available for study; all but 1.6 m of this core is from the Mannville Group. In addition, well 4-11 has 19.3 m of Mannville core. Core recovery from each of the pilot-project wells is shown in Figure 4.1. Detailed studies of the cored intervals of these and 11 other wells in the pilot project were published by Lorsong (1979, 1980, 1981). This data, as well as Dr. Lorsong's unpublished data, proved to be invaluable; a detailed study of the geology would have been beyond the scope of this thesis, and the quality of the cores has deteriorated since they were first studied by Dr. Lorsong. The cores were examined to gain familiarity with Lorsong's nomenclature, to determine features of the core that influenced velocity and density changes, and to correct the core depths to the geophysical-log depths. Other than this, Lorsong's core descriptions were used almost without change.

Lorsong (1979) described six lithofacies based on his examinations of core from the Celtic field; he felt that the scheme was applicable to the Mannville Group throughout west-central Saskatchewan. These lithofacies will be used to describe the core in this study. The only changes made to Lorsong's scheme were in the naming of the shale subfacies. In order to facilitate the computerisation of the data, subfacies S1 was called S and subfacies S2 was called Z. Observations on the cementation in these lithofacies units are from Lorsong (1981).

Facies L (low-angle cross-laminated sandstone)

Facies L is characterised by very fine to fine grained, well sorted, generally unconsolidated quartz-sandstone. Less than 10 per cent of these rocks are cemented, and the predominant cement is clay.

Oil production in the Celtic field is almost exclusively from facies L sand-bodies.

Facies T (trough cross-laminated sandstone)

Facies T is characterised by very fine to fine grained, quartz sandstone that is moderately well sorted. Small amounts of silt and clay may be present. In the pilot area, more than 60 per cent of these rocks are cemented, predominantly by clay and with lesser amounts of calcite. For this reason, oil is seldom produced from facies T sand-bodies.

Facies M (massive sandstone)

Facies M sandstones are fine to medium grained, moderately to poorly sorted, and contain substantial quantities of silt and clay. About half of these units are cemented, commonly by clay, less commonly by calcite or iron-bearing carbonates. Facies M sand bodies are poor oil-producers.

Facies B (bioturbated sandstone and shale)

Facies B is made up of very fine to fine grained, well-sorted sandstones and interbedded shale. About 20 per cent of these rocks are cemented. Clay is the most common cement, followed by calcite, and then by iron-bearing carbonates.

Facies S (shale)

Facies S consists of subfacies S and subfacies Z. Subfacies S is characterised by massive intervals of shale and is never cemented. Subfacies Z consists of massive shale that is similar, but has numerous silty laminae. Less than one per cent of subfacies Z units are cemented.

Facies C (coal)

Facies C is made up of thin beds of lignite and carbonaceous shale.

Cementation does not occur in this lithofacies.

In order to relate the geology seen in the cores to the synthetic seismograms, the core units must be compared to their response on the geophysical logs and, when discrepancies occur, the thicknesses of the core units must be corrected. Poor recovery of core is most common in soft formations and at the ends of the core barrels. The core units were fitted onto the velocity logs using coals, cemented zones, and oil saturated sands as acoustic markers. Resistivity, density, natural gamma, and caliper logs were used for additional checks during this process.

The core-to-log correlation procedure resulted in subsurface geology that is somewhat different from that described solely on the basis of cores (as shown in Lorsong, 1980). In particular, it was necessary to shift the lithofacies boundaries in well 2D8 up by approximately 6 m in order to correlate the cores and logs. Other differences were due to the incomplete recovery of coals, shales, and oil saturated sands.

4.3.2 Geophysical-Log Marker-Beds

The complete suite of geophysical logs was used to pick stratigraphic marker beds in the seven wells, and to make certain that these picks were consistent in all of the wells. Interpreted geophysical-logs for these wells were available, but the way in which the stratigraphic markers were defined and named, and the portion of the well logs examined varied among the sources and even among the wells from any one source. Lorsong (1980) separated the cored intervals of the logs into formations based on his detailed core examinations. The well records of Mobil Oil Canada, Ltd. provided markers for the tops of

the Second White-Speckled Shale and the Mannville formations. The Saskatchewan Department of Mineral Resources consistently picked the top of the Lower Colorado Subgroup, the top and base of the St. Walburg Sandstone, the top of the Mannville Group, and the tops of the Mannville sand bodies. White and von Osinski (1977) showed the Mannville sand horizons present in well 4-11. Simpson (1981) gave an interpreted cross-section of the Colorado Group near the Celtic field.

Within the Mannville Group, the formation boundaries described by Lorsong (1981) were used whenever possible but, because the log-to-core correlations had already been completed (see section 4.3.1), Lorsong's core units could not always be related directly to the geophysical logs. Moreover, the entire Mannville section was not available in any one cored interval. However, by extrapolating the information from well to well, formation markers from the top of the Rex formation to the top of the Colony formation (top of the Mannville Group) could be chosen. These markers were compared with those of Mobil Oil Canada, Ltd. and those of the Saskatchewan Department of Mineral Resources. Once the preliminary interpretation of the logs in each well had been completed, a cross-section through these wells was constructed to ensure that the formation boundaries chosen were consistent. Horizons that proved to be characteristic markers through the cross-section were: 1) a cemented zone of high velocity and density in the Rex formation, 2) a cemented zone of high velocity and density in the G.P. formation, 3) a cemented zone of high velocity and density at the bottom of the Waseca formation (except in well 2D2), 4) a coal bed of low density near the middle of the McLaren formation, and 5) a large natural gamma anomaly at the base of the Colony formation. Also, the oil-saturated sand-bodies were good markers on the resistivity curves, and were visible on the acoustic and

density logs.

During this correlation process it became obvious that the core units in well 2D8 had been placed too deeply. The relative positions of the lithofacies units were adjusted; this required shifting of the formation boundaries chosen by Lorsong.

Once the formation boundaries within the Mannville had been checked, an attempt was made to apply the lithofacies correlations made by Lorsong (1980). This attempt met with little success because some of the lithofacies units had been altered during the log-to-core correlation, and because of the shift in the lithofacies units of well 2D8. Only the major sand beds, such as M2, W6, W4, W3, W1, S3, S2, and G1 were named, and these cannot always be directly linked to the sand beds of Lorsong (1980). A cross-section showing the core and log data for the Mannville portion of the pilot-project wells is shown in Figure 4.5 (in pocket).

The Colorado Group stratigraphic markers were chosen based on the well records of the Saskatchewan Department of Mineral Resources, the well records of Mobil Oil Canada, Ltd., and the cross-sections published by Simpson (1981). Within the Colorado Group, it was possible to consistently pick the following markers: the base of the St. Walburg Sandstone, the top of the St. Walburg Sandstone, the top of the Lower Colorado Subgroup (base of the Second White-Speckled Shale), the top of the Second White-Speckled Shale, and the top of the Colorado Group (base of the Montana Group). As in the Mannville Group, the character of the geophysical-log markers was compared to be sure that they were consistent from well to well. Figure 4.6 shows the stratigraphic marker beds that were picked for well 2D2.

Well 4-11 was interpreted last because its log suite was not as

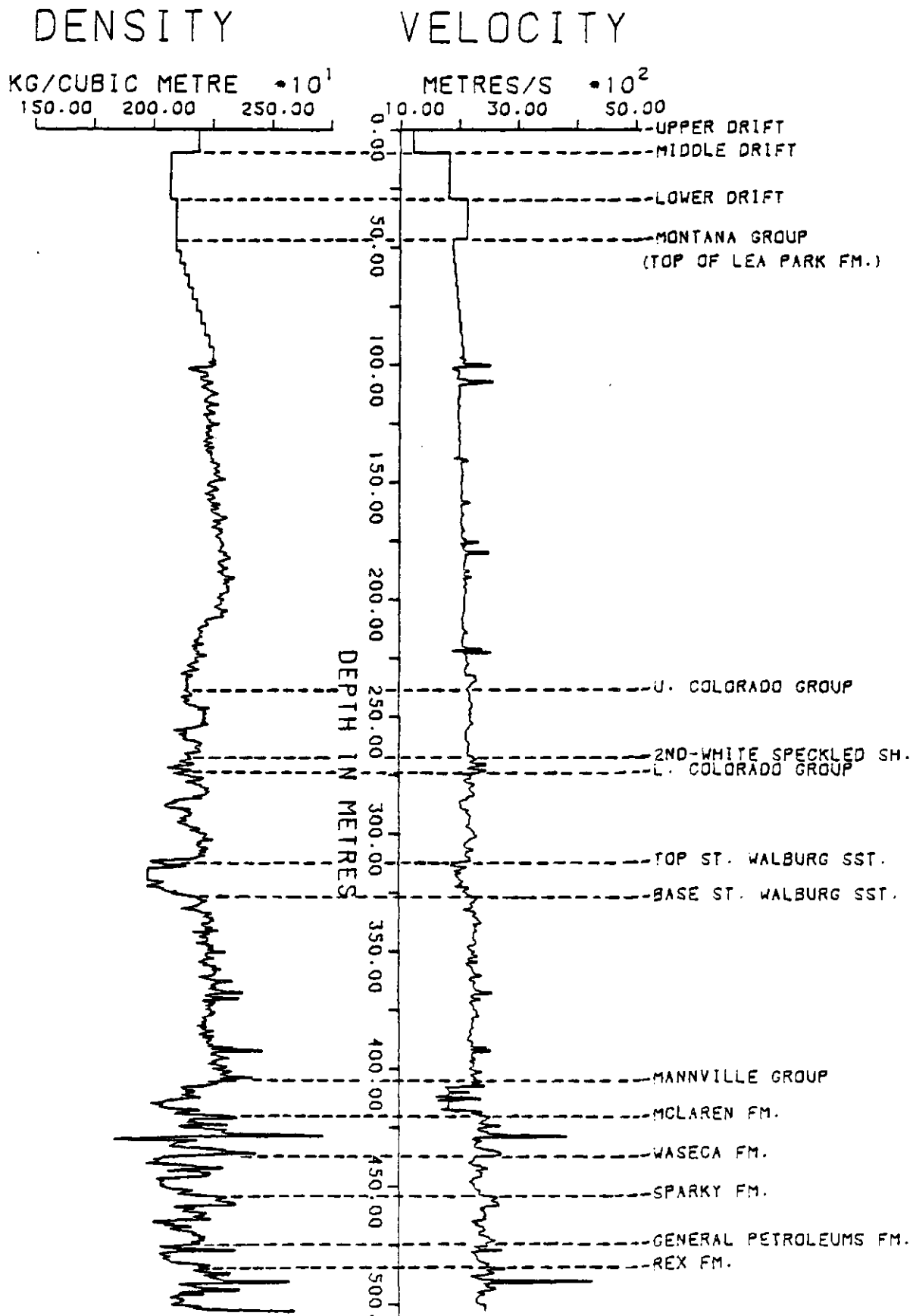


Figure 4.6 - Stratigraphic marker-beds for well 2D2.

extensive as the others, its cored section was of poor quality, and its logs were non-metric. Picking of the marker beds for well 4-11 by using the now well-defined marker-beds of the other six wells resulted in log interpretations that were consistent for all seven wells. The geology in well 4-11 is different from that of the pilot project wells; a thick shale interval is present in the Sparky formation and the Waseca formation is reduced in thickness. The formation boundaries, and the core and log data within the Mannville section of well 4-11 are shown in Figure 4.7 (in pocket). This can be compared to the cross-section through the pilot-project wells in Figure 4.5.

4.3.3 Properties of the Surficial Layers

Surface casing in the boreholes resulted in an absence of geophysical-log data from the surface to depths of between 89 to 124 m, depending on the depth of casing in the well. Although the unconsolidated and weathered surficial-layers are thin and far removed from the zone of interest, they exert a proportionately larger influence on the seismic energy than would be expected. Velocities in these zones are low, and the propagating waveform spends a relatively longer period of time in these layers. Large velocity and density variations, often due to gas content, are characteristic of the surficial layers, and as a result, strong multiple reflections can occur. Moreover, unconsolidated and shallow sequences are highly absorptive.

Information about the rocks within the cased sections of the boreholes was inferred from geophysical logs and descriptions of cuttings from shallow wells. Eleven shallow wells surrounding the pilot project were chosen for this purpose; five are Saskatchewan Research Council stratigraphic testholes and six are wells drilled under a

Saskatchewan Department of Agriculture farm-improvement program. These eleven wells were used to construct three cross-sections through the area of the Celtic field. These lines of the sections did not pass directly through the pilot project, and so, perpendicular projections from the line of section and onto the location of well 2B8 were used to locate the point closest to the centre of the pilot project. The cross-section and well locations relative to the pilot project are shown in Figure 4.8.

When the cross-sections were completed, the results indicated that four distinct surficial layers should be present in the pilot project. These were described (from the surface downward) in the cuttings as: 1) a brown, sandy to silty till, 2) a well consolidated, grey till, 3) sand and gravel interbedded with grey till, and 4) a grey, bedrock shale--the Lea Park Formation. B. Schriener (personal communication, 1981) suggested that unit 1 is the Battleford Formation, and that unit 2 is the Floral Formation. However, as Quaternary stratigraphy is not within the scope of this thesis and because an origin of the sediments is not meant to be implied, units 1, 2, and 3 will be simply referred to as the upper drift, middle drift, and lower drift. Unit 4 was interpreted as the top of the Lea Park Formation.

The elevations of the tops of the three lower layers, at the points closest to the center of the pilot project, were noted for each of the three cross-sections. The thickness of each layer was calculated for all three of the cross-sections; these were then averaged to obtain a representative thickness of each layer in the study area.

Velocity and density values for the surface layers were difficult to obtain and so they were modified from published values for similar lithotypes (Burke, 1968; Christiansen, 1970; Patterson, 1964). These

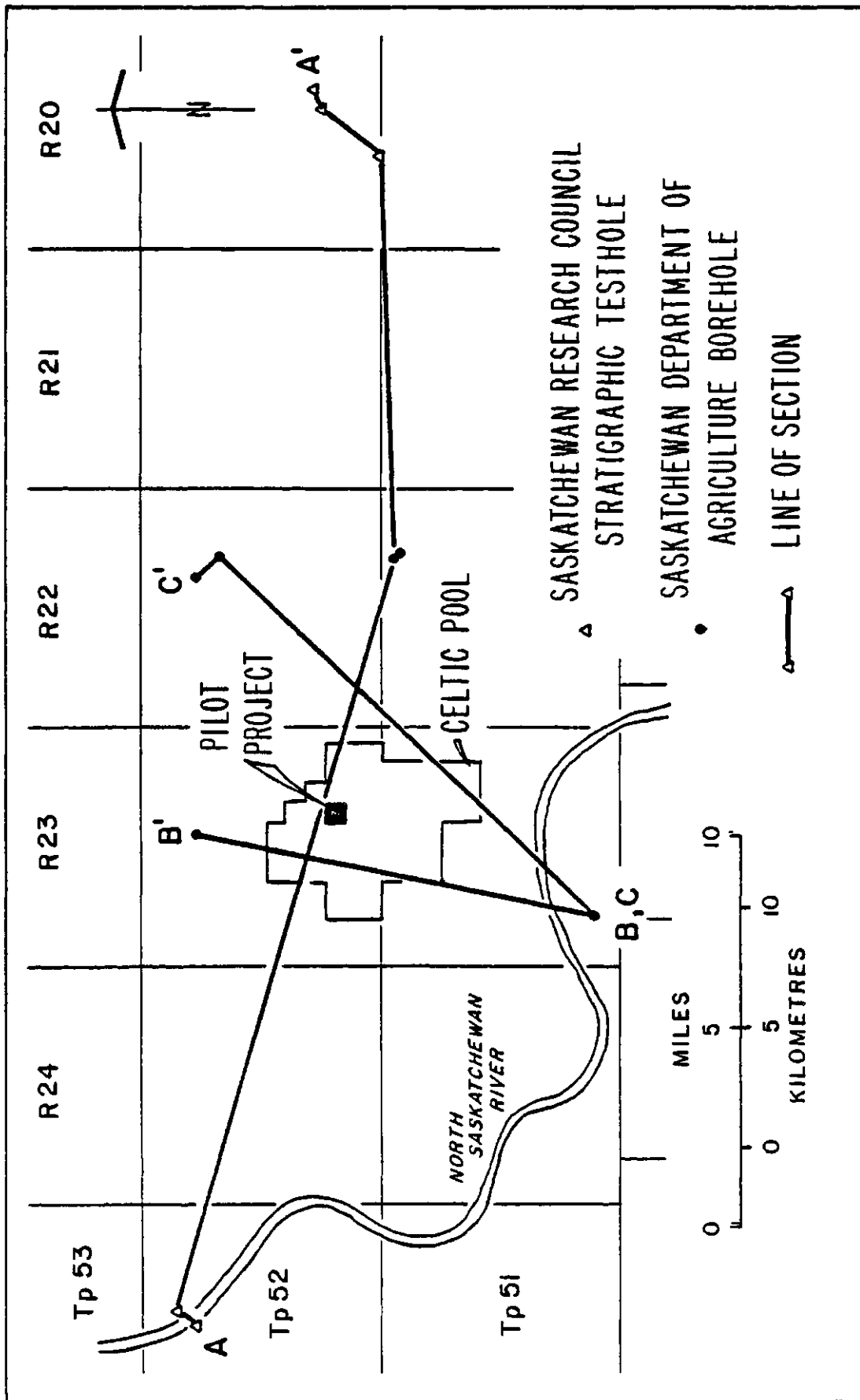


Figure 4.8 - Location map for the shallow wells used to infer information about the surficial layers in the study area.

modifications were based on discussions with geophysicists with long-term Saskatchewan experience (Gendzwil and Hajnal, personal communication, 1982). The average thickness, velocity, and density for each surface layer are given in Table 4.3. These values are constant for all of the wells used in this study and are contained in a data file called GANCEL.DAT, which is used as input to the synthetic seismogram program as well as to several of the plotting routines.

The depths of all of the stratigraphic marker beds, from the surface to the bottom of the hole, for each of the seven wells are shown in Table 4.4. A data file containing these 15 depths was constructed for each of the wells. The files are called PIX.DAT (for example PIX2B8.DAT) and are used as input to plotting programs and to the synthetic seismogram program.

4.4 Core Analyses

The measured rock properties of porosity, permeability, clay content, and oil saturation, as well as the observed type of cementation in the rock, affect the acoustic properties of the rock and also determine its potential for oil production. Analyses of porosity, oil saturation, and permeability to air were performed on the freshly-recovered core of the pilot-project wells by Core Laboratories--Canada Ltd. Porosity and the fraction of pore volume saturated by oil were from Dean Stark analysis, and the permeability to air was determined by small plug analysis. Details of the methods can be found in the API Recommended Practice for Core-Analysis Procedure (1960). The amount and type of cementation, and the per cent of clay content in the rocks were based on core studies (Lorsong, 1981; Lorsong, unpublished data).

TABLE 4.3. SURFICIAL-GEOLOGY DATA

UNIT	DESCRIPTION	DEPTH TO TOP	THICKNESS	VELOCITY	DENSITY
lower drift	brown, sandy to silty till	0.0 m	9.8 m	1219 m/s	2192 kg/cu m
middle drift	well consolidated grey till	9.8m	20.1 m	1829 m/s	2072 kg/cu m
upper drift	sand and gravel interbedded with grey till	29.9 m	16.8 m	2134 m/s	2100 kg/cu m
Lea Park Fm.	grey shale (bedrock)	46.7 m	variable	1890 m/s (at top)	2100 kg/cu m (at top)

TABLE 4.4. STRATIGRAPHIC MARKER-BED DEPTHS

	4B2 (m)	2D2 (m)	4D2 (m)	2B8 (m)	4B8 (m)	2D8 (m)	4-11 (m)
upper drift	0.0	0.0	0.0	0.0	0.0	0.0	0.0
middle drift	9.8	9.8	9.8	9.8	9.8	9.8	9.8
lower drift	29.9	29.9	29.9	29.9	29.9	29.9	29.9
Lea Park Fm.	46.7	46.7	46.7	46.7	46.7	46.7	46.7
U. Colorado Subgroup	234.0	238.0	244.0	243.3	260.9	245.0	264.3
Second White- Speckled Shale	262.5	267.0	272.5	277.3	289.5	301.5	293.3
L. Colorado Subgroup	273.5	273.3	278.6	283.0	295.5	308.0	299.7
top St. Walburg Sandstone	307.2	311.6	314.8	320.6	333.1	346.2	336.9
base St. Walburg Sandstone	321.3	326.5	329.1	335.8	349.0	361.0	352.1
Mannville Group	402.2	404.5	409.5	414.0	427.5	443.3	425.5
McLaren fm.	417.2	420.1	428.7	428.2	440.9	455.2	434.4
Waseca fm.	434.0	437.0	441.4	447.4	459.8	474.7	454.3
Sparky fm.	452.9	453.8	460.9	467.1	479.0	496.1	465.2
G.P. fm.	472.0	474.4	478.0	483.0	496.2	511.7	497.6
Rex fm.	482.3	484.3	488.4	492.9	506.5	523.2	506.8

When several values of core analyses were available for a bed (for example W6), the means were calculated to give representative values of porosity, permeability, and oil saturation for the entire bed. An example sheet of core analysis results is shown in Figure 4.9. In addition to the analyses shown in Figure 4.9, Core Lab determined the lithotype of each sample by visual examination. The first step in reducing the data was to allocate the depth intervals (each of about 20 cm in thickness) used for the Dean Stark analysis to the lithofacies bed to which they belonged. In wells 4B2, 2D2, 4D2, and 2D8 this had already been done (Lorsong, unpublished data). In the remaining two pilot-project wells this was done by comparing the Core Lab lithotype descriptions and depths to the detailed core-descriptions (Lorsong, unpublished data).

The core analyses were almost always made in the sandier, more oil-saturated intervals of the core. For this reason, analyses in beds of uncemented facies L were generally available, data from beds of facies T and M were less common, data from facies B beds were biased toward the sandy intervals, and analyses from cemented intervals or beds of facies S, Z, and C were nonexistent. Furthermore, permeability measurements were not made in every interval. In beds where analyses was not available, data were extrapolated from values in other beds of the same lithofacies. If this was not possible, published measurements of rock properties were used as a guide for selecting a value. Porosities of shales and coals were found in Greensmith (1978, p. 102) and Karr (1978 p. 156), respectively. Permeabilities of sands, sandstones, and shales are available in Pettijohn (1975, p. 78) and Blatt, Middleton, and Murray (1972, p. 347). The range of porosities, oil saturations, and permeabilities of cemented lithofacies L sandstones

Sample Number	Depth Metres (m)	m Rep.	DEAN-STARK ANALYSIS						SMALL PLUG ANALYSIS				
			Bulk Mass Fraction		Porosity (Calculated)	Saturation of Pore Volume (Calculated)		Permeability to Air Millidarcys	Boyle's Law Helium Porosity	Grain Density kg/m ³			
			Oil	Water		Oil	Total Water						
CORE NO. 1 426.00 m - 432.00 m (REC. 4.40 m) (3 BOXES)													
-	426.00-27.46	1.46	-	-	-	-	-	-	-	-	-	-	-
1	427.46-27.74	0.28	0.076	0.094	0.351	0.447	0.553	-	-	-	-	-	-
-	427.74-28.46	0.72	-	-	-	-	-	-	-	-	-	-	-
2	428.46-28.68	0.22	0.043	0.091	0.290	0.321	0.679	-	-	-	-	-	-
3	428.68-28.93	0.25	0.061	0.098	0.333	0.384	0.616	-	-	-	-	-	-
4	428.93-29.23	0.30	0.062	0.074	0.294	0.456	0.544	-	-	-	-	-	-
5	429.23-29.42	0.19	0.068	0.063	0.285	0.519	0.481	-	-	-	-	-	-
6	429.42-29.68	0.26	0.030	0.076	0.238	0.283	0.717	-	-	-	-	-	-
7	429.68-29.93	0.25	0.099	0.074	0.356	0.572	0.428	-	-	-	-	-	-
8	429.93-30.14	0.21	0.081	0.072	0.323	0.529	0.471	-	-	-	-	-	-
9	430.14-30.40	0.26	0.059	0.092	0.320	0.391	0.609	-	-	-	-	-	-
-	430.40-32.00	1.60	-	-	-	-	-	-	-	-	-	-	-
CORE NO. 2 432.00 m - 438.00 m (REC. 5.20 m) (4 BOXES)													
-	432.00-32.32	0.32	-	-	-	-	-	-	-	-	-	-	-
10	432.32-32.49	0.17	0.039	0.026	0.155	0.600	0.400	-	-	-	-	-	-
11	432.49-32.79	0.30	0.033	0.049	0.191	0.402	0.598	-	-	-	-	-	-
12	432.79-33.12	0.33	0.089	0.098	0.378	0.476	0.524	-	-	-	-	-	-
-	433.12-33.97	0.85	-	-	-	-	-	-	-	-	-	-	-
13	433.97-34.30	0.33	0.101	0.048	0.316	0.678	0.522	-	-	-	-	-	-
OB 1	434.30-34.39	0.09	-	-	-	-	-	2180.	0.346	2620	-	-	-
14	434.39-34.71	0.32	0.093	0.050	0.306	0.650	0.350	-	-	-	-	-	-
15	434.71-35.03	0.32	0.096	0.055	0.320	0.636	0.364	-	-	-	-	-	-
16	435.03-35.27	0.24	0.043	0.055	0.223	0.439	0.561	-	-	-	-	-	-
17	435.27-35.48	0.21	0.044	0.088	0.286	0.333	0.667	-	-	-	-	-	-

Figure 4.9 - Example sheet of core-analysis results.

are given in Lorsong (1981).

The amount and type of cementation was determined from the core descriptions (Lorsong, unpublished data). Three types of cement can be distinguished in the cores: clay, calcite, and carbonate (mainly iron carbonate) (Lorsong, 1981). The amount of cementation varies from complete, to partial, to nodular (calcite and carbonate only). Also, a mixture of more than one type of cement was sometimes noted. Cementation often does not extend through the entire lithofacies bed. Because it is such an important factor in the acoustic properties of the rock, lithofacies beds were subdivided so that the type and habit of cementation within each bed was constant.

Average clay content of each lithofacies type was based on discussions with Dr. Lorsong (personal communication, 1982). A constant, average value of clay content as a percentage of rock volume for each lithofacies was used. If a bed was clay cemented, the amount of clay was calculated by assuming that the decrease in porosity of the rock was entirely due to increased clay-content.

Data files called CA.DAT (for example CA2D2.DAT) were used to store the core data for each well. The contents of these CA.DAT files are presented in Appendix A. The files include the unit number, lithofacies type, bed, thickness, and depth (to the top) of each unit. The next column is a code for the cement type; then porosity, oil saturation, permeability, and clay content values follow. CA.DAT files are used as input to plotting routines LOGGRF and CELGRF. The LOGGRF plotting routine was written to allow easy comparison of the velocity and density logs to the oil saturation and cement type of each lithofacies bed. LOGGRF was used to plot the data for each well in the cross-section of Figure 4.5 (a listing of this program can be found in Appendix B). A

portion of the program CELGRF plots all of the core analysis data, but as this program was mainly used to plot the synthetic-seismogram data, CELGRF will be discussed in section 5.1. In both programs, core data are plotted at the same scale as the log data and synthetic seismograms; this allows for easy comparison.

4.5 Q values

Absorption of seismic energy in the Cretaceous sequence of the study area is likely to be a problem because of the shallow occurrence and unconsolidated nature of the beds. The absorptive properties of rocks are specified by many different units of measure, but the most commonly used measures are the absorption coefficient α and the specific attenuation factor, or quality factor, Q (Johnston and Toksoz, 1981). The quantities are related as follows:

$$\frac{1}{Q} = \frac{\alpha}{8.686\pi}$$

Where α is measured in dB/ λ .

Q is an intrinsic property of the rock. It defined as the ratio of 2π times the peak elastic energy per cycle of a harmonic wave, to the energy dissipated in one cycle of the harmonic wave (Ganley, 1979). Q is inversely related to absorption; as absorption increases, Q decreases. In the present study, the absorptive characteristics of each layer of the depth model used to construct the synthetic seismogram were specified by Q.

Measurements of the absorptive behavior of the rocks in the study area were not available; in consequence, the Q values attributed to

these rocks were modified from values published for similar types of rocks in other areas. In order to be directly applicable to the study area, the absorption measurements must be made in situ, at seismic frequencies, and in shallow, unconsolidated sedimentary-rocks. Measurements of this type are relatively rare, but a summary of the published values that fulfill most of these criteria is presented in Table 4.5.

Widely recognized, fundamental trends in the absorptive behavior of rocks were used to modify the published values of Q presented in Table 4.5, so that they would better suit the geologic environment of the study area. These fundamental trends are reviewed briefly in the remainder of this paragraph. Johnston et al. (1979) recognized the following relationships: 1) Q increases with increasing differential pressure (or, in most cases, with depth), 2) Q is higher for dry rocks than for saturated rocks, and 3) Q values obtained by ultrasonic methods are lower than those obtained by lower frequency techniques. Hamilton (1972) related attenuation to the shear, or rigidity, modulus; rocks that are more rigid (that is, cemented or less porous rocks) should have higher Q values. Hauge (1981) noted that as the percentage of sand content in sedimentary rocks increased, the Q of the rocks decreased.

In the present study, the subsurface was separated into five zones for the purpose of allocating Q values. The three drift layers were each given a different Q because of their different lithotypes and degrees of consolidation. The Colorado Group is predominantly shale, therefore, it was treated as one unit. The interbedded sands and shales of the Mannville Group constitute the last unit. The Q values chosen for these units are shown in Figure 4.10. The values for all of the units, except the Colorado Group, are constant. Because the Colorado

TABLE 4.5. SUMMARY OF IN-SITU MEASUREMENTS OF Q FOR COMPRESSIONAL WAVES

ROCK TYPE	DEPTH OF BURIAL	FREQUENCY	Q	REFERENCE
Pierre Shale (U. Cretaceous)	76-229 m	50-600 hz	32	McDonal et <u>al.</u> (1958)
Pierre Shale (U. Cretaceous)	30-1220 m	50-600 hz	97	McDonal et <u>al.</u> (1958)
sandy clay (Pleistocene)	30-152 m	50-400 hz	75	Tullos and Reid (1969)
clay sand (Pleistocene)	152-300 m	50-400 hz	137	Tullos and Reid (1969)
clay sand (Pleistocene)	2.3-30 m	50-400 hz	181	Tullos and Reid (1969)
loam clay (Pleistocene)	.3-3 m	50-400 hz	2	Tullos and Reid (1969)
course gr sand (Sat marn Sed)	.3-.6 m (water depth 32 m)	14 khz	32	Hamilton (1972)
med gr sand (Sat marn Sed)	.3-.6 m (water depth 20 m)	14 khz	31	Hamilton (1972)
fine gr sand (Sat marn Sed)	.3-.6 m (water depth 8 m)	14 khz	31	Hamilton (1972)
vf gr sand (Sat marn Sed)	.3-.6 m (water depth 13 m)	14 khz	32	Hamilton (1972)
sandy silt (Sat marn Sed)	.3-.6 m (water depth 13 m)	100 khz	23	Hamilton (1972)
sand-silt clay (Sat marn Sed)	.3-.6 m (water depth 17 m)	100 khz	31	Hamilton (1972)
clayey silt (Sat marn Sed)	.3-.6 m (water depth 22 m)	100 khz	111	Hamilton (1972)
20% sand, 80% shale (U. Cret)	610-1585 m	seismic	45	Hauge (1981)
45% sand, 55% shale (Miocene)	670-1341 m	15-40 hz	34	Hauge (1981)

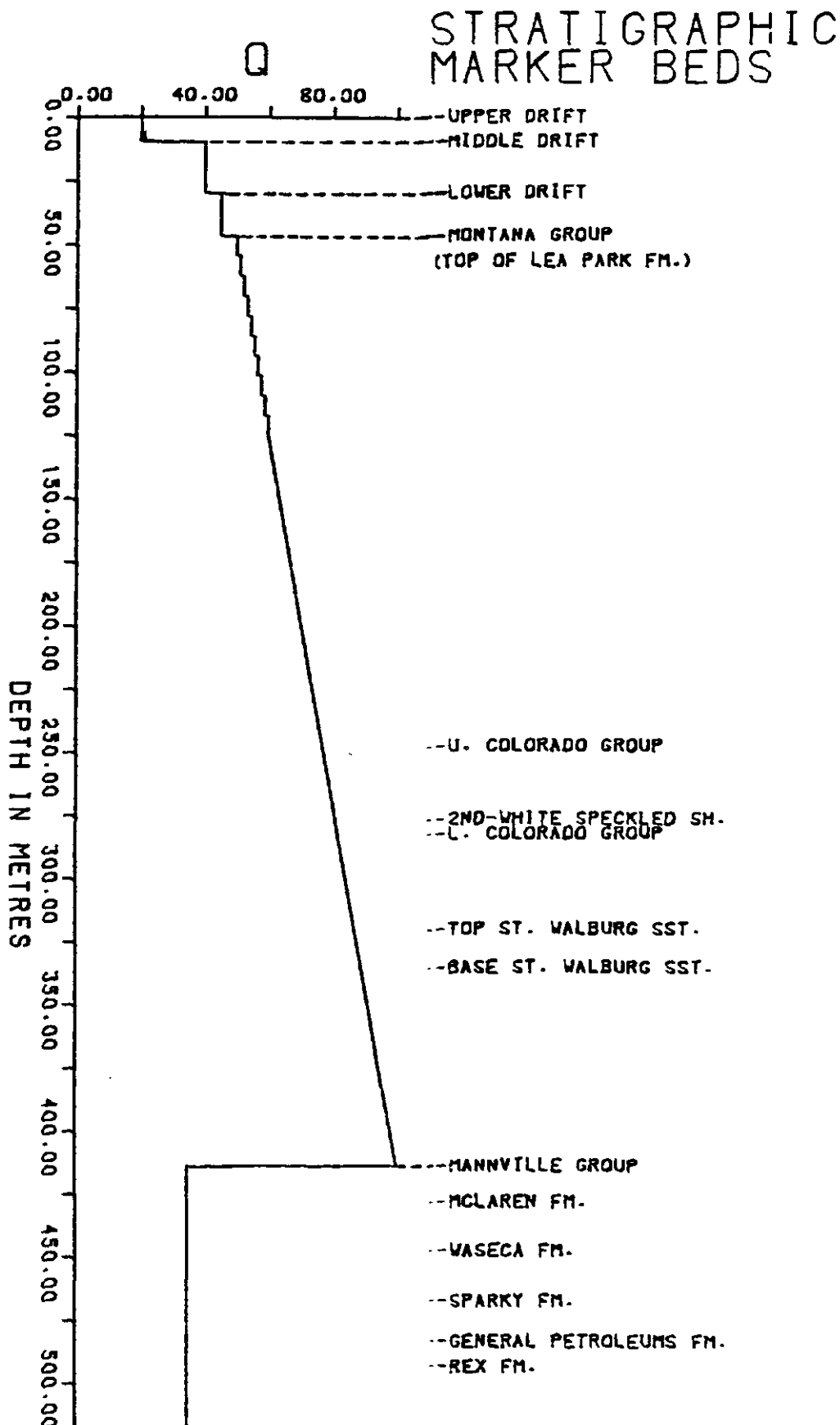


Figure 4.10 - Q values used in the study area.

Group unit is so thick, the Q within this unit was increased linearly from a reasonable value at its shallowest depth to a reasonable value at its deepest depth.

The choice of Q , or the way in which Q varies within the units cannot be rigorously defended. In section 5.3.3 it will be shown that (within reason) it is the average value of Q , rather than the shape of the Q curve that affects the lower portions of the synthetic seismogram. If real seismic data were available, an attempt could be made to model the input Q values until the shape of the synthetic seismogram approximated the shape of the seismic traces. This should be done with traces plotted without gain control.

CHAPTER FIVE

GEOPHYSICAL PROCESSING AND ANALYSIS

5.1 Synthetic Seismograms

The method of synthetic-seismogram synthesis used in this thesis was described in Ganley (1979, 1981). In this method, the communication theory approach to synthetic-seismogram construction is modified to include the effects of absorption and dispersion. Historical developments in the expression of seismic wave propagation through layered media by communication theory were reviewed by Robinson and Treitel (1977). The absorption model used in the program for synthetic-seismogram construction is that of the exponential decay of amplitude as a function of distance. Absorption is mathematically introduced by allowing the elastic modulus in the elastic-wave equation to be a complex function of frequency. As a result, the velocity and wavenumber, as well as the reflection and transmission coefficients become complex functions of frequency. Dispersion is introduced by equations derived by Futterman (1962), which relate dispersion to absorption.

Futterman (1962) demonstrated that if a linear theory of wave propagation is assumed (that is, if the principle of superposition is valid), and the absorption coefficient $\alpha(\omega)$ is strictly linear with frequency over the range of measurement (that is, Q is constant over this range), then the presence of dispersion is a necessary consequence of absorption and is, in fact, determined by it. Using the condition of causality, which states that a signal will not be detected at an apparatus until sufficient time has passed for it to arrive there, Futterman related dispersion to absorption and calculated the dispersion

for three absorption functions. Ganley defined his absorption and dispersion relations by using Futterman's third absorption-dispersion pair.

For typical earth cases (Q greater than 20) and in the frequency range used for seismic exploration, dispersion is small but measurable (Toksoz and Johnston, 1981). Futterman (1962) demonstrated how dispersion caused a propagating pulse to broaden, decrease in amplitude, and become asymmetrical with increasing time. As a result of dispersion, the higher-frequency components of the wave travel with a higher phase velocity; the front of the pulse becomes sharper and the pulse has a definite arrival time. However, as time passes, absorption begins to reduce the high frequency content of the wavelet and the effects of dispersion become less pronounced.

Ganley's original synthetic-seismogram program was tested on the computer facilities available at the University of Saskatchewan by computing and plotting the surface trace of the example synthetic seismogram shown in Ganley (1981). Ganley (1981) described two methods of synthetic seismogram synthesis. The program used in the present study employs the ratio approach, which calculates a synthetic seismogram only at the surface layer. It also has the capability to calculate the surface synthetic-seismogram for a buried source. Modifications to this program were made to suit the present study. The original format required an input thickness, Q value, density, and phase velocity for each depth layer of the model earth. This format was preserved for the layers within the cased portions of the wells, but was changed for the portions of the well where geophysical logs supplied the velocity and density data. The synthetic-seismogram program is called SYNCCEL; it is listed in Appendix B.

A downgoing spike is used as the energy source in the original program. To give an additional choice of wavelet shape a subroutine called PULSE was written. This subroutine generates Ricker wavelets (Ricker, 1953a). Although the viscoelastic model on which the Ricker wavelet is based may not be realistic, the concept of this wavelet has been extensively used in exploration seismology (Toksoz and Johnston, 1981). With PULSE, four different types of Ricker wavelets, of variable peak frequency, can be computed. Of the four, only the direct phase or velocity-type Ricker-wavelet was used in this study. PULSE also includes equations to calculate the phase and amplitude spectra of the wavelet.

The method of constructing the synthetic seismograms was uniform during this study. Due to dispersion, the phase velocity and Q values will vary with frequency. In the present study, the input Q values and phase velocities were at frequencies of 100 hz (as in Ganley, 1981). The low frequency cut-off (as required by Futterman) was at .0017810724 hz.

The synthetic seismograms are calculated as a continuous function of frequency. In order to avoid the effects of aliasing in the time domain when using a discrete Fourier-transform, sampling in the frequency domain must be at a small enough spacing, Δf , that for times greater than $T_n = 1/\Delta f = 2\pi/\Delta \omega$, the amplitude of the synthetic seismogram is negligibly small (Ganley, 1981). Ganley has found that choosing T_n to be four to eight times the two-way time of the model is usually adequate. In the present study, Δf was chosen so that T_n is approximately eight times the two-way time of the model. Inspection of the calculated synthetic-seismograms verified that, at times approaching T_n (4.096 s), the amplitudes are indeed negligibly small. The Fourier

transforms of the synthetic seismograms were evaluated by 2049 discrete frequency-values between 0 and 500 hz, inclusive. In the time domain, 4096 points were calculated, at a time interval of 1 ms.

In order to perform the discrete Fourier-transform, the data must be band limited and the contributions of frequencies beyond a maximum frequency must be eliminated. To reduce any undesirable effects, a Butterworth low-pass filter was used to reduce the amplitudes of frequencies beyond the cut-off frequency (Ganley, 1981). The amplitude response of this filter is 3 decibels down (29.2 per cent reduced from the maximum amplitude) at 250 hz and 72 decibels down (99.9 per cent reduced from the maximum amplitude) at 500 hz. The time domain synthetic now approximates the synthetic that would be recorded through an anti-alias filter with the characteristics of the low-pass Butterworth-filter.

A computer program called CELGRF was written to plot the synthetic seismograms and those properties of the subsurface that could affect the seismic response. The plots include the shape and normalized amplitude spectrum of the Ricker wavelet source (if used); the synthetic seismogram; the Q, velocity, and density values; the stratigraphic markers; and the core properties of porosity, permeability, oil saturation, clay content, cement type, and lithofacies type. The rock properties and synthetic seismograms are plotted at the same scale and as closely together as possible, to facilitate the recognition of cause and effect relationships between the two. The rock properties are plotted versus depth and the seismograms are plotted versus both time and depth. Examples of plots produced by CELGRF are shown in Figures 5.2 through 5.6, 5.8 through 5.13, 5.17, 5.19 through 5.25, 5.30 through 5.37, 5.44 through 5.50, 5.58, 6.1, 6.6, and 6.8 through 6.10.

In order to compensate for the attenuating effects of absorption and short-period multiples, and thus, provide more equal amplitude levels from early to late events, a gain function may be included in the synthetic-seismogram plotting-routine. The gain control is provided by a power gain-function that computes the energy within sliding time-windows and then applies a gain that is inversely proportional to the energy in the time window (Sereda, 1978). Tests were made to determine the optimum window length for the data in this study. The best results were obtained by specifying a window length of 0.10 s.

It is sometimes desirable to plot the synthetic seismogram without gain (a true-amplitude plot). For example, this was done in section 5.3.3 to study the attenuation effects of different Q values. When no gain control is desired (that is, when the window length in CELGRF is set to 0.0 s) the high amplitude, direct-wave arrival on the seismogram is automatically muted. Muting of this arrival is also automatic when the seismic source is buried.

5.2 Spectral Analysis

There is an interchangeability between a waveform as a function of time, such as a seismic trace, and the spectra of the waveform that show amplitude and phase as functions of frequency; "The amplitude and phase spectra, taken together, uniquely define their corresponding composite waveform" (Anstey, 1965, p. 6). Bath (1974) described several advantages of this form of representation. The first is that, when expressing a waveform as functions of frequency (spectral analysis) the whole signal shape is used in the analysis, whereas the common time domain measurements (such as displacement direction, maximum amplitude, or onset time) are point measurements. Spectral analysis can,

therefore, because of its style of presentation, yield more useful information than time measurements. The second advantage is that, when making comparisons of different records it is important to be sure that exactly the same thing is compared in all cases. The frequency-domain representation provides a unique check that the parameters being compared are all referred to the same frequency value. Time domain representations do not provide such reliable control.

Spectral analysis was performed for the Mannville sections of the synthetic seismograms. These amplitude spectra provided a quantitative measure of the changes in amplitude of the frequency components of the propagating seismic energy in the zones of interest, as input parameters to the synthetic seismogram were varied. The input parameters that were varied will be described in the remaining sections of this chapter.

A spectral analysis program call SPECAN was used to calculate these spectra. SPECAN is a generalized spectral-analysis program, employing the efficient fast-Fourier-transform (Rielkoff, 1982). The program was tested by computing the amplitude spectra of sinusoidal time-series. A calcomp plotting routine was added to SPECAN; the amplitude values, were first smoothed by the Hanning method (Titchkosky, 1968, p. 87) and then were normalized and plotted. An example amplitude spectrum is shown in Figure 5.7. The low amplitude of the spectrum from about 250 to 500 hz indicates a lack of energy beyond 250 hz. This is to be expected because the Butterworth low-pass filter used in the synthetic seismogram program severely filters frequencies above 250 hz.

5.3 Model Parameters

5.3.1 Introduction

Tests were made to determine the effect on the synthetic seismogram of variation in the input parameters of the Q value, the depth of burial of the source, the frequency content of the propagating wavelet, and the subsurface geology in the zones of economic interest. Well 2B8 was chosen as the subject of these tests because: 1) it is in the centre of cross-section AA' (see Figure 4.1), 2) it is a typical example of the representative and economically important geologic features of the six pilot-project wells, 3) it has geophysical logs of good quality, and 4) it has a very long cored-section, which includes most of the zone of geologic modelling.

Although only one input parameter at a time was varied, and although the parameters are discussed separately, it is critical to note that it is the combined effect of all of the parameters that determines the output. The testing was an iterative process, in which first one parameter and then another was varied. Earlier tests were often returned to and run again with slightly different input parameters. In order to point out the important synthetic seismogram responses, the variations in the input parameter of subsurface geology are discussed first.

The polarity convention used in this thesis is that a peak is a deflection to the right. It is reflected from an interface in which a layer of higher acoustic-impedance overlies a layer of lower acoustic-impedance. A trough is a deflection to the left and results from the opposite acoustic-impedance layering.

5.3.2 Geologic modelling

The responses of five beds of economic importance were studied by comparing synthetic seismograms constructed with the beds unaltered and altered. The five beds were not actually removed from the wells; instead, their characteristic effects were edited from the velocity and density logs. In Figure 5.1 the edits made for each of the six test cases are shown. For example, when the response of the oil-saturated sand-bed W6 is removed from the synthetic seismogram, the low velocity and density signature of the oil-saturated sand must be removed by increasing the velocity and density of the W6 zone to values similar to that of the unsaturated, shaley sand-beds above and below; the oil-saturated sand-bed is artificially shaled out. The seismograms used for geologic modelling were constructed with the input parameters of an impulse source, the Q curve shown in Figure 4.10, and a source burial of 29.9 m. The input parameters are summarized in Figure 5.2.

When the effects of all of the Waseca formation oil zones (that is, W3, W4, and W6) are deleted from the input logs, the resulting seismogram is as shown in Figure 5.3. The unmodified well logs and their seismic response are shown in Figure 5.4. When comparing these two synthetic seismograms, the most obvious difference between them is that two low amplitude, high frequency peaks at about 0.42 s in Figure 5.4 are eliminated in Figure 5.3. Those waveforms appear to be generated by the oil-saturated sands W6 and W3. To test this hypothesis, the two main oil-zones, W6 and W3, were separately edited to appear shaled out. When the effect of the oil-saturated sand in bed W6 was removed from the well logs, only the upper waveform disappeared from the synthetic seismogram. This is illustrated in Figure 5.5. As is shown in Figure 5.6, when the effect of the oil-saturated sand in bed W3

CELTIC 2B8 10 52 23 W3M

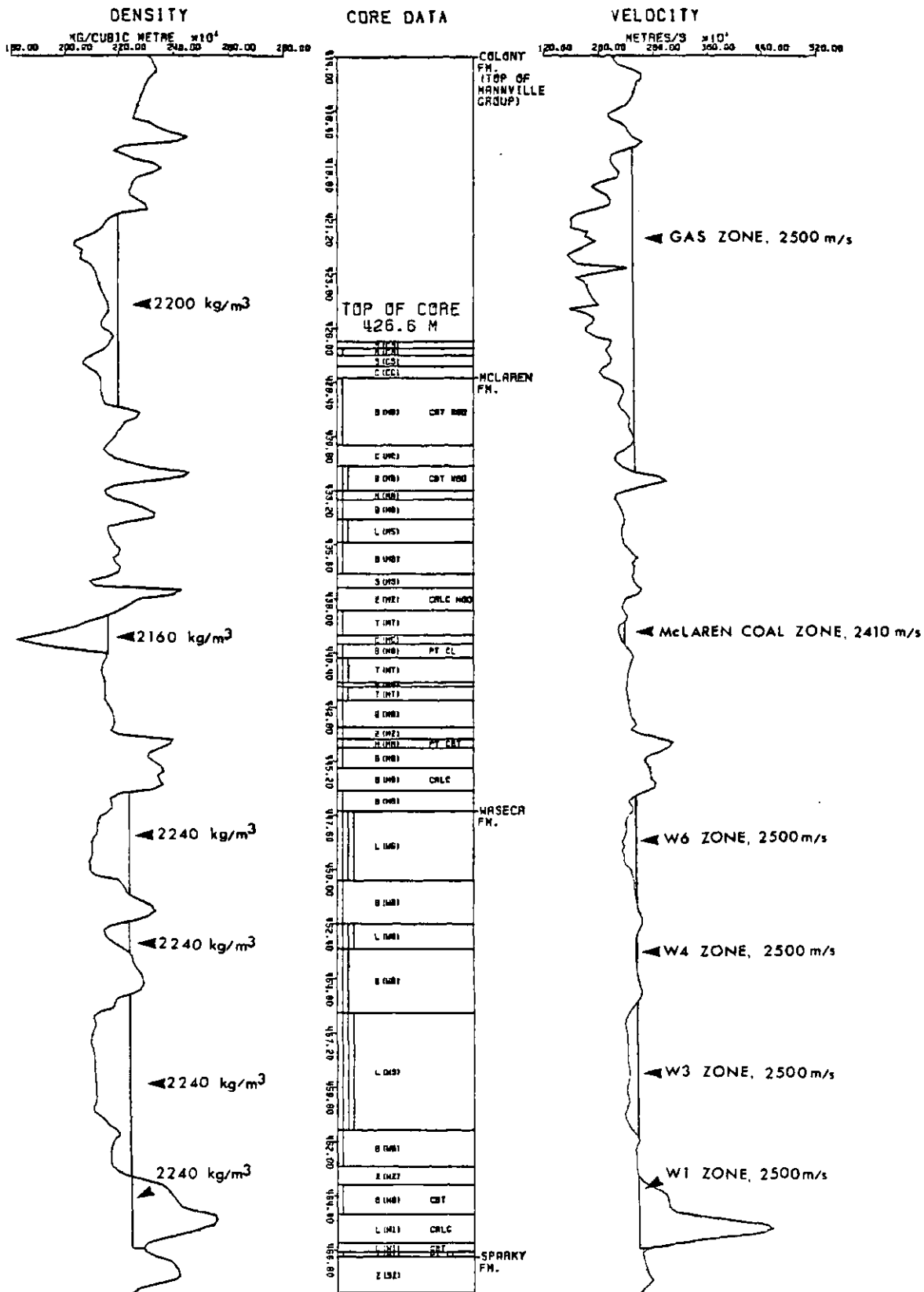


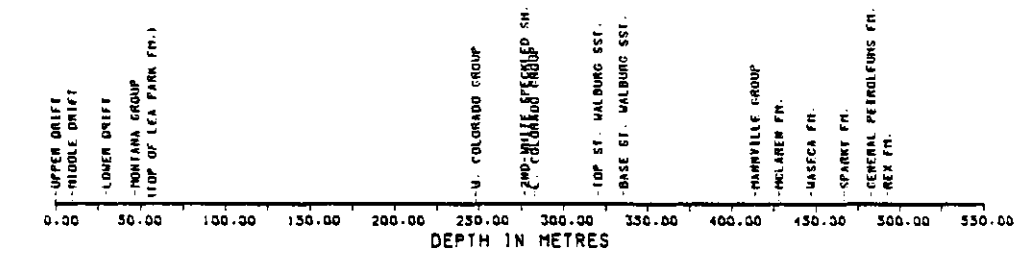
Figure 5.1 - Well-log zones edited for geologic modelling.

NUMBER OF POINTS REQUESTED IN SYNTHETIC TRACE = 4096
SAMPLE INTERVAL FOR SEISMOGRAM AND WAVELET (MS) = 1.
TYPE OF WAVELET = IMPULSE; THE DIRECT WAVE IS MUTED
BUTTERWORTH ANTI-ALIAS FILTER INCLUDED IN SYNTHETIC TRACE
POWER GAIN FUNCTION INCLUDED, WINDOW LENGTH (S) = 0.10
WELL IS CASED TO A DEPTH (M) = 125.4
NUMBER OF CONSTANT VELOCITY LAYERS WITHIN CASED SECTION = 13.
RECEIVERS LOCATED AT TOP OF LAYER 1
DEPTH OF SOURCE BELOW RECEIVERS (M) = 29.9

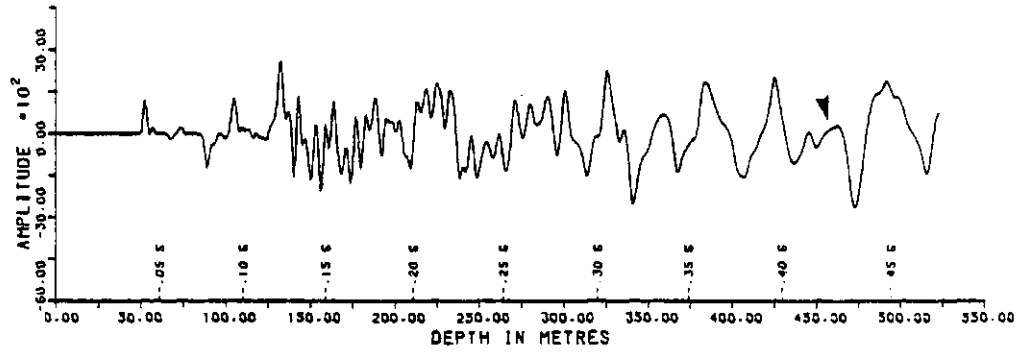
Figure 5.2 - Summary of parameters used to construct synthetic seismograms for geologic modelling.

CELTIC 2B8 10 52 23 W3M

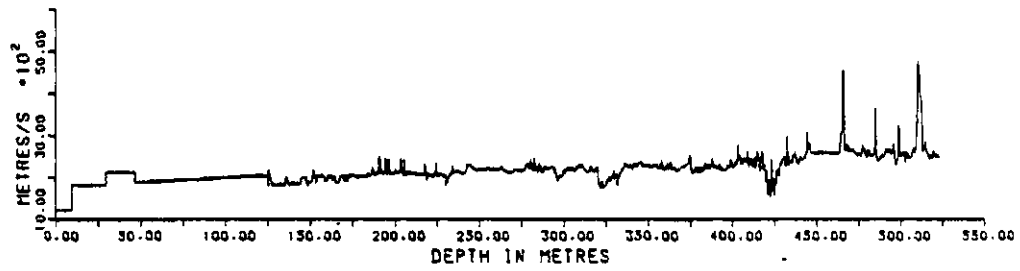
STRATIGRAPHIC
MARKER BEDS



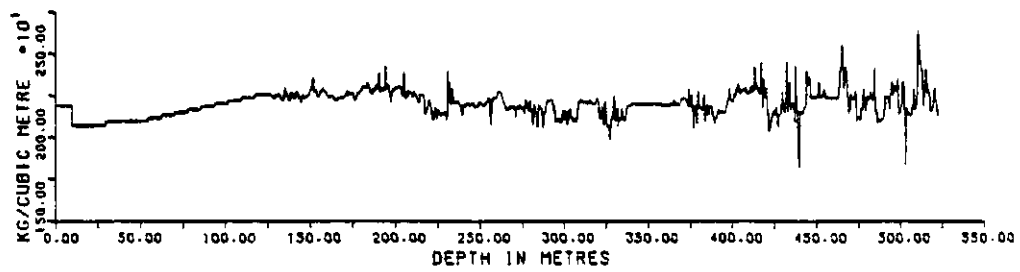
SYNTHETIC
SEISMOGRAM



VELOCITY



DENSITY



Q

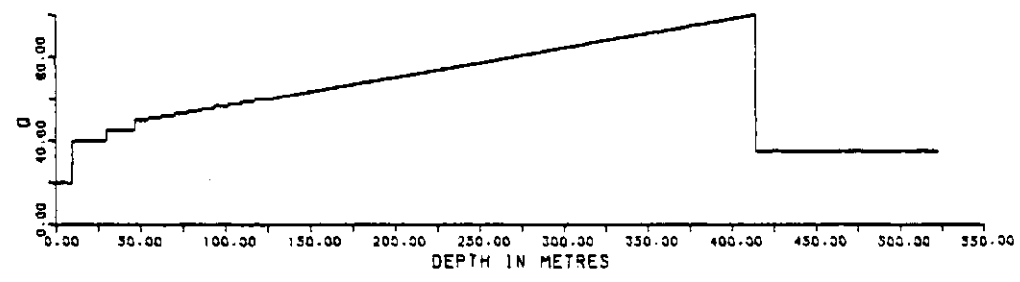
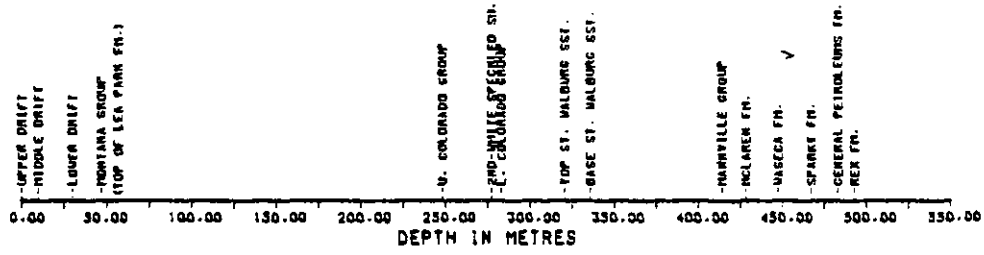


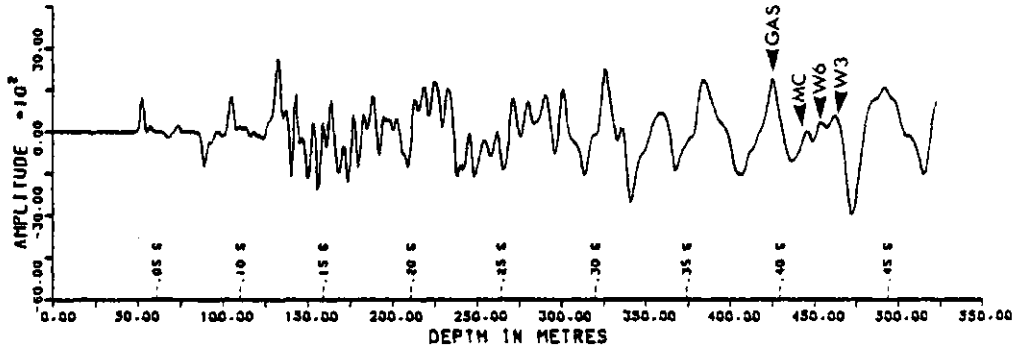
Figure 5.3 - Well logs and seismogram when the Waseca fm. oil-zones are edited to appear shaded out.

CELTIC 2B8 10 52 23 W3M

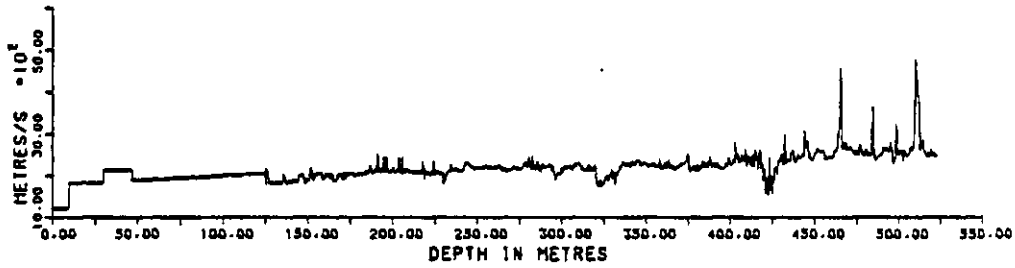
STRATIGRAPHIC MARKER BEDS



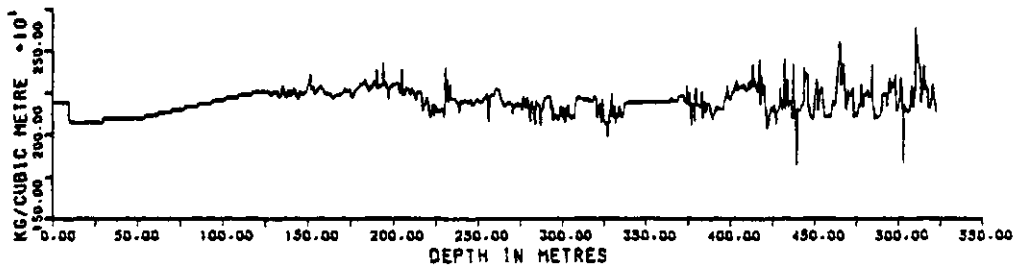
SYNTHETIC SEISMOGRAM



VELOCITY



DENSITY



Q

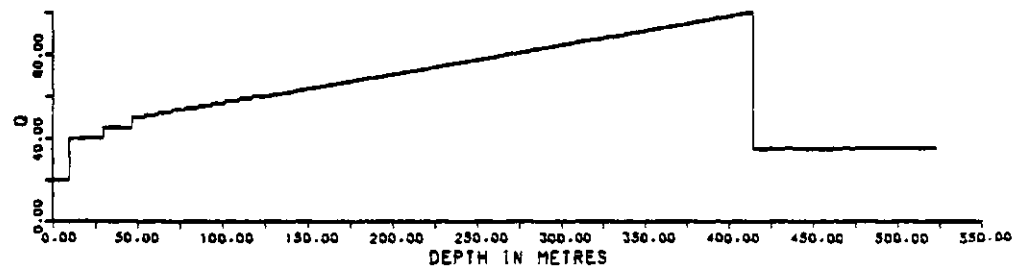
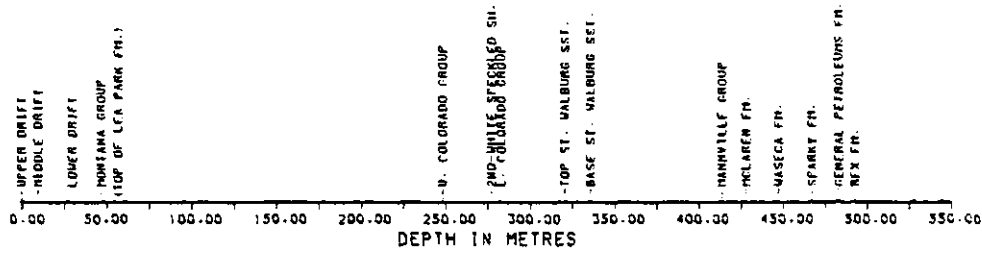


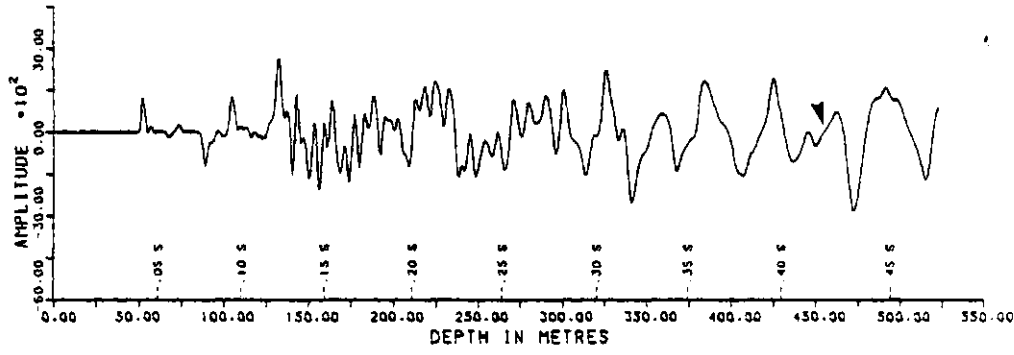
Figure 5.4 - Unmodified well-logs and resulting synthetic seismogram.

CELTIC 288 10 52 23 W3M

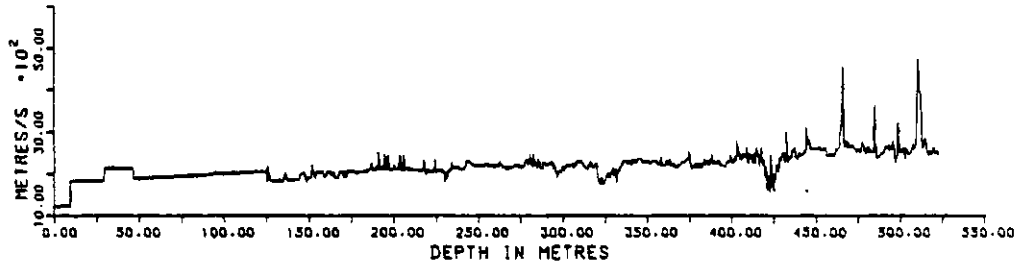
STRATIGRAPHIC
MARKER BEDS



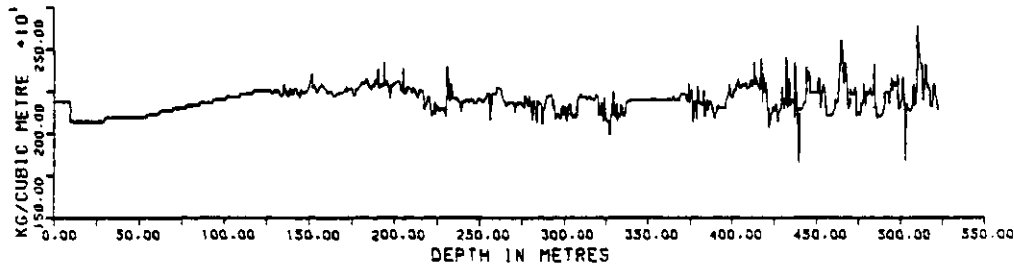
SYNTHETIC
SEISMOGRAM



VELOCITY



DENSITY



0

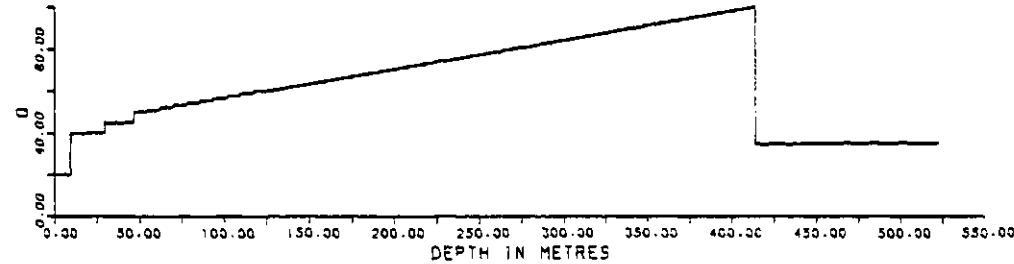


Figure 5.5 - Well logs and seismogram when the W6 oil-zone is edited to appear shaded out.

CELTIC 2B8 10 52 23 W3M

STRATIGRAPHIC
MARKER BEDS

UPPER DRIFT
MIDDLE DRIFT
LOWER DRIFT
MONTANA GROUP
(TOP OF LEE PARK FR.)
U. COLORADO GROUP
2ND COLORADO GROUP CN.
TOP ST. WALBURG SST.
BASE ST. WALBURG SST.
MANNVILLE GROUP
MCLAREN FH.
MABEGA FH.
SPARKS FH.
GENERAL PETROLIFEROUS FH.
REX FH.

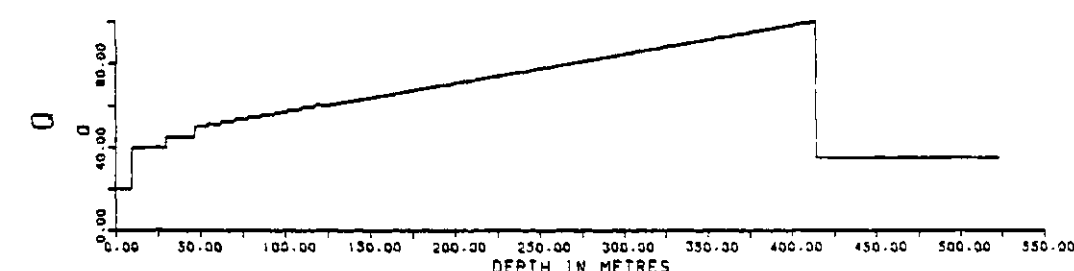
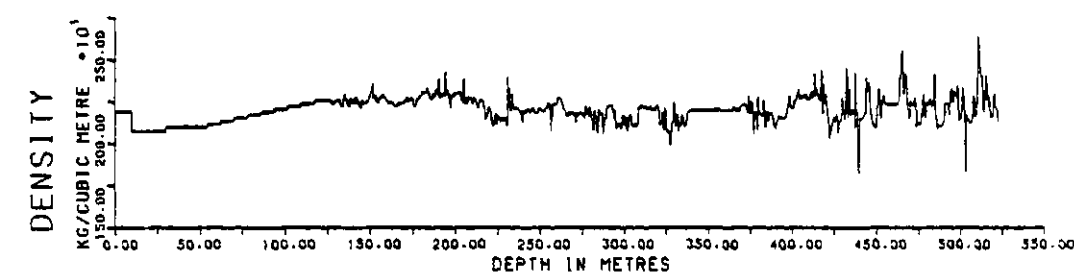
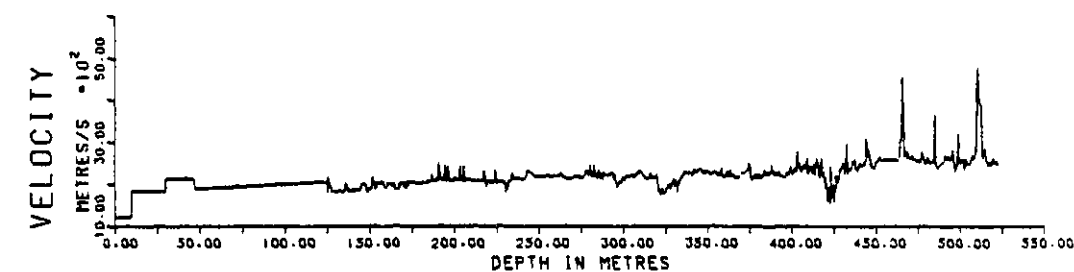
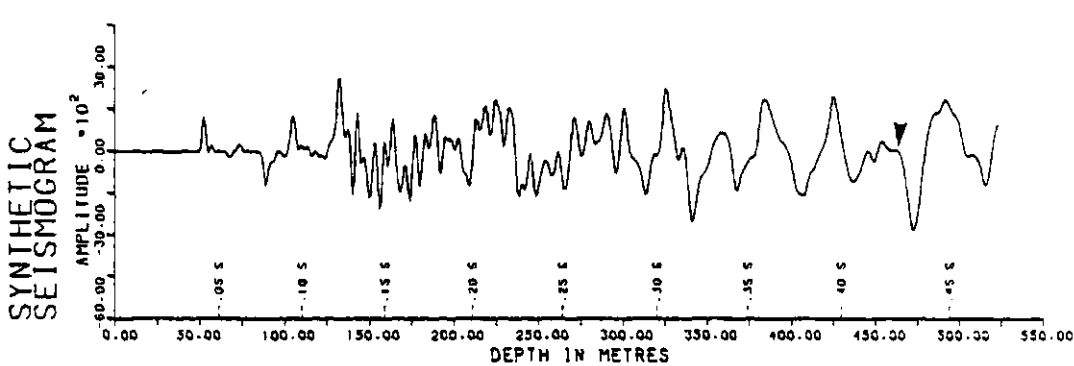


Figure 5.6 - Well logs and seismogram when the W3 oil-zone is edited to appear shaded out.

was removed, only the lower waveform disappeared. These two waveforms are, thus, in direct response to the oil-saturated W6 and W3 beds of the Waseca formation.

The apparent periods of these two waveforms were measured by graphical means. The upper (W6) peak has an approximate period of 9.6 ms, which corresponds to a frequency of 104 hz. The lower (W3) peak has an approximate period of 11.5 ms, which corresponds to a frequency of 87 hz. These values, as well as those measured for the other modelled beds, are presented in Table 5.1. It is important to note that these graphical measures of the wavelet periods are approximate; the time scale of the plotted synthetic seismogram is not linear, and more importantly, due to interference effects, the entire, distinct reflected-waveform cannot be distinguished on the synthetic seismogram. The resolution of these modelled beds is discussed in more detail in section 6.1.

The amplitude spectrum corresponding to the unmodified synthetic seismogram in Figure 5.4 is shown in Figure 5.7. The 104 hz, W6 wavelet has an amplitude of about 25 per cent of the dominant frequency, whereas the 87 hz, W3 wavelet has an amplitude of only 15 per cent of the maximum. The sample interval of all of the amplitude spectra plotted in this study is 7.812 hz. Hanning smoothing was applied to the spectra to decrease the spikiness of the plot. But, for the reasons explained in the preceding paragraph, the wavelet periods cannot be measured accurately, and since only a small change in frequency can make a large difference to the amplitude spectrum, care must be exercised in using the amplitude spectra to determine the amplitude of a specific frequency.

The Colony formation contains gas that is of little economic

TABLE 5.1. SUMMARY OF REFLECTION DATA FROM THE MODELLED ZONES

Reflecting Layer	Measured Period of Reflected Waveform	Measured Frequency of Reflected Waveform	Percentage of the Peak Amplitude Spectrum Response
Colony fm. gas zone	25.0 ms	40 hz	100%
McLaren fm. coal bed, MC	5.8 ms	173 hz	12%
Wasaca fm. oil saturated zone, W6	9.6 ms	104 hz	25%
Waseca fm. oil saturated zone, W3	11.5 ms	87 hz	15%
Waseca fm. cemented zone, W1	no reflected waveform can be distinguished		

CELTIC 2B8 10 52 23 W3M

MINIMUM Q=20 AND MAXIMUM Q=100
 SOURCE BURIED AT A DEPTH (M) = 29.9
 TYPE OF WAVELET : IMPULSE
 BUTTERWORTH ANTI-ALIAS FILTER INCLUDED IN SYNTHETIC TRACE
 TIME GATE (IN S) FOR AMPLITUDE SPECTRUM = .405 TO 0.493
 TIME GATE CORRESPONDS TO:
 TOP OF MANNVILLE GRP. (414.0 M) TO END OF INPUT LOGS (523.2 M)
 SAMPLE INTERVAL IN TIME DOMAIN (S) = .0010
 SAMPLE INTERVAL IN FREQUENCY DOMAIN (HZ) = 7.812
 NUMBER OF FREQUENCIES ANALYSED = 65.
 HANNING SMOOTHING APPLIED TO SPECTRUM
 PERCENT OF TRACE ELEMENTS TAPERED AT EACH END = 10.

AMPLITUDE SPECTRUM OF SYNTHETIC SEISMOGRAM

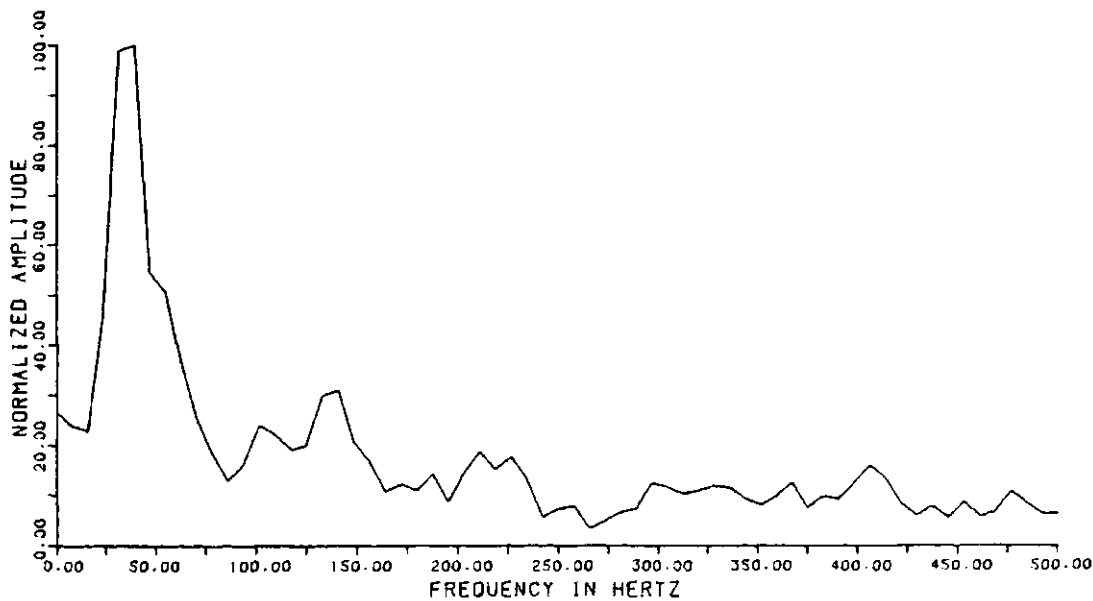


Figure 5.7 - Amplitude spectrum from seismogram constructed using unmodified well-logs.

interest, but is of considerable interest to the geophysicist, as the velocity and density through this zone is strongly affected. Only a 5 per cent concentration of gas is required to reduce severely the velocity of a water saturated rock (Domenico, 1974). When the Colony gas effect was removed by editing the velocity and density logs so that the velocity and density through the gas zone was similar to that of the adjacent rocks that do not contain gas, the change in the seismogram is large and continues throughout seismogram. The geophysical logs were edited to remove the gas effect, as was shown in Figure 5.1, and the resulting seismogram is shown in Figure 5.8. The low frequency, large amplitude peak that occurred at about 0.39 s in Figure 5.4 is no longer visible. This waveform was graphically measured to have a period of about 25 ms and a frequency of 40 hz. The dominant frequency in the amplitude spectrum of Figure 5.7 is 39 hz. When the large-amplitude, 40 hz wavelet resulting from the gas zone is not present there is an extensive effect on the lower portion of the synthetic seismogram because the elimination of this dominant low-frequency makes the higher frequencies more apparent.

Removal of the effect of the very thin but low density, McLaren formation coal-bed MC produces a noticeable reduction in the amplitude of the small peak at about 0.41 s on the seismogram in Figure 5.9. The measured period of this waveform is about 5.8 ms, which corresponds to a frequency of 173 hz. On seismic records, coal beds can be mistaken for oil zones because both are of low velocity and density. Although this is a more serious problem with thicker coal beds, this test provided an indication of the type of event that could be expected. In Figure 5.4 it is interesting to note the similarity of the coal response MC to those of the oil zones W3 and W6.

CELTIC 2B8 10 52 23 W3M

STRATIGRAPHIC
MARKER BEDS

SYNTHETIC
SEISMOGRAM

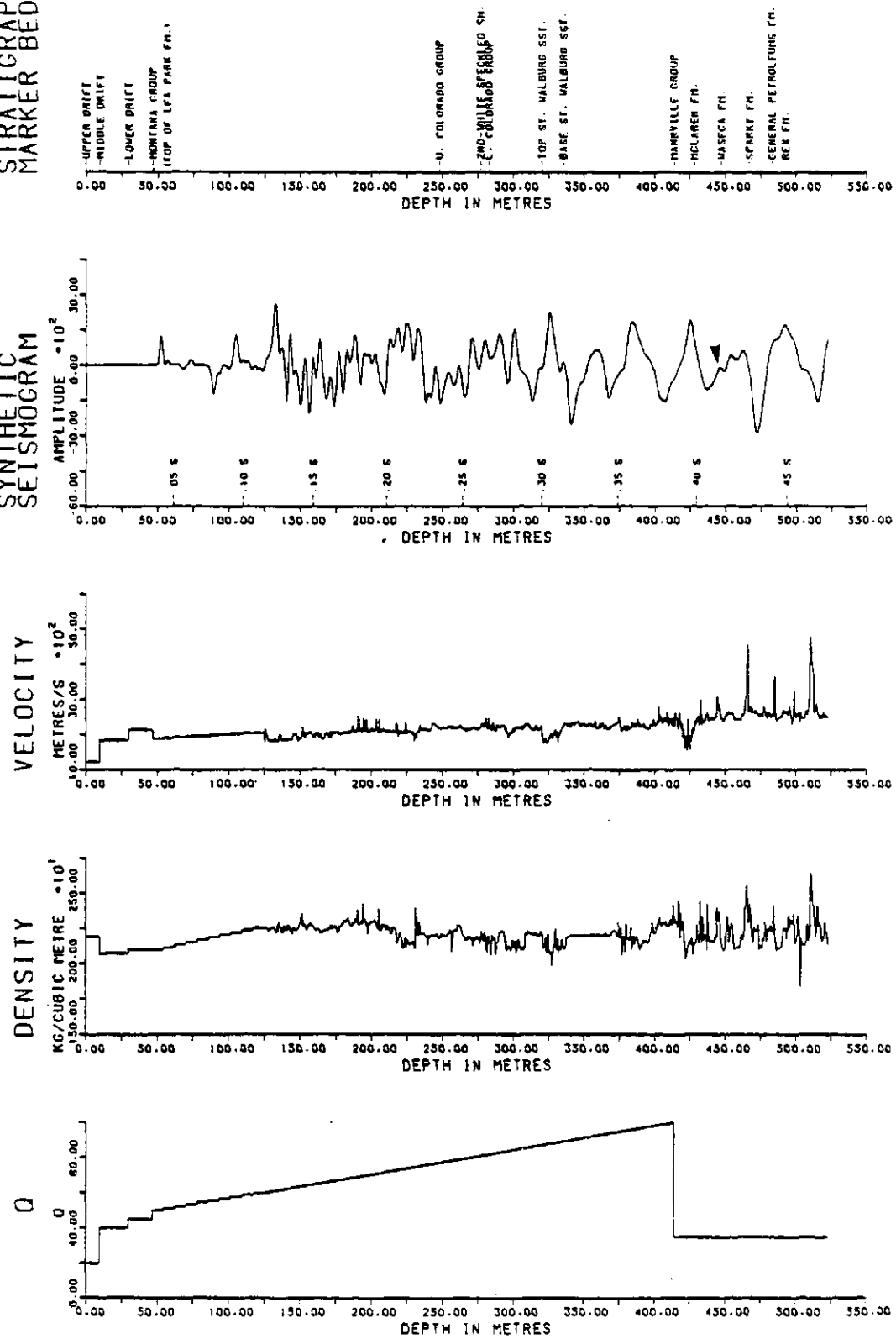


Figure 5.9 - Well logs and seismogram when the MC coal bed is replaced by shale.

Editing of the input well logs to remove the effect of the cemented bed W1, which is located at the base of the Waseca formation, produces very little change of response in the synthetic seismogram, even though the density and velocity of the cemented zone is high and a significant (though high frequency) response was expected. The modified logs and resulting seismogram are shown in Figure 5.10. One can interpret this as showing that the dominance of the low frequencies is so strong that variations in the higher frequencies cannot be recognized at this point in the seismogram. The interference of waveforms will be more thoroughly discussed in sections 5.3.4 and 6.1. Cemented zones are important because they serve as barriers to the flow of heat and fluids (Lorsong, 1981). Knowledge of the locations of these zones is especially important in enhanced-recovery operations.

5.3.3 Q Values

Experimentation in the shape and average value of the Q function was done to determine the effect on the seismogram of variation in these parameters. Tests were made with eight different shapes of Q curves. The main conclusion of these tests was that the frequency content of the seismograms is increased when higher Q-values are used. The other conclusion was that it is the average value of the Q function, and not its shape (within reasonable limits), that is of prime importance to the frequency content of the Mannville portion of the seismograms.

To illustrate these conclusions, synthetic seismograms are presented that were constructed with Q values that are low, average, and high in comparison to the Q function chosen in section 4.5 (see Figure 4.10). This Q function in Figure 4.10 will hereafter be called the standard Q-function. Synthetic seismograms with constant values of Q

CELTIC 2B8 10 52 23 W3M

STRATIGRAPHIC
MARKER BEDS

SYNTHETIC
SEISMOGRAM

VELOCITY

DENSITY

Q

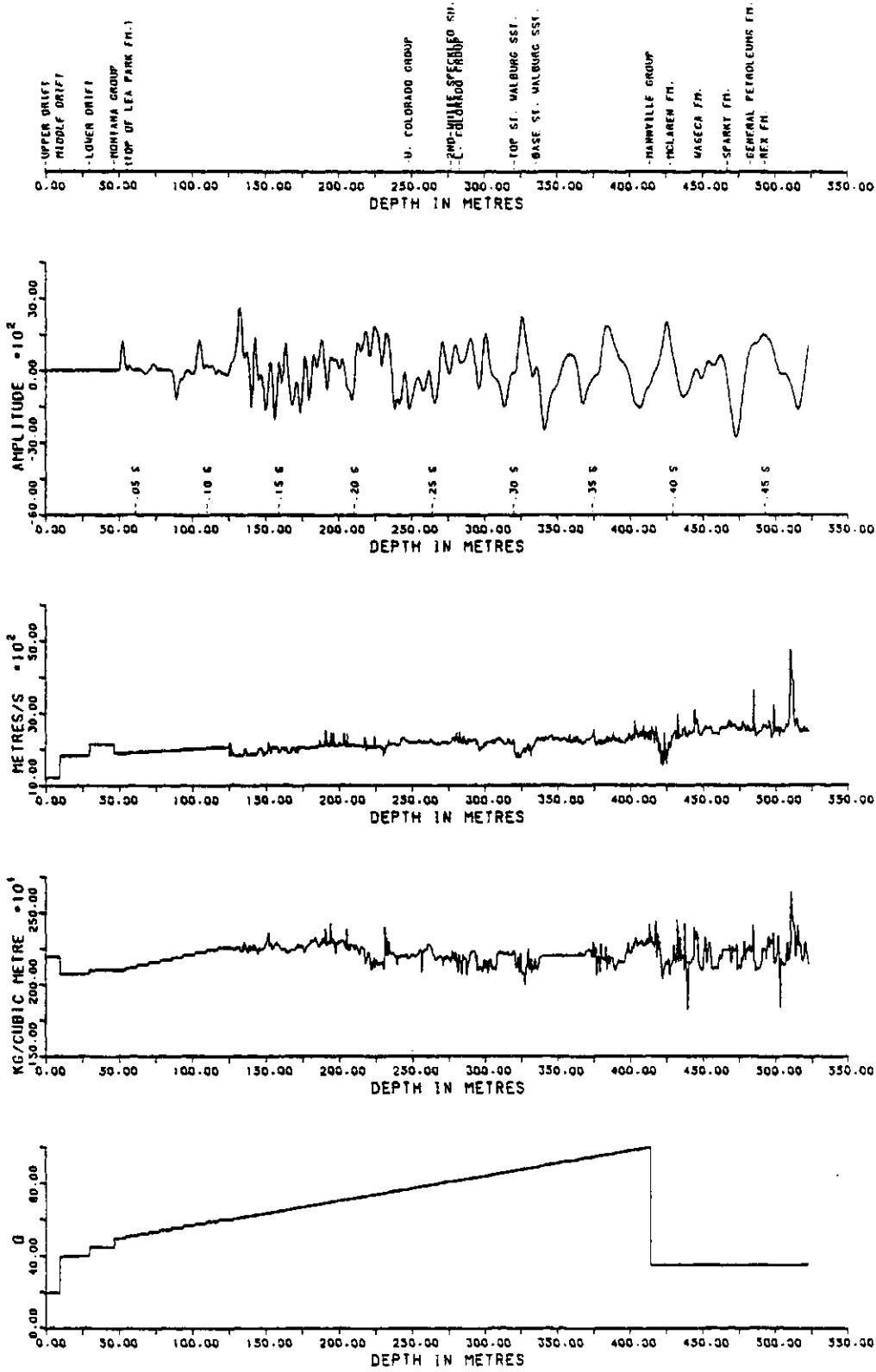


Figure 5.10 - Well logs and seismogram when the W1 cemented-zone is edited to appear non-cemented.

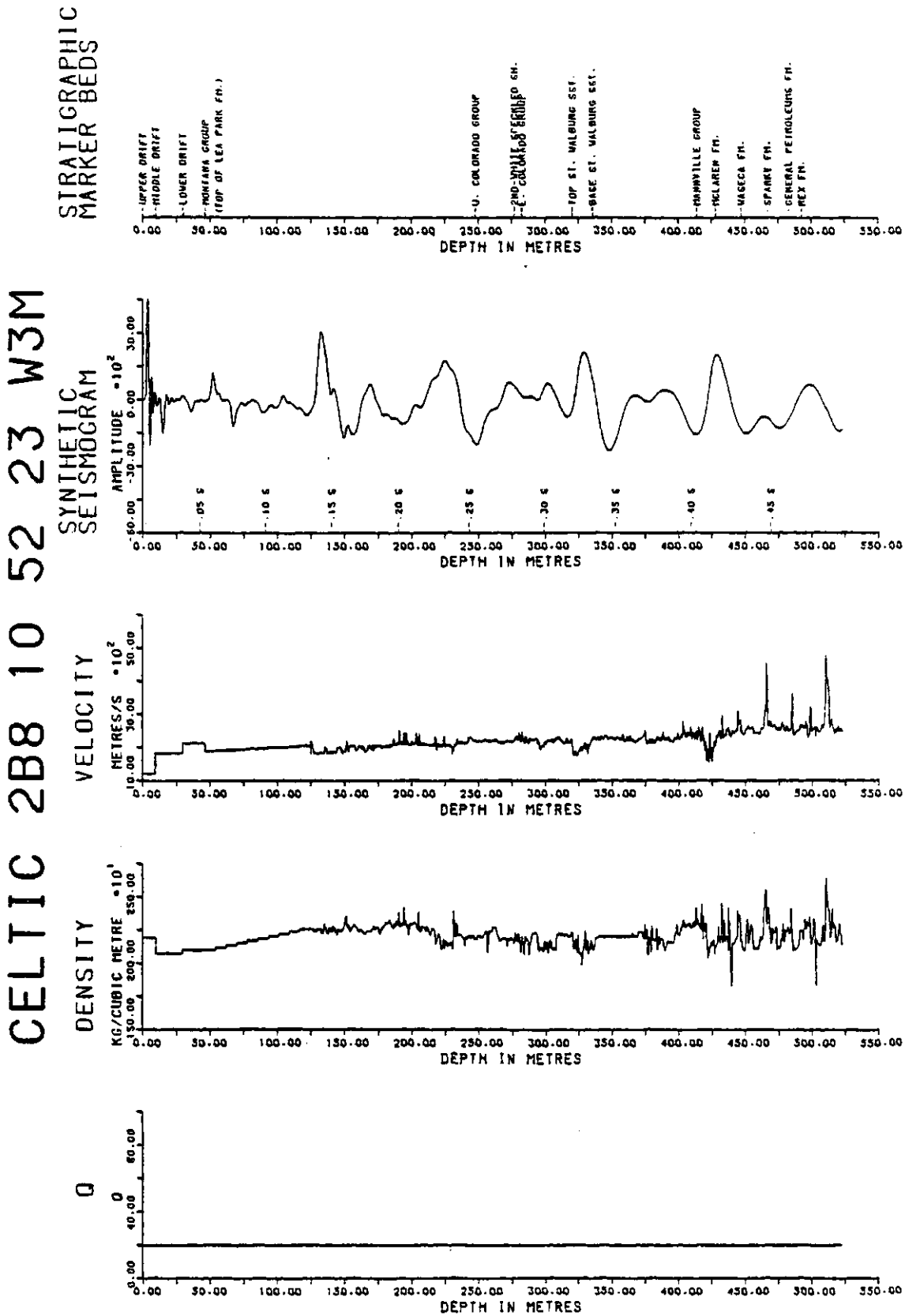


Figure 5.11 - Seismogram with constant Q-value of 20.

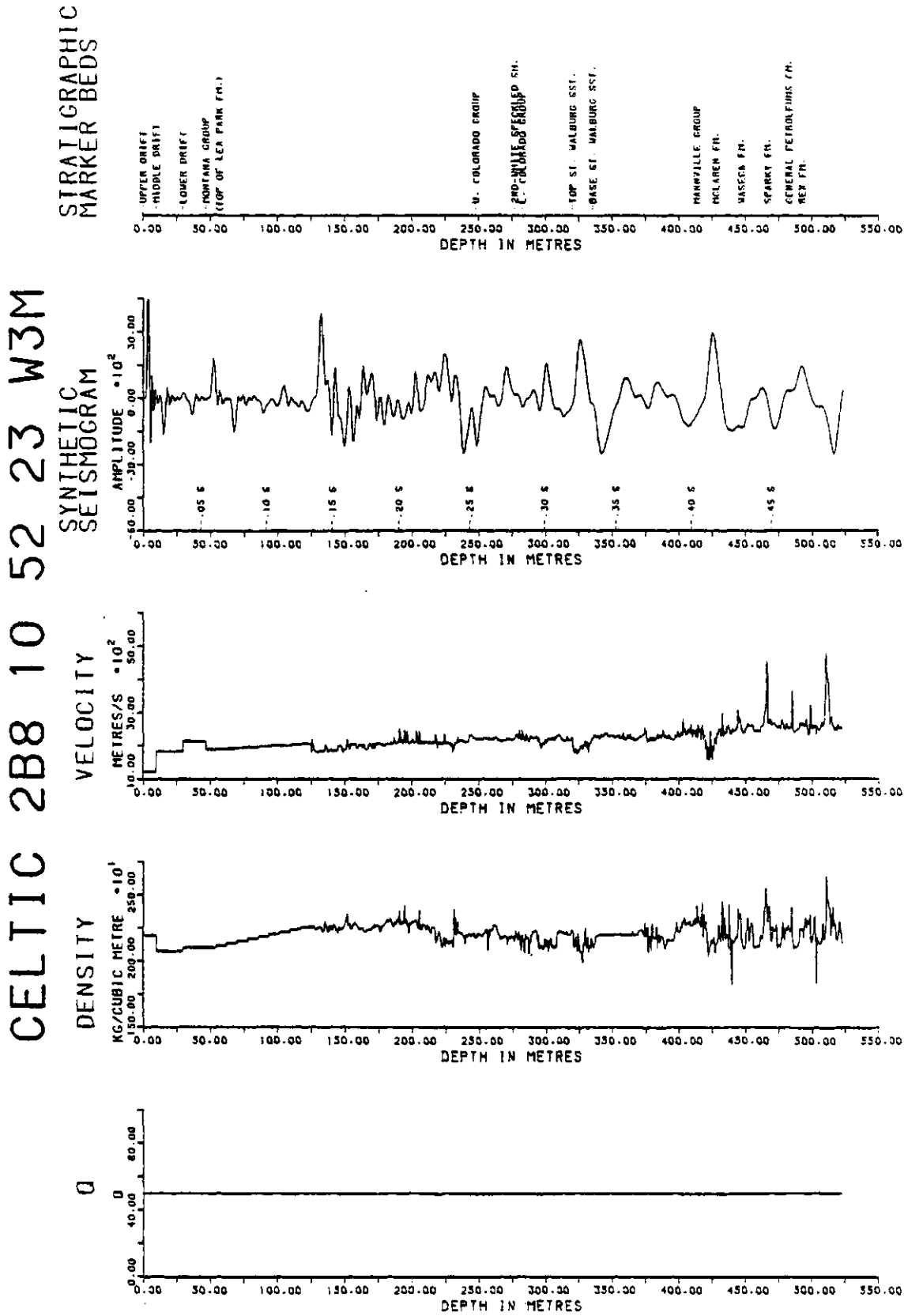


Figure 5.12 - Seismogram with constant Q-value of 50.

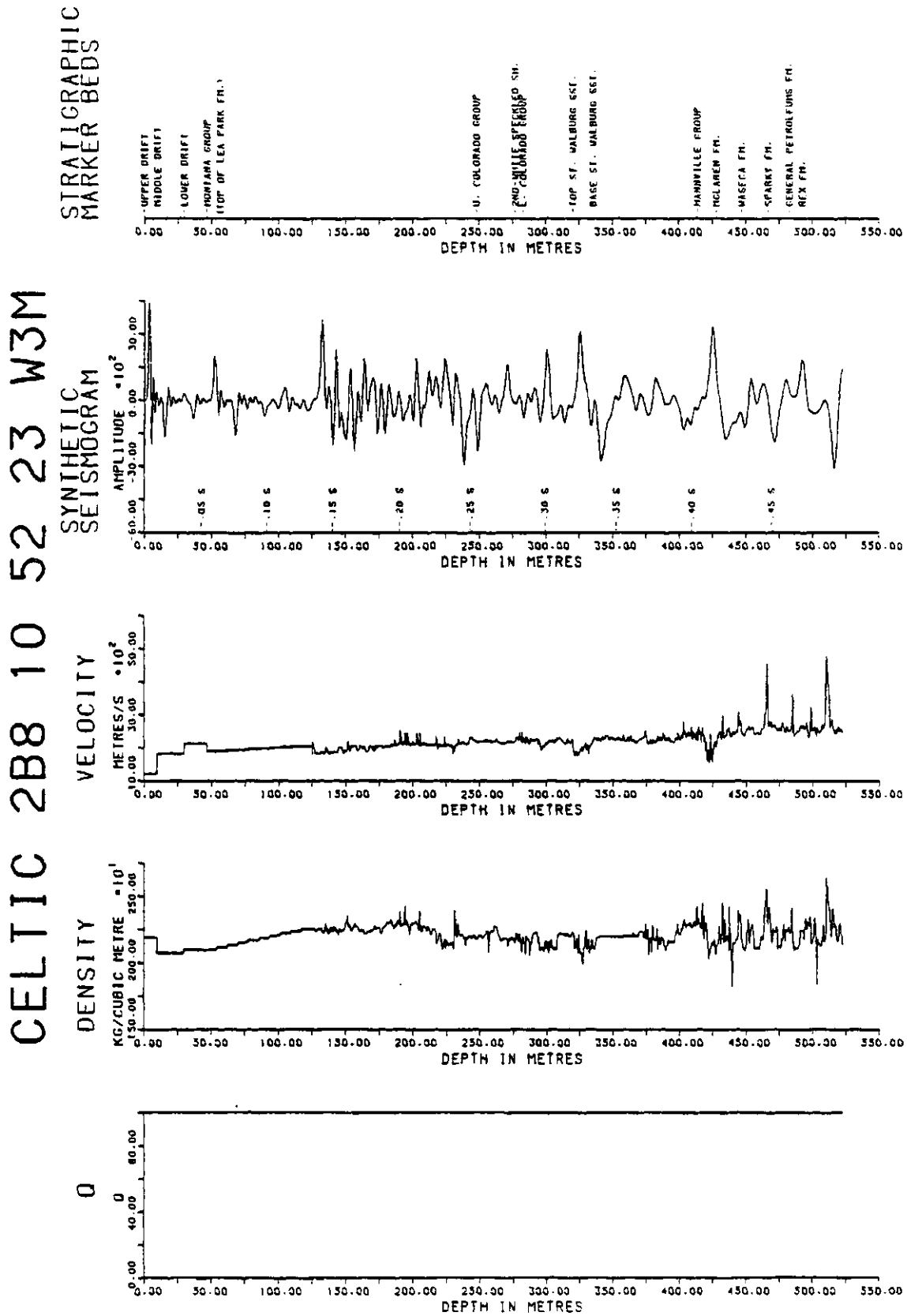


Figure 5.13 - Seismogram with constant Q-value of 100.

equal to 20, 50, and 100 are shown in Figures 5.11, 5.12, and 5.13. The corresponding amplitude-spectra are in Figures 5.14, 5.15, and 5.16. All of these tests were computed with an impulse source buried at 0.0 m; therefore, they must be compared with the seismogram in Figure 5.17, which was also constructed with an impulse source at 0.0 m but with the standard Q function. The amplitude spectrum corresponding to this seismogram is shown in Figure 5.18.

In comparing the seismograms of Figures 5.11 through 5.13, it is immediately noticeable that the frequency content of the Mannville sections is increased in the higher-Q seismograms. This observation is verified by the amplitude spectra in Figures 5.14 through 5.16. With a Q curve equal to 20, the general shape of the Mannville portion of the seismogram of Figure 5.11 is similar to that of Figure 5.17, but the high frequencies required for reflections from the McLaren coal-bed, and the W6 and W3 oil-saturated sands are not present. With a Q curve equal to 100, the general shape of the Mannville portion of the seismogram in Figure 5.13 is also similar to that of Figure 5.17, but the high-frequency content is now enhanced and the McLaren coal-bed, and the W6 and W3 oil zone reflections are distinct and of large amplitude. With a Q curve equal to 50, the Mannville portion of the seismogram in Figure 5.12 is almost identical to that of Figure 5.17. The corresponding amplitude spectra in Figures 5.15 and 5.18 are also similar. The approximate average of the standard Q function is 50. Therefore, the test with Q equal to 50 illustrates that, within reasonable limits, it is the average value of the Q curve, and not its shape, that is more important to the character of the Mannville portion of the resulting seismogram.

The effect of a change in Q is more apparent in true-amplitude

CELTIC 2B8 10 52 23 W3M

CONSTANT $Q=20$.
 SOURCE BURIED AT A DEPTH (M) = 0.0
 TYPE OF WAVELET : IMPULSE
 BUTTERWORTH ANTI-ALIAS FILTER INCLUDED IN SYNTHETIC TRACE
 TIME GATE (IN S) FOR AMPLITUDE SPECTRUM = .405 TO 0.493
 TIME GATE CORRESPONDS TO:
 TOP OF MANNVILLE GRP. (414.0 M) TO END OF INPUT LOGS (523.2 M)
 SAMPLE INTERVAL IN TIME DOMAIN (S) = .0010
 SAMPLE INTERVAL IN FREQUENCY DOMAIN (HZ) = 7.812
 NUMBER OF FREQUENCIES ANALYSED = 65.
 HANNING SMOOTHING APPLIED TO SPECTRUM
 PERCENT OF TRACE ELEMENTS TAPERED AT EACH END = 10.

AMPLITUDE SPECTRUM OF SYNTHETIC SEISMOGRAM

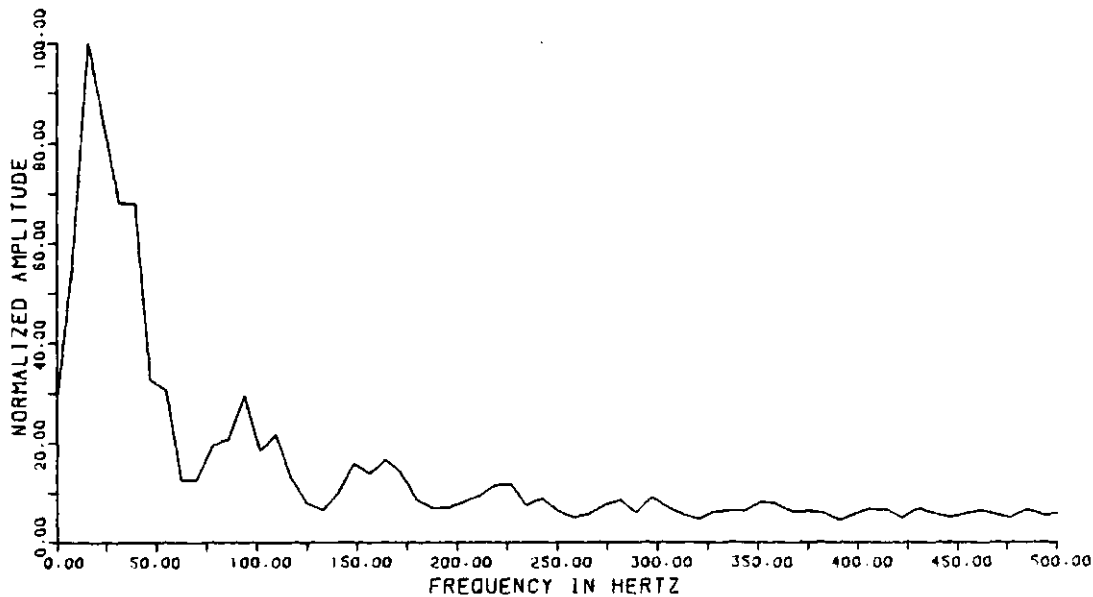


Figure 5.14 - Amplitude spectrum from seismogram constructed with constant Q equal to 20.

CELTIC 2B8 10 52 23 W3M

CONSTANT Q=50.
 SOURCE BURIED AT A DEPTH (M) = 0.0
 TYPE OF WAVELET : IMPULSE
 BUTTERWORTH ANTI-ALIAS FILTER INCLUDED IN SYNTHETIC TRACE
 TIME GATE (IN S) FOR AMPLITUDE SPECTRUM = .405 TO 0.493
 TIME GATE CORRESPONDS TO:
 TOP OF MANNVILLE GRP. (414.0 M) TO END OF INPUT LOGS (523.2 M)
 SAMPLE INTERVAL IN TIME DOMAIN (S) = .0010
 SAMPLE INTERVAL IN FREQUENCY DOMAIN (HZ) = 7.812
 NUMBER OF FREQUENCIES ANALYSED = 65.
 HANNING SMOOTHING APPLIED TO SPECTRUM
 PERCENT OF TRACE ELEMENTS TAPERED AT EACH END = 10.

AMPLITUDE SPECTRUM OF SYNTHETIC SEISMOGRAM

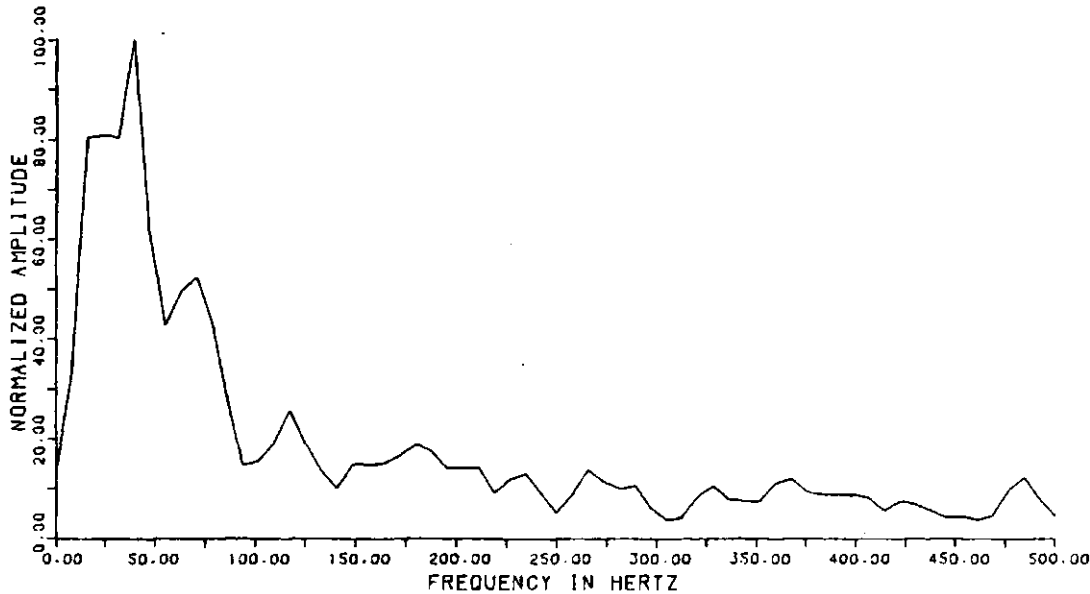


Figure 5.15 - Amplitude spectrum from seismogram constructed with constant Q equal to 50.

CELTIC 2B8 10 52 23 W3M

CONSTANT Q=100.
 SOURCE BURIED AT A DEPTH (M) = 0.0
 TYPE OF WAVELET : IMPULSE
 BUTTERWORTH ANTI-ALIAS FILTER INCLUDED IN SYNTHETIC TRACE
 TIME GATE (IN S) FOR AMPLITUDE SPECTRUM = .405 TO 0.493
 TIME GATE CORRESPONDS TO:
 TOP OF MANNVILLE GRP. (414.0 M) TO END OF INPUT LOGS (523.2 M)
 SAMPLE INTERVAL IN TIME DOMAIN (S) = .0010
 SAMPLE INTERVAL IN FREQUENCY DOMAIN (HZ) = 7.812
 NUMBER OF FREQUENCIES ANALYSED = 65.
 HANNING SMOOTHING APPLIED TO SPECTRUM
 PERCENT OF TRACE ELEMENTS TAPERED AT EACH END = 10.

AMPLITUDE SPECTRUM OF SYNTHETIC SEISMOGRAM

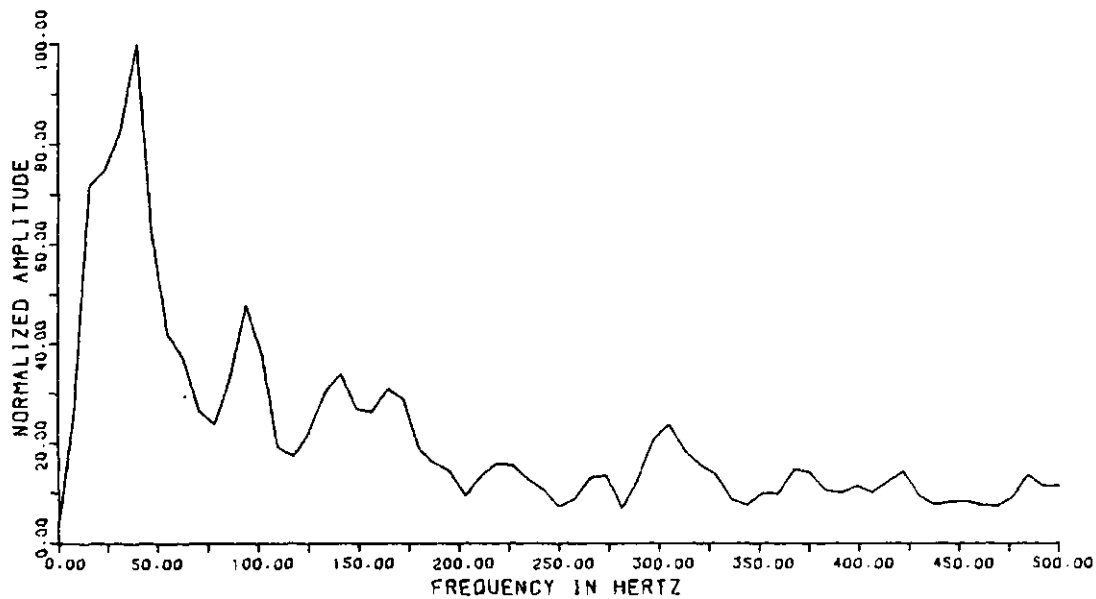


Figure 5.16 - Amplitude spectrum from seismogram constructed with constant Q equal to 100.

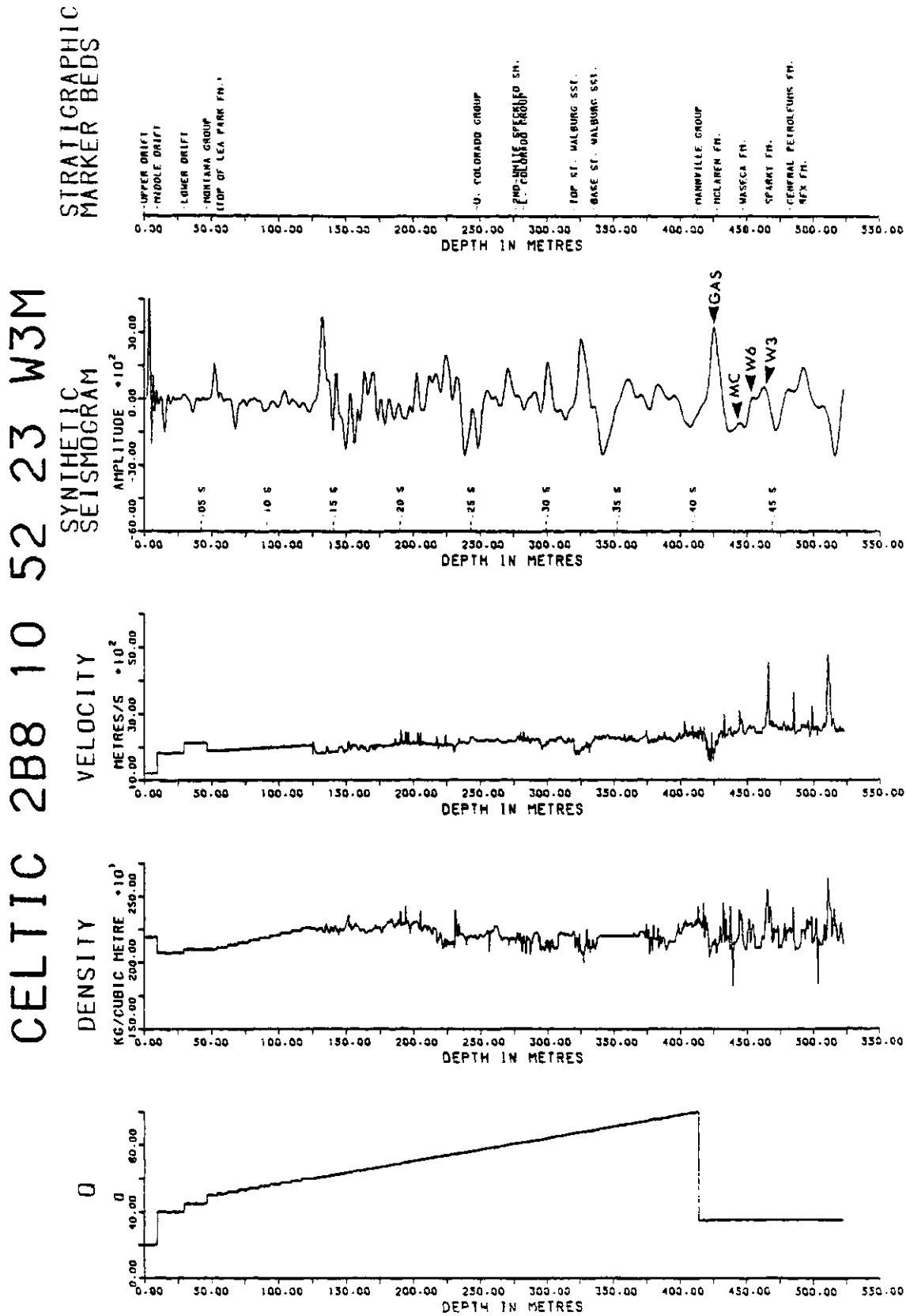


Figure 5.17 - Seismogram with standard Q-function.

CELTIC 2B8 10 52 23 W3M

MINIMUM Q=20 AND MAXIMUM Q=100
 SOURCE BURIED AT A DEPTH (M) = 0.0
 TYPE OF WAVELET : IMPULSE
 BUTTERWORTH ANTI-ALIAS FILTER INCLUDED IN SYNTHETIC TRACE
 TIME GATE (IN S) FOR AMPLITUDE SPECTRUM = .405 TO 0.493
 TIME GATE CORRESPONDS TO:
 TOP OF MANNVILLE GRP. (414.0 M) TO END OF INPUT LOGS (523.2 M)
 SAMPLE INTERVAL IN TIME DOMAIN (S) = .0010
 SAMPLE INTERVAL IN FREQUENCY DOMAIN (HZ) = 7.812
 NUMBER OF FREQUENCIES ANALYSED = 65.
 HANNING SMOOTHING APPLIED TO SPECTRUM
 PERCENT OF TRACE ELEMENTS TAPERED AT EACH END = 10.

AMPLITUDE SPECTRUM OF SYNTHETIC SEISMOGRAM

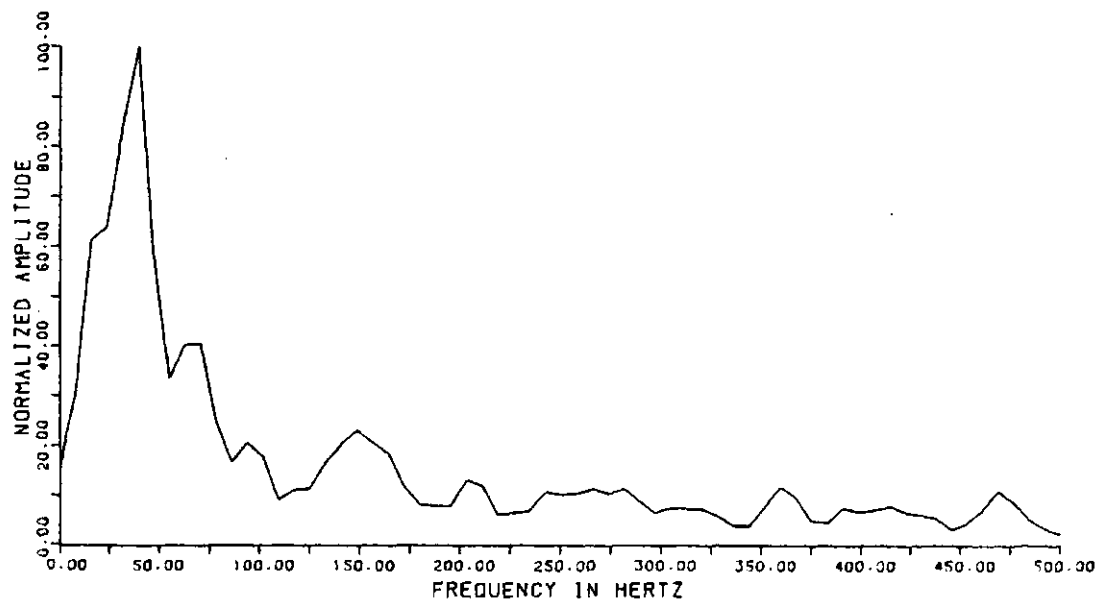


Figure 5.18 - Amplitude spectrum from seismogram constructed with the standard Q-function.

plots. The same synthetic seismograms that were plotted with gain control in Figures 5.11 through 5.13 are shown plotted without gain control in Figures 5.19 through 5.21. In all three true-amplitude plots the high-amplitude, direct-wave has been muted to increase the scaled amplitude of the deeper reflections. Nevertheless, the amplitudes of the reflections are quickly reduced, especially when a low Q value is input. In Figure 5.19 (Q equal to 20), Mannville reflections are barely visible. In Figure 5.20 (Q equal to 50), very low-amplitude McLaren-coal and W6 and W3 oil-zone reflections are visible. In Figure 5.21 (Q equal to 100), the coal and oil-zone reflections are readily visible. Therefore, if the Q function of the earth is similar to, or less than, the standard Q -function chosen in section 4.5 (that is, with an average value equal to or less than 50), then the oil-zone reflections will be very difficult to identify on a true-amplitude plot of real seismic-data. However, if the actual Q -function in the subsurface has an average value that is higher than the standard Q -function chosen for the present study, then the reflections of economic importance should be visible on a true-amplitude seismic-section.

The value of Q is critical in determining the frequency content of the synthetic seismogram; if higher values of Q had been chosen for the standard Q -function (section 4.5), the resulting synthetic seismograms would have contained higher frequencies. A case could be made for using higher Q values than those that were chosen, but these values were considered to be realistic based on the available literature (see Table 4.5). Until in-situ attenuation studies are undertaken in the study area, the Q values can only be estimated.

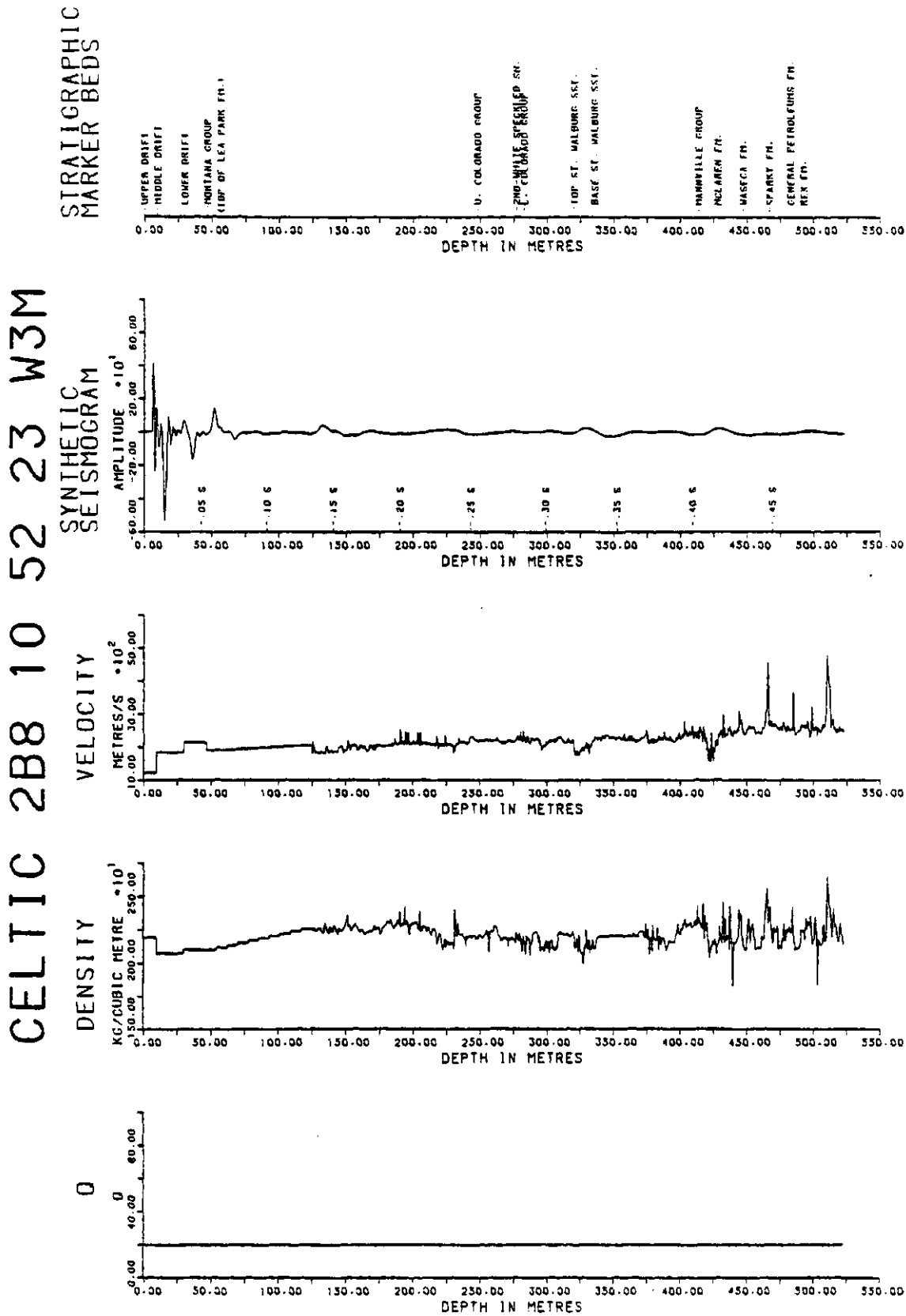


Figure 5.19 - Seismogram with constant Q value of 20; plotted with gain control.

CELTIC 2B8 10 52 23 W3M

STRATIGRAPHIC
MARKER BEDS

SYNTHETIC
SEISMOGRAM

VELOCITY

DENSITY

Q

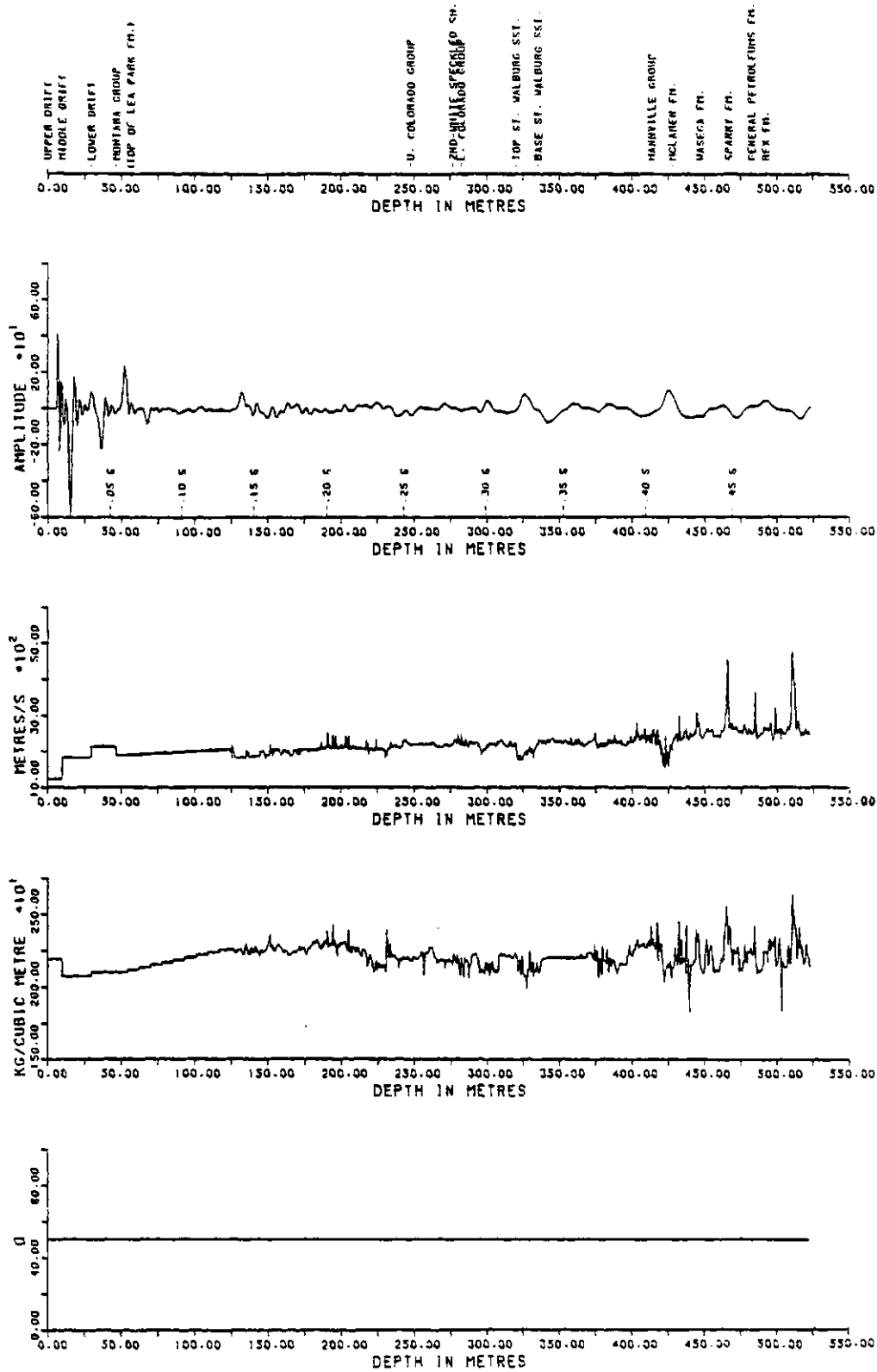


Figure 5.20 - Seismogram with constant Q value of 50; plotted with gain control.

CELTIC 2B8 10 52 23 W3M

STRATIGRAPHIC
MARKER BEDS

SYNTHETIC
SEISMOGRAM

VELOCITY

DENSITY

Q

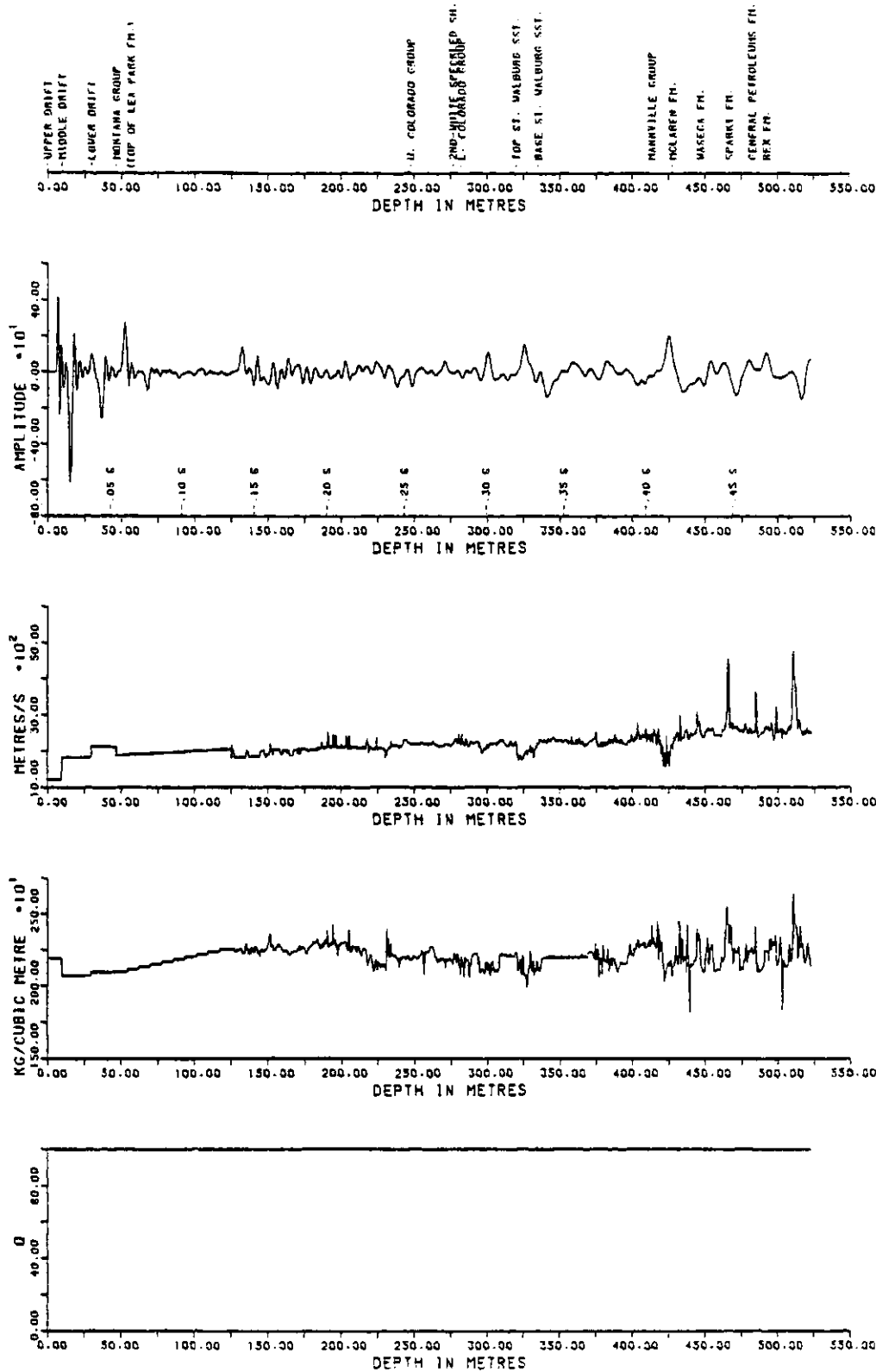


Figure 5.21 - Seismogram with constant Q value of 100; plotted with gain control.

5.3.4 Depth of Source Burial

Tests were made with synthetic seismograms that were constructed as if the source were buried at depths of 0.0 m, 9.8 m, 29.9 m, and 46.7 m. These depths correspond to the tops of the surficial layers, which are in the cased portion of the wells; the time to depth conversion in CELGRF was set up to handle only these depths. Using input parameters of an impulse source and the standard Q-function, the four source-burial cases are shown in Figures 5.22 through 5.25. In each of these plots the direct wave has been muted if the source is located below the surface. The corresponding amplitude spectra are presented in Figures 5.26 through 5.29

As one would expect, when the source is buried more deeply, there is less influence from the highly absorptive surface-layers, and the frequency content of the Mannville section of the seismogram is increased. The amplitude spectra of Figures 5.26 through 5.29 illustrate this tendency.

The overall shape of the lower part of the seismogram varies in Figures 5.22 through 5.25. This is in part due to the change in frequency content that was discussed above, but is mainly the result of interference from a type of multiple reflection called a ghost. Ghost energy travels upward from the shot and is then reflected downward, joining the downward-travelling wave-train and changing its shape (Sheriff, 1973). Since the synthetic seismograms were constructed using a reflection coefficient of the surface (from below) equal to 1.0, the ghost reflections will be of high amplitude.

The response of the geologic zones studied in section 5.3.2 varies among the four source-burial cases. The character of some reflections is significantly altered by different depths of source burial. For

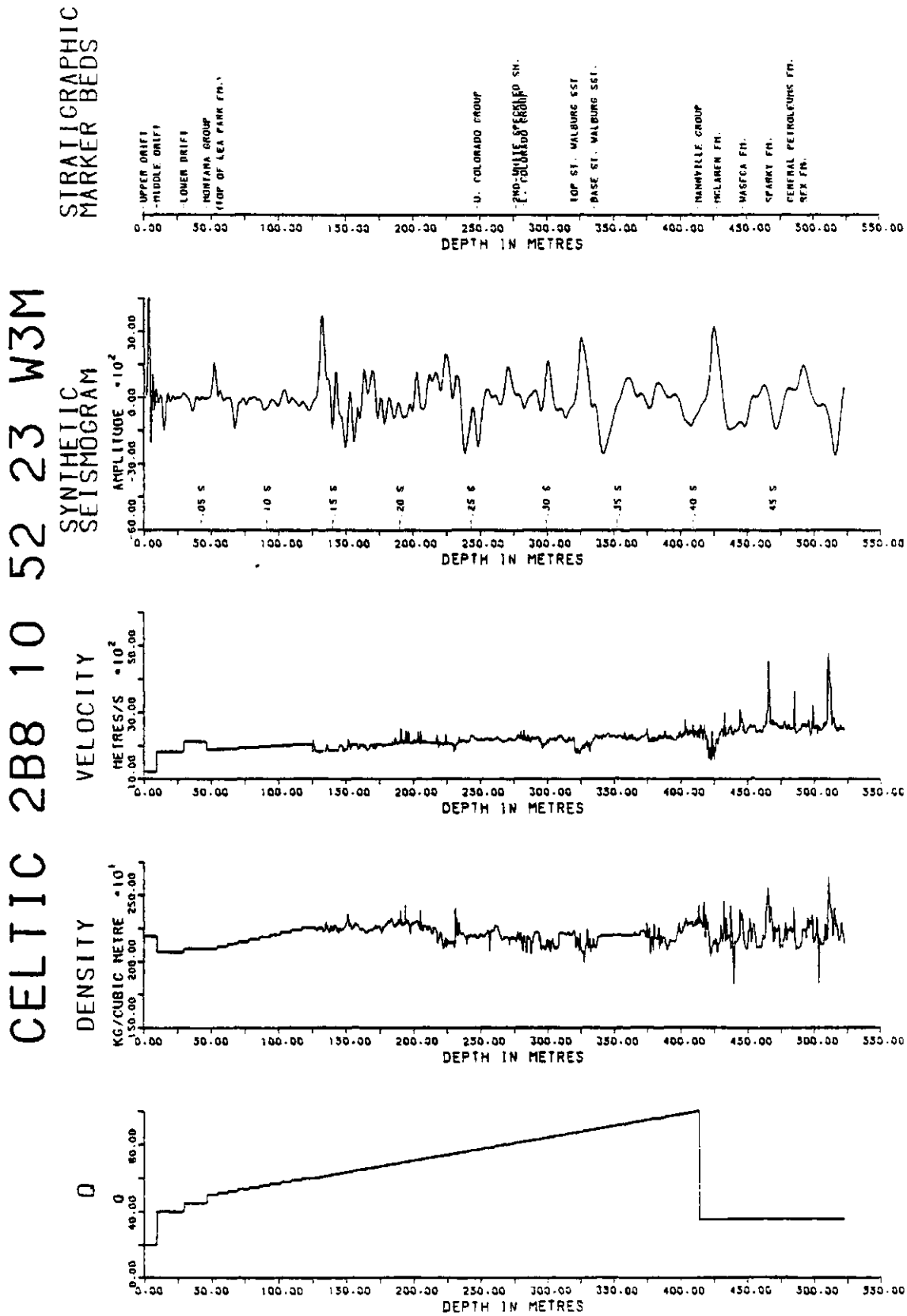
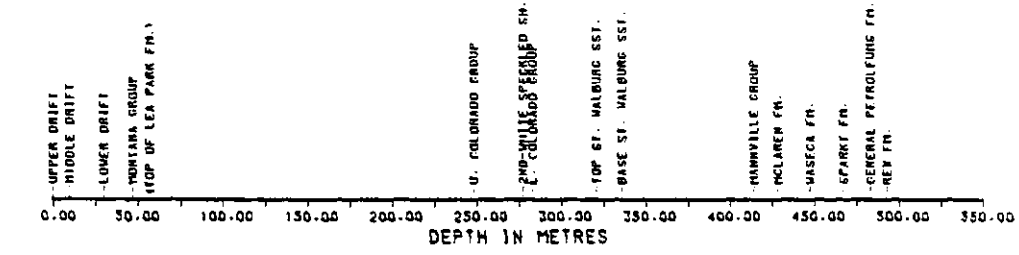


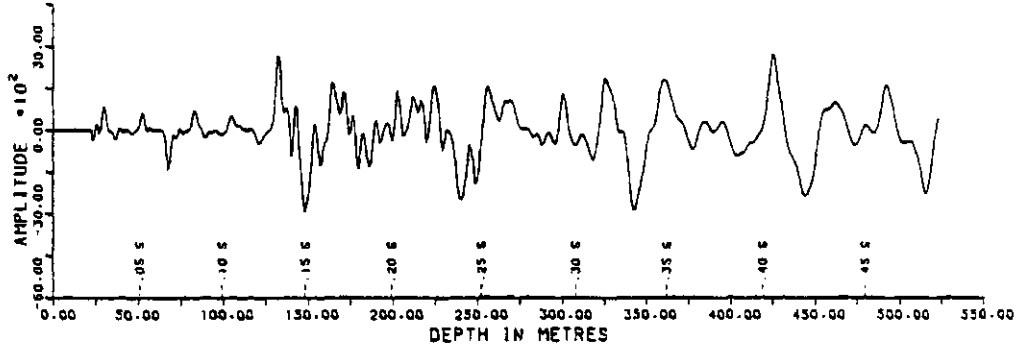
Figure 5.22 - Seismogram with impulse source buried at 0.0 m.

CELTIC 2B8 10 52 23 W3M

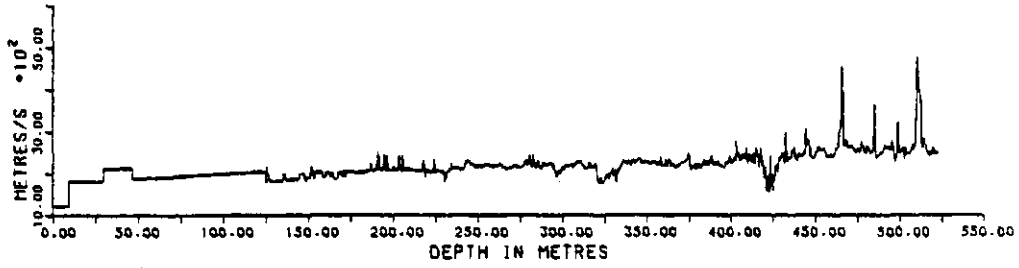
STRATIGRAPHIC
MARKER BEDS



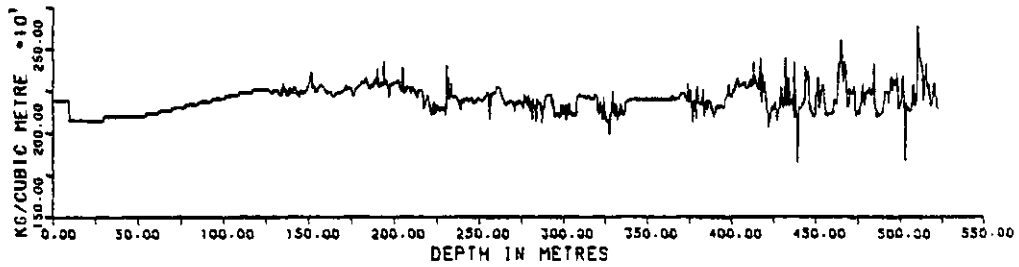
SYNTHETIC
SEISMOGRAM



VELOCITY



DENSITY



Q

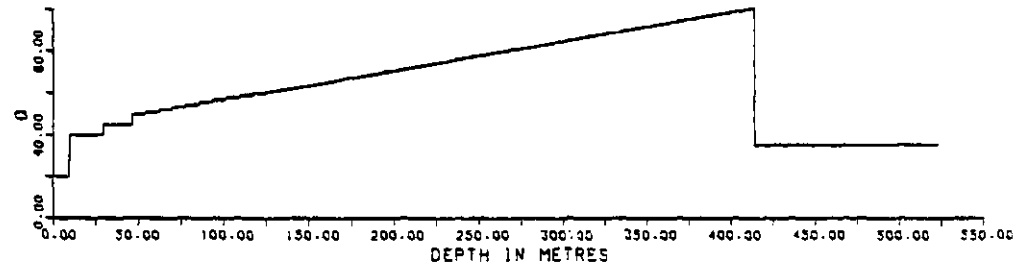


Figure 5.23 - Seismogram with impulse source buried at 9.8 m.

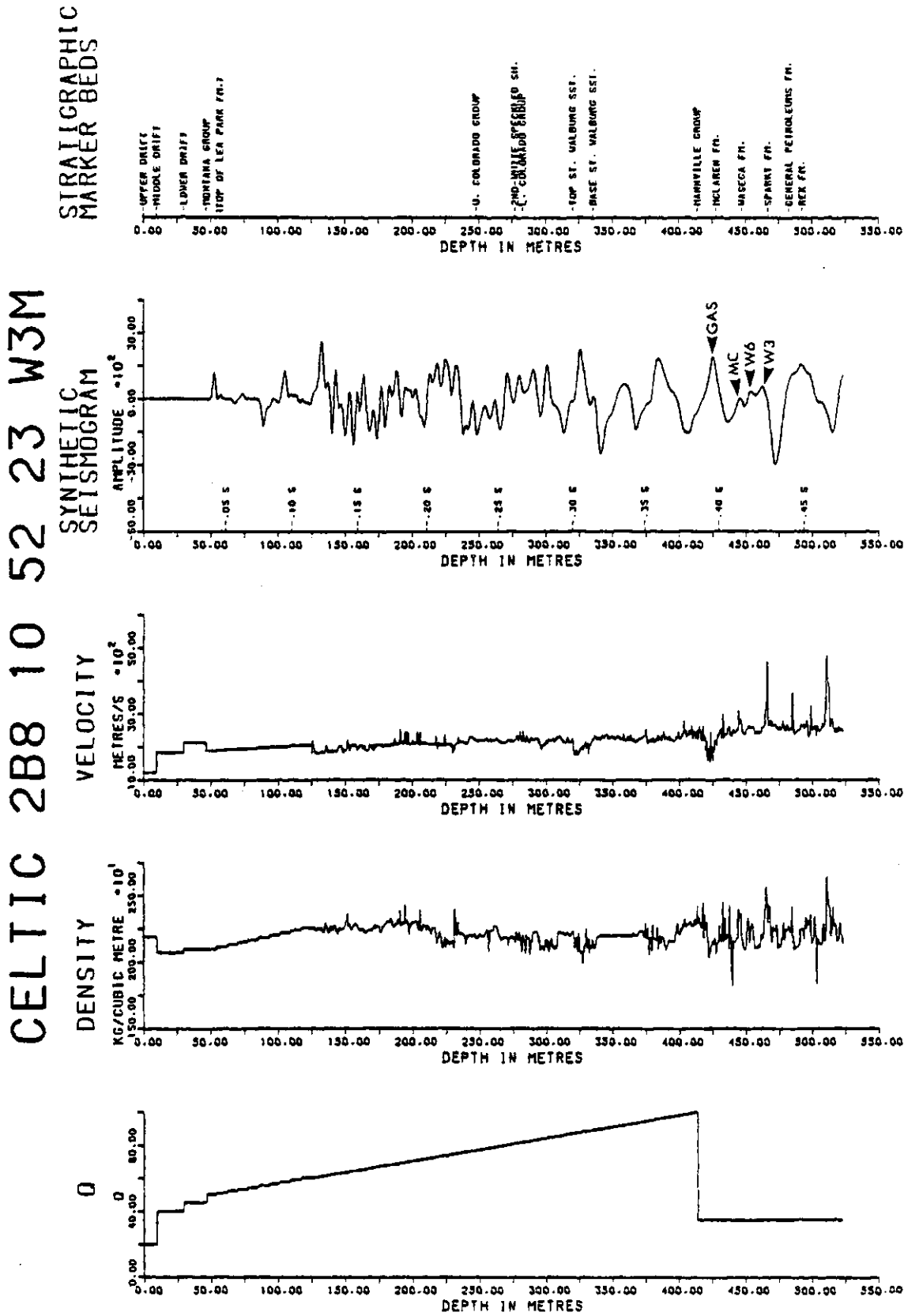


Figure 5.24 - Seismogram with impulse source buried at 29.9 m.

CELTIC 2B8 10 52 23 W3M

MINIMUM Q=20 AND MAXIMUM Q=100
 SOURCE BURIED AT A DEPTH (M) = 0.0
 TYPE OF WAVELET : IMPULSE
 BUTTERWORTH ANTI-ALIAS FILTER INCLUDED IN SYNTHETIC TRACE
 TIME GATE (IN S) FOR AMPLITUDE SPECTRUM = .405 TO 0.493
 TIME GATE CORRESPONDS TO:
 TOP OF MANNVILLE GRP. (414.0 M) TO END OF INPUT LOGS (523.2 M)
 SAMPLE INTERVAL IN TIME DOMAIN (S) = .0010
 SAMPLE INTERVAL IN FREQUENCY DOMAIN (HZ) = 7.812
 NUMBER OF FREQUENCIES ANALYSED = 65.
 HANNING SMOOTHING APPLIED TO SPECTRUM
 PERCENT OF TRACE ELEMENTS TAPERED AT EACH END = 10.

AMPLITUDE SPECTRUM OF SYNTHETIC SEISMOGRAM

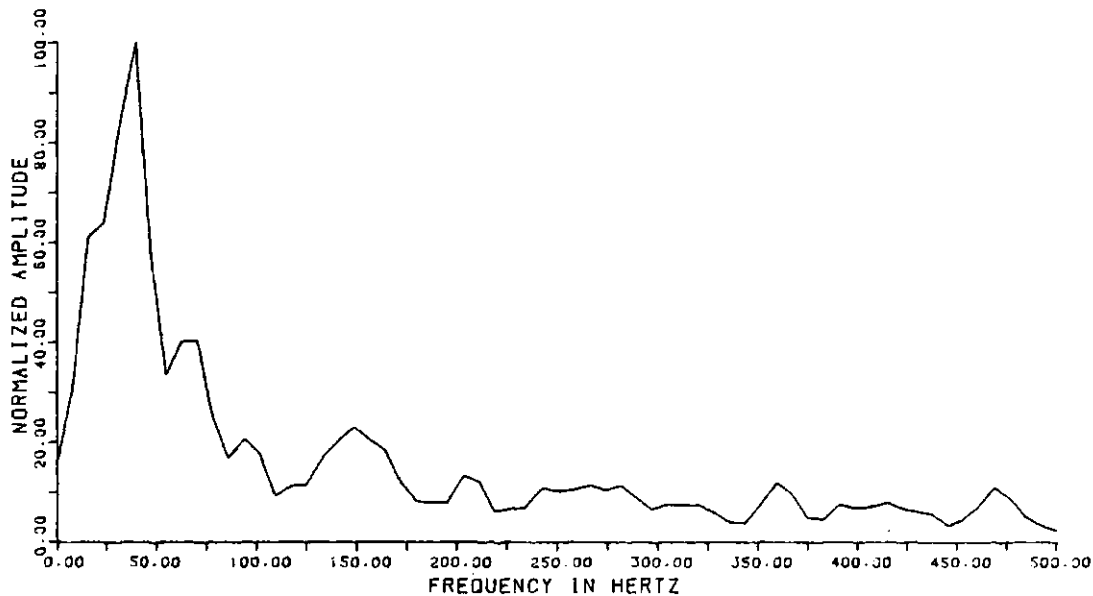


Figure 5.26 - Amplitude spectrum from seismogram constructed with impulse source buried at 0.0 m.

CELTIC 2B8 10 52 23 W3M

MINIMUM Q=20 AND MAXIMUM Q=100.
 SOURCE BURIED AT A DEPTH (M) = 9.8
 TYPE OF WAVELET : IMPULSE
 BUTTERWORTH ANTI-ALIAS FILTER INCLUDED IN SYNTHETIC TRACE
 TIME GATE (IN S) FOR AMPLITUDE SPECTRUM = .405 TO 0.493
 TIME GATE CORRESPONDS TO:
 TOP OF MANNVILLE GRP. (414.0 M) TO END OF INPUT LOGS (523.2 M)
 SAMPLE INTERVAL IN TIME DOMAIN (S) = .0010
 SAMPLE INTERVAL IN FREQUENCY DOMAIN (HZ) = 7.812
 NUMBER OF FREQUENCIES ANALYSED = 65.
 HANNING SMOOTHING APPLIED TO SPECTRUM
 PERCENT OF TRACE ELEMENTS TAPERED AT EACH END = 10.

AMPLITUDE SPECTRUM OF SYNTHETIC SEISMOGRAM

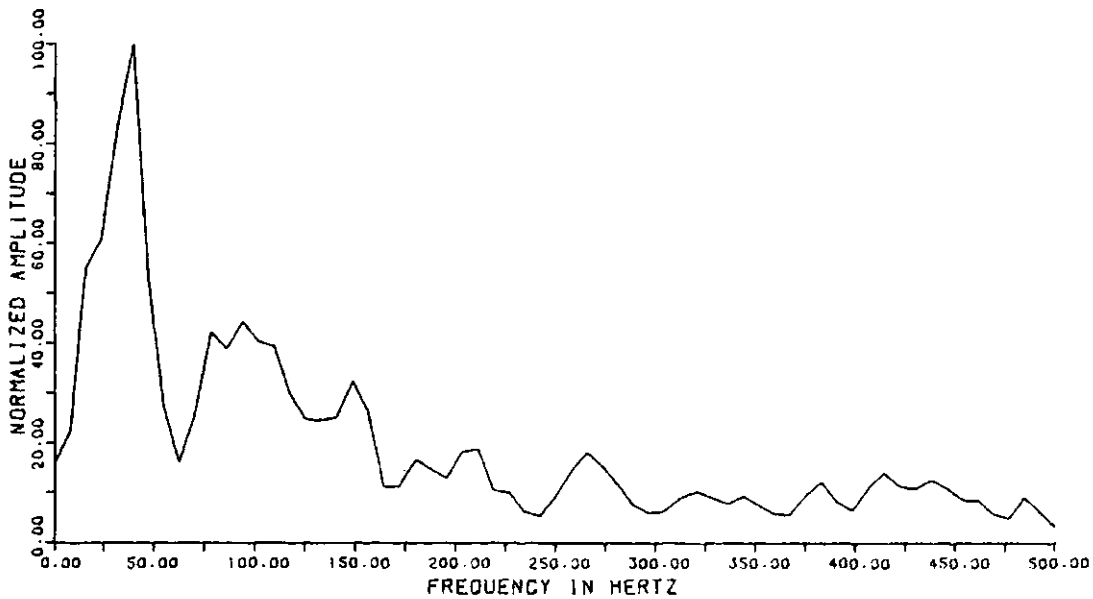


Figure 5.27 - Amplitude spectrum from seismogram constructed with impulse source buried at 9.8 m.

CELTIC 2B8 10 52 23 W3M

MINIMUM Q=20 AND MAXIMUM Q=100
 SOURCE BURIED AT A DEPTH (M) = 29.9
 TYPE OF WAVELET : IMPULSE
 BUTTERWORTH ANTI-ALIAS FILTER INCLUDED IN SYNTHETIC TRACE
 TIME GATE (IN S) FOR AMPLITUDE SPECTRUM = .405 TO 0.493
 TIME GATE CORRESPONDS TO:
 TOP OF MANNVILLE GRP. (414.0 M) TO END OF INPUT LOGS (523.2 M)
 SAMPLE INTERVAL IN TIME DOMAIN (S) = .0010
 SAMPLE INTERVAL IN FREQUENCY DOMAIN (HZ) = 7.812
 NUMBER OF FREQUENCIES ANALYSED = 65.
 HANNING SMOOTHING APPLIED TO SPECTRUM
 PERCENT OF TRACE ELEMENTS TAPERED AT EACH END = 10.

AMPLITUDE SPECTRUM OF SYNTHETIC SEISMOGRAM

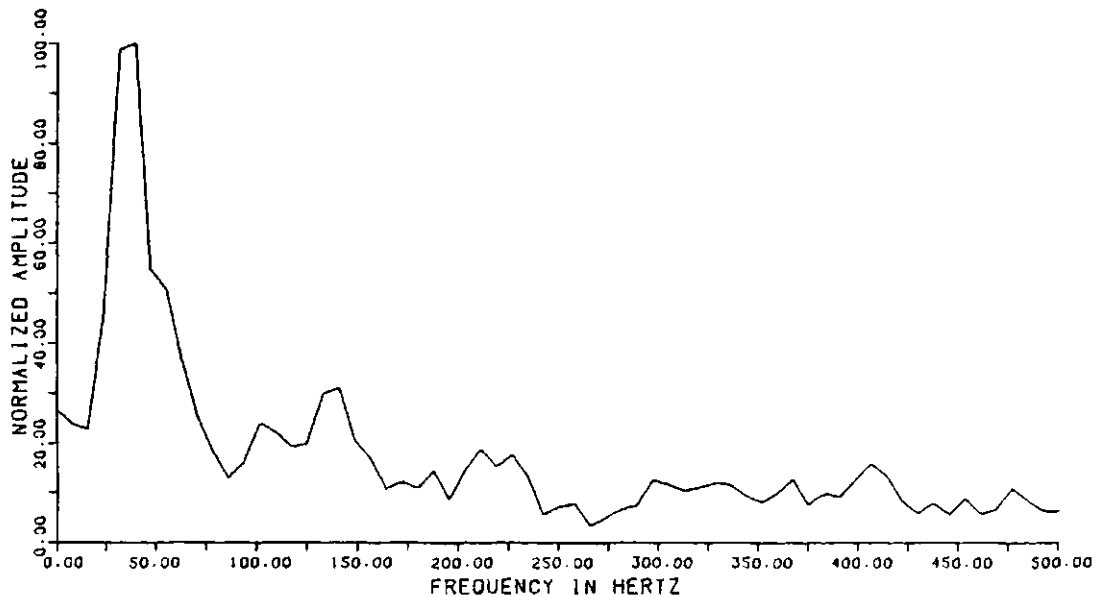


Figure 5.28 - Amplitude spectrum from seismogram constructed with source buried at 29.9 m.

CELTIC 2B8 10 52 23 W3M

MINIMUM Q=20 AND MAXIMUM Q=100.
 SOURCE BURIED AT A DEPTH (M) = 46.7
 TYPE OF WAVELET : IMPULSE
 BUTTERWORTH ANTI-ALIAS FILTER INCLUDED IN SYNTHETIC TRACE
 TIME GATE (IN S) FOR AMPLITUDE SPECTRUM = .405 TO 0.493
 TIME GATE CORRESPONDS TO:
 TOP OF MANNVILLE GRP. (414.0 M) TO END OF INPUT LOGS (523.2 M)
 SAMPLE INTERVAL IN TIME DOMAIN (S) = .0010
 SAMPLE INTERVAL IN FREQUENCY DOMAIN (HZ) = 7.812
 NUMBER OF FREQUENCIES ANALYSED = 65.
 HANNING SMOOTHING APPLIED TO SPECTRUM
 PERCENT OF TRACE ELEMENTS TAPERED AT EACH END = 10.

AMPLITUDE SPECTRUM OF SYNTHETIC SEISMOGRAM

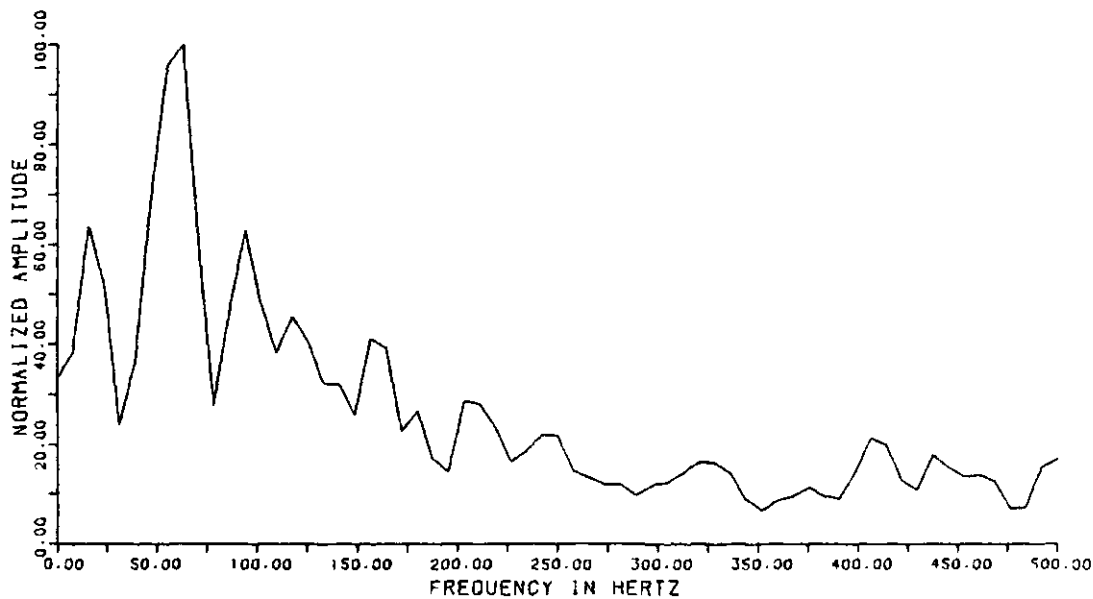


Figure 5.29 - Amplitude spectrum from seismogram constructed with impulse source buried at 46.7 m.

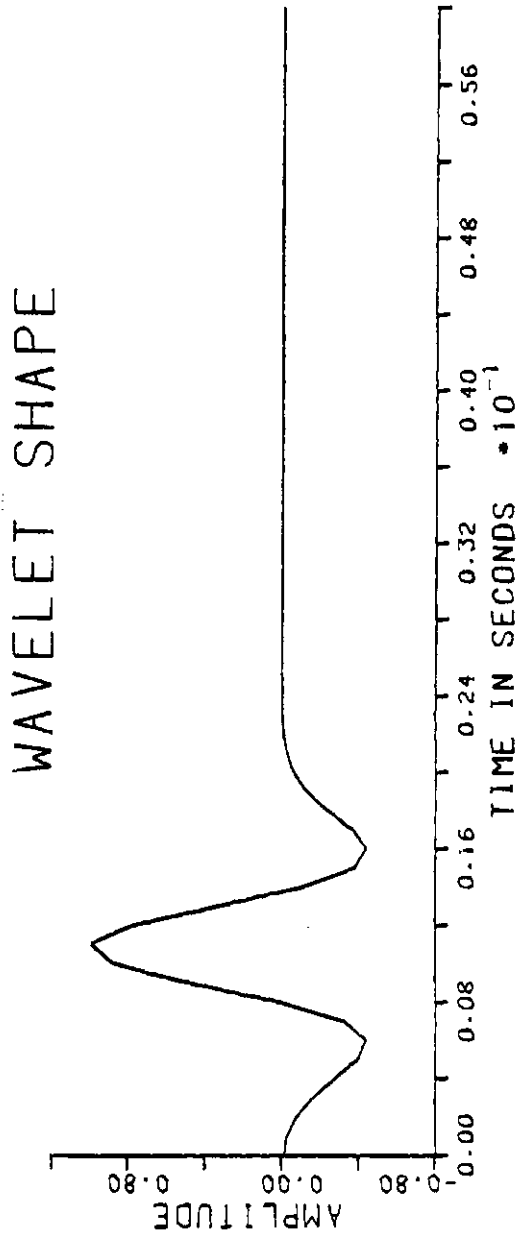


Figure 5.30 - Velocity-type Ricker-wavelet with a peak frequency of 80 hz.

example, the reflection from the McLaren formation coal-bed in Figure 5.22 (0.0 m burial) is similar to that of Figure 5.24 (29.9 m burial), but in Figure 5.23 (9.8 m burial) this reflection is not visible, and in Figure 5.25 (46.7 m burial) the single peak has split into a doublet. The W6 and W3 oil-zone peaks are distinct in all four seismograms, but they are of highest amplitude in Figure 5.25 (46.7 m burial). As was discussed in section 5.3.2, the small trough that was expected in response to the W1 cemented zone did not appear when this zone was modelled. This non-appearance was attributed to interference effects. The large trough that occurs in Figure 5.24, at the time that the small W1 trough was expected, changes in character among the four source burial cases. In fact, if the modelling of the W1 cemented zone were repeated at a source burial different from 29.9 m, the expected W1 response may be visible.

A source burial of 29.9 m was chosen to be the "best" for the present study. Although the burial at 46.7 m returned the highest-frequency reflections from the Mannville beds and the specific reflections of economic interest were the most distinct at this depth, a source burial of 46.7 is too expensive for routine seismic-surveys. It is important to note that, even if a surface source had been used, Figure 5.22 indicates that it is theoretically possible to record the oil-zone reflections. For very detailed work, however, it may be necessary to use a source burial deeper than 29.9 m.

5.3.5 Input Source

Test synthetic-seismograms were constructed using velocity-type Ricker-wavelet sources of peak frequencies from 20 to 220 hz. A Ricker wavelet of this type is shown in Figure 5.30. In Figure 5.31, the

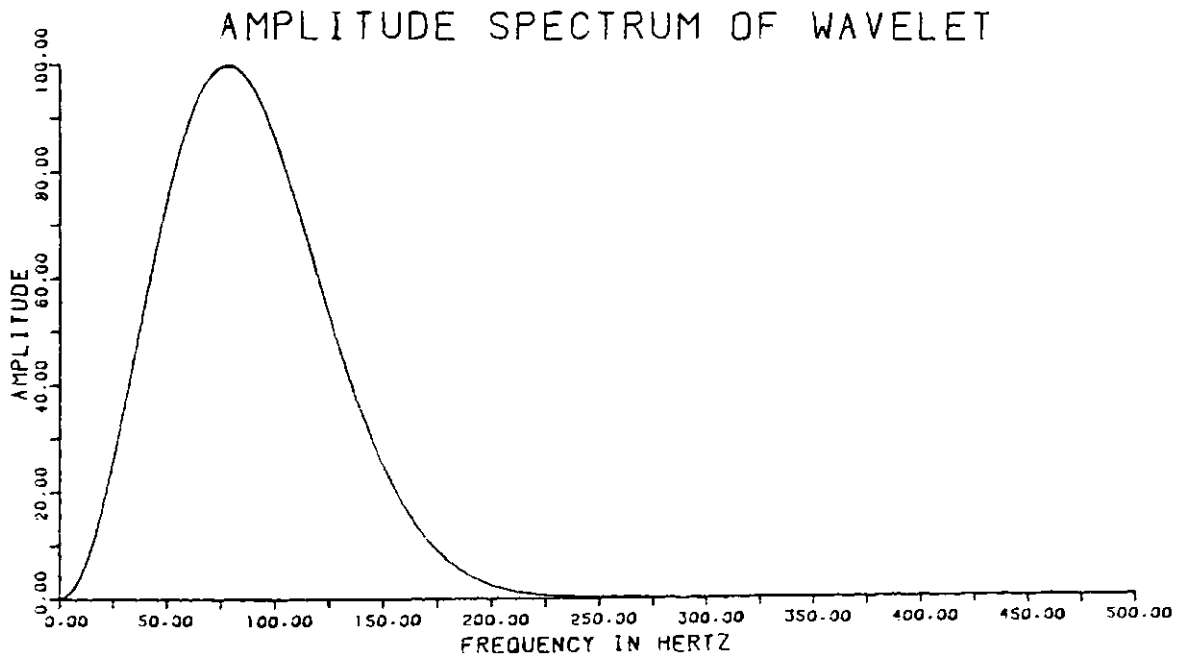
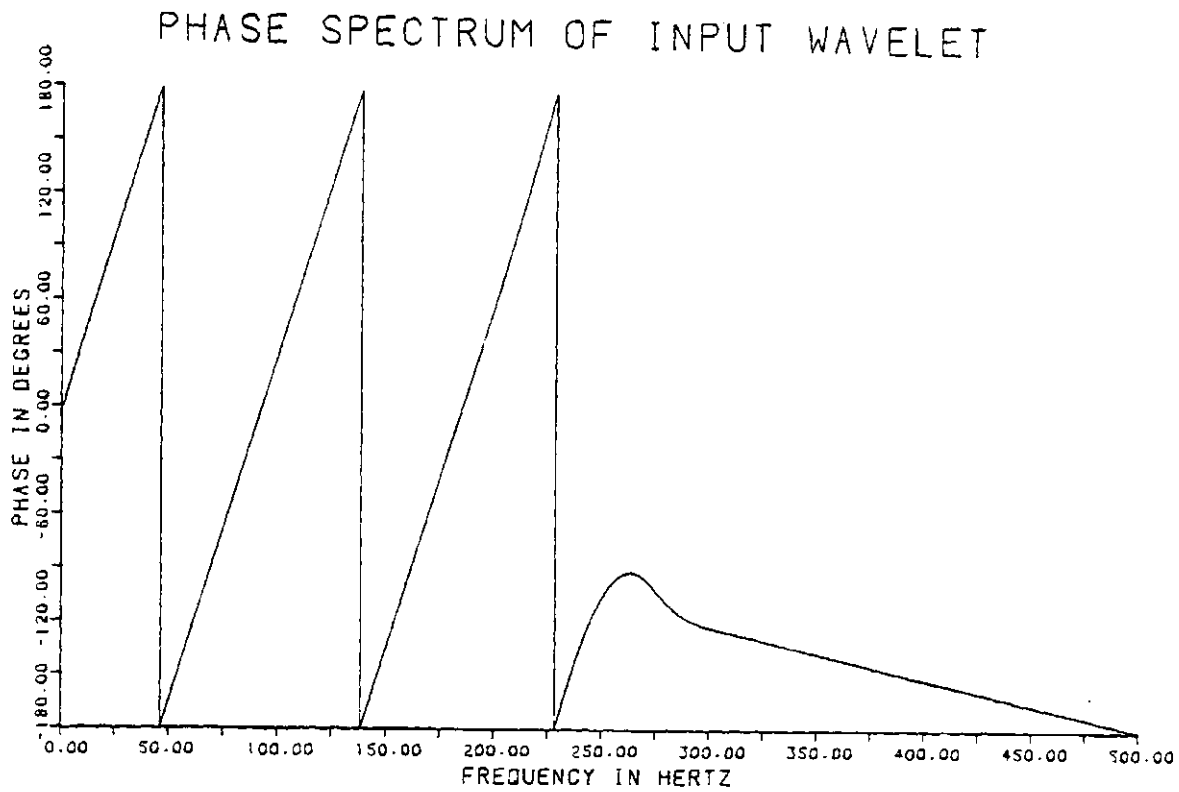


Figure 5.31 - Phase and amplitude spectra of the Ricker wavelet in Figure 5.30.

amplitude and phase spectra of this wavelet are shown. This particular wavelet has a peak frequency of 80 hz and a linear phase-response over the band-pass. A linear-phase filter shifts phase proportional to frequency, thus introducing a constant delay without change of waveshape; the phase spectrum is linear over the band-pass and the intercept must be a multiple of 2π (Sheriff, 1973). These characteristics are seen in the phase spectrum of Figure 5.31. The constant delay introduced by using the linear-phase wavelet may be calculated from the slope of the phase spectrum (Titchkosky, 1968, p. 28-34, p. 37). With the 80 hz wavelet of Figures 5.30 and 5.31, the delay was calculated to be 10.8 ms. At lower peak-frequencies, the slope of the phase spectrum becomes steeper and the calculated delay will be larger.

When the peak frequency of the Ricker-wavelet source is increased, the high-frequency content of the resulting synthetic-seismogram increases and the delay decreases. Seismograms that were constructed using the standard Q-function and a Ricker-wavelet source buried at 29.9 m and of peak frequencies of 60, 80, 100, 140, 180, and 220 hz are shown in Figures 5.32 through 5.37. The corresponding amplitude spectra are in Figures 5.38 through 5.43. The trend of increased high-frequency content with a higher-frequency source can be noted in the seismograms and the amplitude spectra.

The anti-alias filtered, impulse-response seismogram (Figure 5.7) is very similar, in the Mannville section, to the seismogram that was constructed with the 80 hz Ricker-wavelet source (Figure 5.33). Using an 80 hz Ricker-wavelet source corresponds to filtering the impulse response seismogram with a band-limited, 80 hz peak-frequency filter of linear phase. Slight differences in the general shape of the Mannville

CELTIC 2B8 10 52 23 W3M

STRATIGRAPHIC
MARKER BEDS

SYNTHETIC
SEISMOGRAM

VELOCITY

DENSITY

Q

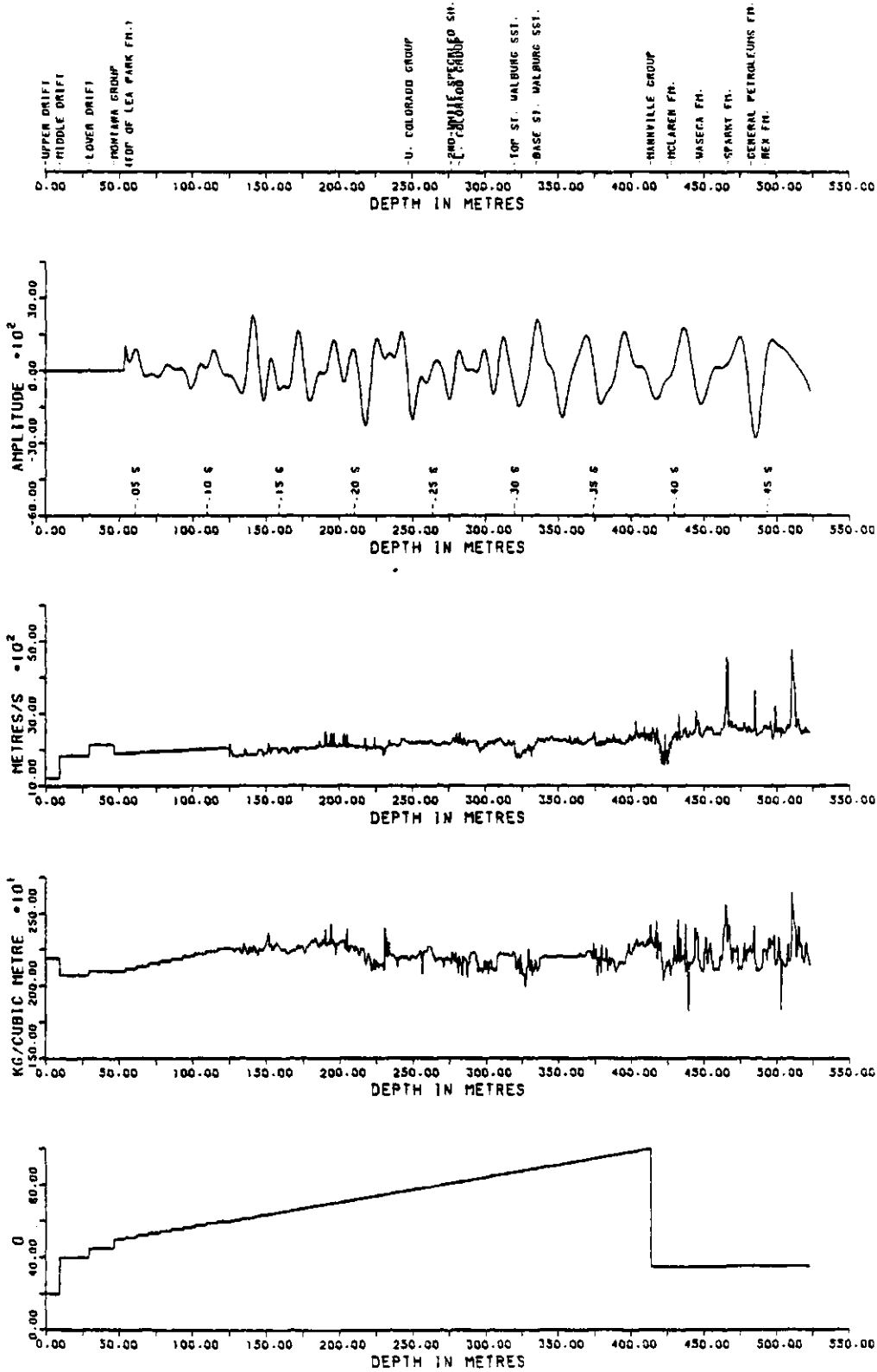


Figure 5.32 - Seismogram constructed using a Ricker-wavelet source with peak frequency of 60 Hz.

CELTIC 2B8 10 52 23 W3M

STRATIGRAPHIC
MARKER BEDS

SYNTHETIC
SEISMOGRAM

VELOCITY

DENSITY

Q

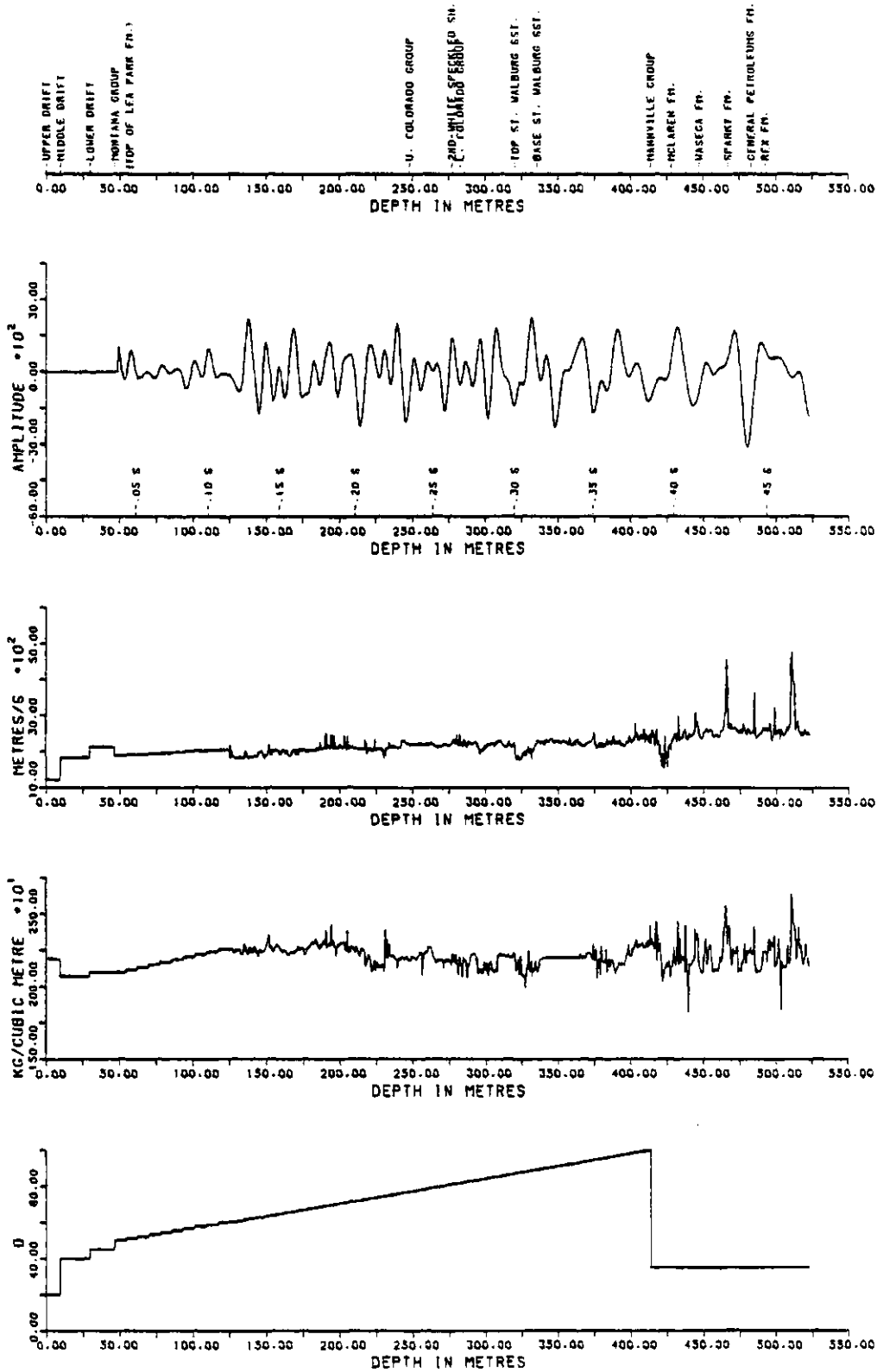


Figure 5.33 - Seismogram constructed using a Ricker-wavelet source with peak frequency of 80 hz.

CELTIC 2B8 10 52 23 W3M

STRATIGRAPHIC
MARKER BEDS

SYNTHETIC
SEISMOGRAM

VELOCITY

DENSITY

0

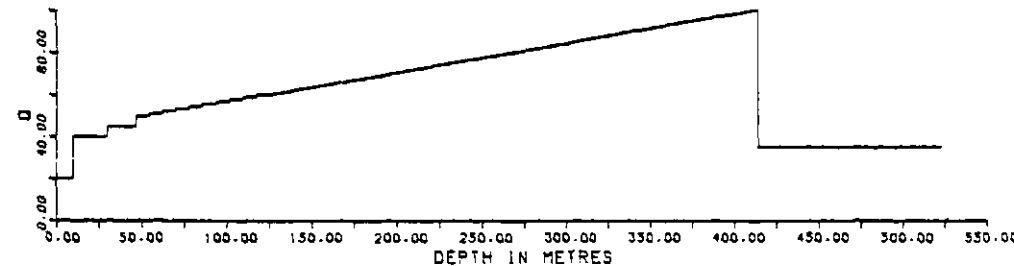
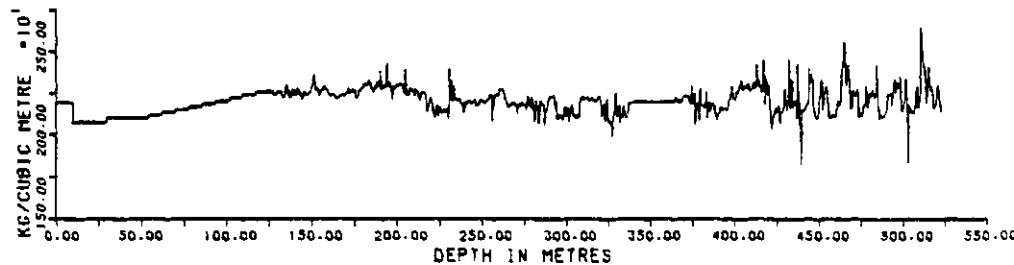
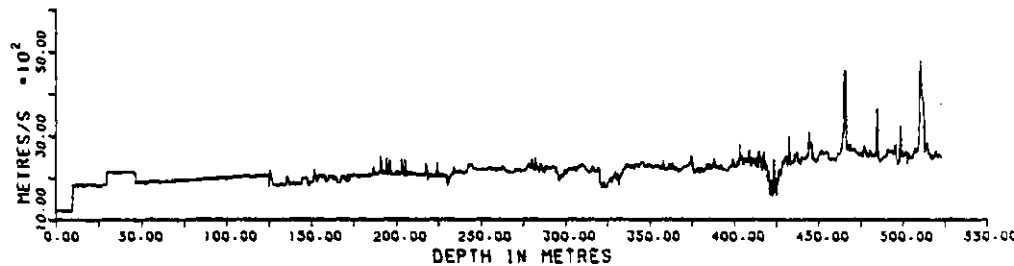
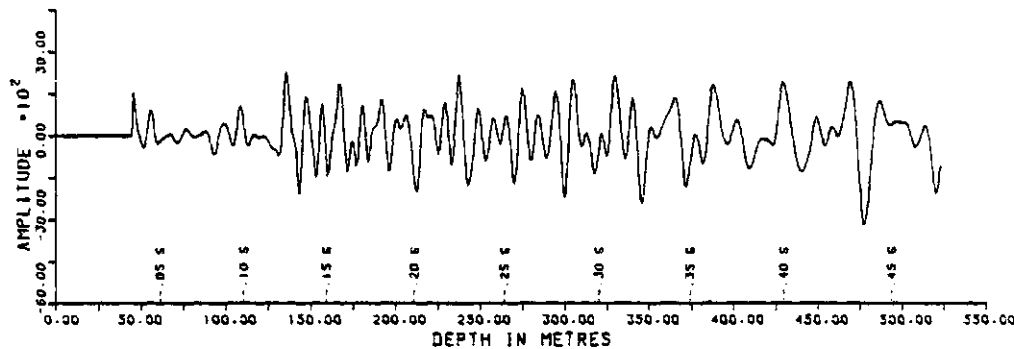
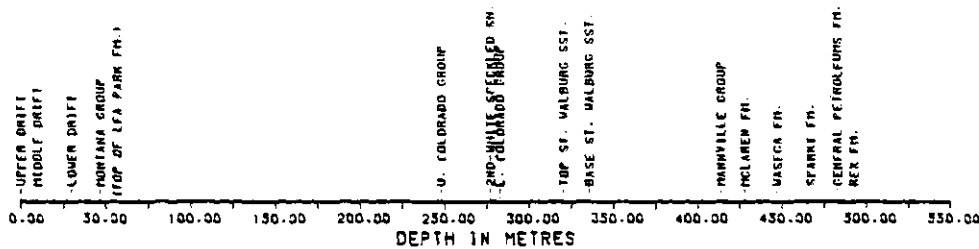


Figure 5.34 - Seismogram constructed using a Ricker-wavelet source with peak frequency of 100 Hz.

CELTIC 2B8 10 52 23 W3M

STRATIGRAPHIC MARKER BEDS

SYNTHETIC SEISMOGRAM

VELOCITY

DENSITY

Q

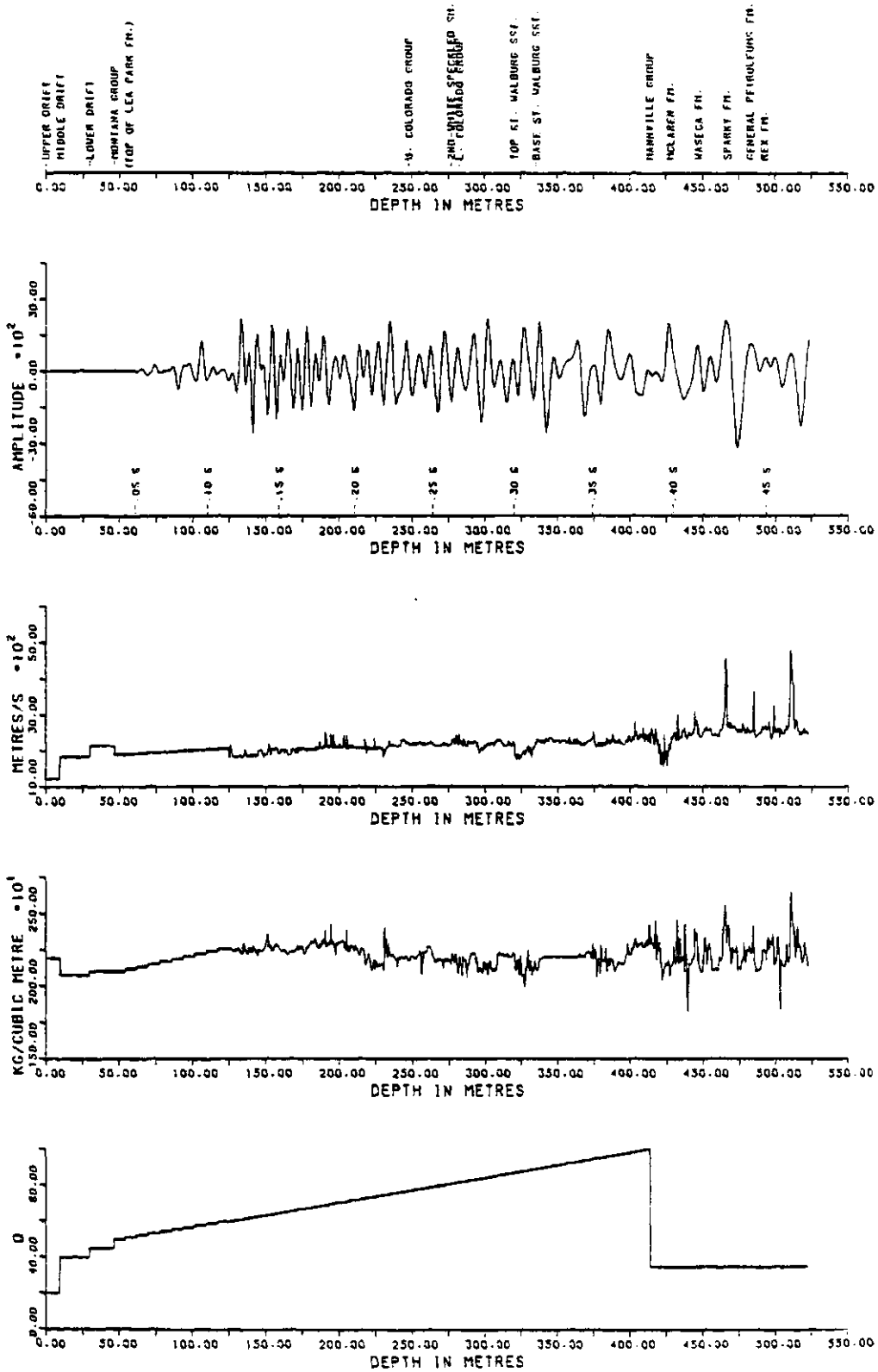


Figure 5.35 - Seismogram constructed using a Ricker-wavelet source with peak frequency of 140 Hz.

CELTIC 2B8 10 52 23 W3M

STRATIGRAPHIC
MARKER BEDS

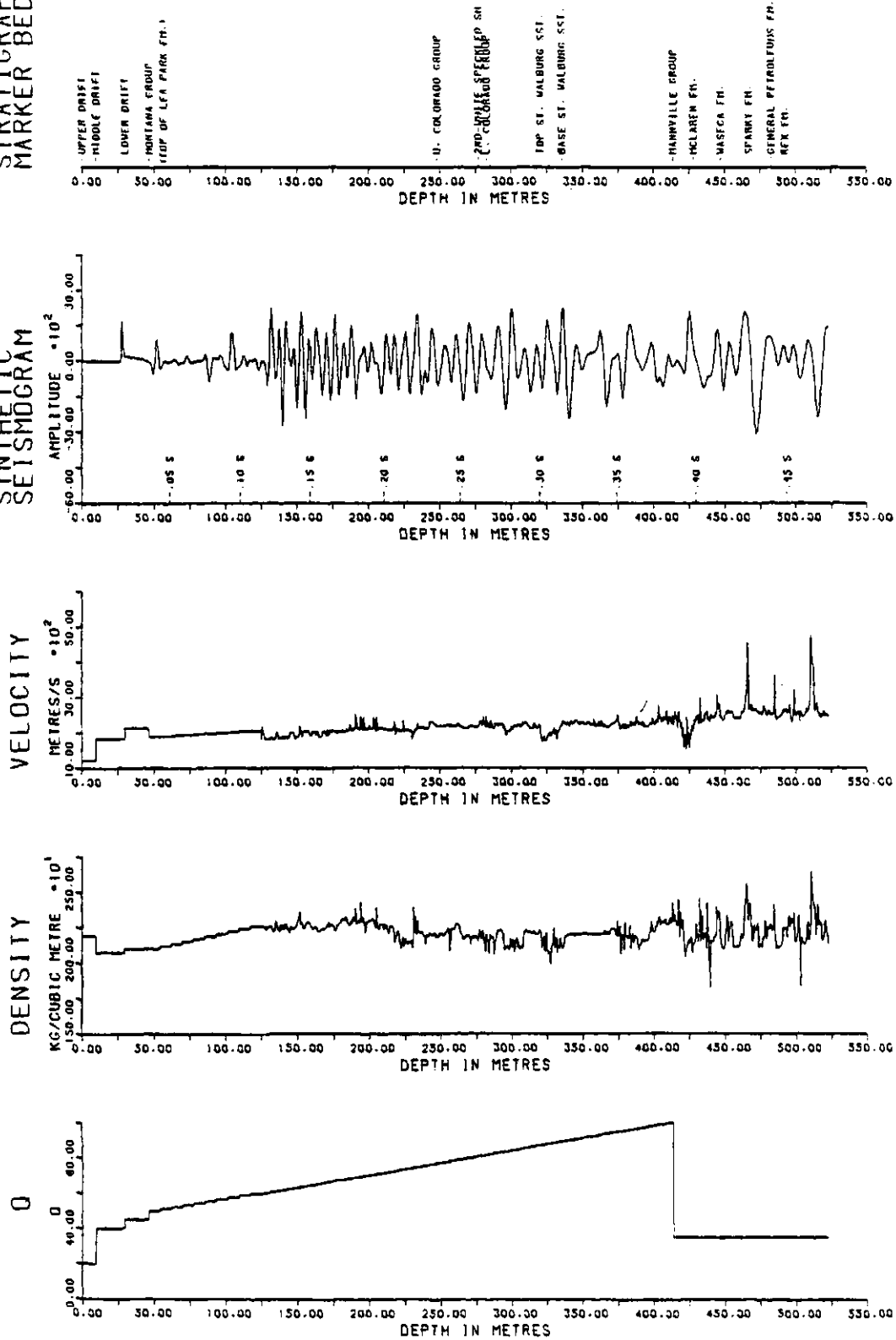


Figure 5.36 - Seismogram constructed using a Ricker-wavelet source with peak frequency of 180 hz.

CELTIC 2B8 10 52 23 W3M

STRATIGRAPHIC
MARKER BEDS

SYNTHETIC
SEISMOGRAM

VELOCITY

DENSITY

Q

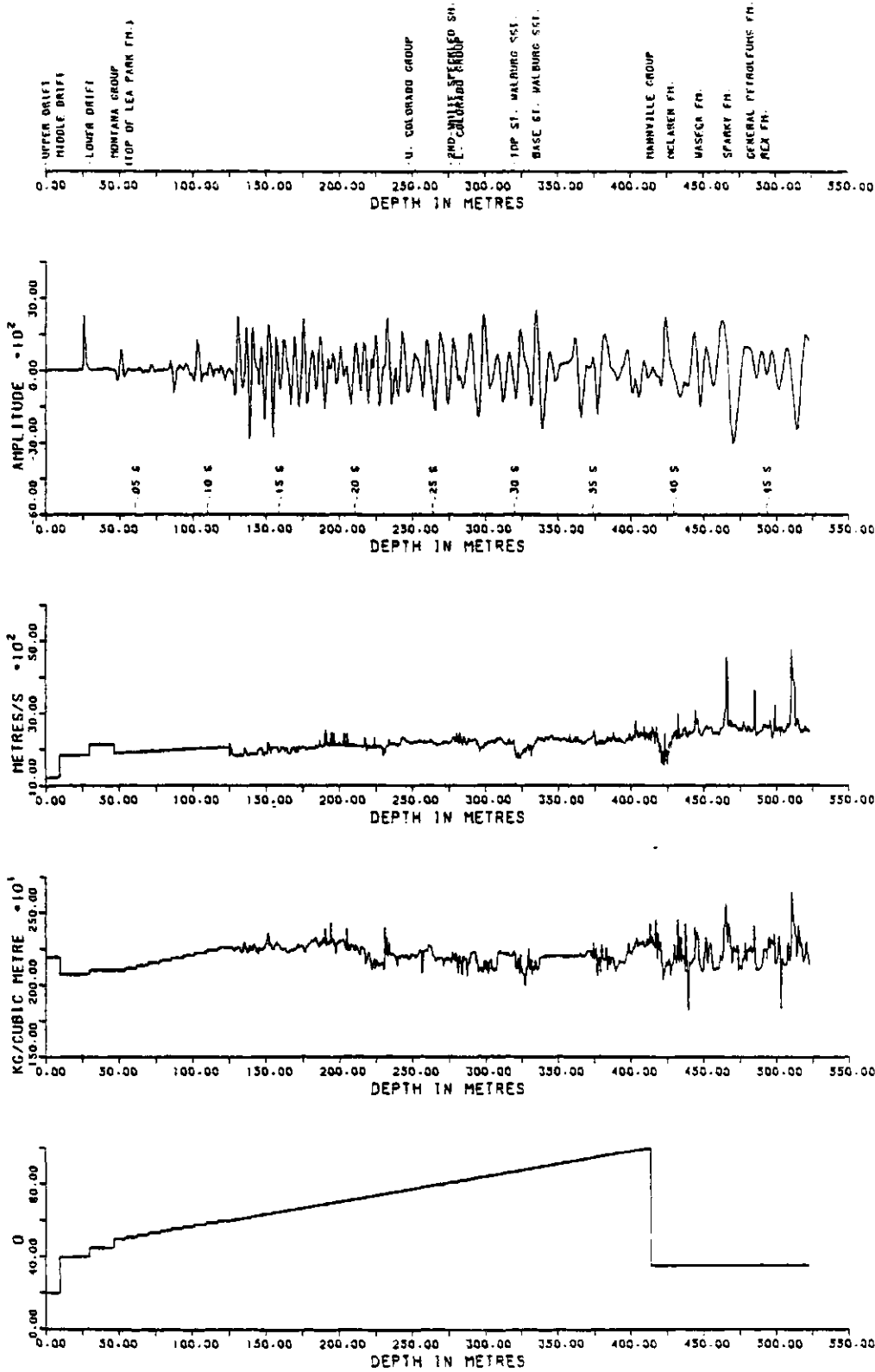


Figure 5.37 - Seismogram constructed using a Ricker-wavelet source with peak frequency of 220 hz.

CELTIC 2B8 10 52 23 W3M

MINIMUM Q=20 AND MAXIMUM Q=100.
 SOURCE BURIED AT A DEPTH (M) = 29.9
 TYPE OF WAVELET : RICKER. WITH CENTRAL FREQUENCY (HZ) APPROX. = 60.

TIME GATE (IN S) FOR AMPLITUDE SPECTRUM = .405 TO 0.493
 TIME GATE CORRESPONDS TO:
 TOP OF MANNVILLE GRP. (414.0 M) TO END OF INPUT LOGS (523.2 M)
 SAMPLE INTERVAL IN TIME DOMAIN (S) = .0010
 SAMPLE INTERVAL IN FREQUENCY DOMAIN (HZ) = 7.812
 NUMBER OF FREQUENCIES ANALYSED = 65.
 HANNING SMOOTHING APPLIED TO SPECTRUM
 PERCENT OF TRACE ELEMENTS TAPERED AT EACH END = 10.

AMPLITUDE SPECTRUM OF SYNTHETIC SEISMOGRAM

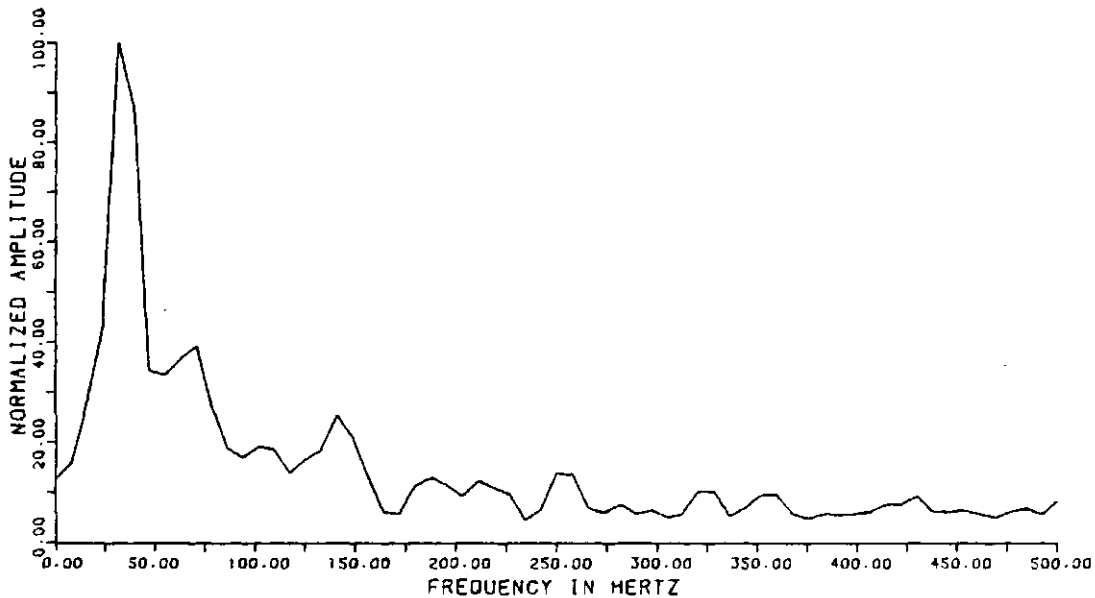


Figure 5.38 - Amplitude spectrum from seismogram constructed using a 60 hz Ricker-wavelet.

CELTIC 2B8 10 52 23 W3M

MINIMUM Q=20 AND MAXIMUM Q=100.
 SOURCE BURIED AT A DEPTH (M) = 29.9
 TYPE OF WAVELET : RICKER. WITH CENTRAL FREQUENCY (HZ) APPROX. = 80.

TIME GATE (IN S) FOR AMPLITUDE SPECTRUM = .405 TO 0.493
 TIME GATE CORRESPONDS TO:
 TOP OF MANNVILLE GRP. (414.0 M) TO END OF INPUT LOGS (523.2 M)
 SAMPLE INTERVAL IN TIME DOMAIN (S) = .0010
 SAMPLE INTERVAL IN FREQUENCY DOMAIN (HZ) = 7.812
 NUMBER OF FREQUENCIES ANALYSED = 65.
 HANNING SMOOTHING APPLIED TO SPECTRUM
 PERCENT OF TRACE ELEMENTS TAPERED AT EACH END = 10.

AMPLITUDE SPECTRUM OF SYNTHETIC SEISMOGRAM

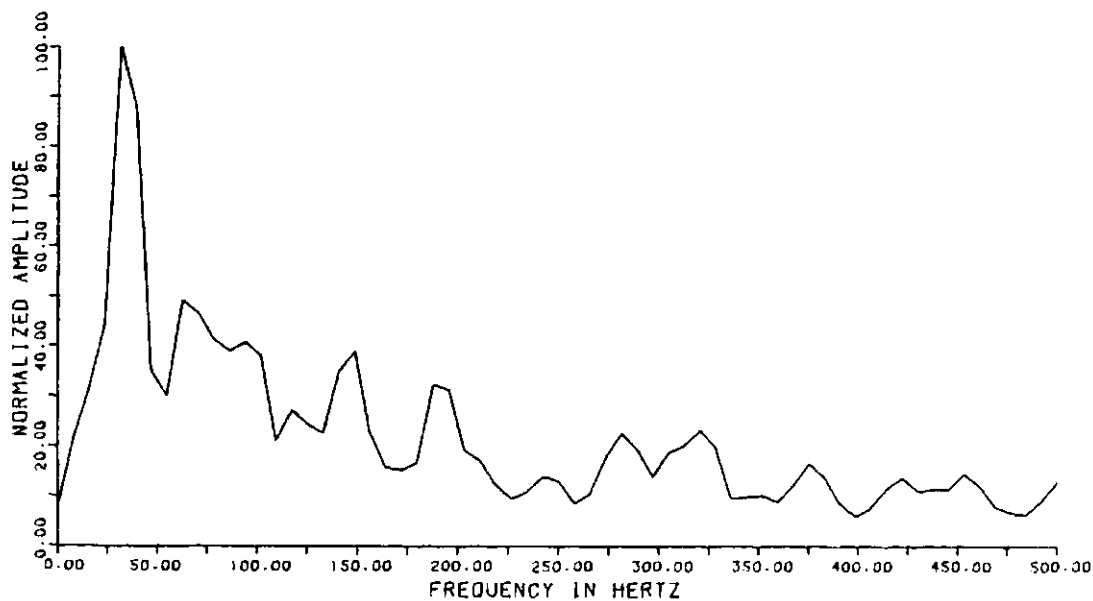


Figure 5.39 - Amplitude spectrum from seismogram constructed using an 80 hz Ricker-wavelet source.

CELTIC 2B8 10 52 23 W3M

MINIMUM Q=20 AND MAXIMUM Q=100
 SOURCE BURIED AT A DEPTH (M) = 29.9
 TYPE OF WAVELET : RICKER. WITH CENTRAL FREQUENCY (HZ) APPROX. = 100.

TIME GATE (IN S) FOR AMPLITUDE SPECTRUM = .405 TO 0.493
 TIME GATE CORRESPONDS TO:
 TOP OF MANNVILLE GRP. (414.0 M) TO END OF INPUT LOGS (523.2 M)
 SAMPLE INTERVAL IN TIME DOMAIN (S) = .0010
 SAMPLE INTERVAL IN FREQUENCY DOMAIN (HZ) = 7.812
 NUMBER OF FREQUENCIES ANALYSED = 65.
 HANNING SMOOTHING APPLIED TO SPECTRUM
 PERCENT OF TRACE ELEMENTS TAPERED AT EACH END = 10.

AMPLITUDE SPECTRUM OF SYNTHETIC SEISMOGRAM

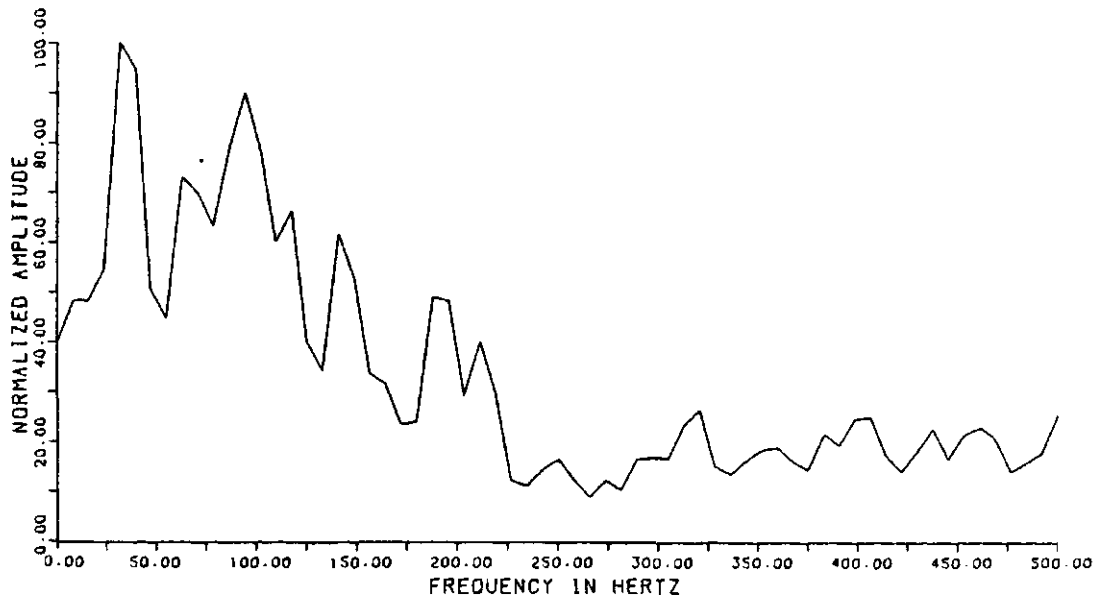


Figure 5.40 - Amplitude spectrum from seismogram constructed using a 100 hz Ricker-wavelet source.

CELTIC 2B8 10 52 23 W3M

MINIMUM Q=20 AND MAXIMUM Q=100.
 SOURCE BURIED AT A DEPTH (M) = 29.9
 TYPE OF WAVELET : RICKER. WITH CENTRAL FREQUENCY (HZ) APPROX. = 140.

TIME GATE (IN S) FOR AMPLITUDE SPECTRUM = .405 TO 0.493
 TIME GATE CORRESPONDS TO:
 TOP OF MANNVILLE GRP. (414.0 M) TO END OF INPUT LOGS (523.2 M)
 SAMPLE INTERVAL IN TIME DOMAIN (S) = .0010
 SAMPLE INTERVAL IN FREQUENCY DOMAIN (HZ) = 7.812
 NUMBER OF FREQUENCIES ANALYSED = 65.
 HANNING SMOOTHING APPLIED TO SPECTRUM
 PERCENT OF TRACE ELEMENTS TAPERED AT EACH END = 10.

AMPLITUDE SPECTRUM OF SYNTHETIC SEISMOGRAM

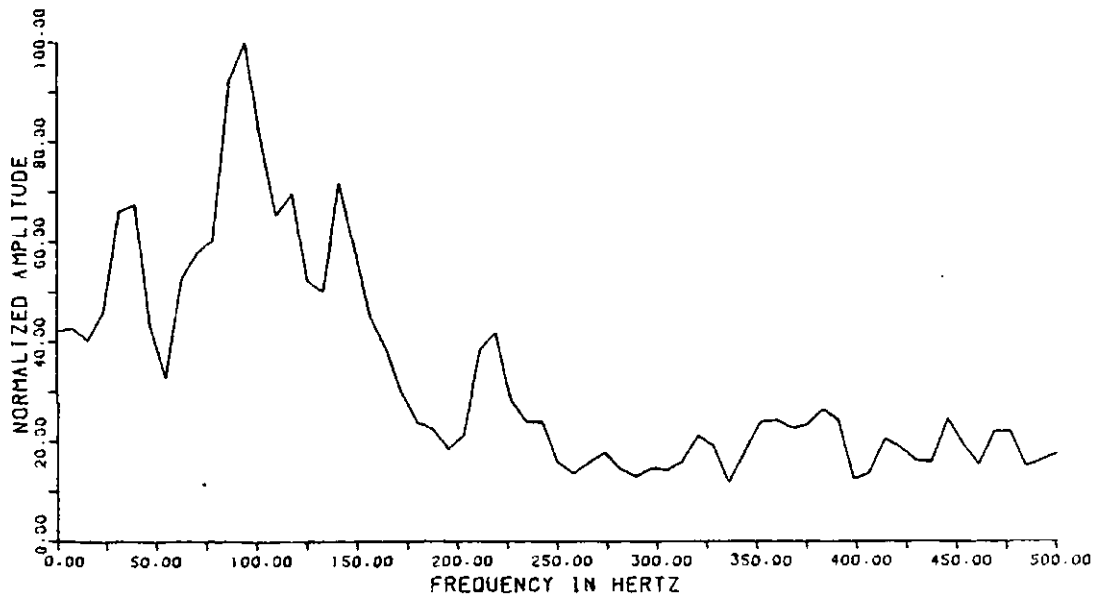


Figure 5.41 - Amplitude spectrum from seismogram constructed using a 140 hz Ricker-wavelet source.

CELTIC 2B8 10 52 23 W3M

MINIMUM Q=20 AND MAXIMUM Q=100.
 SOURCE BURIED AT A DEPTH (M) = 29.9
 TYPE OF WAVELET : RICKER, WITH CENTRAL FREQUENCY (HZ) APPROX. = 178.

TIME GATE (IN S) FOR AMPLITUDE SPECTRUM = .405 TO 0.493
 TIME GATE CORRESPONDS TO:
 TOP OF MANNVILLE GRP. (414.0 M) TO END OF INPUT LOGS (523.2 M)
 SAMPLE INTERVAL IN TIME DOMAIN (S) = .0010
 SAMPLE INTERVAL IN FREQUENCY DOMAIN (HZ) = 7.812
 NUMBER OF FREQUENCIES ANALYSED = 65.
 HANNING SMOOTHING APPLIED TO SPECTRUM
 PERCENT OF TRACE ELEMENTS TAPERED AT EACH END = 10.

AMPLITUDE SPECTRUM OF SYNTHETIC SEISMOGRAM

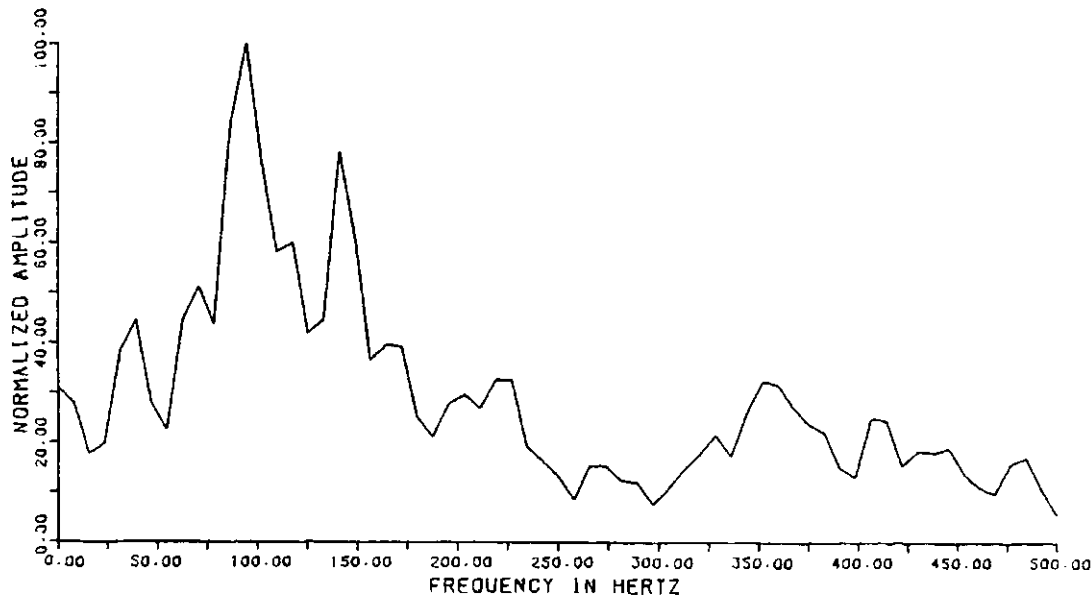


Figure 5.42 - Amplitude spectrum from seismogram constructed using a 180 hz Ricker-wavelet source.

CELTIC 2B8 10 52 23 W3M

MINIMUM Q=20 AND MAXIMUM Q=100.

SOURCE BURIED AT A DEPTH (M) = 29.9

TYPE OF WAVELET : RICKER, WITH CENTRAL FREQUENCY (HZ) APPROX. = 222.

TIME GATE (IN S) FOR AMPLITUDE SPECTRUM = .405 TO 0.493

TIME GATE CORRESPONDS TO:

TOP OF MANNVILLE GRP. (414.0 M) TO END OF INPUT LOGS (523.2 M)

SAMPLE INTERVAL IN TIME DOMAIN (S) = .0010

SAMPLE INTERVAL IN FREQUENCY DOMAIN (HZ) = 7.812

NUMBER OF FREQUENCIES ANALYSED = 65.

HANNING SMOOTHING APPLIED TO SPECTRUM

PERCENT OF TRACE ELEMENTS TAPERED AT EACH END = 10.

AMPLITUDE SPECTRUM OF SYNTHETIC SEISMOGRAM

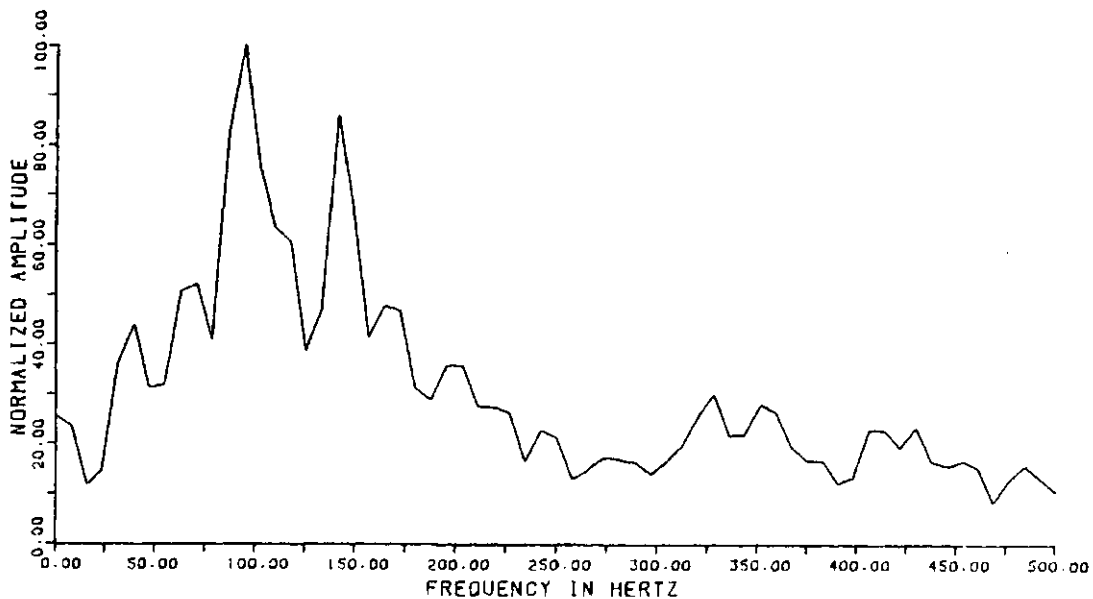


Figure 5.43 - Amplitude spectrum from seismogram constructed using a 220 hz Ricker-wavelet source.

portions of the seismograms in Figures 5.4 and 5.33 are probably as a result of interference from the side lobes of the Ricker wavelet. The seismogram in Figure 5.33 is also delayed, due to the linear-phase characteristic of the Ricker wavelet.

The choice of filter used in synthetic seismogram construction or seismic processing is important. The filter of 80 hz peak frequency provides the most realistic response from the Mannville section because it most closely imitates the (anti-alias filtered) impulse response. If a low-frequency filter is used (for example, one corresponding to the 60 hz wavelet in Figure 5.32), the lower frequency portions of the amplitude spectrum are increased relative to the higher frequency portions and important, high-frequency reflections from the Mannville may be destroyed. If a high-frequency filter is used (for example, one corresponding to the 100, 140, 180, or 220 hz sources of Figures 5.34 through 5.37), the higher-frequency portions of the spectrum are increased relative to the lower frequencies and the important, high-frequency reflections will be accentuated.

For this study, however, the best choice is the impulse source. This is because the impulse source is zero phase and contains all frequencies in equal proportions (Sheriff, 1973). Thus, the impulse response seismogram shows how all of the sampled frequencies (that is, within the theoretically available range of frequencies that is determined by the sampling rate) have responded to the filtering of the simulated earth-model.

5.4 Variation Among Wells

Using the "best" input parameters--an impulse source buried at 29.9 m and the standard Q-function, as were chosen from tests on well 288 in

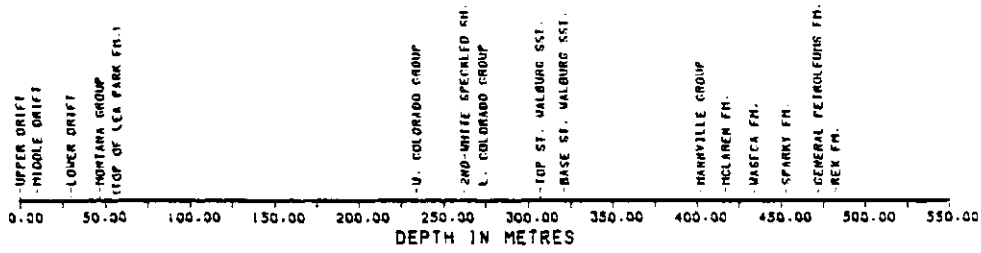
section 5.3, synthetic seismograms were constructed for the pilot-project wells and well 4-11. The synthetic seismograms for these seven wells are shown in Figures 5.44 through 5.50. The amplitude spectra for all seven wells are shown in Figures 5.51 through 5.57.

The Mannville portions of the synthetic seismograms of the six pilot-project wells are not markedly different from one another. The cross-section in Figure 4.5 has already pointed out the geological similarity among the six wells; consequently, the similarity of their synthetic seismograms is not surprising. Still, there are significant differences among the seismograms. A synthetic seismogram cross-section through the pilot-project wells, which is flattened on the top of the Mannville Group, is shown in Figure 5.58. Although the Colony gas-zone, McLaren coal-bed, and Waseca oil-saturated-sand zones reflected responses are visible in each seismogram, the relative sizes of the waveforms vary significantly.

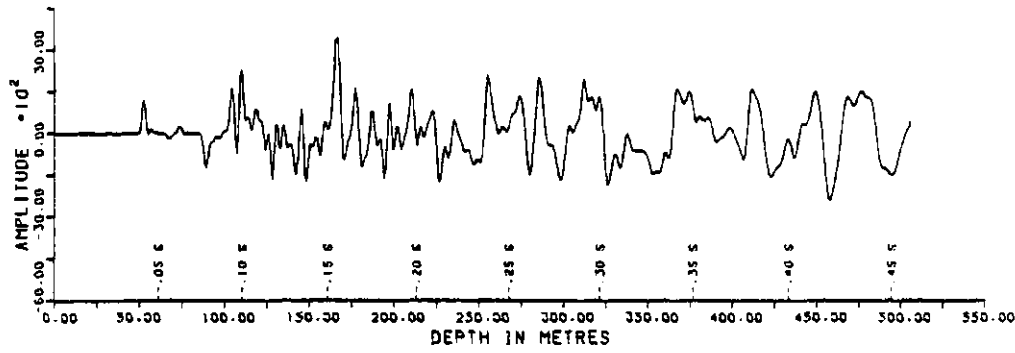
The response of well 4D2 is most different from the others. In comparing the Mannville portions of the synthetic seismograms, the frequencies in well 4D2 (Figures 5.46 and 5.58) are distinctly higher. Whereas the amplitude spectra of the other five pilot project wells have dominant frequencies of 40 hz, well 4D2 (Figure 5.53) has a dominant frequency of 93 hz, the entire range of 55 to 95 hz being over 95 per cent of the peak amplitude. The most probable cause of these high frequencies is found within the Colony gas zone. In well 4D2, the low acoustic impedance gas zone is interrupted by a thin high velocity and density (probably calcite cemented) bed. Due to this zone of high acoustic- impedance, the normally large and broad 40 hz gas-peak is split into two high-frequency peaks and a trough. The measured frequency of these waveforms is approximately 80 hz. From a few ms

CELTIC 4B2 10 52 23 W3M

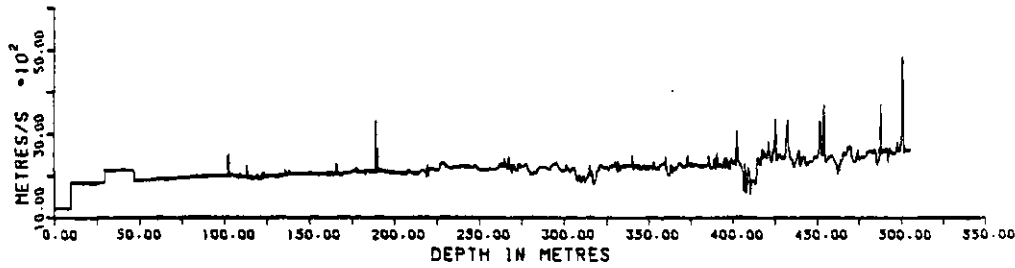
STRATIGRAPHIC
MARKER BEDS



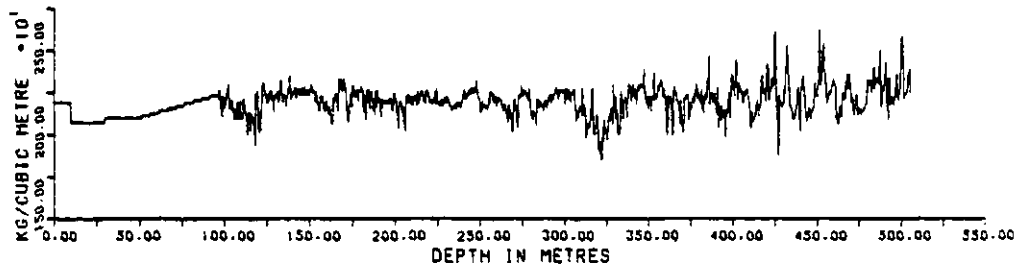
SYNTHETIC
SEISMOGRAM



VELOCITY



DENSITY



0

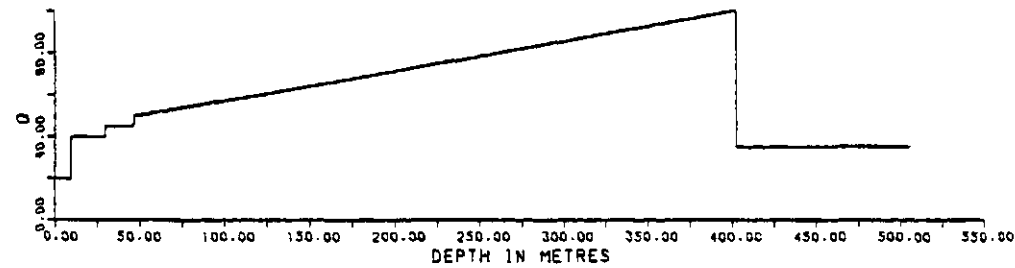
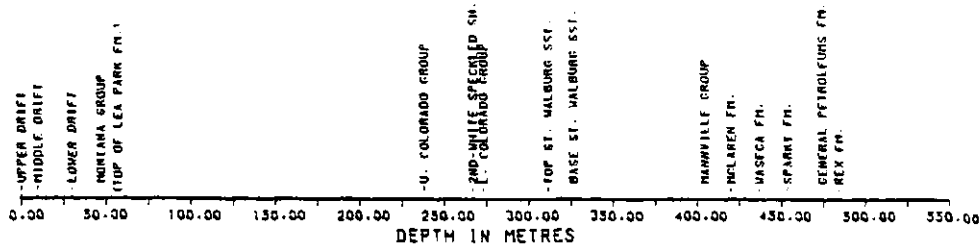


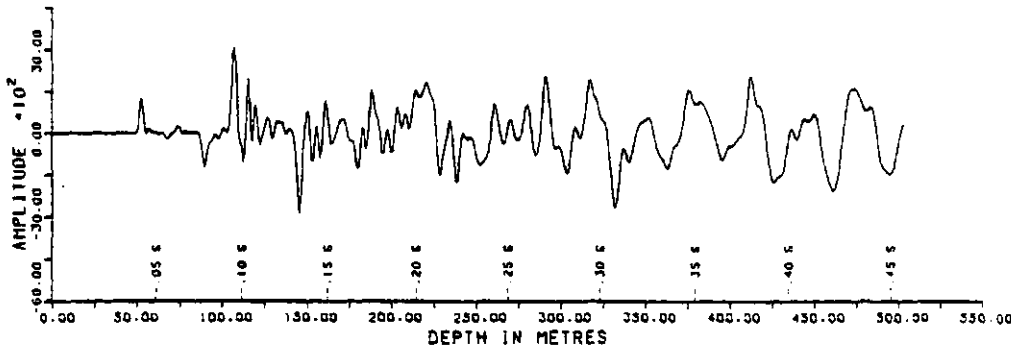
Figure 5.44 - Well logs and synthetic seismogram for well 4B2.

CELTIC 2D2 10 52 23 W3M

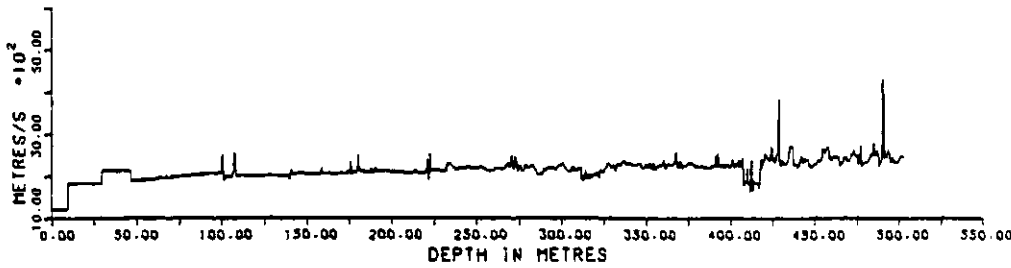
STRATIGRAPHIC
MARKER BEDS



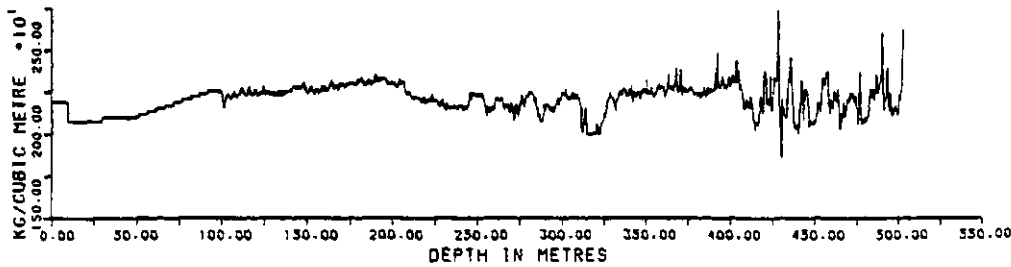
SYNTHETIC
SEISMOGRAM



VELOCITY



DENSITY



0

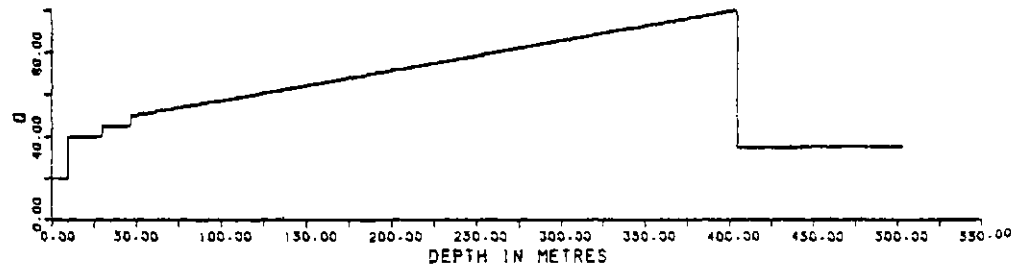


Figure 5.45 - Well logs and synthetic seismogram for well 2D2.

CELTIC 4D2 10 52 23 W3M

STRATIGRAPHIC
MARKER BEDS

SYNTHETIC
SEISMOGRAM

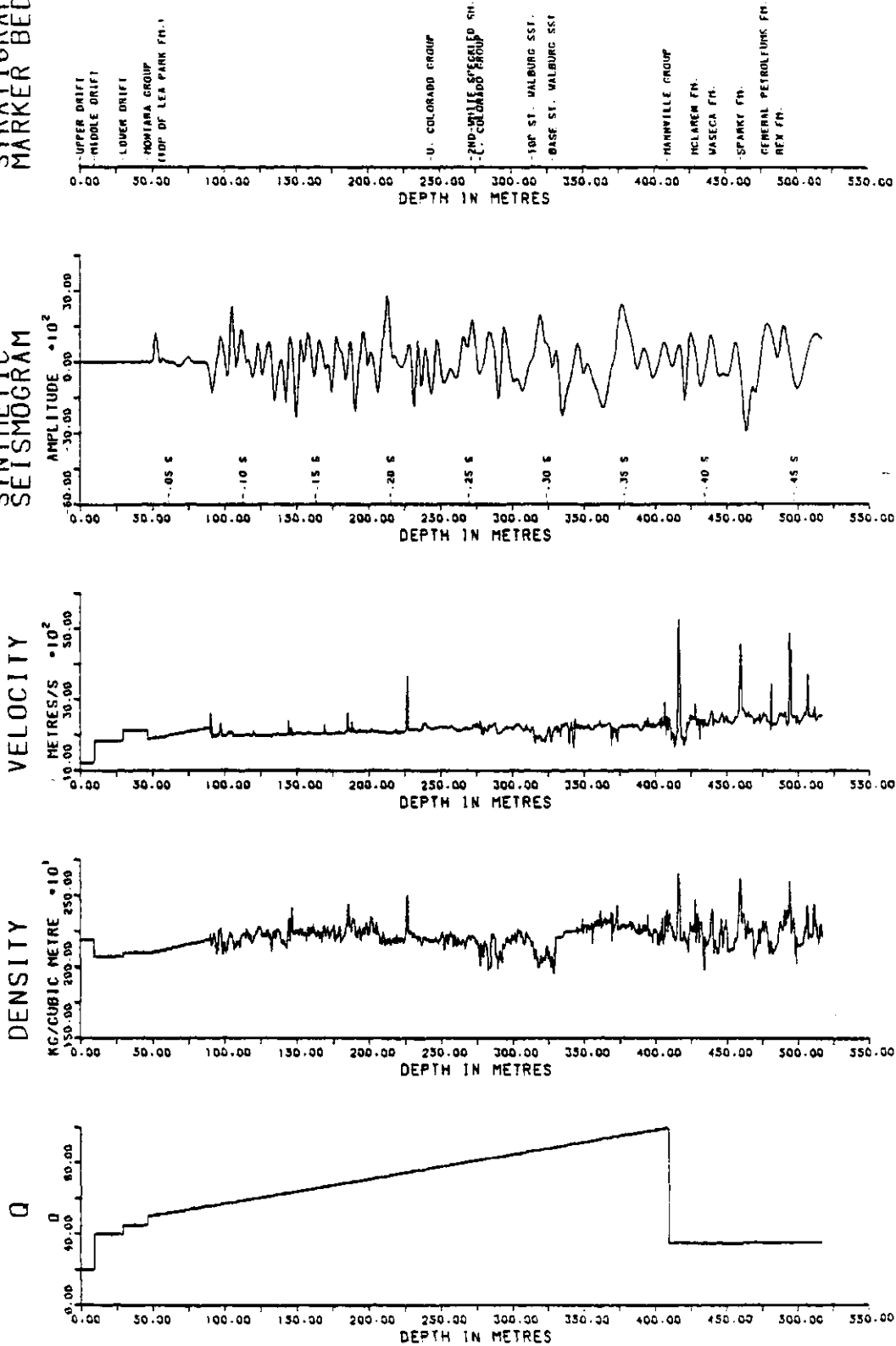
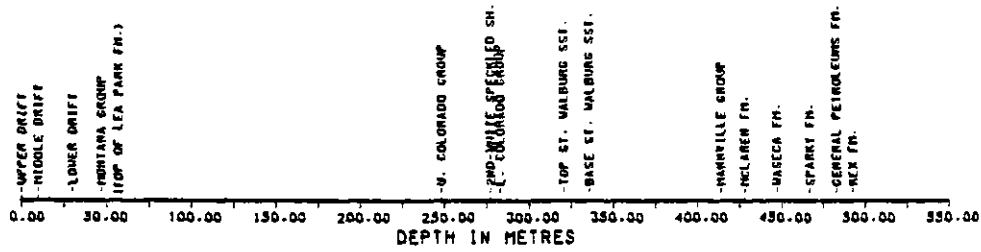


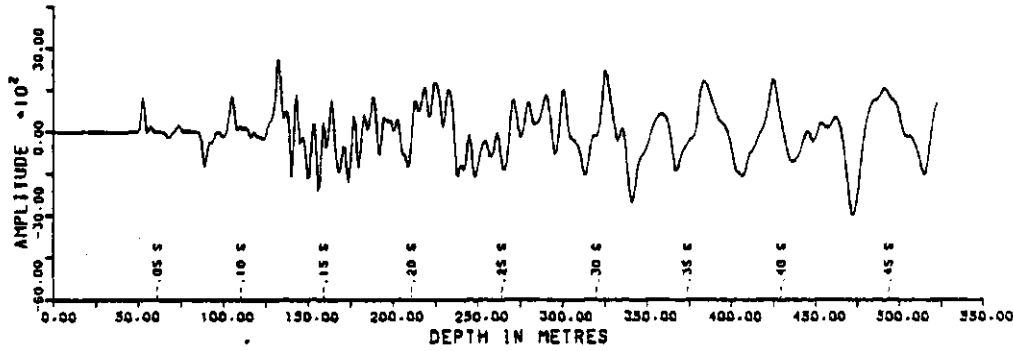
Figure 5.46 - Well logs and synthetic seismogram for well 4D2.

CELTIC 2B8 10 52 23 W3M

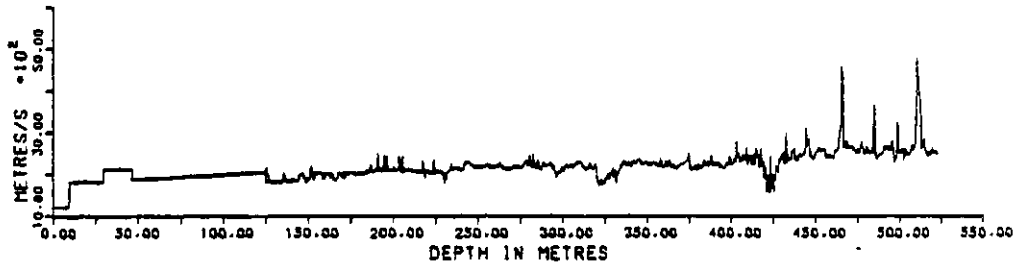
STRATIGRAPHIC
MARKER BEDS



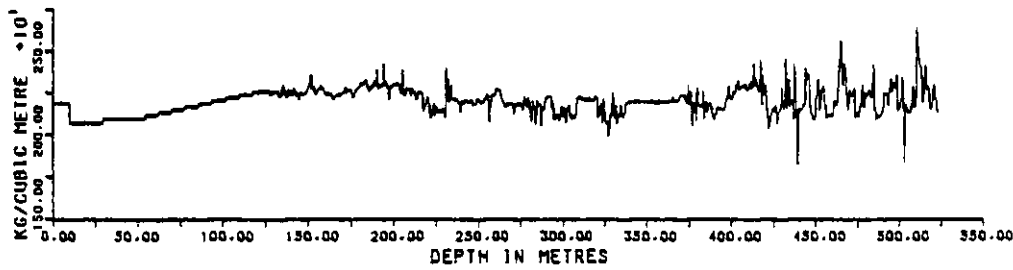
SYNTHETIC
SEISMOGRAM



VELOCITY



DENSITY



Q

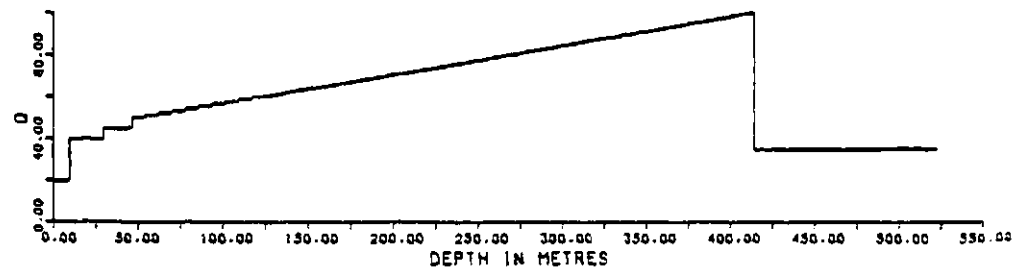
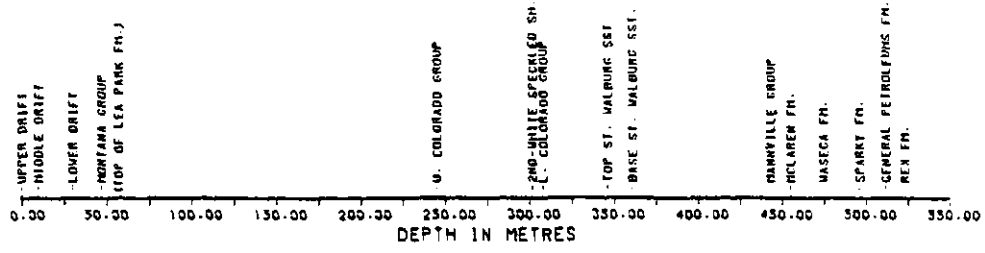


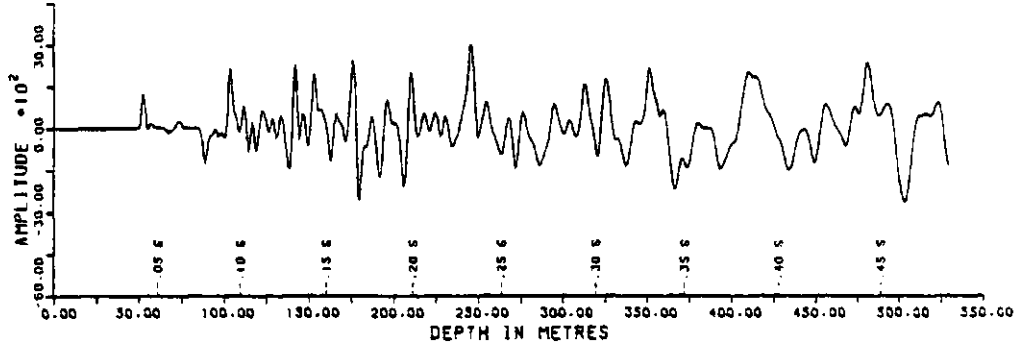
Figure 5.47 - Well logs and synthetic seismogram for well 2B8.

CELTIC 2D8 10 52 23 W3M

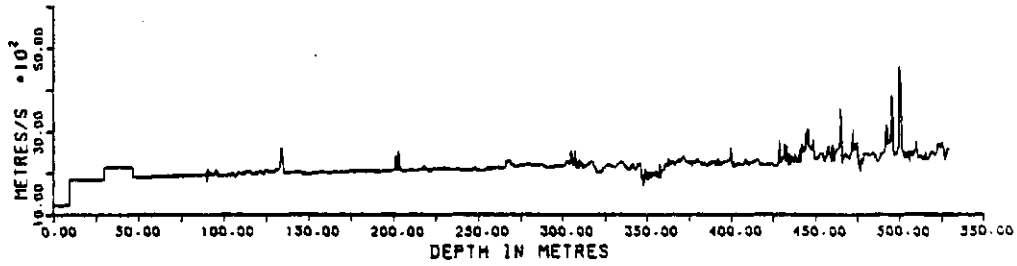
STRATIGRAPHIC
MARKER BEDS



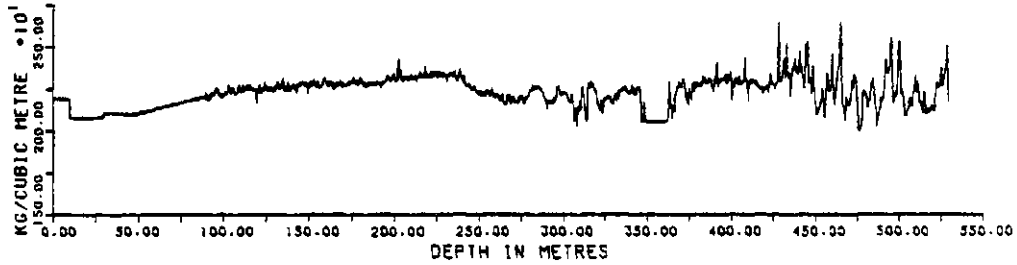
SYNTHETIC
SEISMOGRAM



VELOCITY



DENSITY



0

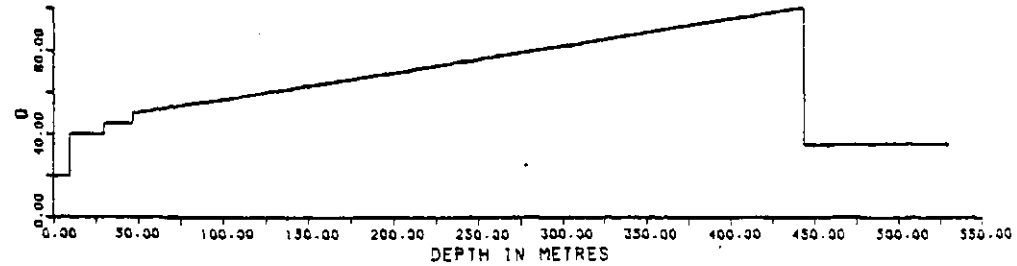
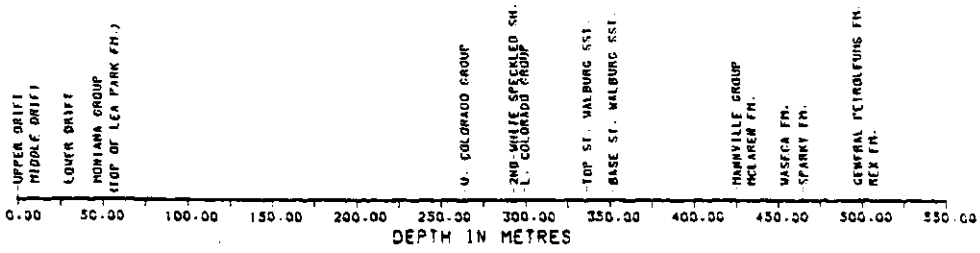


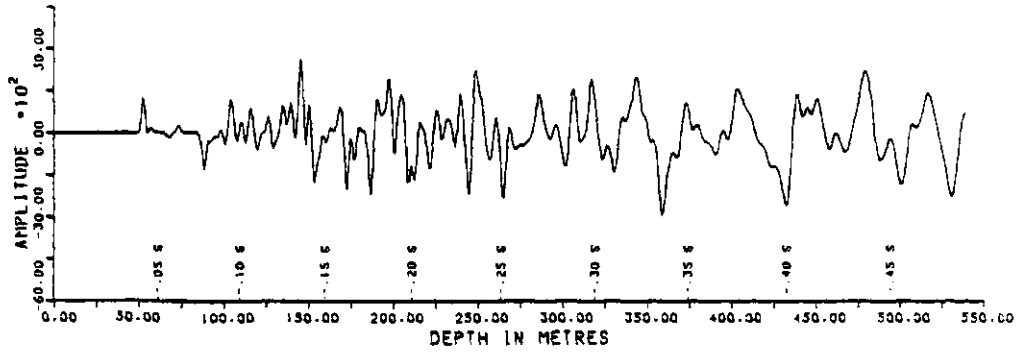
Figure 5.49 - Well logs and synthetic seismogram for well 2D8.

4 11 52 23 W3M

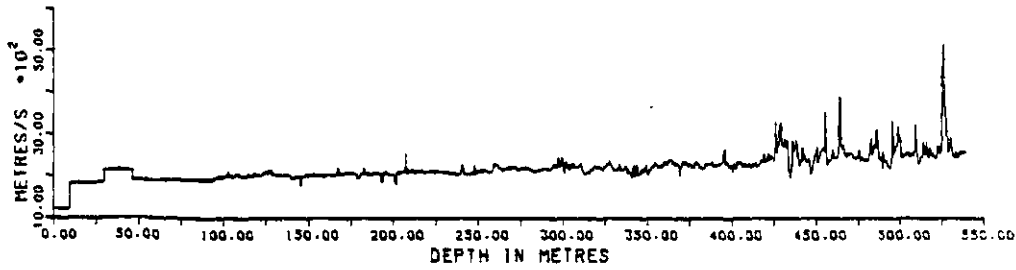
STRATIGRAPHIC
MARKER BEDS



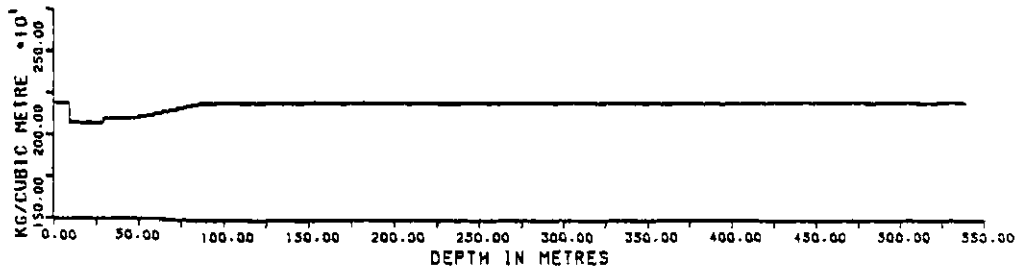
SYNTHETIC
SEISMOGRAM



VELOCITY



DENSITY



0

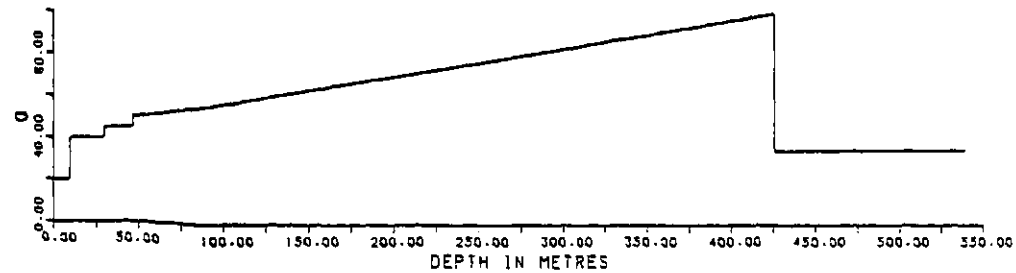


Figure 5.50 - Well logs and synthetic seismogram for well 4-11.

CELTIC 4B2 10 52 23 W3M

MINIMUM Q=20 AND MAXIMUM Q=100
 SOURCE BURIED AT A DEPTH (M) = 29.9
 TYPE OF WAVELET : IMPULSE
 BUTTERWORTH ANTI-ALIAS FILTER INCLUDED IN SYNTHETIC TRACE
 TIME GATE (IN S) FOR AMPLITUDE SPECTRUM = .374 TO 0.443
 TIME GATE CORRESPONDS TO:
 TOP OF MANNVILLE GROUP (402.2 M) TO TOP OF REX FM. (482.3 M)
 SAMPLE INTERVAL IN TIME DOMAIN (S) = .0010
 SAMPLE INTERVAL IN FREQUENCY DOMAIN (HZ) = 7.812
 NUMBER OF FREQUENCIES ANALYSED = 65.
 HANNING SMOOTHING APPLIED TO SPECTRUM
 PERCENT OF TRACE ELEMENTS TAPERED AT EACH END = 10.

AMPLITUDE SPECTRUM OF SYNTHETIC SEISMOGRAM

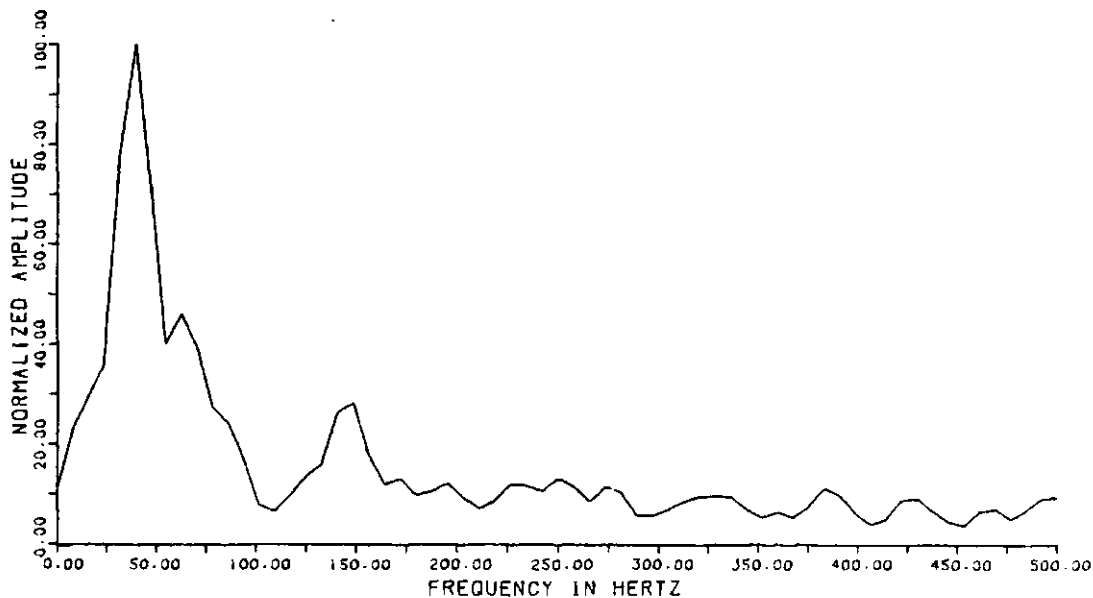


Figure 5.51 - Amplitude spectrum from seismogram for well 4B2.

CELTIC 2D2 10 52 23 W3M

MINIMUM Q=20 AND MAXIMUM Q=100
 SOURCE BURIED AT A DEPTH (M) = 29.9
 TYPE OF WAVELET : IMPULSE
 BUTTERWORTH ANTI-ALIAS FILTER INCLUDED IN SYNTHETIC TRACE
 TIME GATE (IN S) FOR AMPLITUDE SPECTRUM = .374 TO 0.444
 TIME GATE CORRESPONDS TO:
 TOP OF MANNVILLE GROUP (404.5 M) TO TOP OF REX FM. (484.3 M)
 SAMPLE INTERVAL IN TIME DOMAIN (S) = .0010
 SAMPLE INTERVAL IN FREQUENCY DOMAIN (HZ) = 7.812
 NUMBER OF FREQUENCIES ANALYSED = 65.
 HANNING SMOOTHING APPLIED TO SPECTRUM
 PERCENT OF TRACE ELEMENTS TAPERED AT EACH END = 10.

AMPLITUDE SPECTRUM OF SYNTHETIC SEISMOGRAM

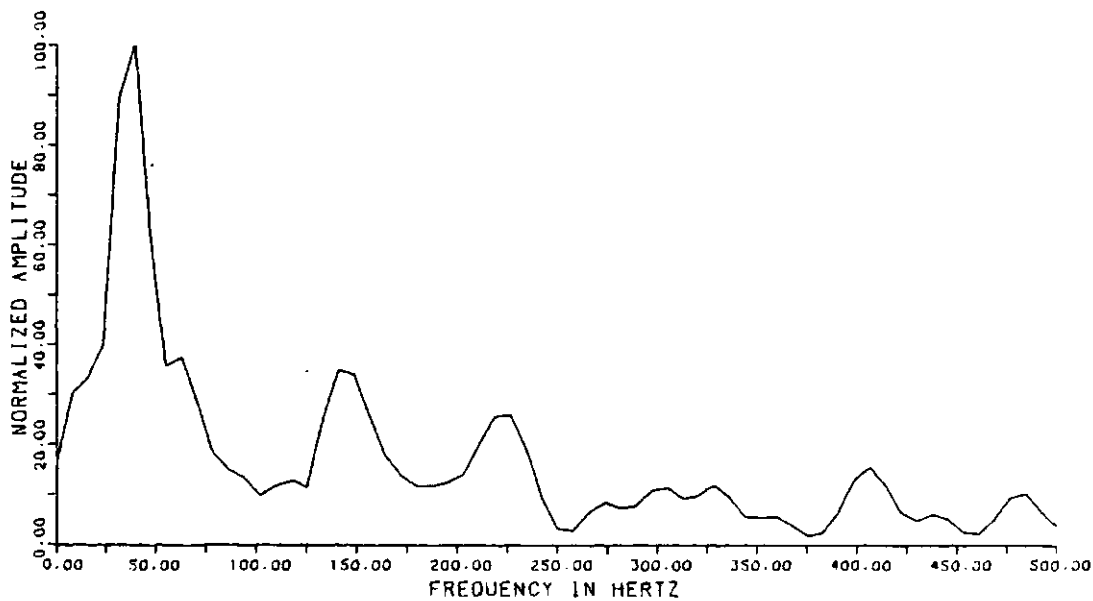


Figure 5.52 - Amplitude spectrum from seismogram for well 2D2.

CELTIC 4D2 10 52 23 W3M

MINIMUM Q=20 AND MAXIMUM Q=100
SOURCE BURIED AT A DEPTH (M) = 29.9
TYPE OF WAVELET : IMPULSE
BUTTERWORTH ANTI-ALIAS FILTER INCLUDED IN SYNTHETIC TRACE
TIME GATE (IN S) FOR AMPLITUDE SPECTRUM = .379 TO 0.446
TIME GATE CORRESPONDS TO:
TOP OF MANNVILLE GRP. (409.5 M) TO TOP OF REX FM. (488.4 M)
SAMPLE INTERVAL IN TIME DOMAIN (S) = .0010
SAMPLE INTERVAL IN FREQUENCY DOMAIN (HZ) = 7.812
NUMBER OF FREQUENCIES ANALYSED = 65.
HANNING SMOOTHING APPLIED TO SPECTRUM
PERCENT OF TRACE ELEMENTS TAPERED AT EACH END = 10.

AMPLITUDE SPECTRUM OF SYNTHETIC SEISMOGRAM

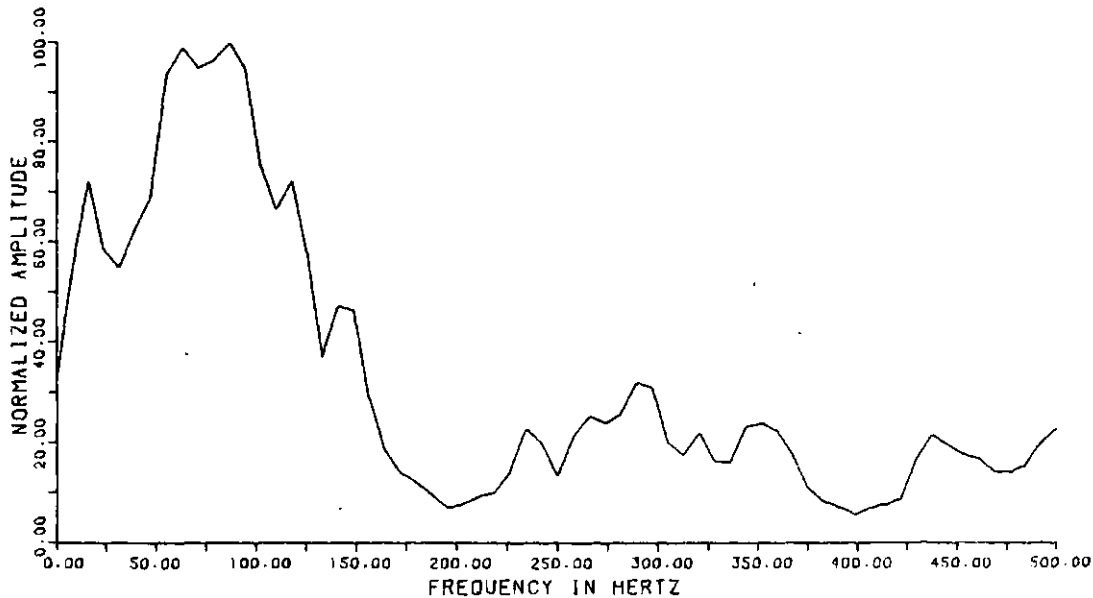


Figure 5.53 - Amplitude spectrum from seismogram for well 4D2.

CELTIC 2B8 10 52 23 W3M

MINIMUM Q=20 AND MAXIMUM Q=100
SOURCE BURIED AT A DEPTH (M) = 29.9
TYPE OF WAVELET : IMPULSE
BUTTERWORTH ANTI-ALIAS FILTER INCLUDED IN SYNTHETIC TRACE
TIME GATE (IN S) FOR AMPLITUDE SPECTRUM = .405 TO 0.471
TIME GATE CORRESPONDS TO:
TOP OF MANNVILLE GRP. (414.0) TO TOP OF REX FM. (492.9 M)
SAMPLE INTERVAL IN TIME DOMAIN (S) = .0010
SAMPLE INTERVAL IN FREQUENCY DOMAIN (HZ) = 7.812
NUMBER OF FREQUENCIES ANALYSED = 65.
HANNING SMOOTHING APPLIED TO SPECTRUM
PERCENT OF TRACE ELEMENTS TAPERED AT EACH END = 10.

AMPLITUDE SPECTRUM OF SYNTHETIC SEISMOGRAM

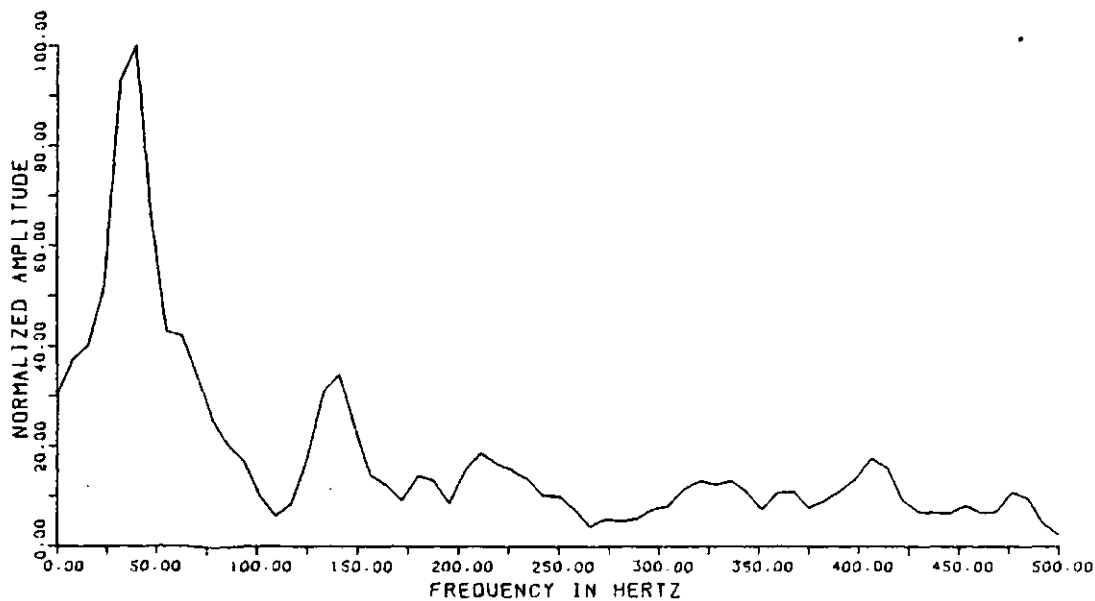


Figure 5.54 - Amplitude spectrum from seismogram for well 2B8.

CELTIC 4B8 10 52 23 W3M

MINIMUM Q=20 AND MAXIMUM Q=100
SOURCE BURIED AT A DEPTH (M) = 29.9
TYPE OF WAVELET : IMPULSE
BUTTERWORTH ANTI-ALIAS FILTER INCLUDED IN SYNTHETIC TRACE
TIME GATE (IN S) FOR AMPLITUDE SPECTRUM = .394 TO 0.459
TIME GATE CORRESPONDS TO:
TOP OF MANNVILLE GROUP (427.5 M) TO TOP OF REX FM. (506.5 M)
SAMPLE INTERVAL IN TIME DOMAIN (S) = .0010
SAMPLE INTERVAL IN FREQUENCY DOMAIN (HZ) = 7.812
NUMBER OF FREQUENCIES ANALYSED = 65.
HANNING SMOOTHING APPLIED TO SPECTRUM
PERCENT OF TRACE ELEMENTS TAPERED AT EACH END = 10.

AMPLITUDE SPECTRUM OF SYNTHETIC SEISMOGRAM

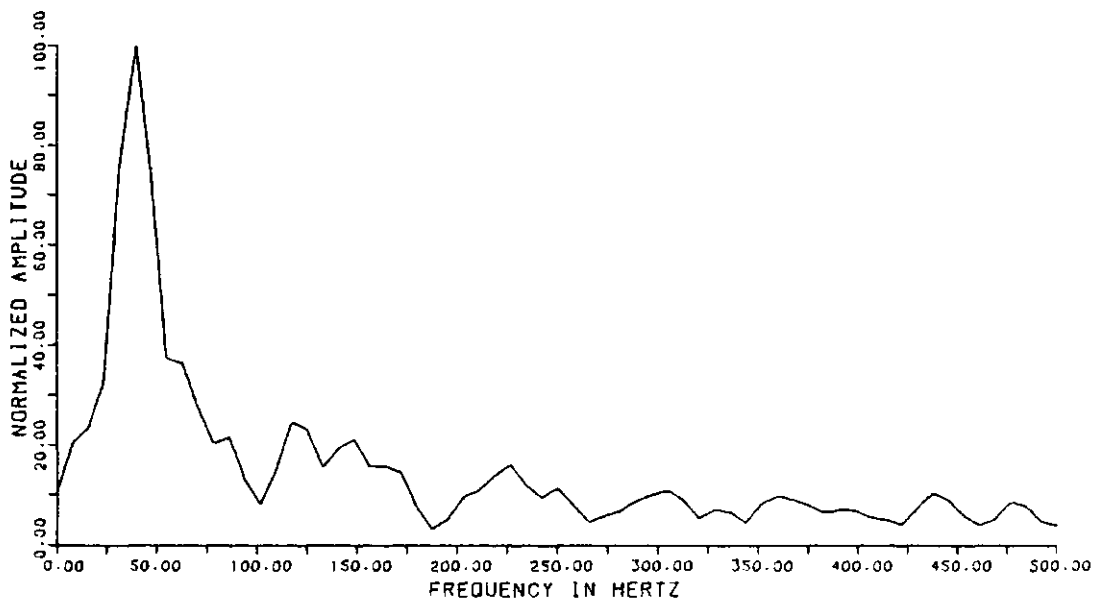


Figure 5.55 - Amplitude spectrum from seismogram for well 4B8.

CELTIC 2D8 10 52 23 W3M

MINIMUM Q=20 AND MAXIMUM Q=100
 SOURCE BURIED AT A DEPTH (M) = 29.9
 TYPE OF WAVELET : IMPULSE
 BUTTERWORTH ANTI-ALIAS FILTER INCLUDED IN SYNTHETIC TRACE
 TIME GATE (IN S) FOR AMPLITUDE SPECTRUM = .414 TO 0.479
 TIME GATE CORRESPONDS TO:
 TOP OF MANNVILLE GROUP (443.3 M) TO TOP OF REX FM. (523.2 M)
 SAMPLE INTERVAL IN TIME DOMAIN (S) = .0010
 SAMPLE INTERVAL IN FREQUENCY DOMAIN (HZ) = 7.812
 NUMBER OF FREQUENCIES ANALYSED = 65.
 HANNING SMOOTHING APPLIED TO SPECTRUM
 PERCENT OF TRACE ELEMENTS TAPERED AT EACH END = 10.

AMPLITUDE SPECTRUM OF SYNTHETIC SEISMOGRAM

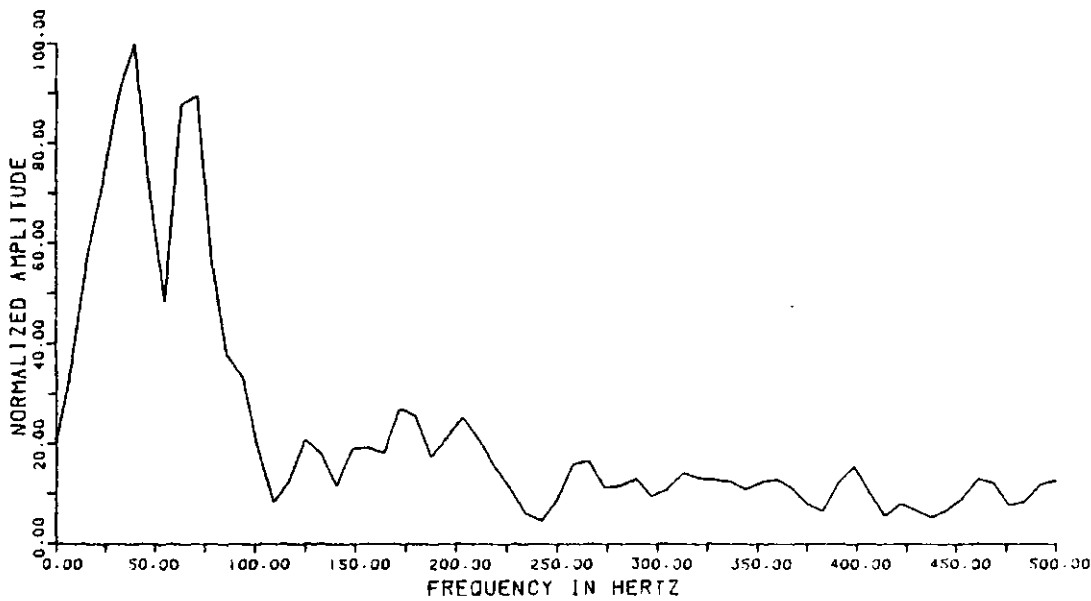


Figure 5.56 - Amplitude spectrum from seismogram for well 2D8.

4 11 52 23 W3M

MINIMUM 0=20 AND MAXIMUM 0=100
 SOURCE BURIED AT A DEPTH (M) = 29.9
 TYPE OF WAVELET : IMPULSE
 BUTTERWORTH ANTI-ALIAS FILTER INCLUDED IN SYNTHETIC TRACE
 TIME GATE (IN S) FOR AMPLITUDE SPECTRUM = .396 TO 0.462
 TIME GATE CORRESPONDS TO:
 TOP OF MANNVILLE GROUP (425.5 M) TO TOP OF REX FM. (406.8 M)
 SAMPLE INTERVAL IN TIME DOMAIN (S) = .0010
 SAMPLE INTERVAL IN FREQUENCY DOMAIN (HZ) = 7.812
 NUMBER OF FREQUENCIES ANALYSED = 65.
 HANNING SMOOTHING APPLIED TO SPECTRUM
 PERCENT OF TRACE ELEMENTS TAPERED AT EACH END = 10.

AMPLITUDE SPECTRUM OF SYNTHETIC SEISMOGRAM

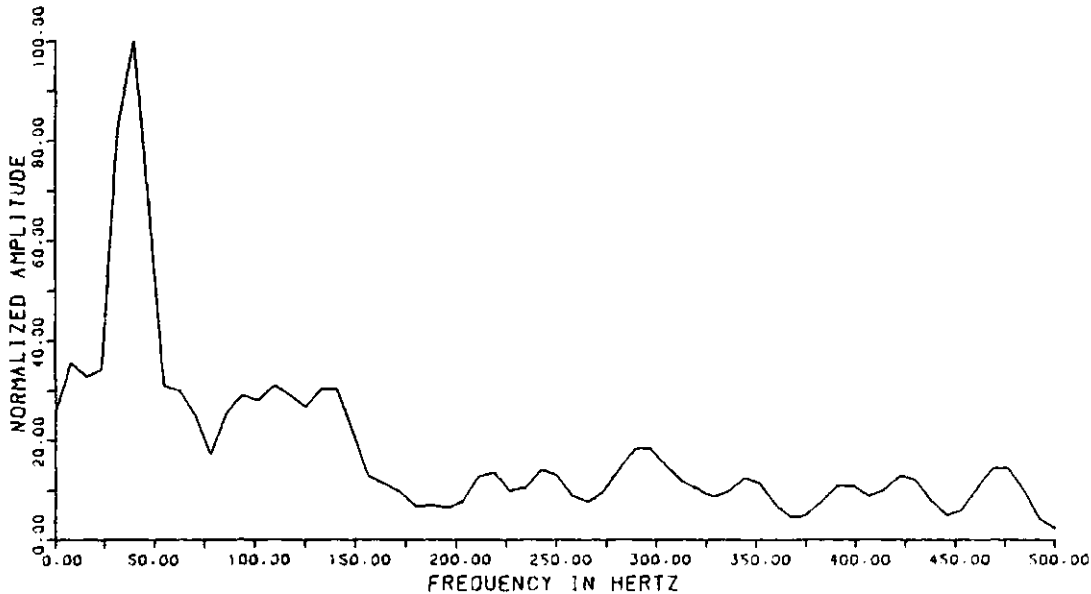


Figure 5.57 - Amplitude spectrum from seismogram for well 4-11.

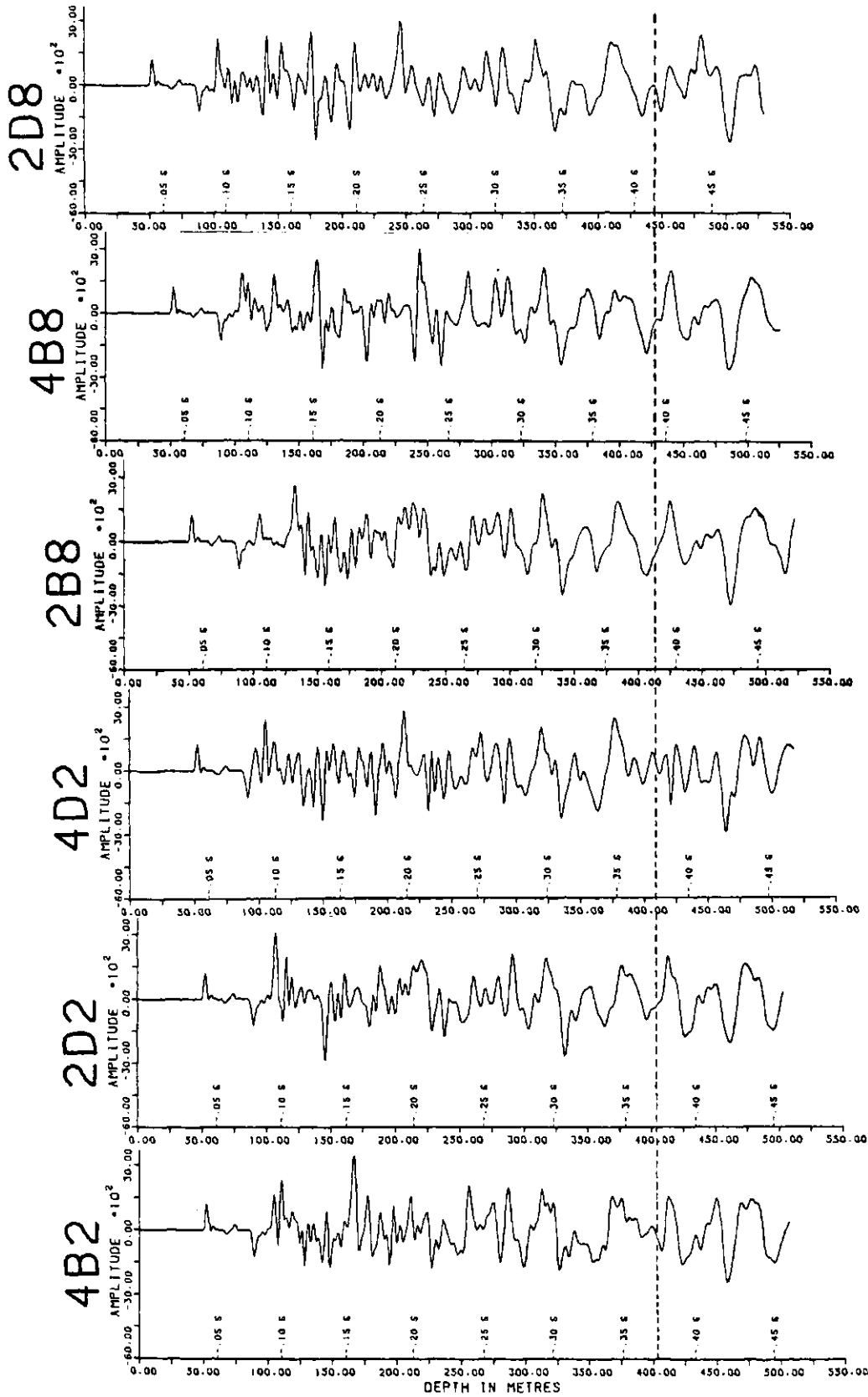


Figure 5.58 - Synthetic-seismogram cross-section, flattened on the top of the Mannville Group.

above the gas-zone peak (due to the zero-phase characteristic of the impulse source) to the end of the seismogram, the higher frequencies predominate. The importance of the gas zone to the Mannville portion of the synthetic seismogram will be discussed further in chapter six.

The McLaren formation coal-bed response varies somewhat from well to well but is always distinctly visible. In wells 4B8 and 2D8, the coal bed response is seen even though the low density character of the beds is very poorly developed. Therefore, the coal bed response is not solely a result of the presence of the coal bed; interference with some other reflection must be accentuating this response.

The opposite situation is seen with the reflections from the W1 cemented-zone. In all six wells, the response is as described for well 2B8 in section 5.3.2. That is, the W1 reflected response is not visible; it is obscured by interference from a larger trough occurring at the same time. Even in well 2D2, where there is no cemented zone at the base of the Waseca formation, this large trough is very similar to that of the wells where the cemented zone is present. In well 4D2, a small waveform is visible just below the larger trough. This may be the W1 zone response; modelling of the cemented zone could test this hypothesis.

Responses from the W6 oil-saturated zone vary from almost undetectable in well 4D2 to very large in well 2D8. Since the W6 zone is only 3 to 4 m thick, its response is weak and interference effects can either accentuate or nearly destroy the reflection.

The response from the W3 oil-saturated zone is clearly visible in all of the six wells. The W3 zone is about 5 or 6 m thick, but for the same reasons as for the W6 zone, its response is somewhat variable.

The Mannville geology of well 4-11 is different from that of the

the pilot-project wells (see section 4.1); thus, the resulting seismogram (in Figure 5.50) is particularly distinctive. The gas, MC, W6, and W3 peaks cannot be picked with confidence. Core control in well 4-11 is poor. The W6 and W3 beds cannot be distinguished on the geophysical logs and are likely not present in the well. There is a high-velocity zone at the base of the Waseca formation and although there is no core for verification, this zone will be called W1. A high-frequency trough, which is likely the response to the cemented zone, occurs at about 0.43 s. Three low amplitude, high frequency peaks are visible between about 0.41 and 0.42 s. These may result from thin oil-saturated sands in the McLaren formation.

If the 4-11 seismogram is shifted up in time by about 15 ms with respect to the 2B8 seismogram, the portion of these seismograms below 0.3 s are more similar than they were before. However, the Mannville formational boundaries no longer correlate. This means that the well-log markers in well 4-11 may not have been correctly chosen, which is possible in a well with poor core control and no density log. The other noticeable effect of shifting the seismograms is that the W6 and W3 peaks of well 2B8 now correspond to one large peak in well 4-11. This is significant because it suggests that, in moving from a well producing from the Waseca formation to a well that does not produce from the Waseca, the oil-zone reflections may change from a high frequency doublet to a low frequency singlet. This is also what the synthetic seismogram of Figure 5.3 showed when the Waseca oil zones was artificially shaled out. Unfortunately, the core and log control in well 4-11 is poor. It would be useful to repeat this test in a field where a dry well of known geology is located next to a producing well.

CHAPTER SIX

INTERPRETATION

6.1 Resolution Limits

When two or more geologic interfaces are located at a time spacing less than the duration of the of the seismic pulse, their reflections will be so close together that they will interfere. As the interval between the reflecting interfaces decreases, there will be less information from each of the individual reflections and more information from the combined reflections, or wavelet complex. Resolution is the process of separating reflections that are very close together, and resolving power is the ability to distinguish between the properties of these reflections (Widess, 1973). In contrast, the layer as a whole may be considered, instead of just the two reflecting surfaces of the layer. The threshold of detectability can then be defined as the minimum thickness that a layer must have in order to produce a visible reflection (de Voogd and den Rooijen, 1983).

Vertical resolution has been studied from different viewpoints by several authors in the past thirty years. Rayleigh chose a spacing of half the breadth of the main lobe of an optical diffraction-pattern to be the separation necessary to resolve the diffraction patterns (Jenkins and White, 1957, p. 299-301). Ricker (1953b) studied the resolving power of two velocity-type Ricker-wavelets of equal amplitude and polarity and determined that these wavelets were resolved at spacings greater than 0.428 of the wavelet breadth. Widess (1973) investigated the change of shape of the composite waveform produced by the interference of two zero-phase reflections, of equal amplitudes and opposite polarities, that were reflected from a progressively thinning

bed. He chose the limit of resolution to occur at one eighth of the predominant period of the incident wavelet, where the predominant period is the breadth of the central lobe of the waveform. Schoenberger (1974) concluded that zero-phase wavelets have better vertical resolving power than do minimum-phase wavelets. Koefoed (1981) proposed that the aspects of the breadth of the central lobe, the side-lobe ratio, and the amplitude of the side-tail oscillations together controlled the resolving power of the seismic wavelet. Most recently, Widess (1982) derived a quantitative formula (expressed by the variables of time, waveform, and signal purity) for the vertical resolving power of a seismic exploration system.

Of the above resolution concepts, that of Widess (1973) has been most commonly used by exploration seismologists. By graphical means, Widess observed that at a reflector spacing of less than one eighth of the predominant period of the incident wavelet, the shape of the composite reflection from the two interfaces of a thinning bed stabilized to a reasonable approximation of the time derivative of the incident wavelet. He defined the theoretical threshold of resolution to occur at that point. However, he qualified this by adding that, in a practical situation, other factors are also involved in determining this threshold. These factors include the presence of noise, the form and duration of the incident wavelet, the degree to which the wavelet is known prior to the analysis, and the analytical tools used. At the limit of resolution, the only information left in the composite waveform is for the combination of the two reflections; none is left for the individual reflections. Using the predominant period and velocity of the bed to compute the predominant wavelength λ_b , Widess defined a thin bed as one whose thickness is less than $\lambda_b/8$.

Reflections from very thin beds may be of surprisingly large amplitude. Widess concluded that the amplitude of a reflection from a thin bed is approximately proportional to the thickness of the bed and inversely proportional to the predominant frequency. For a typical geologic situation, Widess showed that the reflection from a bed of thickness $\lambda b/40$ will be about 0.3 of the amplitude that would result if the bed were very thick.

Maximum constructive interference occurs at a bed thickness of $\lambda b/4$ in Widess' model. This is called the tuning thickness. Interestingly, the spacing required for tuning is equal to the spacing of the Rayleigh criterion for resolution (Kallweit and Wood, 1982).

Kallweit and Wood (1982) studied that work of Rayleigh, Ricker, and Widess in order to develop concepts of resolution to unify the three viewpoints. They discovered that, in the noise-free case, there was no point where the composite wavelet of Widess (1973) stabilized into a replica of the derivative of the incident wavelet, except at zero separation of the reflecting interfaces of the bed. Although the composite waveform does not stabilize to exactly the derivative waveform at a reflector spacing of $\lambda b/8$, the shapes are very similar. Ricker (1953b), Sengbush et al. (1961), Meckel and Nath (1977), Neidell and Poggiagliolmi (1977), Ruter and Schepers (1978), and de Voogd and den Rooijen (1983) have all noted that the reflection from a thin bed approximates the shape of the time-differentiated incident-wavelet. The Widess criterion for resolution will, therefore, be used in this thesis.

Based on the theoretical resolution-limit of $\lambda b/8$, and using the average velocity of the bed, Table 6.1 shows the minimum frequencies necessary to theoretically resolve each of the five modelled zones discussed in section 5.3.2. The tuning frequencies for these zones are

TABLE 6.1. THEORETICAL RESOLUTION OF THE MODELLED ZONES

Edited Zone	Thickness of Edited Zone	Average Velocity of Edited Zone	Two-Way Travel-Time through Edited Zone	Minimum Frequency for Theoretical Resolution (and its Percentage of the Peak-Frequency Amplitude)	Tuning Frequency (and its Percentage of the Peak-Frequency Amplitude)
Colony fm. gas zone	12.5 m	1800 m/s	13.8 ms	18 hz (30%)	36 hz (100%)
McLaren fm. coal bed, MC	2.8 m	2500 m/s	2.2 ms	114 hz (20%)	227 hz (18%)
Waseca fm. oil saturated zone, W6	5.2 m	2400 m/s	4.4 ms	57 hz (45%)	114 hz (22%)
Waseca fm. oil saturated zone, W3	10.0 m	2400 m/s	8.4 ms	30 hz (80%)	60 hz (40%)
Waseca fm. cemented zone, W1	4.6 m	3300 m/s	2.8 ms	90 hz (16%)	179 hz (12%)

also shown. The peak frequency is defined as the frequency component having the largest value in the Fourier amplitude-spectrum (Kallweit and Wood, 1982). In this thesis, the amplitude spectra are plotted so that the peak frequency has an amplitude of 100. Below each frequency value in Table 6.1, the amplitude of this frequency (from Figure 5.7) is expressed as a percentage of the amplitude of the peak frequency.

The highest-amplitude reflection from beds with reflecting surfaces having reflection coefficients of equal magnitudes but opposite polarities occurs at the tuning thickness, $\lambda_b/4$ (Widess, 1973). The five zones modelled in the present study are either of high or low acoustic-impedance with respect to the strata on either side and therefore fit Widess' model. Table 6.1 shows that the gas zone should produce a very large amplitude, tuned-reflection of approximately 36 hz. This is what was observed, although the waveform had a measured frequency of 40 hz (see Table 5.1). The other four zones do not show such good correspondence between the theoretical tuning-frequencies and the measured-waveform frequencies, but the values are nevertheless very similar.

Timing errors and interference effects are partially responsible for the difference between the measured frequencies of the lower four reflected-waveforms in Table 5.1 and the tuning frequencies in Table 6.1. Inaccuracy in measuring the breadth of the reflected waveform is also responsible. At the tuning thickness there is no time error in picking the reflection; that is, the true separation of the reflecting interfaces is equal to the reflected-waveform separation (Widess, 1982). If there is not sufficient tuning-frequency content in the incident seismic-signal, timing errors will occur in the reflected waveforms. Interference effects are also important. Widess considered

an isolated thinning bed for his 1973 model although, in practical situations, the beds of interest are usually not isolated and most reflections will, therefore, be interference composites resulting from several interfaces. If the reflected waveform is not of high amplitude, interference from other reflections are more likely to change its shape. These effects explain why there was more variability seen in the reflection shape of the thinner McLaren coal and W6 zones than in the reflection shape of the thicker Colony gas and W3 zones when the input-parameter tests were made (see chapter 5).

As was illustrated by Meckel and Nath (1977), the amplitude and form of the reflection from a single unit is dependent on the proximity and spacing of acoustic interfaces above and below the unit under consideration. The tuning frequency required for the cemented zone W1 comprises only 12 per cent of the frequency content of the seismic signal in the Mannville section. The W1 reflection must have been of such small amplitude that interference from nearby, stronger reflections obscured the expected small trough.

In addition to the thickness of the unit, the other factor that is critical to the seismic response of a unit is the acoustic impedance difference between the unit and the over- and under-lying strata. A larger difference in acoustic impedance will produce a larger amplitude seismic-response. The nature of the acoustic-impedance boundaries of the unit will also affect the character of the reflected waveform. For example, a transitional upper or lower contact of a thin bed will cause a loss of high frequencies and a decrease in amplitude of the reflected composite waveform (Meckel and Nath, 1977).

6.2 Earth Filter

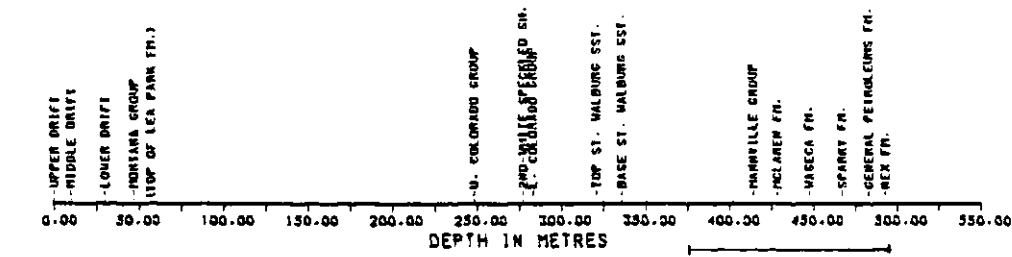
The earth acts as a natural filter to energy introduced into it. Frequency-dependent effects in the earth include absorption, dispersion, and the combined effects of transmission losses and the apparent attenuation due to intrabed multiples. Attenuation was defined by Sheriff (1973) as that portion of the decrease in seismic-signal strength with distance that depends on the physical characteristics of the transmitting media. This can involve reflection, scattering, and absorption. In the present study, a flat-layered model is used (Ganley, 1981) for the seismic synthesis and, therefore, scattering will not occur.

Absorption diminishes seismic amplitudes, as a function of distance travelled, by an irreversible conversion into heat (O'Doherty and Anstey, 1971). This loss is frequency selective and the seismic pulse loses amplitude and broadens by the preferential absorption of its higher frequencies. O'Doherty and Anstey (1971) suspected that absorption exhibits minimum phase behavior. As was discussed in section 5.1, Futterman (1962) proved that dispersion is a necessary consequence of absorption. Unlike absorption, dispersion does not involve a loss of energy. Dispersion affects the phase of the seismic pulse and produces a lengthening of the pulse, thereby decreasing its amplitude. In this thesis, absorption, and therefore, dispersion are determined by the Q value specified for each layer of the earth model.

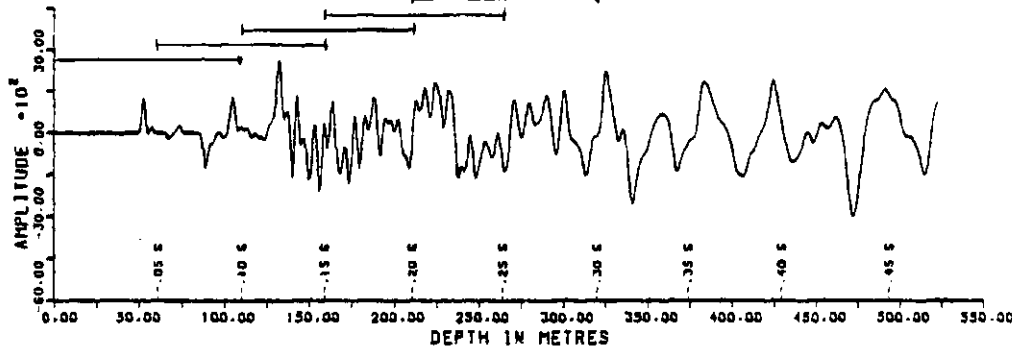
The Q s of the near-surface layers and the Mannville sequence are relatively low and so the largest absorption and dispersion effects will be seen there. The seismic source for the seismogram in Figure 6.1 is an impulse, but the spike shape is distorted (that is, broadened) even for the earliest reflections. With increasing time, the pulse

CELTIC 2B8 10 52 23 W3M

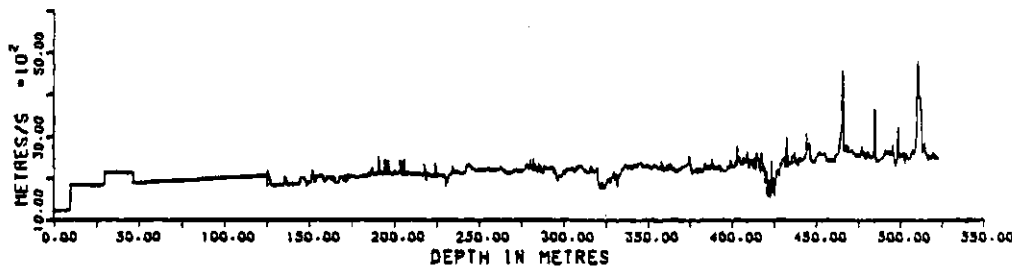
STRATIGRAPHIC
MARKER BEDS



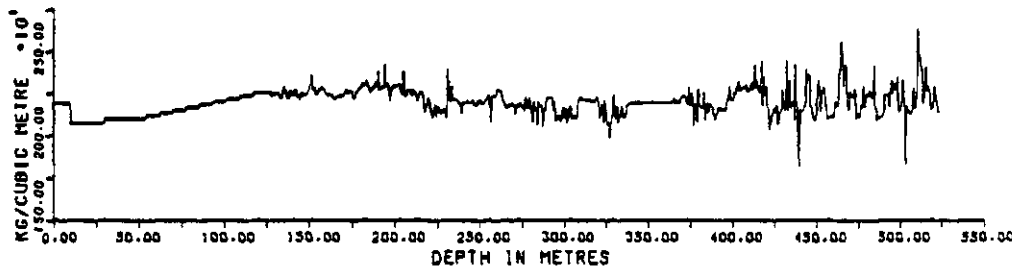
SYNTHETIC
SEISMOGRAM



VELOCITY



DENSITY



Q

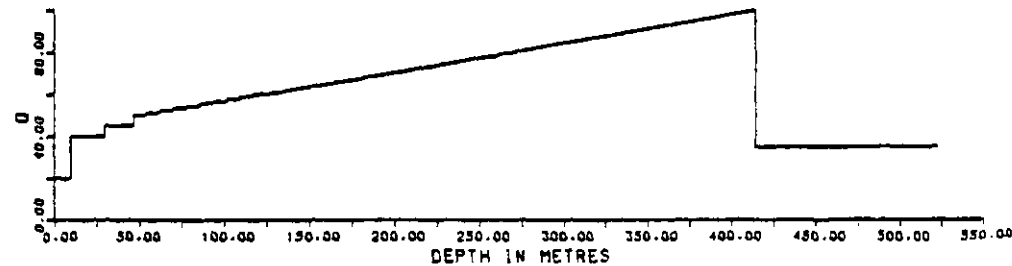


Figure 6.1 - Time gates through the synthetic seismogram constructed using an impulse source.

progressively broadens.

Futterman (1962) studied the time-domain effects of absorption and dispersion on an isolated pulse. When only absorption is present, the wave form is symmetrical about the maximum, its peak travels with a constant velocity, and there is an acausal precursor to the wavelet peak. When absorption and dispersion are both present, the waveform has a lower maximum, a sharpened front, and a definite (that is, causal) arrival time. In a practical seismic-situation, the pulses are not isolated. Instead, there is a complex of overlapping pulses, and the broadening of the pulse by absorption and dispersion increases the chance of overlap. The pulse amplitudes may therefore increase or decrease as a result of constructive or destructive interference.

Unlike absorption, the processes of reflection and transmission do not involve an irreversible loss of energy, but merely a redistribution of it. The reduction in amplitude of the transmitted wave is a natural result of the reflection of energy. For, if energy is reflected from an interface, it cannot be transmitted through it. O'Doherty and Anstey (1971) concisely stated this principle as "more up, less down". The transmission loss associated with a single reflector is insignificant, but the cascaded transmission-losses through a large number of interfaces can be so large that no energy should be propagated. For this reason, O'Doherty and Anstey differentiated between cyclic patterns of sedimentation, which have alternate thin layers of high and low-velocity materials, and transitional patterns of sedimentation, which have steady gradations of velocity within thick layers. The entire logged section of the seven wells used in this study are somewhat cyclic, and the Mannville sections of the wells are decidedly cyclic due to the interbedded, high acoustic-impedance cemented-zones and the low

acoustic-impedance coal and oil-saturated sand-zones.

Transmission losses in the seismic section cannot be considered separately from multiple reflections. Whereas transmission losses lower the amplitudes reasonably uniformly at all frequencies, the constructive effect of many intrabed (or very-short-delay) multiples systematically tends to raise the amplitudes at the low-frequency end of the spectrum and lower those at the high-frequency end (O'Doherty and Anstey, 1971; Schoenberger and Levin, 1974). Schoenberger and Levin (1978) found that these intrabed multiple-reflections were so successful that, at low frequencies, the effect of amplitude reduction due to transmission losses was compensated for almost completely in 23 of the 25 wells that they studied. At reflection times of usual interest, the useful seismic information in a cyclic sequence is carried almost entirely by the very-short-delay reflections (O'Doherty and Anstey, 1971).

In a cyclic sequence, the combined effects of transmission loss and intrabed multiple-reflections are similar to the effects of absorption and, therefore, these effects may be confused. Whereas the effects may be confused, the mechanisms are different; absorption is an intrinsic property of a rock, but the combined effects of transmission loss and intrabed multiples occur simply as a result of the position of the rock layers. The time delay introduced by the transfer of energy to intrabed multiples produces a broadening of the pulse that implies a high-frequency cut similar to that produced by absorption (O'Doherty and Anstey, 1971). Schoenberger and Levin (1974) compared the spectral tilting due to absorption and intrabed multiples and found that both losses can be expressed with an attenuation coefficient that is proportional to the first power of frequency. As well, the intrabed multiple effect is minimum phase (Anstey, 1977, p. 139). The

frequency-dependent loss due to intrabed multiples accounted for between 15 and 70 per cent of the total observed frequency dependent loss in a study of 31 wells (Schoenberger and Levin, 1978).

The effects of wavelet broadening and loss of high frequencies noticed in Figure 6.1 are almost certainly due in part to transmission loss and intrabed multiples. In fact, without the intrabed multiples, it may not be possible to return energy from the Mannville section.

The amplitude spectra in this thesis that were calculated using the impulse source are the amplitude-versus-frequency portion of the transfer function of the modelled earth system. Sheriff (1973) defined the transfer function as the frequency-domain characteristics of a system. The transfer function contains the same information as does the impulse response in the time domain, and is convertible to it through the Fourier transform. The transfer function, contains all of the information about the system and it is represented by both the amplitude and phase spectra. In this study only the amplitude spectra have been calculated and, therefore, only the amplitude-versus-frequency characteristics of the system can be discussed.

The amplitude spectrum portion of the transfer function for the time-gate corresponding to the Mannville portion of the synthetic seismogram is shown in Figure 6.2. In Figure 6.2, one can see that the high frequencies (that is, from 60 to 250 hz) and the very low frequencies (below 25 hz) have been severely attenuated in comparison to the peak frequency of 39 hz. Frequencies from 250 to 500 hz are not included in this discussion of earth filtering as they have been attenuated by the Butterworth low-pass filter discussed in section 5.1. The velocity and density logs of well 2B8 (see Figure 5.4) represent a quasi-cyclic to cyclic sequence and, therefore, the high-cut nature of

CELTIC 2B8 10 52 23 W3M

MINIMUM Q=20 AND MAXIMUM Q=100
 SOURCE BURIED AT A DEPTH (M) = 29.9
 TYPE OF WAVELET : IMPULSE
 BUTTERWORTH ANTI-ALIAS FILTER INCLUDED IN SYNTHETIC TRACE
 TIME GATE (IN S) FOR AMPLITUDE SPECTRUM = .405 TO 0.493
 TIME GATE CORRESPONDS TO:
 TOP OF MANNVILLE GRP. (414.0 M) TO END OF INPUT LOGS (523.2 M)
 SAMPLE INTERVAL IN TIME DOMAIN (S) = .0010
 SAMPLE INTERVAL IN FREQUENCY DOMAIN (HZ) = 7.812
 NUMBER OF FREQUENCIES ANALYSED = 65.
 HANNING SMOOTHING APPLIED TO SPECTRUM
 PERCENT OF TRACE ELEMENTS TAPERED AT EACH END = 10.

AMPLITUDE SPECTRUM OF SYNTHETIC SEISMOGRAM

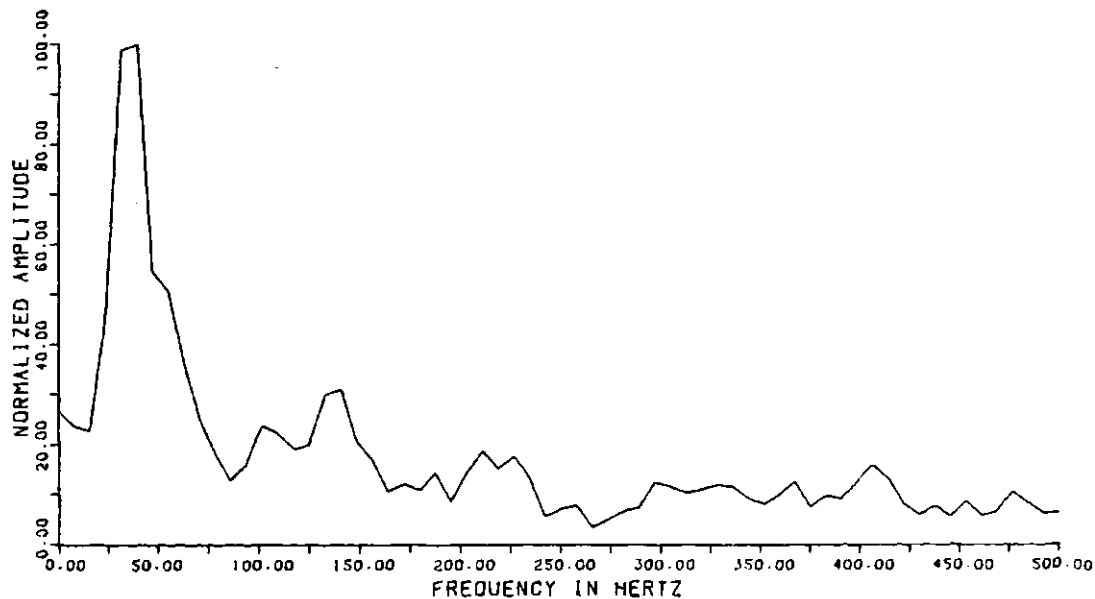


Figure 6.2 - Amplitude spectrum from seismogram constructed using an impulse source.

the impulse function is to be expected. As well, absorption in the subsurface layers contributes to the high-cut form of the amplitude spectrum. It is impossible to say which of the two effects predominates.

The low-cut form of the amplitude spectrum is explainable based on work by Morlet et al. (1982). These authors studied seismic energy propagation through cyclic series and classified it according to the ratio of the signal wavelength to the spatial period of the cyclic medium. For example, in well 2B8, where the thickness of an average acoustic impedance layer is 5 m, the thickness of the spatial period of the cyclic medium will be 10 m. For low frequencies such as 5, 10, and 20 hz, the wavelengths will be (using a velocity of 2500 m/s) 500, 250, and 125 m. In these cases, the ratio of the signal wavelength to the spatial period of the medium falls into the low-frequency category of Morlet et al., and the cyclic medium will appear fully transparent to the propagating seismic-energy. No reflection will be seen. Similarly, the opposite case of superreflectivity of high frequencies (Morlet et al., 1982) will contribute to the high-cut characteristic of the amplitude spectrum.

In Figure 6.1, the dominant frequency content of the seismogram can be seen to change abruptly from relatively high frequencies to much lower frequencies between 0.25 s and 0.30 s. To study the cause of this change in frequency content with depth, amplitude spectra with 0.1 s time gates were calculated at 0.05 s spacings through the seismogram. The amplitude spectrum for the time gate of 0.15 to 0.25 s is shown in Figure 6.3, the amplitude spectrum for the time gate of 0.25 to 0.35 s is shown in Figure 6.4, and the amplitude spectrum for the time gate of 0.30 to 0.40 s is shown in Figure 6.5. The sections of the seismogram

CELTIC 2B8 10 52 23 W3M

MINIMUM Q=20 AND MAXIMUM Q=100
 SOURCE BURIED AT A DEPTH (M) = 29.9
 TYPE OF WAVELET : IMPULSE
 BUTTERWORTH ANTI-ALIAS FILTER INCLUDED IN SYNTHETIC TRACE
 TIME GATE (IN S) FOR AMPLITUDE SPECTRUM = .150 TO 0.250
 TIME GATE CORRESPONDS TO:

SAMPLE INTERVAL IN TIME DOMAIN (S) = .0010
 SAMPLE INTERVAL IN FREQUENCY DOMAIN (HZ) = 7.812
 NUMBER OF FREQUENCIES ANALYSED = 65.
 HANNING SMOOTHING APPLIED TO SPECTRUM
 PERCENT OF TRACE ELEMENTS TAPERED AT EACH END = 10.

AMPLITUDE SPECTRUM OF SYNTHETIC SEISMOGRAM

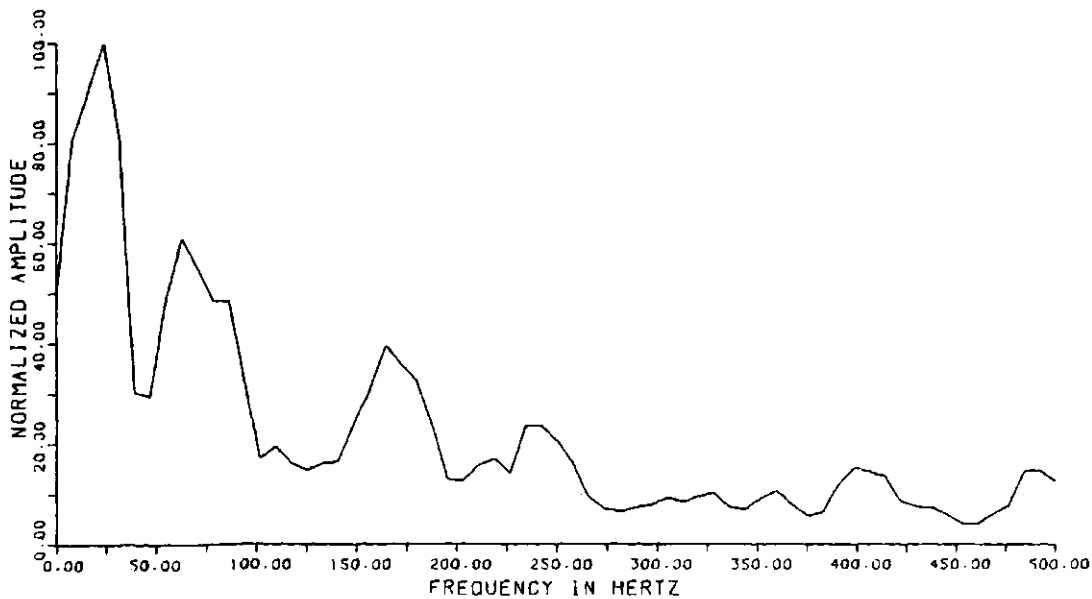


Figure 6.3 - Amplitude spectrum for the time gate from 0.15 to 0.25 s.

CELTIC 2B8 10 52 23 W3M

MINIMUM Q=20 AND MAXIMUM Q=100
 SOURCE BURIED AT A DEPTH (M) = 29.9
 TYPE OF WAVELET : IMPULSE
 BUTTERWORTH ANTI-ALIAS FILTER INCLUDED IN SYNTHETIC TRACE
 TIME GATE (IN S) FOR AMPLITUDE SPECTRUM = .250 TO 0.350
 TIME GATE CORRESPONDS TO:

SAMPLE INTERVAL IN TIME DOMAIN (S) = .0010
 SAMPLe INTERVAL IN FREQUENCY DOMAIN (HZ) = 7.812
 NUMBER OF FREQUENCIES ANALYSED = 65.
 HANNING SMOOTHING APPLIED TO SPECTRUM
 PERCENT OF TRACE ELEMENTS TAPERED AT EACH END = 10.

AMPLITUDE SPECTRUM OF SYNTHETIC SEISMOGRAM

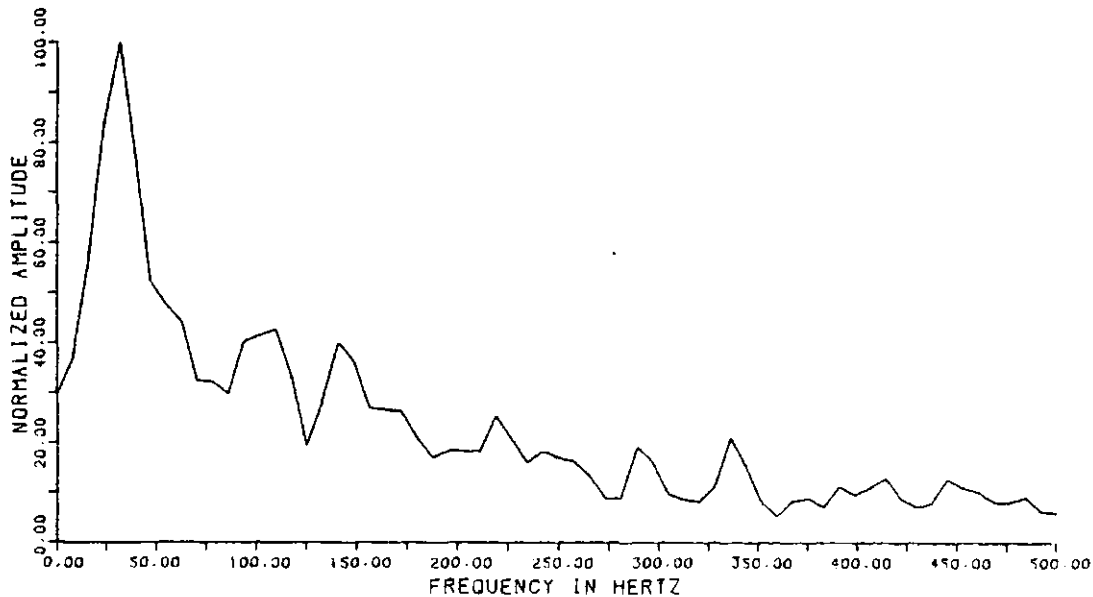


Figure 6.4 - Amplitude spectrum for the time gate from 0.25 to 0.35 s.

CELTIC 2B8 10 52 23 W3M

MINIMUM Q=20 AND MAXIMUM Q=100
 SOURCE BURIED AT A DEPTH (M) = 29.9
 TYPE OF WAVELET : IMPULSE
 BUTTERWORTH ANTI-ALIAS FILTER INCLUDED IN SYNTHETIC TRACE
 TIME GATE (IN S) FOR AMPLITUDE SPECTRUM = .300 TO 0.400
 TIME GATE CORRESPONDS TO:

SAMPLE INTERVAL IN TIME DOMAIN (S) = .0010
 SAMPLE INTERVAL IN FREQUENCY DOMAIN (HZ) = 7.812
 NUMBER OF FREQUENCIES ANALYSED = 65.
 HANNING SMOOTHING APPLIED TO SPECTRUM
 PERCENT OF TRACE ELEMENTS TAPERED AT EACH END = 10.

AMPLITUDE SPECTRUM OF SYNTHETIC SEISMOGRAM

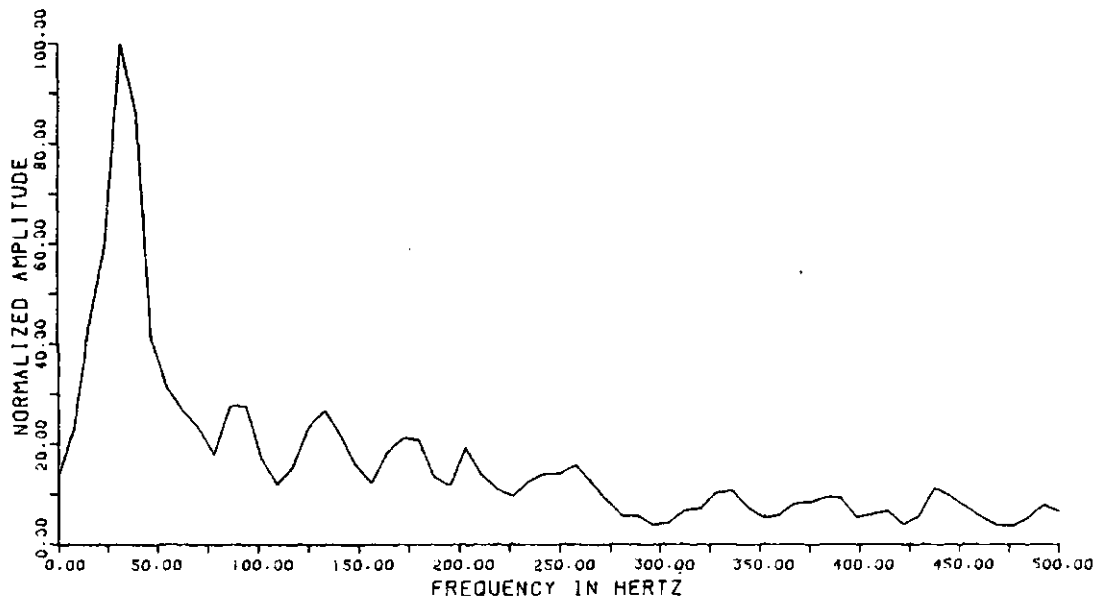


Figure 6.5 - Amplitude spectrum for the time gate from 0.30 to 0.40 s.

included in each amplitude spectrum are marked on Figure 6.1. In comparing the time gate of 0.15 to 0.25 s (Figure 6.3) to the time gate of 0.25 to 0.35 s (Figure 6.4), the peak frequency in Figure 6.4 has stabilized at 39 hz. At a time gate of 0.30 to 0.40 s, the amplitude spectrum is very similar to that of the Mannville section (Figure 6.2).

A series of three layers with alternating high and low acoustic-impedances, each averaging 15 m in thickness, is postulated to be the cause of this sudden change to a 39 hz dominant-frequency. The top of the shallowest layer occurs at 290 m, or approximately 0.28 s. The deepest layer is of low velocity and density and corresponds to the St. Walburg Sandstone. The shallowest layer has a similar velocity and density and may correspond to an unnamed sandstone-layer. In any case, the tuning frequency for this series of three, 15 m thick layers will occur at 37 hz (using an average velocity of 2200 m/s). As was mentioned in section 6.1, at the tuning thickness the reflection amplitudes, for beds with interfaces having reflection-coefficients of opposite polarity will be at the maximum. But, in this case, the reflection amplitudes will be even larger than the tuning response for a single bed. This is because, as Sengbush et al. (1961) noted, "Tuning of two or more reflections results in the increased reflection amplitude due to constructive addition. Additional properly spaced interfaces will continue to increase the maximum amplitude....".

Approximately 75 m deeper in the section, the Colony gas-zone, which is 12.5 m thick in well 2B8, again sets up a high-amplitude tuned-reflection of about 37 hz. Due to these tuned reflections, it is not surprising that the dominant frequency in the amplitude-spectrum portion of the transfer function of the Mannville sequence (Figure 6.2) is at 39 hz.

The amplitude spectra of six of the seven wells studied (Figures 5.51 through 5.57) have peak frequencies of 39 hz. The only exception is the amplitude spectrum of well 4D2, which has a peak frequency of 93 hz (Figure 5.53). To determine the cause of this difference, amplitude spectra were constructed at time gates through the 4D2 synthetic seismogram, in the same way as was done for well 2B8. The frequency content and general shape of the 2B8 and 4D2 seismograms were similar until about 0.37 s on the 4D2 seismogram. At this point, the frequency content increased dramatically. The velocity and density logs for the two wells were compared to determine the cause of the increased frequency content. The main difference between the two wells is that, in well 4D2 the Colony gas-zone is interrupted by a thin, very high-velocity and density layer. Therefore, instead of re-inforcing the 40 hz tuning-frequency of the upper portion of the seismogram, the interrupted gas-zone of well 4D2 introduces a higher frequency-content to the lower sections of the seismogram.

Based on the above study of the filtering effects of the earth model used to construct the synthetic seismograms, it is unlikely that dominant frequencies higher than 40 hz will be recorded from the Mannville section of the Celtic pool, or from the Mannville section of any area of similar geology, if there is gas present in the Colony formation. In the noiseless theoretical-situation, the amplitudes of the frequency components required to detect the zones of economic interest are high enough to make the reflections visible, even when the dominant frequency is only 40 hz. However, in well 4D2, the dominant frequency is higher and the amplitudes of these economically-important reflections are also higher, (with the exception of the W6 reflection, which is probably reduced in amplitude due to destructive interference)

and these reflections are more likely to be seen in the presence of noise. In the case of real seismic-recording, noise levels could obscure the low-amplitude, high-frequency reflections from the oil zones unless special care is taken to enhance the necessary frequency range.

6.3 Physical Rock-Properties

The rock bulk-properties of velocity, density, and quality factor (Q) control the seismic data that are recorded. But, these rock bulk-properties are affected by fundamental, physical rock-properties, such as mineral composition, grain-size distribution and shape, cementation, porosity, pore size and shape, and the density of the rock framework and pore fluid. In the preceding sections of this thesis, the calculated, theoretical seismic-reflections have been compared only to the rock bulk-properties. In this section, the measured, physical rock-properties of porosity, permeability, oil saturation, and clay content, which were discussed in section 4.4, will be compared to the rock bulk-properties of velocity and density, which were derived from geophysical logs. Factors affecting the Q value have been discussed in section 4.5. In addition, comments will be made about the significance of the lithotype, amount and type of cementation, and the type of pore fluid.

A theoretical approach to the study of elastic-wave propagation in porous media that will fit all types of rocks and environmental situations has not yet been developed. The contributions of the physical rock-properties to the rock bulk-properties are interrelated and may vary greatly depending on environmental factors such as differential pressure, degree of fluid saturation, and temperature. Theories relating the physical properties of the rock framework and the

pore-fluid saturant to the rock bulk-properties have been proposed by Gassman (1951), Brandt (1955), Wyllie et al. (1956), Biot (1956a, 1956b), Geertsma (1961), Kuster and Toksoz (1974), O'Connell and Budiansky (1974), and Walsh and Grosenbaugh (1979).

If a model to relate fundamental, or physical rock-properties to rock bulk-properties were available, it would then be possible to directly determine, or to infer fundamental rock-properties that were previously not easily derived from seismic information. For example, the physical rock-properties of porosity, permeability, cementation, lithotype, and type of pore fluid would be of economic interest to heavy-oil exploration and development. However, no single theoretical model is suitable and, therefore, in this section, the relationship between the physical rock-properties obtained from core analyses and the rock bulk-properties obtained from the geophysical logs will be compared both to observed experimental results and to the theoretical models.

For any depth of burial (that is, differential pressure), the velocity of unconsolidated sands in young sedimentary basins is an approximate linear function of porosity; as porosity increases, velocity decreases (Gardner et al., 1974). In Figure 6.6, the velocity, density, core data, and porosity for the upper portion of the cored interval of well 2B8 are shown. A key to the core-data symbols is presented in Figure 6.7. The general relationship of increased velocity with decreased porosity can be seen in Figure 6.6; the cemented zones of any lithofacies have the lowest porosities and highest velocities, whereas, the uncemented lithofacies L, T, and M sand beds have the highest porosities and lowest velocities. There is also a direct correspondence between rock bulk-density and porosity, since, fluid-filled pore-space is much less dense than rock. As with velocity,

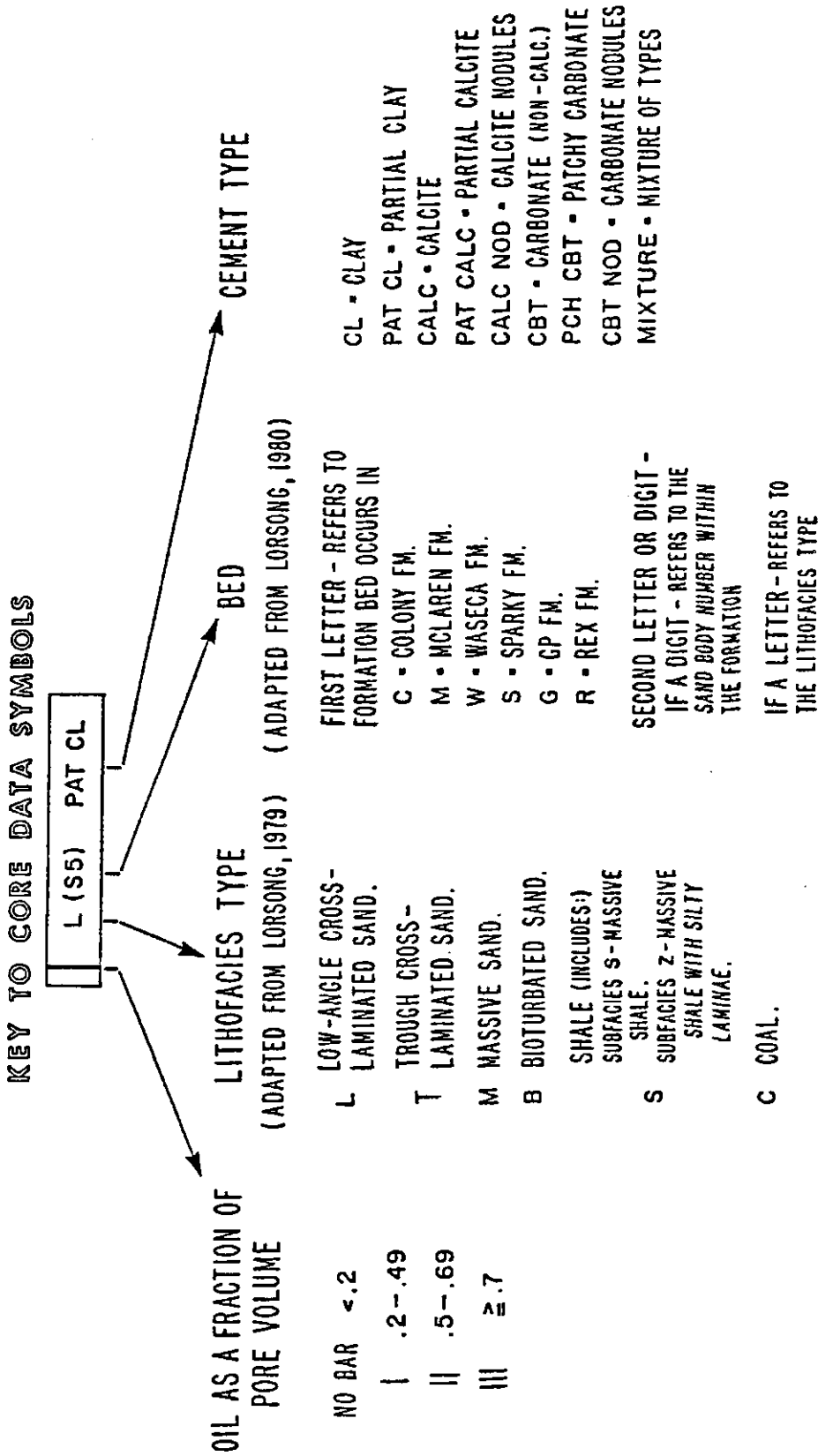


Figure 6.7 - Key to the core-data symbols.

this relationship is best documented in the cemented zones and sand beds. The coal beds show the only major departure from the rule. In those beds, the density, velocity, and porosity are all low. Porosity is an important parameter in determining the rock bulk-properties. Each of the eight theoretical models for elastic-wave propagation mentioned above include porosity as a variable.

Permeability normally increases as porosity increases (Gregory, 1977). This would be expected, since permeability is defined as a measure of the ease with which a fluid can pass through the pore spaces of a formation (Sheriff, 1973). Figure 6.8 shows permeability-to-air plotted beside the same data as in Figure 6.6. In general, velocity and density decrease as the permeability to air increases. This is the same relationship that was noted for porosity in Figure 6.6. Specific examples of this trend can be seen in the lithofacies L beds; the three highest permeability values are from facies L beds and all of the other high permeability values are from high sand-content, facies B beds or from facies L beds. These same beds are almost always of lower velocity and density than the adjacent, lower permeability beds. Lithofacies T and M sand beds do not show high permeabilities, although their porosities are relatively high, and so, one can infer that only a small amount of clay is needed to reduce the permeability severely.

Permeability is usually ignored in the theoretical formulations of wave propagation. In fact, one of the restrictions of the Biot theory (Biot, 1956a, 1956b) and the Geertsma theory (Geertsma, 1961) is that the walls of the main pores are impervious (King, 1966). The Kuster-Toksoz theory (Kuster and Toksoz, 1974) also assumes non-interaction between pore spaces or inclusions. Only the Walsh-Grosenbaugh theory (Walsh and Grosenbaugh, 1979) recognizes that the pore phase of rocks is a

CELTIC 2B8 10 52 23 W3M

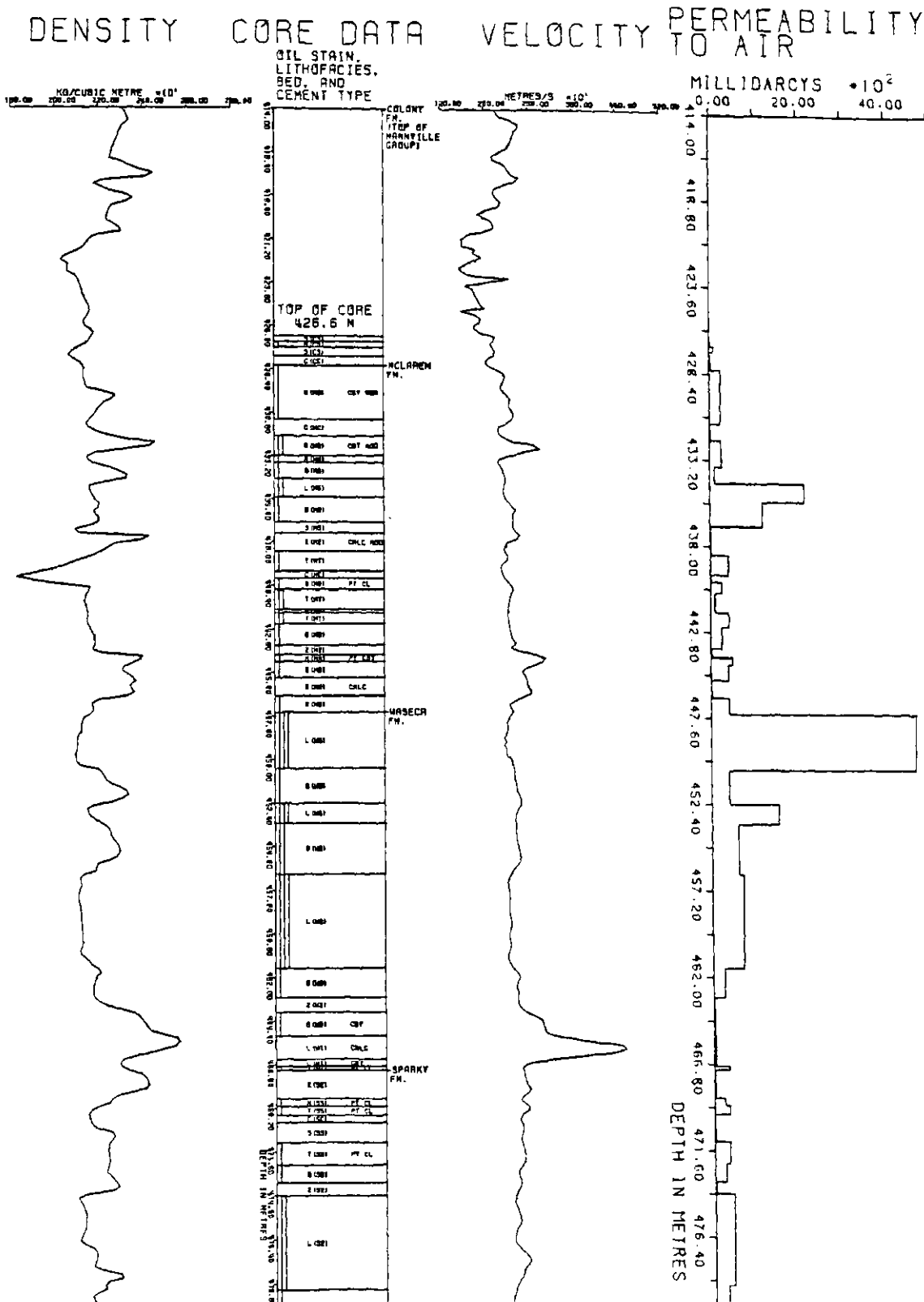


Figure 6.8 - Relationships among permeability to air values, well logs, and core data.

continuous network of cavities.

Porosity and permeability are directly related to the amount of cementation. The code for the type of cementation observed in the core samples is explained in Figure 6.7. Cemented beds show a reduced porosity and permeability, and an increased velocity and density in Figures 6.6 and 6.8. For example, there is a zone at the base of the Waseca formation and top of the Sparky formation that is partially cemented for about 10 m. This zone has very low average-porosities and permeabilities in comparison to the rest of the cored section. Only the coal beds have lower porosities.

Clay content as a percentage of rock volume (see Figure 6.9) is directly related to lithofacies type. Clay content ranges from 2 per cent for lithofacies-type L to 75 per cent for subfacies-type S. Gardner et al. (1974) have plotted velocity versus density relationships in rocks of different lithotypes for a large number of sedimentary rocks from a variety of geologic environments. The range of velocities and densities for the shales and sandstones in their plot is large. Moreover, there is extensive overlap of the values in shales and sandstones. Sandstone velocities and densities, however, may reach slightly higher values than those for shale. As would be expected from the above discussion the clay content values in Figure 6.9 do not show an obvious relationship to velocity and density. Other factors, such as saturation effects, porosity, and cementation affect these values more. For example, lithofacies L beds have the lowest clay contents, but their velocities and densities may be low if the sand is porous and oil saturated (as in beds W3 and W6), or high if the sand is cemented and non-porous (as in bed W1). On the other hand, the subfacies S and Z beds have the highest clay contents but their densities and velocities

CELTIC 2B8 10 52 23 W3M

DENSITY CORE DATA VELOCITY CLAY CONTENT

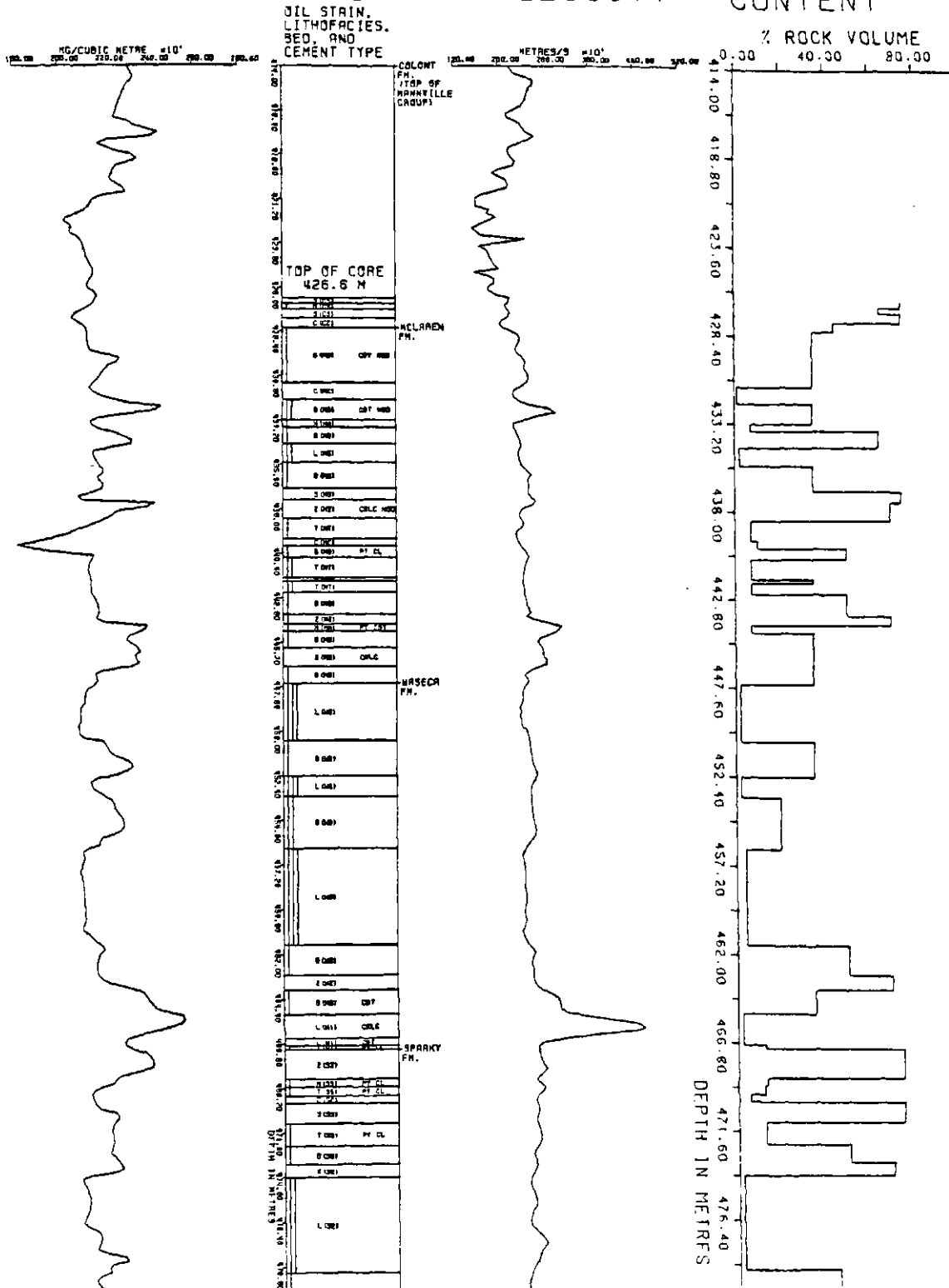


Figure 6.9 - Relationships among clay content, well logs, and core data.

are unexceptional. The amount of clay content is not directly included in any of the theoretical models for elastic wave-propagation, but its effect would be indirectly felt through its influence on other parameters in the formulae.

Velocity, and to a lesser extent density, are strongly dependent on saturation conditions. Saturation conditions include the type of pore fluid (for example, water, brine, gas, or oil) and the degree of saturation (that is, complete or partial saturation). Numerous laboratory and theoretical studies of saturation effects have been made. All of the theoretical models for elastic wave-propagation include parameters that are directly or indirectly affected by the pore fluid. Saturation effects have been studied with respect to porosity, pore shape, pressure, and the distribution of the fluids within the pore spaces. General conclusions of this work and their applications to the present study are as follows:

1. The velocity difference between fluid and gas saturated rocks is distinguishable only at shallow depths, that is, low differential pressures (Wyllie et al., 1958; Geertsma, 1961; Gardner et al., 1974; Toksoz et al., 1976). Toksoz et al. (1976) estimated that at differential pressures corresponding to depths of greater than 2500 m, in normally-pressured zones, the gas effect will not be visible. Due to the shallow depth of the Mannville rocks in the study area, the gas effect should be readily visible.
2. A small quantity of gas (about 5 per cent) in a water saturated rock reduces the rock velocity significantly, especially at lower differential-pressure, as are present in the study area. On the other hand, the presence of oil in water-filled pores has a much less pronounced effect, and oil content is more linearly related to velocity

(Domenico, 1974, 1976, 1977). The effect of gas saturation should be much stronger than that of oil saturation in the study area.

3. The compressional-wave velocity in a rock with pore fluid that is about 5 per cent gas in brine could be lower than the velocity in a pure gas-saturated rock (Toksoz et al., 1976). This means that the amount of gas in the Colony formation will not be linearly related to its effect on the seismogram.

4. Velocity has little diagnostic value in differentiating between oil and water reservoirs, and the prospect for identifying the gravity of crude oil from velocity data is very poor (Gregory, 1976). This means that the low velocity noticed in the W6 and W3 oil saturated sands is more likely due to their high porosities than their high oil contents.

In Figure 6.10, lithofacies beds with a high percentage of oil saturation show a generally lower velocity and density. Both Gregory (1976) and Domenico (1974) predicted that the effect of oil versus water saturation would cause only slightly decreased rock velocities. Because oil saturated zones are also of high porosity, part of the low velocity effect in the oil zones must be due to their high porosity.

The Colony gas zone has a low velocity, as would be expected for even small amount of gas saturation. Density values through this zone are affected to a relatively lesser degree than are the velocity values, suggesting that the gas concentration is small.

6.4 Possible Correlation to Real Seismic-Data

Synthetic seismograms have been used since the late 1950s because they provide a good fit to seismic traces in most cases. Synthetic seismograms allow geologic insight to the seismic section, and without this type of control, the significance of the subtle waveform changes

CELTIC 2B8 10 52 23 W3M

DENSITY CORE DATA VELOCITY OIL SATURATION

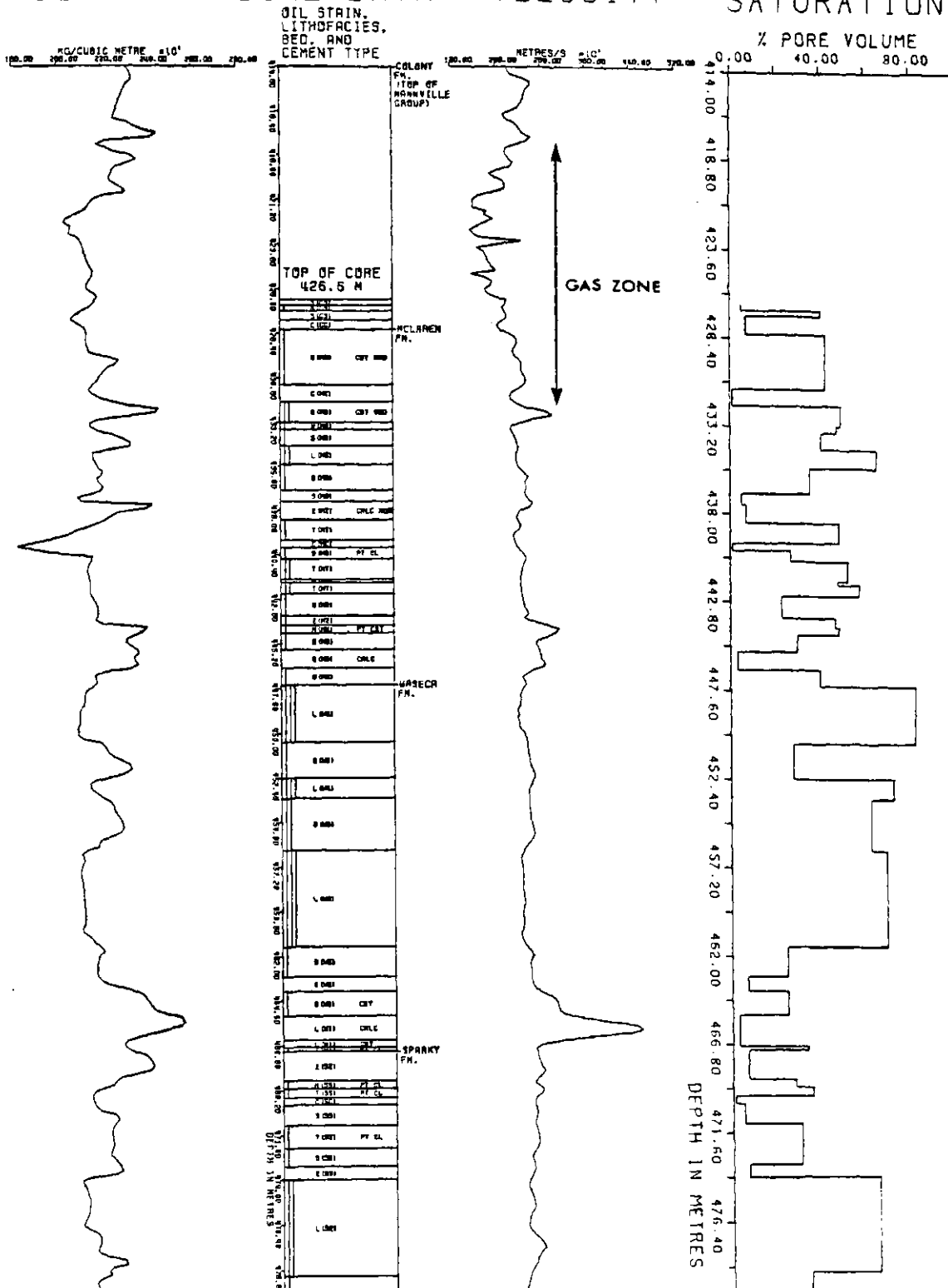


Figure 6.10 - Relationships among oil-saturation values, presence of gas, well logs, and core data.

important to stratigraphic seismic mapping cannot be evaluated. In this study, synthetic seismograms were used to verify that thin beds within the Mannville can be mapped. They were also used to analyse the effect of replacing the coal beds, oil-saturated sand-beds, and gas zone with brine-saturated, shaley beds. If real seismic-data were available in the study area, the synthetic seismograms would provide a link between the geology and the seismic section. In addition, the synthetic seismograms have demonstrated that frequencies in the 60 to 115 Hz range will provide the strongest reflections from the thin, oil-saturated sand-beds in the Waseca formation. Data acquisition and processing techniques can now be directed toward improving the amplitudes of the frequencies in this range. Techniques for high-resolution seismic-recording are discussed by Farr (1976), Ziolkowski and Lerwill (1979), and Denham (1981).

There can be many differences between synthetic and real seismic-data, but if care is taken in selecting the synthetic-seismogram algorithm, in choosing and correcting the data used to construct the synthetic seismogram, and in processing the real seismic-section, many of these differences lose their significance. Assumptions made in the synthetic-seismogram algorithm and the importance of these assumptions to the present study were discussed in chapter three. In chapter four, the collection and preparation of the data used to construct the synthetic seismogram was examined. No real seismic-data was available in the study area, therefore, the substantial subject of processing the seismic data to more closely resemble the synthetic data was not considered.

Many of the differences between synthetic and real seismic-data stem from the inherent differences in what seismic traces and well logs

measure. Sheriff (1977) and Ausburn et al. (1978) studied these differences and the steps that may be taken to reduce their effects. However, one of the differences between well-log and seismic data can be turned to the advantage of this study. Well logs measure rock properties in a limited zone surrounding the borehole, and so, the invasion of mud filtrate will usually reduce the effect of hydrocarbons on well-log measurements (Ausburn, 1977). Seismic waves, however, are reflected from large areas called Fresnel zones. Synthetic seismograms are constructed from well logs and, therefore, the hydrocarbon effects seen on seismograms are minimum effects. In other words, the response to hydrocarbons could be more prominent on real seismic-traces than on synthetic seismic-traces. In the present study, this would mean that the gas, W6, and W3 peaks resulting from the presence of hydrocarbons (Figure 5.4) could be more pronounced on real seismic-data, if the deleterious effects of factors such as noise are not severe.

CHAPTER SEVEN

CONCLUSION

The seismic-reflection method is potentially useful to map zones of economic interest in the Celtic field, if sufficiently high frequencies can be returned from the Mannville section. Based on studies of synthetic seismograms, these frequencies are in the range of 60 to 115 hz. But, the natural filtering of the earth forces a dominant frequency of 40 hz on the Mannville section of the majority of wells studied. In the synthetic-seismic data, a signal with the 40 hz predominant frequency had enough high-frequency content to detect the zones of interest. However, this synthetic data is noise-free; in real-seismic records, noise may mask the low-amplitude, high-frequency content. Before seismic programs are started, techniques of data acquisition and processing must be chosen to accentuate frequencies in the desired range.

There is a simple one-to-one relationship between the zones of economic interest and their theoretical seismic response. Subtle stratigraphic changes, or even changes in the saturating fluids in the strata can be directly detected if sufficiently high frequencies and low noise levels are present.

Mannville geology is extremely variable. The specific results of this thesis will not likely be applicable in other heavy-oil fields, but the method used in this study could certainly be applied to other heavy-oil areas, and even to coal or mineral exploration and development.

REFERENCES

- American Petroleum Institute, 1960, API recommended practice for core-analysis procedure: Washington, American Petroleum Institute.
- Anstey, N.A., 1966, Wiggles: Tulsa, Seismograph Service Corporation.
- 1977, Seismic interpretation: the physical aspects: Boston, International Human Resources Development Corporation.
- Ausburn, B.E., 1977, Well log editing in support of detailed seismic studies: Presented at the SPWLA eighteenth Annual Logging Symposium.
- Ausburn, B.E., Nath, A.K., and Wittick, T.R., 1978, Modern seismic methods--An aid for the petroleum engineer: J. of Petroleum Technology, v. 20, p. 1519-1529.
- Bath, M., 1974, Spectral analysis in geophysics: Amsterdam, Elsevier Scientific Publishing Co.
- Biot, M.A., 1956a, Theory of propagation of elastic waves in a fluid-saturated porous solid; I: Low frequency range: J. of the Acoustical Soc. of America, v. 28, p. 168-178.
- 1956b, Theory of propagation of elastic waves in a fluid-saturated porous solid; II: Higher frequency range: J. of the Acoustical Soc. of America, v. 28, p. 179-191.
- Blatt, H., Middleton, G., and Murray, R., 1972, Origin of Sedimentary Rocks: Englewood Cliffs, Prentice-Hall.
- Brandt, H., 1955, A study of the speed of sound in porous granular media: J. of Applied Mechanics, v. 22. p. 479-486.
- Burke, K.B.S., 1968, A seismic study of the surficial deposits in the Stenen area, Saskatchewan: Geol. Survey of Canada, Paper 68-60.

- Christiansen, E.A. (editor), 1970, Physical environment of Saskatoon, Canada: National Research Council of Canada publication number 11378.
- Christopher, J.E., 1974, The Upper Jurassic Vanguard and Lower Cretaceous Mannville Groups of south-western Saskatchewan: Sask. Dept. of Mineral Resources Report 151.
- 1980, The Lower Cretaceous Mannville Group of Saskatchewan--A tectonic overview: Sask. Geol. Soc. Special Publ. No. 5, p. 3-32.
- Christopher, J.E., Kent, D.M., and Simpson, F., 1971 Hydrocarbon potential of Saskatchewan: Sask. Dept. of Mineral Resources Report 157.
- Crain, E.R., and Boyd, J.D., 1979, Determination of seismic response using edited well log data: Presented at the Seventh Formation Evaluation Symposium of the Canadian Well Logging Soc.
- Denham, L.R., 1981, Extending the resolution of seismic reflection exploration: J. of the Canadian Soc. of Exploration Geophysicists, v. 17, p. 43-54.
- Domenico, S.N., 1974, Effect of water saturation on seismic reflectivity of sand reservoirs encased in shale: Geophysics, v. 39, p. 759-769.
- 1976, Effect of brine-gas mixture on velocity in an unconsolidated sand reservoir: Geophysics, v. 41, p. 882-894.
- 1977, Elastic properties of unconsolidated porous sand reservoirs: Geophysics, v. 42, p. 1339-1368.
- Dunning, N.E., Henley, H.J., and Lange, A.G., 1980, The Freemont field: An exploration model for the Lloydminster area: Sask. Geol. Soc. Special Publ. No. 5, p. 132-148.

- Farr J.B., 1976, How high is high resolution?: Presented at the 46th Annual Meeting of the Soc. of Exploration Geophysicists.
- Focht, G.W., and Baker, F.E., 1979, Geophysical Case History of the Two Hills Colony gas field of Alberta: Presented at the 49th Annual Meeting of the Soc. of Exploration Geophysicists.
- Fuglem, M.O., 1970, Use of core in evaluation of productive sands, Lloydminster area; in: Bundle, J.E. and Holmberg, R.A. (editors), Saskatchewan Mesozoic core seminar, Sask. Geol. Soc.
- Futterman, W.I., 1962, Dispersive body waves: J. of Geophysical Research, v. 67, p. 5279-5291.
- Ganley, D.C., 1979, The measurement of Q from seismic data: Ph.D. thesis, University of Alberta, Edmonton, unpublished.
- 1981, A method for calculating synthetic seismograms which include the effects of absorption and dispersion: Geophysics, v. 46, p. 1100-1107.
- Gardner, G.H.F., Gardner, L.W., and Gregory, A.R., 1974, Formation velocity and density--The diagnostic basics for stratigraphic traps: Geophysics, v. 39, p. 770-780.
- Gary, M., McAfee, R.Jr., and Wolf, C.L., 1974, Glossary of Geology: Washington, American Geological Institute.
- Gassman, F., 1951, Elastic waves through a packing of spheres: Geophysics, v. 16, p. 673-685.
- Gendzwill, D.J., 1982, Personal Communication, Dept. of Geological Sciences, U. of Saskatchewan, Saskatoon.
- Geertsma, J., 1961, Velocity log interpretation: The effect of rock bulk compressibility: Soc. of Petroleum Engineers Journal, v. 1, p. 235-248.

- Greensmith, J.T., 1978, Petrology of the sedimentary rocks: Great Britian, George Allen and Unwin Ltd.
- Gregory, A.R., 1976, Fluid saturation effects on dynamic elastic properties of sedimentary rocks: Geophysics, v. 41, p. 895-921.
- 1977, Aspects of rock physics from laboratory and log data that are important to seismic interpretation: American Association of Petroleum Geologists Memoir 26, p. 15-46.
- Gross, A.A., 1980, Mannville channels in east-central Alberta: Sask. Geol. Soc. Special Publ. No. 5, p. 33-63.
- Haidl, F., 1980, Correlation of lithofacies and lithostratigraphic units in the Mannville Group, Lloydminster area, Saskatchewan: Sask. Geol. Soc. Special Publ. No. 5, p. 218-235.
- 1981, Personal Communication, Serendipity Geological Consultants Ltd., Regina, Sask.
- Hajnal, Z., 1982, Personal Communication, Dept. of Geological Sciences, U. of Saskatchewan, Saskatoon.
- Hamilton, E.L., 1972, Compressional-wave attenuation in marine sediments: Geophysics, v. 37, p. 620-646.
- Hauge, P.S., 1981, Measurements of attenuation from vertical seismic profiles: Geophysics, v. 46, p. 1548-1558.
- Jenkins, F.A., and White, H.E., 1957, Fundamentals of optics: New York, McGraw-Hill Book Company, Inc.
- Johnston, D.H., Toksoz, M.N., and Timur, A., 1979, Attenuation of seismic waves in dry and saturated rocks: II. Mechanisms: Geophysics, v. 44, p. 691-711.
- Johnson, D.H., and Toksoz, M.N., 1981, Definitions and terminology; in: Seismic wave attenuation, Soc. of Exploration Geophysicists reprint series No. 2, p. 1-5.

- Kallweit, R.S., and Wood, L.C., 1982, The limits of resolution of zero-phase wavelets: *Geophysics*, v. 47, p.1035-1046.
- Karr, C.Jr., 1978, Analytical methods for coal and coal products, volume 1: New York, Academic Press.
- King, M.S., 1966, Wave velocities in rocks as a function of changes in over-burden pressure and pore fluids: *Geophysics*, v. 31, p. 50-73.
- Koefoed, O., 1981, Aspects of vertical seismic resolution: *Geophysical Prospecting*, v. 29, p. 21-30.
- Kuster, G.T., and Toksoz, M.N., 1974, Velocity and attenuation of seismic waves in two-phase media: Part I. Theoretical formulations: *Geophysics*, v. 39, p.587-606.
- Lorsong, J.A., 1979, Lithofacies of the Lower Cretaceous Mannville Group, west-central Saskatchewan: Sask. Dept. of Mineral Resources Misc. Report 80-4, p. 109-111.
- 1980, Geometry of nearshore sand bodies in the Upper Mannville Group, Celtic field, Saskatchewan: Sask. Geol. Soc. Special Publ. No. 5, p. 236-266.
- 1981, Diagenesis and heavy oil emplacement in Upper Mannville reservoirs, Celtic field, west-central Saskatchewan: Sask. Dept. of Mineral Resources Misc. Report 81-4, p. 141-148.
- 1981, Personal Communication, Serendipity Geological Consultants Ltd., Regina, Sask.
- 1982, Personal Communication, Serendipity Geological Consultants Ltd., Regina, Sask.
- Meckel, L.D.Jr., and Nath, A.K., 1977, Geological considerations for stratigraphic modeling and interpretations: *American Association of Petroleum Geologists Memoir* 26, p. 417-438.

- Morlet, J., Arens, G., Fourceau, E., and Giard, D., 1982, Wave propagation and sampling theory--Part 1: Complex signal and scattering in multilayered media: *Geophysics*, v. 47, p. 203-221.
- Nafe, J.E., and Drake, C.L., 1963, Physical properties of marine sediments; in: Hill, M.N. (editor), *The earth beneath the sea--History*: New York, Interscience publishers, p.794-815.
- Neidell, N.S. and Poggiagliolmi, E., 1977, Stratigraphic modeling and interpretation--Geophysical principles and techniques: *American Association of Petroleum Geologists Memoir 26*, p. 389-416.
- North, B.R., and Caldwell, W.G.E., 1975, Foraminiferal faunas in the Cretaceous system of Saskatchewan: *Geol. Association of Canada Special Paper No. 13*, p. 303-331.
- Patterson, A.R., 1964, Datum corrections in glacial drift: *Geophysics*, v. 29, p. 957-967.
- Pettijohn, F.T., 1975, *Sedimentary rocks*, third edition: New York, F.T. Pettijohn.
- Peterson, R.A., Fillippone, W.R., and Coker, F.B., 1955, The synthesis of seismograms from well log data: *Geophysics*, v. 20, p. 516-538.
- O'Connell, R.J., and Budiansky, B., 1974, Seismic velocities in dry and saturated cracked solids: *J. of Geophysical Research*, v. 79, p. 5412-5426.
- O'Doherty, R.F., and Anstey, N.A., 1971, Reflections on amplitudes: *Geophysical prospecting*, v. 19, p. 430-458.
- Orr, R.D., Johnston, J.R., and Manko, E.M., 1977, Lower Cretaceous geology and heavy-oil potential of the Lloydminster area: *Bull. of Canadian Petroleum Geology*, v. 25, p. 1187-1221.

- Putman, P.E., 1980, Fluvial deposition within the Upper Mannville of west-central Saskatchewan: Stratigraphic implications: Sask. Geol. Soc. Special Publ. No. 5, p. 197-216.
- Reilkoff, B.R., 1982, Processing reflection seismic data from the Athabasca Basin: M.Sc. thesis, University of Saskatchewan, Saskatoon, unpublished.
- Ricker, N., 1953a, The form and laws of propagation of seismic wavelets: Geophysics, v. 18, p. 10-40.
- 1953b, Wavelet contraction, wavelet expansion and the control of seismic resolution: Geophysics, v. 18, p. 769-792.
- Robinson, E.A., and Treitel, S., 1977, The spectral function of a layered system and the determination of the waveform at depth: Geophysical Prospecting, v. 25, p. 434-459.
- Ruter, H., and Schepers, R., 1978, Investigation of the seismic response of cyclically layered carboniferous rock by means of synthetic seismograms: Geophysical Prospecting, v. 26, p. 29-47.
- Sask. Dept. of Mineral Resources, 1979, Reservoir annual 1978: Sask. Dept. of Mineral Resources Misc. Report 79-8.
- Sask. Dept. of Mineral Resources, 1983, Personal Communication, Geology and Mines Geodata Division, Regina.
- Schoenberger, M., 1974, Resolution comparison of minimum-phase and zero-phase signals: Geophysics, v. 39, p. 826-833.
- Schoenberger, M., and Levin, F.K., 1974, Apparent attenuation due to intrabed multiples: Geophysics, v. 39, p. 278-291.
- 1978, Apparent attenuation due to intrabed multiples, II: Geophysics, v. 43, p. 730-737.
- Schriener, B., 1981, Personal Communication, Sask. Research Council, Saskatoon.

- Sengbush, R.L., Lawrence, P.L., and McDonal, F.J., 1961, Interpretation of synthetic seismograms: Geophysics, v. 26, p138-157.
- Sereda, I.T., 1978, A crustal reflection expanding-spread study in southeast Saskatchewan and southwest Manitoba: M.Sc. thesis, University of Saskatchewan, Saskatoon, unpublished.
- Sheriff, R.E., 1973, Encyclopedic dictionary of exploration geophysics: Tulsa, Society of Explortion Geophysicists.
- 1977, Limitations on resolution of seismic reflections and geologic detail derivable from them: American Association of Petroleum Geologists Memoir 26, p. 3-14.
- Simpson, F., 1975, Marine lithofacies and biofacies of the Colorado Group (Middle Albian to Santonian) in Saskatchewan: Geol. Association of Canada Special Paper No. 13, p. 553-587.
- Simpson, F., 1981, Low-permeability gas reservoirs in marine Cretaceous sandstones of Saskatchewan: 13. Upper Colorado (Turonian to Santonian) strata of west-central Saskatchewan: Sask. Dept. of Mineral Resources Misc. Report 81-4, p. 159-162.
- Stone, D.G., 1980, Statistical relations between borehole and surface data: Presented at the 50th Annual Meeting of the Society of Exploration Geophysicists.
- Titchkosky, K.A., 1968, Seismic deconvolution, volume II: Calgary, Evelyn DeMille Books Ltd.
- Toksoz, M.N., Cheng, C.H., and Timur, A., 1976, Velocities of seismic waves in porous rocks: Geophysics, v. 41, p. 621-645.
- Toksoz, M.N., and Johnston, D.H. (editors), 1981, Field measurements of attenuation; in: Seismic wave attenuation, Soc. of Exploration Geophysicists Geophysics reprint series No. 2, p. 250-251.

- Vigrass, L.W., 1965, General geology of heavy oil accumulations in western Canada (including the Athabasca tar sands): The J. of Canadian Petroleum Technology, v. 4, p. 87-94.
- Vigrass, L.W., 1977, Trapping of oil at intra-Mannville (Lower Cretaceous) disconformity in Lloydminster area, Alberta and Saskatchewan: The American Association of Petroleum Geologists Bull., v. 61, p. 1010-1028.
- de Voogd, N., and den Rooijen, H., 1983, Thin layer response and spectral bandwidth: Geophysics, v.48, p. 12-18.
- Walsh, J.B., and Grosebaugh, M.A., 1979, A new model for analyzing the effect of fractures on compressibility: J. of Geophysical Research, v. 84, p.3532-3536.
- Wennekers, J.H.N., Ryckborst, H., Abougoush, M.S., McCreary, R.K.V., and Letkeman, J.P., 1979, Heavy oil, tar sands play key role in Alberta, Saskatchewan production, Part 1: Oil and Gas J., v. 77, p. 290-304.
- White, W.I., and von Osinski, W.D., 1977, Geology and heavy oil reserves of the Mannville Group, Lloydminster-North Battleford area, Saskatchewan: Sask. Dept. of Mineral Resources, Petroleum and Natural Gas Branch.
- Widess, M.B., 1973, How thin is a thin bed: Geophysics, v. 38, p. 1176-1180.
- Widess, M.B., 1982, Quantifying resolving power of seismic systems: Geophysics, v. 47, p. 1160-1173.
- Williams, G.D., 1963, The Mannville Group (Lower Cretaceous) of central Alberta: Bull. of Canadian Petroleum Geology, v. 11, p. 350-368.

Wyllie, M.R.J., Gregory, A.R., and Gardner, L.W., 1956, Elastic wave velocities in heterogeneous and porous media: *Geophysics*, v. 21, p. 41-70.

Wyllie, M.R.J., Gregory, A.R., and Gardner, G.H.F., 1958, An experimental investigation of factors affecting elastic wave velocities in porous media: *Geophysics*, v. 23, p. 459-493.

Ziolkowski, A., and Lerwill, W.E., 1979, A simple approach to high resolution seismic profiling for coal: *Geophysical Prospecting*, v. 27, p. 360-393.

APPENDIX A

Core-analysis data, as stored in the CA.DAT files

CA4B2.DAT

01	B	WB	.3	452.1	4	.26	.10	257.	35.
02	L	W1	.3	451.8	3	.19	.03	10.	3.
03	B	WB	2.8	449.0	0	.27	.28	260.	35.
04	L	W3	5.4	443.6	0	.35	.72	1037.	3.
05	B	WB	2.6	441.0	0	.30	.46	400.	35.
06	L	W4	1.0	440.0	0	.35	.56	2920.	3.
07	B	WB	1.5	438.5	0	.27	.28	260.	35.
08	L	W6	4.5	434.0	0	.33	.74	6115.	2.
09	B	MB	.8	433.2	1	.19	.03	10.	60.
10	B	MB	.2	433.0	6	.19	.03	10.	40.
11	B	MB	.1	432.9	3	.19	.03	10.	40.

CA2D2.DAT

01	L	S2	2.2	467.1	0	.29	.72	1540.	2.
02	Z	SZ	.1	467.0	0	.22	.07	10.	55.
03	L	S2	2.6	464.4	0	.35	.77	1540.	2.
04	Z	SZ	.8	463.6	0	.22	.07	10.	55.
05	B	SB	1.4	462.2	0	.28	.43	260.	35.
06	T	S3	1.6	460.6	2	.27	.31	500.	12.
07	L	S3	1.1	459.5	2	.28	.46	890.	4.
08	Z	SZ	.5	459.0	0	.22	.07	10.	65.
09	B	SB	.8	458.2	0	.30	.47	500.	20.
10	Z	SZ	4.4	453.8	8	.21	.07	8.	50.
11	B	WB	2.3	451.5	0	.27	.31	300.	30.
12	L	W3	.8	450.7	0	.36	.69	1540.	3.
13	B	WB	.3	450.4	0	.28	.43	400.	30.
14	L	W3	4.1	446.3	0	.35	.70	1540.	2.
15	B	WB	2.6	443.7	0	.33	.67	600.	20.
16	L	W4	.9	442.8	0	.33	.66	1540.	3.
17	B	WB	1.6	441.2	0	.28	.43	400.	35.
18	L	W6	4.2	437.0	0	.39	.80	1540.	2.
19	B	MB	3.6	433.4	2	.29	.48	260.	35.
20	T	M2	2.9	430.5	2	.33	.60	350.	12.
21	C	MC	.5	430.0	0	.06	.01	1.	1.
22	L	M4	.8	429.2	0	.35	.67	600.	3.
23	Z	MZ	1.8	427.4	4	.22	.07	10.	70.
24	S	MS	1.6	425.8	0	.23	.05	2.	75.
25	B	MB	1.4	424.4	2	.28	.43	260.	35.
26	T	MT	.5	423.9	0	.28	.56	420.	5.
27	C	MC	.2	423.7	0	.26	.07	10.	35.
28	S	MS	.6	423.1	0	.23	.05	2.	75.
29	B	MB	.5	422.6	0	.32	.67	546.	20.
30	T	M5	2.5	420.1	0	.29	.45	420.	13.
31	S	CS	.4	419.7	0	.23	.05	2.	75.
32	T	C1	.7	419.0	0	.31	.51	570.	5.
33	Z	CZ	1.2	417.8	0	.22	.07	10.	70.
34	T	C1	.4	417.4	0	.32	.51	570.	5.
35	S	CS	.4	417.0	0	.22	.07	10.	75.
36	T	CT	4.1	412.9	2	.31	.40	570.	5.
37	S	CS	.3	412.6	0	.22	.07	10.	75.

38	M	CM	1.2	411.4	1	.21	.07	228.	14.
39	S	CS	.2	411.2	0	.22	.07	10.	75.
40	T	CT	3.2	408.0	1	.21	.07	228.	14.

CA4D2.DAT

01	B	RB	2.4	488.4	0	.27	.51	400.	35.
02	S	GS	1.7	486.7	0	.23	.05	2.	75.
03	L	G1	5.1	481.6	0	.35	.72	1585.	2.
04	B	GB	.2	481.4	0	.27	.20	260.	50.
05	L	G1	.4	481.0	3	.14	.68	24.	3.
06	L	G1	1.2	479.8	0	.32	.66	1088.	3.
07	T	G1	1.8	478.0	1	.29	.38	80.	13.
08	S	SS	.3	477.7	0	.23	.05	2.	75.
09	B	SB	3.9	473.8	0	.29	.34	400.	35.
10	T	S2	1.1	472.7	0	.34	.71	2388.	5.
11	B	SB	.3	472.4	0	.24	.41	100.	65.
12	L	S2	3.8	468.6	0	.35	.71	764.	3.
13	S	SS	.3	468.3	0	.23	.05	2.	75.
14	Z	SZ	.4	467.9	0	.22	.07	10.	70.
15	B	SB	.9	467.0	0	.28	.39	500.	35.
16	L	S3	1.5	465.5	2	.28	.40	44.	12.
17	S	SS	.4	465.1	0	.23	.05	2.	75.
18	Z	SZ	.3	464.8	0	.22	.07	10.	70.
19	S	SS	.7	464.1	0	.23	.05	2.	75.
20	T	S5	.3	463.8	0	.33	.40	1200.	5.
21	S	SS	.3	463.5	0	.23	.05	2.	75.
22	M	S5	.5	463.0	2	.27	.26	55.	12.
23	S	SS	1.3	461.7	8	.22	.05	2.	75.
24	Z	SZ	.8	460.9	8	.21	.07	8.	65.
25	T	W1	2.8	458.1	9	.21	.22	100.	10.
26	B	WB	2.3	455.8	0	.27	.33	300.	35.
27	L	W3	4.8	451.0	0	.35	.74	770.	2.
28	B	WB	2.3	448.7	0	.31	.64	600.	20.
29	L	W4	1.6	447.1	0	.33	.72	1432.	2.
30	B	WB	1.8	445.3	0	.28	.49	500.	30.
31	L	W6	3.9	441.4	0	.35	.79	3199.	2.

CA2B8.DAT

01	B	RB	1.1	492.9	0	.30	.39	400.	35.
02	Z	GZ	.2	492.7	0	.22	.07	10.	70.
03	S	GS	1.9	490.8	0	.23	.05	2.	75.
04	L	G1	4.5	486.3	0	.34	.71	1493.	2.
05	T	G1	.4	485.9	0	.36	.51	400.	5.
06	M	G1	.5	485.4	0	.32	.57	501.	7.
07	T	G1	.7	484.7	3	.14	.03	30.	5.
08	T	G1	1.7	483.0	2	.27	.30	350.	12.
09	S	SS	.5	482.5	0	.23	.05	2.	75.
10	B	SB	3.4	479.1	0	.28	.35	300.	45.
11	L	S2	5.1	474.0	0	.33	.66	434.	2.
12	Z	SZ	.7	473.3	0	.22	.07	10.	70.
13	B	SB	1.0	472.3	0	.26	.31	260.	50.
14	T	S3	1.2	471.1	2	.25	.31	350.	12.
15	S	SS	1.1	470.0	0	.23	.05	2.	75.
16	C	SC	.4	469.6	0	.06	.01	1.	5.
17	T	S5	.5	469.1	2	.23	.36	350.	12.
18	M	S5	.4	468.7	2	.25	.28	228.	13.
19	Z	SZ	1.6	467.1	0	.22	.07	10.	75.
20	T	WT	.2	466.9	2	.23	.34	350.	12.
21	L	W1	.4	466.5	6	.14	.03	30.	2.
22	L	W1	1.3	465.2	3	.14	.03	30.	2.
23	B	WB	1.3	463.9	6	.19	.25	10.	35.
24	Z	WZ	.8	463.1	0	.22	.07	10.	70.
25	B	WB	1.6	461.5	0	.27	.25	260.	50.
26	L	W3	5.2	456.3	0	.35	.70	713.	4.
27	B	WB	2.8	453.5	0	.30	.63	600.	20.
28	L	W4	1.1	452.4	0	.32	.73	1540.	2.
29	B	WB	1.9	450.5	0	.31	.28	400.	35.
30	L	W6	3.1	447.4	0	.36	.83	4710.	2.
31	B	MB	.9	446.5	0	.32	.40	400.	35.
32	B	MB	1.0	445.5	3	.19	.03	10.	35.
33	B	MB	.9	444.6	0	.32	.30	400.	35.
34	M	MM	.4	444.2	7	.27	.49	500.	7.
35	Z	MZ	.5	443.7	0	.19	.47	10.	70.
36	B	MB	1.2	442.5	0	.29	.23	260.	50.
37	T	MT	.6	441.9	0	.34	.58	420.	7.
38	B	MB	.2	441.7	0	.32	.48	400.	35.
39	T	MT	1.1	440.6	0	.31	.53	93.	7.
40	B	MB	.6	440.0	2	.27	.27	260.	50.
41	C	MC	.4	439.6	0	.06	.01	1.	10.
42	T	MT	1.1	438.5	0	.37	.49	420.	7.
43	Z	MZ	1.0	437.5	5	.22	.07	10.	70.
44	S	MS	.6	436.9	0	.23	.05	2.	75.
45	B	MB	1.4	435.5	0	.27	.36	1210.	35.
46	L	M5	1.0	434.5	0	.31	.66	2180.	2.
47	B	MB	.9	433.6	0	.23	.41	100.	65.
48	M	MM	.4	433.2	0	.38	.48	280.	7.
49	B	MB	1.1	432.1	8	.17	.50	257.	35.
50	C	MC	.9	431.2	0	.06	.01	1.	1.
51	B	MB	3.0	428.2	8	.31	.43	257.	35.
52	C	CC	.5	427.7	0	.26	.07	10.	45.
53	S	CS	.5	427.2	0	.23	.07	2.	75.

54	B	CB	.3	426.9	0	.23	.41	100.	65.
55	S	CS	.3	426.6	0	.23	.05	2.	75.

CA4B8.DAT

01	M	R1	.5	513.1	1	.24	.07	220.	13.
02	M	R1	.7	512.4	3	.14	.03	30.	7.
03	M	R1	.2	512.2	1	.24	.07	220.	13.
04	Z	RZ	.4	511.8	0	.22	.07	10.	70.
05	S	RS	1.6	510.2	0	.23	.05	2.	75.
06	Z	RZ	2.0	508.2	0	.22	.07	10.	70.
07	B	RB	1.7	506.5	6	.26	.22	257.	35.
08	Z	GZ	1.2	505.3	0	.22	.07	10.	70.
09	L	G1	5.6	499.7	0	.34	.64	1447.	2.
10	B	GB	.5	499.2	7	.24	.41	100.	65.
11	L	G1	.7	498.5	0	.31	.48	1227.	3.
12	T	G1	.9	497.6	2	.26	.28	350.	13.
13	M	G1	.3	497.3	2	.27	.31	200.	12.
14	T	G1	1.1	496.2	2	.30	.37	400.	7.
15	S	SS	1.1	495.1	0	.23	.05	2.	75.
16	B	SB	3.4	491.7	8	.28	.37	400.	35.
17	L	S2	1.4	490.3	0	.31	.47	181.	4.
18	B	SB	.3	490.0	0	.28	.41	400.	35.
19	L	S2	3.1	486.9	0	.32	.74	1031.	2.
20	S	SS	.7	486.2	0	.23	.05	2.	75.
21	L	S3	2.2	484.0	2	.24	.25	500.	12.
22	B	SB	.7	483.3	2	.28	.33	350.	40.
23	C	SC	.4	482.9	0	.06	.01	1.	5.
24	Z	SZ	.9	482.0	0	.22	.07	10.	70.
25	B	S5	.7	481.3	8	.33	.40	450.	35.
26	T	S5	.6	480.7	1	.26	.27	300.	13.
27	Z	SZ	1.7	479.0	9	.22	.07	10.	70.
28	T	W1	1.2	477.8	7	.25	.30	350.	5.
29	T	W1	.6	477.2	3	.13	.03	30.	5.
30	B	WB	1.0	476.2	3	.19	.03	10.	35.
31	B	WB	1.8	474.4	0	.28	.15	260.	35.
32	L	W3	5.1	469.3	0	.35	.67	557.	4.
33	B	WB	1.2	468.1	0	.30	.42	400.	35.
34	Z	WZ	.8	467.3	0	.22	.07	10.	10.

CA2D8.DAT

01	B	SB	.3	506.7	0	.34	.16	600.	20.
02	T	S2	.8	505.9	0	.32	.19	545.	5.
03	L	S2	3.2	502.7	0	.34	.57	700.	4.
04	Z	SZ	.8	501.9	0	.22	.07	10.	70.
05	M	S3	.6	501.3	0	.26	.26	31.	7.
06	T	S3	.6	500.7	0	.26	.29	68.	5.
07	M	S3	1.4	499.3	3	.14	.03	30.	7.
08	M	S3	.6	498.7	2	.28	.32	32.	7.
09	S	SS	.2	498.5	0	.23	.05	2.	75.
10	L	S5	1.2	497.3	2	.29	.39	66.	4.
11	S	SS	.5	496.8	0	.23	.05	2.	75.
12	L	SL	.3	496.5	2	.32	.30	66.	12.
13	Z	SZ	.4	496.1	0	.22	.07	10.	70.
14	M	W1	.9	495.2	3	.14	.03	30.	7.
15	M	W1	.6	494.6	2	.26	.30	32.	12.
16	Z	WZ	1.7	492.9	0	.22	.07	10.	70.
17	T	WT	1.1	491.8	1	.24	.07	30.	5.
18	Z	WZ	.3	491.5	0	.22	.07	10.	70.
19	B	WB	.8	490.7	0	.30	.40	400.	35.
20	L	WL	.3	490.4	1	.22	.24	30.	13.
21	B	WB	1.4	489.0	0	.30	.40	400.	35.
22	L	W3	2.0	487.0	0	.33	.56	275.	4.
23	B	WB	.8	486.2	0	.29	.21	260.	35.
24	S	WS	.5	485.7	0	.23	.05	2.	75.
25	L	WL	.3	485.4	0	.31	.51	1320.	4.
26	B	WB	2.7	482.7	0	.27	.36	546.	30.
27	L	W4	.5	482.2	0	.35	.46	1320.	4.
28	B	WB	.2	482.0	0	.27	.36	546.	30.
29	L	W4	1.8	480.2	0	.33	.57	1419.	3.
30	B	WB	1.7	478.5	0	.37	.43	546.	20.
31	L	W6	.5	478.0	2	.30	.59	67.	12.
32	L	W6	3.3	474.7	0	.40	.83	4912.	2.
33	B	MB	.3	474.4	2	.23	.23	250.	65.
34	Z	MZ	.4	474.0	3	.21	.07	2.	70.
35	B	MB	1.2	472.8	2	.26	.22	257.	50.
36	L	ML	.8	472.0	9	.29	.67	541.	8.
37	B	MB	.8	471.2	0	.23	.41	100.	65.
38	M	MM	.2	471.0	0	.26	.28	731.	7.
39	B	MB	.7	470.3	0	.30	.40	546.	30.
40	L	M2	3.6	466.7	0	.32	.51	257.	4.
41	C	MC	.2	466.5	0	.24	.07	10.	40.
42	L	M4	.9	465.6	0	.34	.63	606.	3.
43	Z	MZ	1.7	463.9	4	.21	.07	2.	70.
44	S	MS	1.3	462.6	0	.23	.05	2.	75.
45	L	ML	1.8	460.8	0	.28	.52	446.	4.
46	B	MB	1.1	459.7	7	.26	.23	257.	35.
47	L	ML	2.0	457.7	0	.30	.37	404.	4.
48	S	MS	.5	457.2	0	.23	.05	2.	75.
49	B	MB	.5	456.7	0	.27	.36	546.	30.
50	L	ML	1.5	455.2	0	.34	.62	1824.	2.
51	C	CC	.2	455.0	0	.24	.07	10.	40.
52	7	CZ	.8	454.2	0	.26	.07	15.	65.
53	S	CS	.7	453.5	0	.23	.05	2.	75.

54	C	CC	.1	453.4	0	.26	.07	10.	40.
55	T	C2	3.2	450.2	0	.32	.18	541.	5.
56	M	C2	.7	449.5	1	.15	.08	291.	7.
57	S	CS	.2	449.3	0	.23	.05	2.	75.
58	B	CB	1.2	448.1	2	.31	.17	257.	50.
59	S	CS	.3	447.8	0	.23	.05	2.	75.
60	T	CT	1.4	446.4	1	.24	.07	230.	13.
61	Z	CZ	.2	446.2	0	.22	.07	10.	70.
62	T	CT	.8	445.4	1	.24	.07	230.	13.
63	Z	CZ	.3	445.1	0	.22	.07	10.	70.
64	T	CT	1.8	443.3	1	.24	.07	230.	13.
65	Z	LZ	1.1	442.2	0	.22	.07	10.	70.
66	S	LS	.5	441.7	0	.23	.05	2.	75.

CA411.DAT

01	L	GL	3.1	497.6	7	.00	.00	0.	0.
02	S	SS	1.5	496.1	0	.00	.00	0.	0.
03	L	SL	1.0	495.1	0	.00	.00	0.	0.
04	S	SS	.3	494.8	0	.00	.00	0.	0.
05	C	SC	1.6	493.2	0	.00	.00	0.	0.
06	S	SS	9.7	483.5	0	.00	.00	0.	0.
07	B	SB	1.8	481.7	0	.00	.00	0.	0.
08	L	SL	.3	481.4	0	.00	.00	0.	0.

APPENDIX B

Listings of computer programs

```

C*****
C
C
C           C E L G R F
C
C*****
C
C
C PURPOSE:  CELGRF IS USED TO PLOT THE SYNTHETIC SEISMOGRAM
C           PRODUCED BY SYNCAL.  CELGRF PLOTS THE SYNTHETIC SEISMOGRAM
C           VERSUS TIME AND DEPTH; THE SHAPE AND NORMALIZED AMPLITUDE
C           SPECTRUM OF THE RICKER-WAVELET SOURCE (IF IT IS USED);
C           THE Q, VELOCITY AND DENSITY VALUES FOR THE WELL; THE
C           STRATIGRAPHIC MARKERS; AND THE CORE PROPERTIES OF
C           POROSITY, PERMEABILITY, OIL SATURATION, CLAY CONTENT,
C           CEMENT TYPE, AND LITHOFACIES TYPE
C
C           AS SEVERAL PAGES OF PLOTS ARE PRODUCED,
C           2-STEP CALCOMP PLOTTING IS SUGGESTED
C
C PROGRAMMER:  M.K. LOMAS
C              DEPT. OF GEOLOGICAL SCIENCES (GEOPHYSICS)
C              U. OF SASKATCHEWAN
C              SASKATOON
C              1982
C
C           SCALING FACTORS ARE SPECIFIED IN THE PROGRAM
C           A FILE CALLED SPECAN.DAT IS WRITTEN TO DISK AND CAN BE USED
C           AS INPUT TO THE SPECTRAL ANALYSIS PROGRAM SPECAN.FOR
C
C*****
C
C*****
C           DIMENSION SECTION
C*****
C           REAL*8 DELT,DELTIM,S(8192),PWR
C           INTEGER UNIT(100),CEM(100),PO,LABEL1(5),LBL2(11),LBL3(11),LBL4(12)
C           *,LBL5(9),LBL6(12),LBL7(4),LBL8(8),LBL9(7),LBL10(11),LBL11(2),
C           *LBL12(2),LBL13(7),LBL14(7),LBL15(11),LBL16(6)
C           REAL INTIME(4001),LCOLO,MANN,MONTAN,LEAPK,MCLARN
C           DIMENSION Z(4001),CO(4001),QO(4001),RHO(4001),TT(4001),
C           .ADEPTH(4001),ATIME(4001),AZ(4001),ACO(4001),ARHO(4001),AQO(4001)
C           DIMENSION XT(8192),TWTIME(8192),TDEPTH(4001),SYNDEP(8192),
C           .FREQ(10000),WAVAMP(10000),SS(10000),TTIME(4001),CCO(100),RRHO(100)
C           DIMENSION FAC(100),BED(100,2),THICK(100),TOPBED(100),
C           *POR(100),OILSAT(100),PERM(100),CLAY(100),WAVE(5000),WAVTIM(5000)
C
C*****
C           OPEN STATEMENTS
C*****
C           OPEN(UNIT=21,DEVICE='DSK',ACCESS='SEQIN',FILE='SYNGAN.DAT',
C           .DIALOG)
C           OPEN(UNIT=22,DEVICE='DSK',ACCESS='SEQIN',FILE='GANCEL.DAT',
C           .DIALOG)
C           OPEN(UNIT=23,DEVICE='DSK',ACCESS='SEQIN',FILE='AU.DAT',DIALOG)
C           OPEN(UNIT=24,DEVICE='DSK',ACCESS='SEQIN',FILE='DEN.DAT',DIALOG)
C           OPEN(UNIT=25,DEVICE='DSK',ACCESS='SEQIN',FILE='WAVE.DAT',DIALOG)

```

```

OPEN(UNIT=26,DEVICE='DSK',ACCESS='SEQIN',FILE='WAVAMP.DAT',
.DIALOG)
OPEN(UNIT=28,DEVICE='DSK',ACCESS='SEQIN',FILE='COQO.DAT',DIALOG)
OPEN(UNIT=30,DEVICE='DSK',ACCESS='SEQIN',FILE='PIX.DAT',DIALOG)
OPEN(UNIT=31,DEVICE='DSK',ACCESS='SEQIN',FILE='CA.DAT',DIALOG)
OPEN(UNIT=32,DEVICE='DSK',ACCESS='SEQOUT',FILE='SPECAN.DAT',
.DIALOG)
OPEN(UNIT=1,DEVICE='DSK',ACCESS='SEQIN',FILE='SYNGRF.DAT',DIALOG)
C*****
C LABELS FOR THE PLOTS
C*****
DATA LBL2/'NUMBE','R OF ','POINT','S REQ','UESTE','D IN ',
*'SYNTH','ETIC ','TRACE',' = ',' /',
*LBL3/'SAMPL','E INT','ERVAL',' FOR ','SEISM','OGRAM',' AND ',
*'WAVEL','ET (M','S) = ',' /',
*LBL4/'BUTTE','RWORT','H ANT','I-ALI','AS FI','LTER ',
*'INCLU','DED I','N SYN','THETI','C TRA','CE '/,
*LBL5/'DEPTH',' OF S','OURCE',' BELO','W REC','EIVER','S (M)',
*' = ',' /',
*LBL6/'NUMBE','R OF ','CONST','ANT V','ELOCI','TY LA','YERS ',
*'WITHI','N CAS','ED SE','CTION',' = ',' /',
*LBL7/'TYPE ','OF WA','VELET',' = ',' /',
*LBL8/'RECEI','VERS ','LOCAT','ED AT',' TOP ','OF LA','YER ',
*' /',
*LBL9/'WELL ','IS CA','SED T','O A D','EPH ','(M) =',
*' /',
*LBL10/'POWER',' GAIN',' FUNC','TION ','INCLU','DED ','WINDO',
*'W LEN','GTH ('','S) = ',' /',
*LBL11/' RICK','ER '/,
*LBL12/'IMPUL','SE '/,
*LBL13/'TOP O','F COR','ED SE','CTION',' , AT ',' M '/,
*LBL14/'END O','F COR','ED SE','CTION',' , AT ',' M '/,
*LBL15/'TRUE ','AMPLI','TUDE ','SEISM','OGRAM','S; TH','E DIR',
*'ECT W','AVE I','S MUT','ED '/,
*LBL16/'; THE',' DIRE','CT WA','VE IS',' MUTE','D '/
C*****
C READ IN THE PARAMETERS USED IN THE CONSTRUCTION OF THE
C SYNTHETIC SEISMOGRAM
C*****
READ (21,1) NPTS,DT,IBF,SDEPTH,FC,NLAYER,IPULS,PERIOD,PO,
.DEPCOR,NUNIT,DEPCAS,WD
C*****
C NPTS = NUMBER OF POINTS DESIRED IN SYNTHETIC TRACE
C MAXIMUM IS 4096 AND NPTS SHOULD BE POWER OF 2
C DT = SAMPLE INTERVAL IN MILLISECONDS
C IBF = 5 MEANS TO INCLUDE THE BUTTERWORTH ANTI-ALIAS FILTER
C SDEPTH = DEPTH OF SOURCE. THIS DEPTH CAN BE ZERO, BUT THE
C DEPTH MUST BE AT A LAYER BOUNDARY OR AN ERROR MESSAGE
C WILL RESULT.
C FC = FREQUENCY AT WHICH VELOCITY AND Q ARE INPUT
C NLAYER = NUMBER OF LAYERS ABOVE WHERE THE LOGS BEGIN
C IPULS=1,2,3, OR 4 DEPENDING ON THE TYPE OF RICKER WAVELET DESIRED
C IF IPULS=0,NO WAVELET IS CONVOLVED
C PERIOD=THE APPROXIMATE PERIOD (IN SECONDS) OF THE INPUT PULSE
C FOR THE SYNTHETIC SEISMOGRAM. ACTUALLY, THE CENTRAL

```

```

C          FREQUENCY IS ABOUT 20% LESS THAN (1/PERIOD)
C          PO=1 MEANS THAT THE LIMITING VALUES OF PHASE VELOCITY AND Q AS
C          FREQUENCY APPROACHES ZERO ARE WRITTEN INTO THE OUTPUT FILE
C          CO QO.DAT.
C          DEPCOR = DEPTH TO THE BOTTOM OF THE CORED SECTION
C          NUNIT = NUMBER OF FACIES UNITS IN CORED SECTION
C          DEPCAS = DEPTH OF THE FIRST DIGITIZED WELL LOG VALUES
C          WD = WINDOW LENGTH (IN SEC.) FOR THE AUTOMATIC GAIN CONTROL
C          SUBROUTINE
C          IF NO AGC IS REQUIRED, SET WD=0.0
C*****
C          1 FORMAT (2X,I5,F5.0,I5,F5.1,F5.0,2I5,F7.4,I5,F7.1,I3,4X,F5.1,F5.2)
C          WRITE(6,1) NPTS,DT,IBF,SDEPTH,FC,NLAYER,IPULS,PERIOD,PO,
C          .DEPCOR,NUNIT,DEPCAS,WD
C          IF (IPULS.EQ.0) GO TO 105
C*****
C          READ IN THE DATA NECESSARY TO PLOT THE INPUT WAVELET
C          THEN, CALCULATE THE TIME AT EACH WAVELET SAMPLE
C*****
C          READ (25,30) NSAMP,LOG2N
C          WRITE (6,30) NSAMP,LOG2N
C          30 FORMAT(2I5)
C          READ(25,12) (WAVE(I),I=1,NSAMP)
C          12 FORMAT(8F10.3)
C          DO 100 I=1,NSAMP
C          WAVTIM(I)=I*DT*.001
C          100 CONTINUE
C          WRITE(6,31) WAVTIM(1),WAVTIM(NSAMP),DT
C          31 FORMAT(' ',3F7.4)
C*****
C          WAVE(I)=INPUT WAVELET AMPLITUDES AT THE TIME SAMPLES
C          NSAMP=(IFIX(6.*PERIOD/TAU)+1)
C          =NUMBER OF TIME SAMPLES (AT SPACING DT) FOR THE INPUT WAVE
C          LOG2N=2**LOG2N GIVES THE NUMBER OF POINTS IN THE INPUT AND
C          OUTPUT TIME SERIES (LOG2N.LE.13)
C*****
C          NPTS=2**LOG2N
C          NBY2=NPTS/2
C          MPTS=NBY2+1
C          TAU=1./(2.*(1./(2.*DT*.001)))
C*****
C          CALCULATE THE ARRAY OF FREQUENCY VALUES AT WHICH THE AMPLITUDES
C          OF THE WAVELET HAVE BEEN CALCULATED
C          READ IN THE AMPLITUDES NECESSARY TO PLOT THE AMPLITUDE SPECTRUM
C          OF THE INPUT PULSE
C*****
C          FINTL=.5/TAU/FLOAT(NBY2)
C          DO 102 I=1,MPTS
C          FREQ(I)=(I-1)*FINTL
C          102 CONTINUE
C          READ(26,14) (WAVAMP(I),I=1,MPTS)
C          14 FORMAT(8F10.3)
C*****
C          NORMALIZE THE AMPLITUDE SPECTRUM
C*****

```

```

TMAX=0.0
DO 103 I=1,MPTS
IF (WAVAMP(I) .GE. TMAX) TMAX=WAVAMP(I)
103 CONTINUE
DO 104 I=1,MPTS
WAVAMP(I)=(WAVAMP(I)/TMAX)*100.
104 CONTINUE
WRITE(6,36) FINTL,MPTS,FREQ(1),FREQ(MPTS),TMAX
36 FORMAT(' ',F10.4,I8,3F10.3)
C*****
C FINTL=FREQUENCY INTERVAL BETWEEN POINTS ON THE AMPLITUDE SPECTRUM
C FREQ=ARRAY FREQUENCY VALUES AT WHICH THE AMPLITUDE SPECTRUM IS
C CALCULATED
C WAVAMP=ARRAY OF AMPLITUDE SPECTRUM VALUES
C*****
C
C
C 105 IF(PO.NE.1) GO TO 115
C
C*****
C READ IN NZ1 AND THE LIMITING VALUES OF PHASE VELOCITY AND Q,
C AS FREQUENCY APPROACHES ZERO
C*****
110 READ(28,18) NZ1
WRITE(6,18) NZ1
18 FORMAT (I5)
C*****
C NZ1=THE TOTAL NUMBER OF LAYERS IN THE MODEL
C MAXIMUM NUMBER OF LAYERS IS 4000
C*****
READ(28,19) (CO(I),I=1,NZ1)
READ(28,19) (QO(I),I=1,NZ1)
19 FORMAT(8F10.3)
C*****
C TO READ IN THE DEPTHS TO THE TOP OF THE VARIOUS MARKER HORIZONS
C*****
115 READ (30,25) LABEL1
25 FORMAT(5A5)
WRITE (6,25) LABEL1
READ (30,4) DRIFTU,DRIFTM,DRIFTL,LEAPK,UCOLO,SWHSP,LCOLO,TWAL,
*BWAL,MANN,MCLARN,WASECA,SPARKY,GP,REX
C*****
C DRIFTU = UPPER DRIFT LAYER (BATTLEFORD FM.?)
C DRIFTM = MIDDLE DRIFT LAYER (FLORAL FM.?)
C DRIFTL = LOWER DRIFT LAYER (SANDS AND GRAVELS)
C LEAPK = LEA PARK FM. (ALSO TOP OF THE MONTANA GROUP)
C UCOLO = UPPER COLORADO GROUP (ALSO THE TOP OF THE FIRST WHITE
C SPECKLED SHALE)
C SWHSP = SECOND WHITE SPECKLED SHALE
C LCOLO = LOWER COLORADO GROUP
C TWAL = TOP OF THE ST. WALBURG SANDSTONE (WITHIN THE LOWER COLORADO
C GROUP)
C BWAL = BASE OF THE ST. WALBURG SANDSTONE
C MANN = MANNVILLE GROUP (ALSO THE TOP OF THE COLONY FM.)
C MCLARN = MCLAREN FM. (OF THE MANNVILLE GROUP)

```

```

C      WASECA = WASECA FM. (MANNVILLE GROUP)
C      SPARKY = SPARKY FM. (MANNVILLE GROUP)
C      GP = GENERAL PETROLEUM FM. (MANNVILLE GROUP)
C      REX = REX FM. (MANNVILLE GROUP)
C*****
  4 FORMAT (10(F7.1),/,5(F7.1))
    WRITE (6,4) DRIFTU,DRIFTM,DRIFTL,LEAPK,UCOLO,SWHSP,LCOLO,TWAL,
      *BWAL,MANN,MCLARN,WASECA,SPARKY,GP,REX
C*****
C      TO READ IN THE DATA ON THE CORED SECTIONS OF THE WELL
C*****
      DO 120 I=1,NUNIT
      READ (31,5) UNIT(I),FAC(I),(BED(I,J),J=1,2),THICK(I),TOPBED(I),
      *CEM(I),POR(I),OILSAT(I),PERM(I),CLAY(I)
C*****
C      UNIT(I) = THE FACIES UNIT NUMBER.  NOTE, SOME OF JIM LORSONG'S
C              FACIES UNITS WERE SUBDIVIDED BY CEMENT TYPE; THESE ARE
C              CONSIDERED AS SEPARATE FACIES UNITS.
C      FAC(I) = THE FACIES TYPE
C      BED(I,J) = FIRST DIMENSION IS THE FIRST LETTER OF THE FACIES TO
C                WHICH THE BED BELONGS
C                SECOND DIMENSION IS THE FACIES TYPE, OR SAND BODY
C                NUMBER OF THE BED
C      THICK(I) = THICKNESS OF THE FACIES UNIT
C      TOPBED(I) = DEPTH TO THE TOP OF THE FACIES UNIT
C      CEM(I) = TYPE OF CEMENTATION IN THE FACIES UNIT
C              0=NO CEMENT
C              1=CLAY CEMENT
C              2=PARTIAL CLAY CEMENT
C              3=CALCITE CEMENT
C              4=PARTIAL CALCITE CEMENT
C              5=NODULES OF CALCITE
C              6=CARBONATE (NON-CALCITE) CEMENT
C              7=PARTIAL CARBONATE CEMENT
C              8=CARBONATE NODULES
C              9=A MIXTURE OF CEMENT TYPES
C      POR(I) = MEAN POROSITY OF THE FACIES UNIT (SOMETIMES ESTIMATED)
C      OILSAT(I) = MEAN OIL SATURATION--FRACTION OF PORE VOLUME
C                (SOMETIMES ESTIMATED)
C      PERM(I) = MEAN PERMEABILITY TO AIR, IN MILLIDARCIES
C                (SOMETIMES ESTIMATED)
C      CLAY(I) = ESTIMATED CLAY AND SILT CONTENT (BY VOLUME OF THE ROCK)
C*****
  5 FORMAT(I4,2X,A1,2X,2(A1),F5.1,F7.1,I3,2(F5.2),F7.0,F5.0)
    WRITE (6,5) UNIT(I),FAC(I),(BED(I,J),J=1,2),THICK(I),TOPBED(I),
      *CEM(I),POR(I),OILSAT(I),PERM(I),CLAY(I)
  120 CONTINUE
      DEPTH=0.0
      TIME=0.0
C*****
C      TO READ IN VALUES TO THE BOTTOM OF THE CASING
C*****
      DO 125 I=1,NLAYER
      NZ1=I
      READ (22,2) Z(I),CO(I),RHO(I),QO(I)

```

```

C*****
C   Z(I) = THICKNESS OF I'TH LAYER
C   =99999 FOR LAST LAYER
C   CO(I) = PHASE VELOCITY IN I'TH LAYER
C   RHO(I)=DENSITY IN I'TH LAYER
C   QO(I) = SPECIFIC ATTENUATION FACTOR IN I'TH LAYER
C   MAXIMUM NUMBER OF LAYERS IS 4000
C   THE THICKNESS OF Z(NLAYER) IS CALCULATED
C*****
      IF (I.EQ.NLAYER) Z(I)=DEPCAS-DEPTH
      TTIME(I)=TIME
      TIME=TIME+Z(I)/CO(I)
      TDEPTH(I)=DEPTH
      DEPTH=DEPTH+Z(I)
125 CONTINUE
      2 FORMAT (5X,4F7.1)

C
C   DEVIDE THE PORTION OF THE LEA PARK FM. THAT IS WITHIN THE CASED
C   SECTION OF THE WELL INTO AN ARBITRARY NUMBER OF DEPTH INTERVALS
C   (IE-10), TO ALLOW A STEP LIKE CHANGE IN Q, VELOCITY, AND
C   DENSITY VALUES FROM THE TOP OF THE LEA PARK FM. TO THE START
C   OF THE GEOPHYSICAL LOGS.
C
      DLEAPK=DEPCAS-LEAPK
      DINCR=DLEAPK/10.
      NLEAPK=NLAYER+9
      XLEAPK=NLEAPK+0.0
      WRITE (6,28) XLEAPK
28 FORMAT('0',F5.1)
      Z(NLAYER)=DINCR
      DEPTH=TDEPTH(NLAYER)+Z(NLAYER)
      TIME=TTIME(NLAYER)+Z(NLAYER)/CO(NLAYER)

C
C   THE FIRST 7 DIGITIZED VELOCITY AND DENSITY VALUES ARE
C   USED TO COMPUTE AN AVERAGE AND THEN AN
C   INCREMENT, WHICH IS THEN ADDED WITHIN EACH DEPTH INTERVAL
C
      READ (23,11) (DDD,(TT(I),I=1,7))
      READ (24,11) (DDD,(RRHO(I),I=1,7))
      COSUM=0.0
      RHOSUM=0.0
      DO 126 K=1,7
      CCO(K)=(1/TT(K))*1000000
      COSUM=COSUM+CCO(K)
      RHOSUM=RHOSUM+RRHO(K)
126 CONTINUE
      COAV=COSUM/7
      RHOAV=RHOSUM/7
      QOINC=((100.-50.)/(MANN-LEAPK-DINCR))*DINCR
      COINC=((COAV-CO(NLAYER))/(DLEAPK-DINCR))*DINCR
      RHOINC=((RHOAV-RHO(NLAYER))/(DLEAPK-DINCR))*DINCR

C
      N=0
      DO 128 I=NLAYER+1,NLEAPK
      N=N+1

```

```

Z(I)=DINCR
QO(I)=QO(NLAYER)+(N*QOINC)
CO(I)=CO(NLAYER)+(N*COINC)
RHO(I)=RHO(NLAYER)+(N*RHOINC)
TTIME(I)=TIME
TIME=TIME+Z(I)/CO(I)
TDEPTH(I)=DEPTH
DEPTH=DEPTH+Z(I)
128 CONTINUE
DO 129 I=1,NLEAPK
129 CONTINUE
C*****
C TO READ IN VELOCITY AND DENSITY VALUES FROM THE LOGS
C*****
NZ1=NLEAPK
REWIND 23
REWIND 24
NLAYER=NLEAPK
NEND=NLAYER
DO 130 J=1,(4000-NLAYER)/7
NZ1=NZ1+7
NBEG=NEND+1
NEND=NBEG+6
READ (23,11)(DDD,(TT(I),I=NBEG,NEND))
READ (24,11)(DDD,(RHO(I),I=NBEG,NEND))
11 FORMAT(' ',8F10.3)
L=0
DO 131 K=NBEG,NEND
IF (TT(K).EQ.9999.000) GO TO 135
CO(K)=(1/TT(K))*1000000
L=L+1
131 CONTINUE
130 CONTINUE
135 NZ1=NZ1-7+L
NZ=NZ1-1
C*****
C TO READ IN Q AND DEPTH VALUES TO THE END OF THE LOGS
C*****
QOINC=((100.-50.)/(MANN-LEAPK-DINCR))*2
QUAL=QO(NLAYER)
WRITE(6,*) NLAYER,QO(NLAYER),QOINC
DO 136 I=NLAYER+1,NZ
Z(I)=.2
QUAL=QUAL+QOINC
IF (DEPTH.GE.(MANN)) QUAL=35.
QO(I)=QUAL
TDEPTH(I)=DEPTH
TTIME(I)=TIME
DEPTH=DEPTH+Z(I)
TIME=TIME+Z(I)/CO(I)
136 CONTINUE
Z(NZ1)=99999.
QO(NZ1)=QUAL
TDEPTH(NZ1)=DEPTH
C

```

```

DO 138 I=1,50
WRITE(6,9) I,TDEPTH(I),TTIME(I),Z(I),CO(I),RHO(I),QO(I)
138 CONTINUE
9 FORMAT(I5,F8.2,F8.6,F8.2,F10.3,F10.3,F7.1)
WRITE (6,9) NZ1,TDEPTH(NZ1),TTIME(NZ1),Z(NZ1),CO(NZ1),RHO(NZ1),
*QO(NZ1)
C*****
C
C THE INPUT VALUES USED TO CONSTRUCT THE
C SYNTHETIC SEISMOGRAM MUST BE RENAMED
C*****
C
ANZ1=NZ1
ANZ=ANZ1-1
510 DO 515 I=1,NZ1
ATIME(I)=TTIME(I)
ADEPTH(I)=TDEPTH(I)
AZ(I)=Z(I)
ACO(I)=CO(I)
ARHO(I)=RHO(I)
AQO(I)=QO(I)
515 CONTINUE
C
C*****
C THE INTEGRATED 2-WAY TIME FOR EACH DEPTH LAYER IS CALCULATED
C CASED INTERVAL
C IF THE SOURCE IS BURIED, A ONE-WAY TIME (OWTIME) TO THAT DEPTH
C MUST BE SUBTRACTED FROM ALL INTIME(I).
C*****
C
J=0
DO 518 I=1,NLAYER
518 IF(SDEPTH .EQ. ADEPTH(I)) J=J+1
K=0
DO 520 I=1,NLAYER
K=K+1
IF (SDEPTH .GE. ADEPTH(I)) INTIME(I)=ATIME(I)
IF (SDEPTH .LT. ADEPTH(I)) GO TO 522
OWTIME=ATIME(I)
520 CONTINUE
522 DO 523 I=K,ANZ1
523 INTIME(I)=(2*ATIME(I))-OWTIME
DO 525 I=1,50
525 WRITE(6,20)ADEPTH(I),INTIME(I),ATIME(I),AZ(I),ACO(I),ARHO(I),
*AQO(I)
20 FORMAT(F8.2,1X,F8.6,2X,F8.6,2X,F8.2,1X,F8.3,2X,F8.3,2X,F6.1)
WRITE (6,*) ANZ1
WRITE (6,20) ADEPTH(ANZ1),INTIME(ANZ1),ATIME(ANZ1),AZ(ANZ1),
*ACO(ANZ1),ARHO(ANZ1),AQO(ANZ1)
C
C*****
C READ IN THE AMPLITUDE VALUES FOR THE SYNTHETIC SEISMOGRAM
C APPLY THE AUTOMATIC GAIN CONTROL IF REQUIRED
C*****
READ (1,3) (XT(I),I=1,NPTS)

```

```

3 FORMAT(8F10.3)
IF (WD .EQ. 0.) GO TO 139
CALL PWRGFN (XT,NPTS,S,WD,DT)
IF (SDEPTH .NE. 0.0) GO TO 139
GO TO 143

```

```

C*****
C   IF WD=0., TRUE AMPLITUDE SEISMOGRAMS ARE REQUESTED
C   TO MAKE THE TRUE AMPLITUDE GRAPH MORE MEANINGFUL, THE HIGH
C   AMPLITUDE DIRECT WAVE IS MUTED
C   THE SYNTHETIC SEISMOGRAM VALUES FROM 0 SECONDS
C   TO A CALCULATED TIME MUTIME (CORRESPONDING TO THE INPUT
C   WAVELET LENGTH) ARE SET EQUAL TO ZERO
C   NOTE-THE INPUT WAVELET PERIOD IS ACTUALLY =1.2*PERIOD
C   -AN MULTIPLICATION FACTOR IS ADDED TO HELP
C   ACCOUNT FOR WAVELET BROADENING DUE TO DISPERSION
C   -WHEN THE INPUT SOURCE IS AN IMPULSE, MUTIME IS SET
C   TO 10 MS, BASED ON OBSERVATION
C   THE DIRECT WAVE IS ALSO MUTED IF THE SOURCE IS BURIED

```

```

C*****
C
139 MUTIME=IFIX((1.5*(1.2*PERIOD*1000)/DT)+(OWTIME*1000/DT))
IF (IPULS .EQ. 0) MUTIME=IFIX(10./DT+1.5*(OWTIME*1000/DT))
DO 142 I=1,MUTIME
XT(I)=0.0
142 CONTINUE

```

```

C*****
C   CREATE X AXIS ARRAY OF TWO-WAY TIMES

```

```

C*****
143 TIME=0.0
DO 145 I=1,NPTS
TWTIME(I)=TIME+DT/1000.
TIME=TWTIME(I)
145 CONTINUE

```

```

C*****
C   FOR THE ADJUSTED LAYER VALUES:
C   CONVERT THIS TWO-WAY TIME ARRAY TO A DEPTH ARRAY
C   TDEPTH(I)=TOTAL DEPTH TO THE TOP OF EACH DEPTH LAYER
C           I=1 TO ANZ1
C   INTIME(I)=INTEGRATED TWO-WAY TIME FOR EACH DEPTH LAYER
C           I=1 TO ANZ1
C   TWTIME(I)=INTEGRATED TWO-WAY TIME FOR EACH TIME LAYER
C           I=1 TO NPTS
C   XT(I)=AMPLITUDE VALUES FOR THE SYNTHETIC SEISMOGRAM, FOR EACH TIME
C   LAYER
C           I=1 TO NPTS
C   SYNDEP=TOTAL DEPTH CORRESPONDING TO THE TOP OF EACH TIME LAYER
C   WITHIN THE DEPTH OF THE WELL
C           I=1 TO J

```

```

C*****
DEP=0.

```

```

C*****
C   FOR THE UPPER, CONSTANT VELOCITY LAYERS
C*****
J=1
TIMLAY=0.0

```

```

DO 150 IJ=1,(NLAYER-LAYBEG+1)
DO 155 K=J,NPTS
SYNDEP(J)=(ACO(IJ)*(TWTIME(J)-TIMLAY)/2)+DEP
IF (SYNDEP(J).GE.ADEPTH(IJ+1)) GO TO 152
J=J+1
155 CONTINUE
152 SYNDEP(J)=ADEPTH(IJ+1)+((TWTIME(J)-INTIME(IJ+1))/2*ACO(IJ+1))
TIMLAY=TWTIME(J)
DEP=SYNDEP(J)
J=J+1
150 CONTINUE
IJ=IJ-1
JSTART=J
C*****
C   FOR THE LOWER LAYERS, WHICH WERE READ OFF THE LOGS
C*****
DO 200 J=JSTART,NPTS
IF (SYNDEP(J-1).LT..0001) GO TO 201
IF (INTIME(IJ).GE.TWTIME(J)) GO TO 190
C*****
C   DO LOOP TO INCREMENT INTIME(IJ) UNTIL IT IS GREATER THAN OR
C   EQUAL TO TWTIME(J)
C*****
160 DO 170 I=IJ,ANZ
IF (INTIME(IJ).GT.TWTIME(J)) GO TO 180
IJ=IJ+1
C
170 CONTINUE
C*****
C   CALCULATE THE TIME INTERVAL BETWEEN THE TWO BRACKETING
C   INTEGRATED TIMES AND THE AVERAGE VELOCITY OVER THAT INTERVAL
C*****
180 TIMINT=INTIME(IJ)-INTIME(IJ-1)
VAV=(ACO(IJ)+ACO(IJ-1))/2
C*****
C   INCREMENT INTIME(IJ-1) UNTIL THE CLOSEST TIME TO TWTIME(J)
C   IS FOUND
C*****
DELT=TIMINT/100
DO 185 K=1,1000
DELTIM=DELT*K
TI=INTIME(I-1)+DELTIM
IF (TI.LT.TWTIME(J)) GO TO 185
SYNDEP(J)=ADEPTH(I-1)+(VAV*DELTIM/2)
GO TO 200
185 CONTINUE
190 SYNDEP(J)=ADEPTH(IJ)
IJ=IJ+1
GO TO 200
200 CONTINUE
201 J=J-2
C
WRITE (6,24) (I, TWTIME(I),SYNDEP(I),XT(I),I=1,J,50)
24 FORMAT (I5,F10.4,2F10.3)
C*****

```

```

C     CALCULATE THE STARTING POINT FOR THE BLOWUP PLOTS
C*****
C
C     CALCULATE THE DEPTH LAYER NUMBER THAT CORRESPONDS TO THE
C     FIRST TDEPTH ARRAY POINT BELOW THE TOP OF THE MANNVILLE
C
      DO 220 I=1,NZ
      IF (TDEPTH(I) .LT. MANN) GO TO 220
      ISTART=I
      GO TO 221
220  CONTINUE
221  WRITE (6,27) ISTART,TDEPTH(ISTART),MANN
      27  FORMAT('- ',I5,2F10.3)
C
C     CALCULATE THE TWTIME CORRESPONDING TO THE FIRST SYNDEP ARRAY
C     POINT BELOW THE TOP OF THE MANNVILLE.  ADD THE DEPTH
C     DELAY, SO THAT SYNDEP IS MEASURED BELOW GROUND LEVEL
C
      DO 225 I=1,J
225  SYNDEP(I)=SYNDEP(I)+DEPDEL
      DO 230 I=1,J
      IF (SYNDEP(I) .LT. MANN) GO TO 230
      JSTART=I
      GO TO 231
230  CONTINUE
231  WRITE(6,27) JSTART,SYNDEP(JSTART),MANN
      SYNSTR=SYNDEP(JSTART)
C*****
C     CALCULATE THE TWTIME OF THE SYNDEP ARRAY POINT CORRESPONDING
C     TO THE TOP OF THE REX FM.(JREX).
C     NREX=NO. OF TWTIME POINTS BETWEEN JSTART AND JREX
C     J= THE NO. OF THE SYNDEP ARRAY POINTS CORRESPONDING
C     TO THE END OF THE INPUT LOGS.
C     NEND=NO. OF TWTIME POINTS BETWEEN JSTART AND J
C     ONE MAY USE N=NEND OR NREX IN SPECAN.DAT BELOW
C*****
      DO 235 I=JSTART,J
      IF(SYNDEP(I) .LT. REX) GO TO 235
      JREX=I
      GO TO 236
235  CONTINUE
236  NREX=(JREX-JSTART+1)
      NEND=(J-JSTART+1)
      WRITE(6,27) JREX,SYNDEP(JREX),REX
      WRITE(6,27) J,SYNDEP(J),TDEPTH(ANZ1)
      WRITE(6,33) NREX,NEND
      33  FORMAT('- ',2I5)
C*****
C     CONSTRUCT THE INPUT FILE (SPECAN.DAT) TO THE
C     SPECTRAL ANALYSIS PROGRAM SPECAN.
C     NTS=NO. OF TRACES TO BE SKIPPED BEFORE ANALYSIS
C     NIT=NO. OF INPUT TRACES
C     ST=STARTING TIME OF DESIRED WINDOW
C     N=NO. OF POINTS IN TIME WINDOW
C     DT=DIGITAL INTERVAL IN SECONDS

```

```

C      NPTS=NO. OF POINTS IN INPUT TIME SERIES
C*****
      NTS=0
      NIT=1
      ST=JSTART/1000.
      N=NREX
      DT=DT/1000.
      WRITE(32,34)NTS,NIT,ST,N
34  FORMAT(I4,2X,I2,2X,F5.3,2X,I4)
      WRITE(32,35)DT,NPTS
35  FORMAT(F5.4,2X,I4)
C*****
C      REWIND DATA FILES TO READ THE VALUES USED IN THE PLOT
C      DOCUMENTATION
C*****
      REWIND 21
      READ (21,50) LBL2(11),LBL3(11),LBL5(9),LBL14(6),LBL8(8)
*,LBL9(7),LBL10(11)
50  FORMAT (2X,1X,A4,3X,A2,5X,1X,A4,5X,3X,2X,17X,2X,A5,3X,
*,2X,A1,1X,A5,1X,A4)
      WRITE (6,53) LBL14
53  FORMAT(7A5)
C
      REWIND 31
      DO 250 I=1,NUNIT-1
      READ (31,52)
52  FORMAT(48X)
250  CONTINUE
      READ (31,51) LBL13(6)
51  FORMAT(18X,A5,25X)
      WRITE(6,53) LBL13
C*****
C      BEGIN THE PLOT
C*****
      CALL PLOTS(0,0,5)
C
C      POSITION PEN AT THE RIGHT HAND CORNER OF THE PAPER
C
C*****
C      PLOT THE SYNTHETIC SEISMOGRAM VERSUS TIME VALUES
C*****
      CALL PLOT(2.0,24.0,-3)
      CALL SYMBOL(3.0,3.0,1.0,LABEL1(1),0.0,25)
      CALL SYMBOL(0.0,1.5,.5,'SYNTHETIC SEISMOGRAM',0.0,20)
      CALL SCALE(TWTIME,21.0,NPTS,1)
      IF (WD .EQ. 0.) GO TO 270
      XT(NPTS+1)=-4000.
      XT(NPTS+2)=2000.
      GO TO 275
270  CALL SCALE(XT,10.0,NPTS,1)
C
275  CALL AXIS(0.0,0.0,'TWO-WAY TIME IN SECONDS',-23,21.0,270.0,0.00,
*,TWTIME(NPTS+2))
      CALL AXIS(0.0,0.0,'AMPLITUDE',9,10.0,0.0,XT(NPTS+1),XT
*(NPTS+2))

```

```

CALL PLOT(XT(1)/XT(NPTS+2)-XT(NPTS+1)/XT(NPTS+2),
*-(TWTIME(1))/TWTIME(NPTS+2),3)
DO 280 I=1,NPTS
CALL PLOT(XT(I)/XT(NPTS+2)-XT(NPTS+1)/XT(NPTS+2),
*-(TWTIME(I))/TWTIME(NPTS+2),2)
280 CONTINUE
C*****
C   WRITE THE PLOT DOCUMENTATION
C*****
CALL PLOT(15.0,1.0,-3)
CALL SYMBOL(0.0,0.0,.3,LBL2(1),0.0,55)
CALL SYMBOL(0.0,-.5,.3,LBL3(1),0.0,55)
CALL SYMBOL(0.0,-1.0,.3,LBL7(1),0.0,20)
IF (IPULS .NE. 0) GO TO 290
CALL SYMBOL(5.5,-1.0,.3,LBL12(1),0.0,10)
GO TO 293
290 CALL SYMBOL(5.5,-1.0,.3,LBL11(1),0.0,10)
293 IF (SDEPTH .EQ. 0.0) GO TO 295
CALL SYMBOL(7.7,-1.0,.3,LBL16(1),0.0,30)
295 IF (IBF .NE. 5) GO TO 296
CALL SYMBOL(0.0,-1.5,.3,LBL4(1),0.0,60)
296 IF(WD .EQ. 0.) GO TO 300
CALL SYMBOL(0.0,-2.0,.3,LBL10(1),0.0,55)
GO TO 303
300 CALL SYMBOL(0.0,-2.0,.3,LBL15(1),0.0,55)
303 CALL SYMBOL(0.0,-2.5,.3,LBL9(1),0.0,35)
CALL SYMBOL(0.0,-3.0,.3,LBL6(1),0.0,60)
CALL NUMBER(18.0,-3.0,.3,XLEAPK,0.0,0)
CALL SYMBOL(0.0,-3.5,.3,LBL8(1),0.0,40)
CALL SYMBOL(0.0,-4.0,.3,LBL5(1),0.0,45)
C
IF (IPULS .EQ. 0) GO TO 306
C*****
C   IF A WAVELET IS CONVOLVED, PLOT THE WAVELET SHAPE
C*****
CALL PLOT(2.0,-10.5,-3)
CALL SYMBOL(5.0,5.0,0.5,'WAVELET SHAPE',0.0,13)
CALL SCALE(WAVTIM,15.0,NSAMP,1)
CALL SCALE(WAVE,5.0,NSAMP,1)
CALL AXIS(0.0,0.0,'TIME IN SECONDS',-15,15.0,0.0,0.0,WAVTIM(NSAMP
.+2))
CALL AXIS(0.0,0.0,'AMPLITUDE',9,5.0,90.0,WAVE(NSAMP+1),WAVE
.(NSAMP+2))
CALL LINE(WAVTIM,WAVE,NSAMP,1,0,1)
C
C*****
C   PLOT THE AMPLITUDE SPECTRUM OF THE WAVELET
C*****
CALL PLOT(-2.0,-13.5,-3)
CALL SYMBOL(3.0,10.5,0.5,'AMPLITUDE SPECTRUM OF WAVELET',0.0,29)
CALL SCALE(WAVAMP,10.0,MPTS,1)
FREQ(MPTS+1)=0.
FREQ(MPTS+2)=FREQ(MPTS)/20.
CALL AXIS(0.0,0.0,'FREQUENCY IN HERTZ',-18,20.0,0.0,0.0,FREQ
.MPTS+2))

```

```

CALL AXIS(0.0,0.0,'AMPLITUDE',9,10.0,90.0,WAVAMP(MPTS+1),
.WAVAMP(MPTS+2))
CALL LINE(FREQ,WAVAMP,MPTS,1,0,1)
C
C
C*****
C    PLOT THE VALUES VERSUS DEPTH
C*****
    CALL PLOT(26.0,23.0,-3)
    GO TO 307
306 CALL PLOT(26.0,-1.0,-3)
307 CALL SYMBOL(4.0,3.0,1.0,LABEL1(1),0.0,25)
    TDEPTH(NZ+2)=25.0
C*****
C    ATTENUATION COEFFICIENT PLOT
C*****
    CALL SYMBOL(2.5,1.5,.5,'Q',0.0,1)
    QO(NZ+1)=0.
    QO(NZ+2)=20.
    CALL AXIS(0.0,0.0,'Q',1,5.0,0.0,QO(NZ+1),QO(NZ+2))
    CALL AXIS(0.0,0.0,'DEPTH IN METRES',-15,24.0,270.0,0.0,
*TDEPTH(NZ+2))
    CALL PLOT(QO(1)/QO(NZ+2)-QO(NZ+1)/QO(NZ+2),0.,3)
    DO 308 I=1,NLAYER
    CALL PLOT(QO(I)/QO(NZ+2)-QO(NZ+1)/QO(NZ+2),
*-(TDEPTH(I)+Z(I))/TDEPTH(NZ+2),2)
    CALL PLOT(QO(I+1)/QO(NZ+2)-QO(NZ+1)/QO(NZ+2),
*-(TDEPTH(I)+Z(I))/TDEPTH(NZ+2),2)
308 CONTINUE
    DO 310 I=NLAYER+1,NZ
    CALL PLOT(QO(I)/QO(NZ+2)-QO(NZ+1)/QO(NZ+2),
*-TDEPTH(I)/TDEPTH(NZ+2),2)
310 CONTINUE
C*****
C    DENSITY PLOT
C*****
    CALL PLOT(7.5,0.0,-3)
    CALL SYMBOL(0.0,1.5,.5,'DENSITY',0.0,7)
    RHO(NZ+1)=1500.
    RHO(NZ+2)=250.
    CALL AXIS(0.0,0.0,'KG/CUBIC METRE',14,5.0,0.0,RHO(NZ+1),
*RHO(NZ+2))
    CALL AXIS(0.0,0.0,'DEPTH IN METRES',-15,24.0,270.0,0.0,
*TDEPTH(NZ+2))
    CALL PLOT(RHO(1)/RHO(NZ+2)-RHO(NZ+1)/RHO(NZ+2),0.,3)
    DO 315 I=1,NLAYER
    CALL PLOT(RHO(I)/RHO(NZ+2)-RHO(NZ+1)/RHO(NZ+2),
*-(TDEPTH(I)+Z(I))/TDEPTH(NZ+2),2)
    CALL PLOT(RHO(I+1)/RHO(NZ+2)-RHO(NZ+1)/RHO(NZ+2),
*-(TDEPTH(I)+Z(I))/TDEPTH(NZ+2),2)
315 CONTINUE
    DO 320 I=NLAYER+1,NZ
    CALL PLOT(RHO(I)/RHO(NZ+2)-RHO(NZ+1)/RHO(NZ+2),
*-TDEPTH(I)/TDEPTH(NZ+2),2)
320 CONTINUE

```

```

C*****
C   VELOCITY PLOT
C*****
  CALL PLOT(7.5,0.0,-3)
  CALL SYMBOL(0.0,1.5,.5,'VELOCITY',0.0,8)
  CO(NZ+1)=1000.
  CO(NZ+2)=1000.
  CALL AXIS(0.0,0.0,'METRES/S',8,5.0,0.0,CO(NZ+1)
*,CO(NZ+2))
  CALL AXIS(0.0,0.0,'DEPTH IN METRES',-15,24.0,270.0,0.0,
*TDEPTH(NZ+2))
  CALL PLOT(CO(1)/CO(NZ+2)-CO(NZ+1)/CO(NZ+2),0.,3)
  DO 325 I=1,NLAYER
  CALL PLOT(CO(I)/CO(NZ+2)-CO(NZ+1)/CO(NZ+2),
*-(TDEPTH(I)+Z(I))/TDEPTH(NZ+2),2)
  CALL PLOT(CO(I+1)/CO(NZ+2)-CO(NZ+1)/CO(NZ+2),
*-(TDEPTH(I)+Z(I))/TDEPTH(NZ+2),2)
325 CONTINUE
  DO 330 I=NLAYER+1,NZ
  CALL PLOT(CO(I)/CO(NZ+2)-CO(NZ+1)/CO(NZ+2),
*-(TDEPTH(I))/TDEPTH(NZ+2),2)
330 CONTINUE
C*****
C   SYNTHETIC SEISMOGRAM PLOT
C*****
  CALL PLOT(7.5,0.0,-3)
  CALL SYMBOL(0.0,2.0,.5,'SYNTHETIC',0.0,9)
  CALL SYMBOL(0.0,1.4,.5,'SEISMOGRAM',0.0,10)
  IF (WD .EQ. 0.) GO TO 335
  XT(J+1)=-4000.
  XT(J+2)=2000.
  GO TO 338
335 CALL SCALE(XT,7.0,J,1)
338 CALL AXIS(0.0,0.0,'AMPLITUDE',9,7.0,0.0,XT(J+1),
*XT(J+2))
  CALL AXIS(0.0,0.0,'DEPTH IN METRES',-15,24.0,270.0,0.0,
*TDEPTH(NZ+2))
  CALL PLOT(XT(1)/XT(J+2)-XT(J+1)/XT(J+2),
*-(SYNDEP(1))/TDEPTH(NZ+2),3)
  DO 340 I=1,J
  CALL PLOT(XT(I)/XT(J+2)-XT(J+1)/XT(J+2),
*-(SYNDEP(I))/TDEPTH(NZ+2),2)
340 CONTINUE
C
C   PLOT TWO-WAY TRAVEL TIMES
C
C   K=0
C
  DO 350 I=1,J
  K=K+1
  IF (TWTIME(I) .LT. .05) GO TO 350
  CALL SYMBOL(0.0,-(SYNDEP(I)/TDEPTH(NZ+2))-.1,.2,'--.05 S',0.0,7)
  GO TO 354
350 CONTINUE
C

```

```
354 DO 355 I=K,J
      K=K+1
      IF (TWTIME(I) .LT. .1) GO TO 355
      CALL SYMBOL(0.0,-(SYNDEP(I)/TDEPTH(NZ+2))-.1,.2,'---.10 S',0.0,7)
      GO TO 359
355 CONTINUE
C
359 DO 360 I=K,J
      K=K+1
      IF (TWTIME(I) .LT. .15) GO TO 360
      CALL SYMBOL(0.0,-(SYNDEP(I)/TDEPTH(NZ+2))-.1,.2,'---.15 S',0.0,7)
      GO TO 364
360 CONTINUE
C
364 DO 365 I=K,J
      K=K+1
      IF (TWTIME(I) .LT. .2) GO TO 365
      CALL SYMBOL(0.0,-(SYNDEP(I)/TDEPTH(NZ+2))-.1,.2,'---.20 S',0.0,7)
      GO TO 369
365 CONTINUE
C
369 DO 370 I=K,J
      K=K+1
      IF (TWTIME(I) .LT. .25) GO TO 370
      CALL SYMBOL(0.0,-(SYNDEP(I)/TDEPTH(NZ+2))-.1,.2,'---.25 S',0.0,7)
      GO TO 374
370 CONTINUE
C
374 DO 375 I=K,J
      K=K+1
      IF (TWTIME(I) .LT. .3) GO TO 375
      CALL SYMBOL(0.0,-(SYNDEP(I)/TDEPTH(NZ+2))-.1,.2,'---.30 S',0.0,7)
      GO TO 379
375 CONTINUE
C
379 DO 380 I=K,J
      K=K+1
      IF (TWTIME(I) .LT. .35) GO TO 380
      CALL SYMBOL(0.0,-(SYNDEP(I)/TDEPTH(NZ+2))-.1,.2,'---.35 S',0.0,7)
      GO TO 384
380 CONTINUE
C
384 DO 385 I=K,J
      K=K+1
      IF (TWTIME(I) .LT. .4) GO TO 385
      CALL SYMBOL(0.0,-(SYNDEP(I)/TDEPTH(NZ+2))-.1,.2,'---.40 S',0.0,7)
      GO TO 389
385 CONTINUE
C
389 DO 390 I=K,J
      K=K+1
      IF (TWTIME(I) .LT. .45) GO TO 390
      CALL SYMBOL(0.0,-(SYNDEP(I)/TDEPTH(NZ+2))-.1,.2,'---.45 S',0.0,7)
      GO TO 394
390 CONTINUE
```

```

C
394 DO 395 I=K,J
      K=K+1
      IF (TWTIME(I) .LT. .5) GO TO 395
      CALL SYMBOL(0.0,-(SYNDEP(I)/TDEPTH(NZ+2))-.1,.2,'--.50 S',
*0.0,7)
      GO TO 400
395 CONTINUE
C*****
C      PLOT THE STRATIGRAPHIC MARKER HORIZONS
C*****
400 CALL PLOT (9.5,0.0,-3)
      CALL SYMBOL(0.0,2.0,.5,'STRATIGRAPHIC',0.0,13)
      CALL SYMBOL(0.0,1.4,.5,'MARKER BEDS',0.0,11)
      CALL AXIS(0.0,0.0,'DEPTH IN METRES',-15,24.0,270.0,0.0,
*TDEPTH(NZ+2))
      CALL SYMBOL(0.0,-(DRIFTU/TDEPTH(NZ+2))-.1,.2,'_UPPER DRIFT',0.0,
*13)
      CALL SYMBOL(0.0,-(DRIFTM/TDEPTH(NZ+2))-.1,.2,'_MIDDLE DRIFT',0.0
*,14)
      CALL SYMBOL(0.0,-(DRIFTL/TDEPTH(NZ+2))-.1,.2,'_LOWER DRIFT',
*0.0,13)
      CALL SYMBOL(0.0,-(LEAPK/TDEPTH(NZ+2))-.1,.2,'_MONTANA GROUP',0.0
*,15)
      CALL SYMBOL(0.1,-(LEAPK/TDEPTH(NZ+2))-.5,.2,'(TOP OF LEA
*PARK FM.)',0.0,21)
      CALL SYMBOL(0.0,-(UCOLO/TDEPTH(NZ+2))-.1,.2,'_U. COLORADO GROUP',
*0.0,19)
      CALL SYMBOL(0.0,-(SWHSP/TDEPTH(NZ+2))-.1,.2,'_2ND WHITE SPECKLED
* SH.',0.0,24)
      CALL SYMBOL(0.0,-(LCOLO/TDEPTH(NZ+2))-.1,.2,'_L. COLORADO GROUP',
*0.0,19)
      CALL SYMBOL(0.0,-(TWAL/TDEPTH(NZ+2))-.1,.2,'_TOP ST. WALBURG SST
*.',0.0,22)
      CALL SYMBOL(0.0,-(BWAL/TDEPTH(NZ+2))-.1,.2,'_BASE ST. WALBURG SST
*.',0.0,23)
      CALL SYMBOL(0.0,-(MANN/TDEPTH(NZ+2))-.1,.2,'_MANNVILLE GROUP',0.0
*,17)
      CALL SYMBOL(0.0,-(MCLARN/TDEPTH(NZ+2))-.1,.2,'_MCLAREN FM.',0.0,
*13)
      CALL SYMBOL(0.0,-(WASECA/TDEPTH(NZ+2))-.1,.2,'_WASECA FM.',0.0,
*12)
      CALL SYMBOL(0.0,-(SPARKY/TDEPTH(NZ+2))-.1,.2,'_SPARKY FM.',0.0,
*12)
      CALL SYMBOL(0.0,-(GP/TDEPTH(NZ+2))-.1,.2,'_GENERAL PETROLEUM FM
*.',0.0,23)
      IF (REX .EQ. 999.9) GO TO 405
      CALL SYMBOL(0.0,-(REX/TDEPTH(NZ+2))-.1,.2,'_REX FM.',0.0,9)
C
C
C*****
C      DRAW THE BLOWN UP MANNVILLE PLOTS
C*****
405 CALL PLOT(18.0,-23.5,-3)
      CALL SYMBOL(-7.0,2.0,1.0,LABEL1(1),90.0,25)

```

```

CALL SYMBOL(-5.4,-.5,.6,'BLOWUP TO GEOPHYSICAL LOG SCALE (1 CM
*= 2.4 M)',90.0,46)
CALL SYMBOL(-4.0,-.2,.6,'MANNVILLE PORTION OF THE SYNTHETIC
* SEISMOGRAM',90.0,45)
TDEPTH(NZ+1)=MANN
TDEPTH(NZ+2)=2.4
IF (WD .EQ. 0.) GO TO 407
XT(J+1)=-4500.
XT(J+2)=350.
GO TO 408
407 CALL SCALE(XT,27.0,J,1)
C*****
C    SYNTHETIC SEISMOGRAM PLOT
C*****
408 CALL SYMBOL(-1.5,0.0,.5,'SYNTHETIC SEISMOGRAM',90.0,20)
CALL AXIS(0.0,0.0,'AMPLITUDE',9,27.0,90.0,XT(J+1),XT(J+2))
CALL AXIS(0.0,0.0,'DEPTH IN METRES',-15,50.0,0.0,TDEPTH(NZ+1),
*TDEPTH(NZ+2))
CALL PLOT(((SYNSTR-TDEPTH(NZ+1))/TDEPTH(NZ+2),
*(XT(JSTART)-XT(J+1))/XT(J+2),3)
DO 410 I=JSTART,J
CALL PLOT(((SYNDEP(I)-TDEPTH(NZ+1))/TDEPTH(NZ+2),
*(XT(I)-XT(J+1))/XT(J+2),2)
410 CONTINUE
C*****
C    NEW PAGE
C*****
CALL PLOT(85.0,0.0,-3)
CALL SYMBOL(-8.0,2.0,1.0,LABEL1(1),90.0,25)
CALL SYMBOL(-6.4,-.5,.6,'BLOWUP TO GEOPHYSICAL LOG SCALE (1 CM
*= 2.4 M)',90.0,46)
CALL SYMBOL(-5.0,5.0,.6,'MANNVILLE PORTION OF THE DATA',90.0,29)
C
C
C*****
C    PLOT THE FORMATION TOPS
C*****
CALL SYMBOL(-2.0,0.0,.5,'FORMATION',90.0,9)
CALL SYMBOL(-1.4,0.0,.5,'TOPS',90.0,4)
CALL AXIS(0.0,0.0,'DEPTH IN METRES',-15,50.0,0.0,TDEPTH(NZ+1),
*TDEPTH(NZ+2))
CALL SYMBOL(((MANN-TDEPTH(NZ+1))/TDEPTH(NZ+2))+.1,0.0,.2,
*'-COLONY FM.',90.0,12)
CALL SYMBOL(((MANN-TDEPTH(NZ+1))/TDEPTH(NZ+2))+.5,0.1,.2,
*'(TOP OF MANNVILLE GRP.)',90.0,23)
CALL SYMBOL(((MCLARN-TDEPTH(NZ+1))/TDEPTH(NZ+2))+.1,0.0,.2,
*'-MCLAREN FM.',90.0,13)
CALL SYMBOL(((WASECA-TDEPTH(NZ+1))/TDEPTH(NZ+2))+.1,0.0,.2,
*'-WASECA FM.',90.0,12)
CALL SYMBOL(((SPARKY-TDEPTH(NZ+1))/TDEPTH(NZ+2))+.1,0.0,.2,
*'-SPARKY FM.',90.0,12)
CALL SYMBOL(((GP-TDEPTH(NZ+1))/TDEPTH(NZ+2))+.1,0.0,.2,
*'-GENERAL PETROLEUM FM.',90.0,23)
IF (REX .EQ. 999.9) GO TO 415
CALL SYMBOL(((REX-TDEPTH(NZ+1))/TDEPTH(NZ+2))+.1,0.0,.2,

```

```

*'---REX FM.',90.0,9)
C*****
C   PLOT THE LITHOFACIES TYPE, CEMENT TYPE, AND THE DEGREE OF
C   OIL STAIN
C*****
415 CALL PLOT(0.0,6.3,-3)
    CALL SYMBOL(-2.6,0.0,.5,'OIL STAIN',90.0,10)
    CALL SYMBOL(-2.0,0.0,.5,'LITHOFACIES',90.0,12)
    CALL SYMBOL(-1.4,0.0,.5,'AND CEMENT TYPE',90.0,15)
    CALL AXIS(0.0,0.0,'DEPTH IN METRES',-15,50.0,0.0,TDEPTH
*(NZ+1),TDEPTH(NZ+2))
    CALL PLOT(0.0,7.0,2)
    IF (TOPBED(NUNIT) .LT. MANN) GO TO 417
    CALL SYMBOL(-.2,0.0,.2,'OIL STAIN',90.0,9)
    CALL SYMBOL(-.2,2.0,.2,' LITHOFACIES',90.0,12)
    CALL SYMBOL(-.2,4.5,.2,' CEMENT TYPE',90.0,13)

C
C   DRAW IN THE LAYER BOUNDARIES
C
417 DO 420 I=1,NUNIT
    CALL PLOT((TOPBED(I)-TDEPTH(NZ+1))/TDEPTH(NZ+2),0.0,3)
    CALL PLOT((TOPBED(I)-TDEPTH(NZ+1))/TDEPTH(NZ+2),7.0,2)
420 CONTINUE
    CALL PLOT((TOPBED(1)+THICK(1)-TDEPTH(NZ+1))/
*TDEPTH(NZ+2),0.0,3)
    CALL PLOT((TOPBED(1)+THICK(1)-TDEPTH(NZ+1))/
*TDEPTH(NZ+2),7.0,2)

C
C   WRITE IN THE DEPTH OF THE TOP AND BOTTOM OF THE CORED SECTION
C
    CALL SYMBOL(((TOPBED(NUNIT)-TDEPTH(NZ+1))/TDEPTH(NZ+2))- .2,
*0.1,.2,LBL13(1),90.0,35)
    CALL SYMBOL(((TOPBED(1)+THICK(1)-TDEPTH(NZ+1))/
*TDEPTH(NZ+2))+.4,0.1,.2,LBL14(1),90.0,35)

C
C   PLOT THE DEGREE OF OIL SATURATION
C
    CALL PLOT((TOPBED(1)+THICK(1)-TDEPTH(NZ+1))/TDEPTH(NZ+2),0.1,3)
    DO 422 I=1,NUNIT
    XX=(TOPBED(I)-TDEPTH(NZ+1))/TDEPTH(NZ+2)
    IF (OILSAT(I) .LE. 0.19) GO TO 421
    CALL PLOT (XX,0.1,2)
    IF (OILSAT(I) .GE. 0.50) GO TO 422
    CENTRE=.1+((THICK(I)-.2)/2.4)/2.
    CALL SYMBOL(XX+CENTRE,0.5,.1,'MODERATE',90.0,8)
421 CALL PLOT(XX,0.1,3)
422 CONTINUE

C
    CALL PLOT((TOPBED(1)+THICK(1)-TDEPTH(NZ+1))/TDEPTH(NZ+2),0.2,3)
    DO 426 I=1,NUNIT
    XX=(TOPBED(I)-TDEPTH(NZ+1))/TDEPTH(NZ+2)
    IF (OILSAT(I) .LE. 0.49) GO TO 425
    CALL PLOT (XX,0.2,2)
    IF (OILSAT(I) .GE. 0.70) GO TO 426
    CENTRE=.1+((THICK(I)-.2)/2.4)/2.

```

```

CALL SYMBOL (XX+CENTRE,0.5,.1,'HEAVY',90.0,5)
425 CALL PLOT (XX,0.2,3)
426 CONTINUE
C
CALL PLOT ((TOPBED(1)+THICK(1)-TDEPTH(NZ+1))/TDEPTH(NZ+2),0.3,3)
DO 430 I=1,NUNIT
XX=(TOPBED(I)-TDEPTH(NZ+1))/TDEPTH(NZ+2)
IF (OILSAT(I) .LE. 0.69) GO TO 429
CALL PLOT (XX,0.3,2)
CENTRE=.1+((THICK(I)-.2)/2.4)/2.
CALL SYMBOL (XX+CENTRE,0.5,.1,'SATURATED',90.0,9)
429 CALL PLOT (XX,0.3,3)
430 CONTINUE
C
C
C
PLOT THE LITHOFACIES TYPE
DO 435 I=1,NUNIT
XX=(TOPBED(I)-TDEPTH(NZ+1))/TDEPTH(NZ+2)
CENTRE=.1+((THICK(I)-.2)/2.4)/2.
CALL SYMBOL (XX+CENTRE,3.5,.1,FAC(I),90.0,1)
435 CONTINUE
C
C
C
PLOT THE CEMENT TYPE
DO 440 I=1,NUNIT
XX=(TOPBED(I)-TDEPTH(NZ+1))/TDEPTH(NZ+2)
CENTRE=.1+((THICK(I)-.2)/2.4)/2.
IF (CEM(I) .EQ. 0) GO TO 440
IF (CEM(I) .EQ. 1) CALL SYMBOL (XX+CENTRE,5.0,.1,'CLAY',
*90.0,4)
IF (CEM(I) .EQ. 2) CALL SYMBOL (XX+CENTRE,5.0,.1,'PATCHY
* CLAY',90.0,11)
IF (CEM(I) .EQ. 3) CALL SYMBOL (XX+CENTRE,5.0,.1,'CALCITE',
*90.0,7)
IF (CEM(I) .EQ. 4) CALL SYMBOL (XX+CENTRE,5.0,.1,'PATCHY
* CALCITE',90.0,14)
IF (CEM(I) .EQ. 5) CALL SYMBOL (XX+CENTRE,5.0,.1,'CALCITE
* NODULES',90.0,15)
IF (CEM(I) .EQ. 6) CALL SYMBOL (XX+CENTRE,5.0,.1,'CARBONATE
* (NON-CALC)',90.0,20)
IF (CEM(I) .EQ. 7) CALL SYMBOL (XX+CENTRE,5.0,.1,'PCH CBT
* (NON-CALC)',90.0,18)
IF (CEM(I) .EQ. 8) CALL SYMBOL (XX+CENTRE,5.0,.1,'CBT (NON-
*CALC) NOD',90.0,18)
IF (CEM(I) .EQ. 9) CALL SYMBOL (XX+CENTRE,5.0,.1,'MIXTURE',
*90.0,7)
440 CONTINUE
C*****
C VELOCITY PLOT
C*****
CALL PLOT (0.0,8.8,-3)
CALL SYMBOL (-1.5,0.0,.5,'VELOCITY',90.0,8)
CALL AXIS (0.0,0.0,'METRES/S',8,5.0,90.0,CO(NZ+1),CO(NZ+2))
CALL AXIS (0.0,0.0,'DEPTH IN METRES',-15,50.0,0.0,TDEPTH(NZ+1),
*TDEPTH(NZ+2))

```

```

CALL PLOT((TDEPTH(ISTART)-TDEPTH(NZ+1))/TDEPTH(NZ+2),
*(CO(ISTART)-CO(NZ+1))/CO(NZ+2),3)
DO 450 I=ISTART,NZ
CALL PLOT((TDEPTH(I)-TDEPTH(NZ+1))/TDEPTH(NZ+2),
*(CO(I)-CO(NZ+1))/CO(NZ+2),2)
450 CONTINUE
C*****
C    DENSITY PLOT
C*****
CALL PLOT(0.0,6.8,-3)
CALL SYMBOL(-1.5,0.0,.5,'DENSITY',90.0,7)
CALL AXIS(0.0,0.0,'KG/CUBIC METRE',14,5.0,90.0,RHO(NZ+1),
*RHO(NZ+2))
CALL AXIS(0.0,0.0,'DEPTH IN METRES',-15,50.0,0.0,TDEPTH(NZ+1),
*TDEPTH(NZ+2))
CALL PLOT((TDEPTH(ISTART)-TDEPTH(NZ+1))/TDEPTH(NZ+2),(RHO(ISTART)-
*RHO(NZ+1))/RHO(NZ+2),3)
DO 460 I=ISTART,NZ
CALL PLOT((TDEPTH(I)-TDEPTH(NZ+1))/TDEPTH(NZ+2),(RHO(I)-
*RHO(NZ+1))/RHO(NZ+2),2)
460 CONTINUE
C*****
C    NEW PAGE
C*****
CALL PLOT(84.0,-21.9,-3)
CALL SYMBOL(-8.0,2.0,1.0,LABEL1(1),90.0,25)
CALL SYMBOL(-6.4,-.5,.6,'BLOWUP TO GEOPHYSICAL LOG SCALE (1 CM
*= 2.4 M)',90.0,46)
CALL SYMBOL(-5.0,0.0,.6,'MANNVILLE PORTION OF THE CORE ANALYSES
* DATA',90.0,43)
C*****
C    PLOT THE MEAN POROSITY FOR EACH UNIT IN THE CORED SECTION
C*****
CALL SYMBOL(-1.5,0.0,.5,'POROSITY',90.0,8)
DO 465 I=1,NUNIT
465 POR(I)=100*POR(I)
POR(NUNIT+1)=0.
POR(NUNIT+2)=10.
CALL AXIS(0.0,0.0,'% ROCK VOLUME',13,5.0,90.0,POR(NUNIT+1),
*POR(NUNIT+2))
CALL AXIS(0.0,0.0,'DEPTH IN METRES',-15,50.0,0.0,TDEPTH(NZ+1),
*TDEPTH(NZ+2))
CALL PLOT((TOPBED(1)+THICK(1)-TDEPTH(NZ+1))/TDEPTH(NZ+2),
*(POR(1)-POR(NUNIT+1))/POR(NUNIT+2),3)
DO 470 I=1,NUNIT
IF (TOPBED(I) .LT. MANN) GO TO 471
CALL PLOT((TOPBED(I)-TDEPTH(NZ+1))/TDEPTH(NZ+2),
*(POR(I)-POR(NUNIT+1))/POR(NUNIT+2),2)
IF (I .EQ. NUNIT) GO TO 470
CALL PLOT((TOPBED(I)-TDEPTH(NZ+1))/TDEPTH(NZ+2),
*(POR(I+1)-POR(NUNIT+1))/POR(NUNIT+2),2)
470 CONTINUE
C*****
C    PLOT THE MEAN PERMEABILITY TO AIR FOR EACH UNIT IN THE CORED
C    SECTION

```

C*****

```

471 CALL PLOT(0.0,7.0,-3)
    CALL SYMBOL(-2.0,0.0,.5,'PERMEABILITY',90.0,12)
    CALL SYMBOL(-1.4,0.0,.5,'TO AIR',90.0,6)
    PERM(NUNIT+1)=0.
    PERM(NUNIT+2)=1000.
    CALL AXIS(0.0,0.0,'MILLIDARCYS',11,6.0,90.0,PERM(NUNIT+1),
*PERM(NUNIT+2))
    CALL AXIS(0.0,0.0,'DEPTH IN METRES',-15,50.0,0.0,TDEPTH(NZ+1),
*TDEPTH(NZ+2))
    CALL PLOT((TOPBED(1)+THICK(1)-TDEPTH(NZ+1))/TDEPTH(NZ+2),
*(PERM(1)-PERM(NUNIT+1))/PERM(NUNIT+2),3)
    DO 475 I=1,NUNIT
    IF (TOPBED(I) .LT. MANN) GO TO 476
    CALL PLOT((TOPBED(I)-TDEPTH(NZ+1))/TDEPTH(NZ+2),
*(PERM(I)-PERM(NUNIT+1))/PERM(NUNIT+2),2)
    IF (I .EQ. NUNIT) GO TO 475
    CALL PLOT((TOPBED(I)-TDEPTH(NZ+1))/TDEPTH(NZ+2),
*(PERM(I+1)-PERM(NUNIT+1))/PERM(NUNIT+2),2)
475 CONTINUE

```

C*****

```

C    PLOT THE MEAN OIL SATURATION FOR EACH UNIT IN THE CORED
C    SECTION

```

C*****

```

476 CALL PLOT(0.0,8.0,-3)
    DO 478 I=1,NUNIT
478 OILSAT(I)=100*OILSAT(I)
    CALL SYMBOL(-2.0,0.0,.5,'OIL',90.0,3)
    CALL SYMBOL(-1.4,0.0,.5,'SATURATION',90.0,10)
    OILSAT(NUNIT+1)=0.
    OILSAT(NUNIT+2)=20.
    CALL AXIS(0.0,0.0,'% PORE VOLUME',13,5.0,90.0,OILSAT(NUNIT+1),
*OILSAT(NUNIT+2))
    CALL AXIS(0.0,0.0,'DEPTH IN METRES',-15,50.0,0.0,TDEPTH(NZ+1),
*TDEPTH(NZ+2))
    CALL PLOT((TOPBED(1)+THICK(1)-TDEPTH(NZ+1))/TDEPTH(NZ+2),
*(OILSAT(1)-OILSAT(NUNIT+1))/OILSAT(NUNIT+2),3)
    DO 480 I=1,NUNIT
    IF (TOPBED(I) .LT. MANN) GO TO 481
    CALL PLOT((TOPBED(I)-TDEPTH(NZ+1))/TDEPTH(NZ+2),
*(OILSAT(I)-OILSAT(NUNIT+1))/OILSAT(NUNIT+2),2)
    IF (I .EQ. NUNIT) GO TO 480
    CALL PLOT((TOPBED(I)-TDEPTH(NZ+1))/TDEPTH(NZ+2),
*(OILSAT(I+1)-OILSAT(NUNIT+1))/OILSAT(NUNIT+2),2)
480 CONTINUE

```

C*****

```

C    PLOT THE MEAN (ESTIMATED) CLAY CONTENT FOR EACH UNIT IN
C    THE CORED SECTION

```

C*****

```

481 CALL PLOT(0.0,7.0,-3)
    CALL SYMBOL(-2.0,0.0,.5,'CLAY',90.0,4)
    CALL SYMBOL(-1.4,0.0,.5,'CONTENT',90.0,7)
    CLAY(NUNIT+1)=0.
    CLAY(NUNIT+2)=20.
    CALL AXIS(0.0,0.0,'% ROCK VOLUME',13,5.0,90.0,CLAY(NUNIT+1),

```

```

*CLAY(NUNIT+2))
  CALL AXIS(0.0,0.0,'DEPTH IN METRES',-15,50.0,0.0,TDEPTH(NZ+1),
*TDEPTH(NZ+2))
  CALL PLOT((TOPBED(1)+THICK(1)-TDEPTH(NZ+1))/TDEPTH(NZ+2),
*(CLAY(1)-CLAY(NUNIT+1))/CLAY(NUNIT+2),3)
  DO 485 I=1,NUNIT
  IF (TOPBED(I) .LT. MANN) GO TO 486
  CALL PLOT((TOPBED(I)-TDEPTH(NZ+1))/TDEPTH(NZ+2),
*(CLAY(I)-CLAY(NUNIT+1))/CLAY(NUNIT+2),2)
  IF (I .EQ. NUNIT) GO TO 485
  CALL PLOT((TOPBED(I)-TDEPTH(NZ+1))/TDEPTH(NZ+2),
*(CLAY(I+1)-CLAY(NUNIT+1))/CLAY(NUNIT+2),2)
485 CONTINUE
486 CALL PLOT(0.0,0.0,999)
  CLOSE(UNIT=1)
  CLOSE(UNIT=21)
  CLOSE(UNIT=22)
  CLOSE(UNIT=23)
  CLOSE(UNIT=24)
  CLOSE(UNIT=25)
  CLOSE(UNIT=26)
  CLOSE(UNIT=28)
  CLOSE(UNIT=30)
  CLOSE(UNIT=31)
  CLOSE(UNIT=32)
  STOP
  END

```

C

C

C*****

C

SUBROUTINE PWRGFN(C,NPS,S,WD,DT)

C

C*****

C

WRITTEN BY I. SEREDA

C

REAL C(8192)

REAL*8 S(8192),PWR

DTI=1/(DT*.001)

NWD=INT(WD*DTI+.5)

DO 1 I=1,NPS

1 S(I)=C(I)*C(I)

C

NW2=NWD/2

NW1=NW2+1

C

PWR=0.0

NORM=0

C

DO 2 J=1,NW1

NORM=NORM+1

2 PWR=PWR+S(J)

C

PWRN=PWR/NORM

RMS=SQRT(PWRN)

```
IF(RMS.EQ.0.0)RMS=1000.  
GN=1000./RMS  
C(1)=C(1)*GN
```

C

```
DO 3 K=2,NPS  
L=K-NW1  
IF(L.LT.1) GO TO 10  
PWR=PWR-S(L)  
GO TO 13  
10 NORM=NORM+1  
13 M=K+NW2  
IF (M.GT.NPS) GO TO 12  
PWR=PWR+S(M)  
GO TO 11  
12 NORM=NORM-1  
11 PWRN=PWR/NORM  
RMS=SQRT(PWRN)  
IF (RMS.EQ.0.0) RMS=1000.  
GN=1000./RMS  
C(K)=C(K)*GN  
3 CONTINUE  
RETURN  
END
```

```

C*****
C
C           L O G G R F
C
C*****
C   PURPOSE:  TO PLOT THE MANNVILLE PORTION OF THE CORE
C             AND LOG DATA FOR THE WELLS IN THE CELTIC FIELD
C
C   PROGRAMMER:  MARGARET LOMAS
C                DEPT. OF GEOL. SCIENCES (GEOPHYSICS)
C                SASKATOON
C                1982
C*****
C
C*****
C   DIMENSION SECTION
C*****
C   INTEGER UNIT(100),CEM(100),PO,LABEL1(5),LBL13(3),LBL14(3),
C   *LBL15(2),LBL16(2)
C   REAL INTIME(4001),LCOLO,MANN,MONTAN,LEAPK,MCLARN
C   DIMENSION Z(4001),CO(4001),QO(4001),RHO(4001),TT(4001)
C   DIMENSION TDEPTH(4001),TTIME(4001),CCO(100),RRHO(100)
C   DIMENSION FAC(100),BED(100),THICK(100),TOPBED(100),
C   * POR(100),OILSAT(100),PERM(100),CLAY(100)
C
C*****
C   OPEN STATEMENTS
C*****
C   OPEN(UNIT=21,DEVICE='DSK',ACCESS='SEQIN',FILE='SYNGAN.DAT',
C   *DIALOG)
C   OPEN(UNIT=22,DEVICE='DSK',ACCESS='SEQIN',FILE='GANCEL.DAT',
C   *DIALOG)
C   OPEN(UNIT=23,DEVICE='DSK',ACCESS='SEQIN',FILE='AU.DAT',
C   *DIALOG)
C   OPEN(UNIT=24,DEVICE='DSK',ACCESS='SEQIN',FILE='DEN.DAT',
C   *DIALOG)
C   OPEN(UNIT=30,DEVICE='DSK',ACCESS='SEQIN',FILE='PIX.DAT',
C   *DIALOG)
C   OPEN(UNIT=31,DEVICE='DSK',ACCESS='SEQIN',FILE='CA.DAT',
C   *DIALOG)
C*****
C   LABELS FOR PLOTS
C*****
C   DATA LBL13/'TOP O','F COR','E'  '/',
C   *LBL14/'END O','F COR','E'  '/',
C   *LBL15/'      ',' M'  '/',
C   *LBL16/'      ',' M'  /
C*****
C   READ IN THE INPUT PARAMETERS; THIS IS THE SAME FILE AS IS
C   USED FOR INPUT TO SYNCEL.FOR
C*****
C   READ (21,1) NPTS,DT,IBF,SDEPTH,FC,NLAYER,IPULS,PERIOD,PO,
C   .DEPCOR,NUNIT,DEPCAS,WD
C*****
C   NPTS = NUMBER OF POINTS DESIRED IN SYNTHETIC TRACE

```

```

C          MAXIMUM IS 4096 AND NPTS SHOULD BE POWER OF 2
C          DT = SAMPLE INTERVAL IN MILLISECONDS
C          IBF = 5 MEANS TO INCLUDE THE BUTTERWORTH ANTI-ALIAS FILTER
C          SDEPTH = DEPTH OF SOURCE. THIS DEPTH CAN BE ZERO, BUT THE
C          DEPTH MUST BE AT A LAYER BOUNDARY OR AN ERROR MESSAGE
C          WILL RESULT.
C          FC = FREQUENCY AT WHICH VELOCITY AND Q ARE INPUT
C          NLayer = NUMBER OF LAYERS ABOVE WHERE THE LOGS BEGIN
C          IPULS=1,2,3, OR 4 DEPENDING ON THE TYPE OF RICKER WAVELET DESIRED
C          IF IPULS=0,NO WAVELET IS CONVOLVED
C          PERIOD=PERIOD OF THE DESIRED RICKER WAVELET (IN SECONDS)
C          PO=1 MEANS THAT THE LIMITING VALUES OF PHASE VELOCITY AND Q AS
C          FREQUENCY APPROACHES ZERO ARE WRITTEN INTO THE OUTPUT FILE
C          CO QQ.DAT.
C          DEPCOR = DEPTH TO THE BOTTOM OF THE CORED SECTION
C          NUNIT = NUMBER OF FACIES UNITS IN CORED SECTION
C          DEPCAS = DEPTH OF THE FIRST DIGITIZED WELL LOG VALUES
C          WD = WINDOW LENGTH (IN SEC.) FOR THE AUTOMATIC GAIN CONTROL
C          SUBROUTINE
C          IF NO AGC IS REQUIRED, SET WD=0.0
C*****
C          1 FORMAT (2X,I5,F5.0,I5,F5.1,F5.0,2I5,F7.4,I5,F7.1,I3,4X,F5.1,F5.2)
C          WRITE(6,1) NPTS,DT,IBF,SDEPTH,FC,NLayer,IPULS,PERIOD,PO,
C          .DEPCOR,NUNIT,DEPCAS,WD
C*****
C          TO READ IN THE DEPTHS TO THE TOP OF THE VARIOUS MARKER HORIZONS
C*****
C          115 READ (30,25) LABEL1
C          25 FORMAT(5A5)
C          WRITE (6,25) LABEL1
C          READ (30,4) DRIFTU,DRIFTM,DRIFTL,LEAPK,UCOLO,SWHSP,LCOLO,TWAL,
C          *BWAL,MANN,MCLARN,WASECA,SPARKY,GP,REX
C*****
C          DRIFTU = UPPER DRIFT LAYER (BATTLEFORD FM.?)
C          DRIFTM = MIDDLE DRIFT LAYER (FLORAL FM.?)
C          DRIFTL = LOWER DRIFT LAYER (SANDS AND GRAVELS)
C          LEAPK = LEA PARK FM. (ALSO TOP OF THE MONTANA GROUP)
C          UCOLO = UPPER COLORADO GROUP (ALSO THE TOP OF THE FIRST WHITE
C          SPECKLED SHALE)
C          SWHSP = SECOND WHITE SPECKLED SHALE
C          LCOLO = LOWER COLORADO GROUP
C          TWAL = TOP OF THE ST. WALBURG SANDSTONE (WITHIN THE LOWER COLORADO
C          GROUP)
C          BWAL = BASE OF THE ST. WALBURG SANDSTONE
C          MANN = MANNVILLE GROUP (ALSO THE TOP OF THE COLONY FM.)
C          MCLARN = MCLAREN FM. (OF THE MANNVILLE GROUP)
C          WASECA = WASECA FM. (MANNVILLE GROUP)
C          SPARKY = SPARKY FM. (MANNVILLE GROUP)
C          GP = GENERAL PETROLEUM FM. (MANNVILLE GROUP)
C          REX = REX FM. (MANNVILLE GROUP)
C*****
C          4 FORMAT (10(F7.1),/,5(F7.1))
C          WRITE (6,4) DRIFTU,DRIFTM,DRIFTL,LEAPK,UCOLO,SWHSP,LCOLO,TWAL,
C          *BWAL,MANN,MCLARN,WASECA,SPARKY,GP,REX
C*****

```

```

C      TO READ IN THE DATA ON THE CORED SECTIONS OF THE WELL
C*****
      DO 120 I=1,NUNIT
      READ (31,5) UNIT(I),FAC(I),BED(I),THICK(I),TOPBED(I),
      *CEM(I),POR(I),OILSAT(I),PERM(I),CLAY(I)
C*****
C      UNIT(I) = THE FACIES UNIT NUMBER.  NOTE, SOME OF JIM LORSONG'S
C              FACIES UNITS WERE SUBDIVIDED BY CEMENT TYPE; THESE ARE
C              CONSIDERED AS SEPARATE FACIES UNITS.
C      FAC(I) = THE FACIES TYPE
C      BED(I) = FIRST CHARACTER IS THE FIRST LETTER OF THE FORMATION TO
C              WHICH THE BED BELONGS
C              SECOND CHARACTER IS THE FACIES TYPE, OR SAND BODY
C              NUMBER OF THE BED
C      THICK(I) = THICKNESS OF THE FACIES UNIT
C      TOPBED(I) = DEPTH TO THE TOP OF THE FACIES UNIT
C      CEM(I) = TYPE OF CEMENTATION IN THE FACIES UNIT
C              0=NO CEMENT
C              1=CLAY CEMENT
C              2=PARTIAL CLAY CEMENT
C              3=CALCITE CEMENT
C              4=PARTIAL CALCITE CEMENT
C              5=NODULES OF CALCITE
C              6=CARBONATE (NON-CALCITE) CEMENT
C              7=PARTIAL CARBONATE CEMENT
C              8=CARBONATE NODULES
C              9=A MIXTURE OF CEMENT TYPES
C      POR(I) = MEAN POROSITY OF THE FACIES UNIT (SOMETIMES ESTIMATED)
C      OILSAT(I) = MEAN OIL SATURATION--FRACTION OF PORE VOLUME
C                (SOMETIMES ESTIMATED)
C      PERM(I) = MEAN PERMEABILITY TO AIR, IN MILLIDARCIES
C                (SOMETIMES ESTIMATED)
C      CLAY(I) = ESTIMATED CLAY AND SILT CONTENT (BY VOLUME OF THE ROCK)
C*****
      5 FORMAT(I4,2X,A1,2X,A2,F5.1,F7.1,I3,2(F5.2),F7.0,F5.0)
      WRITE (6,5) UNIT(I),FAC(I),BED(I),THICK(I),TOPBED(I),
      *CEM(I),POR(I),OILSAT(I),PERM(I),CLAY(I)
      120 CONTINUE
      DEPTH=0.0
      TIME=0.0
C*****
C      TO READ IN VALUES TO THE BOTTOM OF THE CASING
C*****
      DO 125 I=1,NLAYER
      NZ1=I
      READ (22,2) Z(I),CO(I),RHO(I),QO(I)
C*****
C      Z(I) = THICKNESS OF I'TH LAYER
C              =99999 FOR LAST LAYER
C      CO(I) = PHASE VELOCITY IN I'TH LAYER
C      RHO(I)=DENSITY IN I'TH LAYER
C      QO(I) = SPECIFIC ATTENUATION FACTOR IN I'TH LAYER
C      MAXIMUM NUMBER OF LAYERS IS 4000
C      THE THICKNESS OF Z(NLAYER) IS CALCULATED
C*****

```

```

IF (I.EQ.NLAYER) Z(I)=DEPCAS-DEPTH
TTIME(I)=TIME
TIME=TIME+Z(I)/CO(I)
TDEPTH(I)=DEPTH
DEPTH=DEPTH+Z(I)
125 CONTINUE
  2 FORMAT (5X,4F7.1)
C
C   DEVIDE THE PORTION OF THE LEA PARK FM. THAT IS WITHIN THE CASED
C   SECTION OF THE WELL INTO AN ARBITRARY NUMBER OF DEPTH INTERVALS
C   (IE-10), TO ALLOW A STEP LIKE CHANGE IN Q, VELOCITY, AND
C   DENSITY VALUES FROM THE TOP OF THE LEA PARK FM. TO THE START
C   OF THE GEOPHYSICAL LOGS.
C
DLEAPK=DEPCAS-LEAPK
DINCR=DLEAPK/10.
NLEAPK=NLAYER+9
XLEAPK=NLEAPK+0.0
WRITE (6,28) XLEAPK
28 FORMAT('0',F5.1)
Z(NLAYER)=DINCR
DEPTH=TDEPTH(NLAYER)+Z(NLAYER)
TIME=TTIME(NLAYER)+Z(NLAYER)/CO(NLAYER)
C
C   THE FIRST 7 DIGITIZED VELOCITY AND DENSITY VALUES ARE
C   USED TO COMPUTE AN AVERAGE AND THEN AN
C   INCREMENT, WHICH IS THEN ADDED WITHIN EACH DEPTH INTERVAL
C
READ (23,11) (DDD,(TT(I),I=1,7))
READ (24,11) (DDD,(RRHO(I),I=1,7))
COSUM=0.0
RHOSUM=0.0
DO 126 K=1,7
CCO(K)=(1/TT(K))*1000000
COSUM=COSUM+CCO(K)
RHOSUM=RHOSUM+RRHO(K)
126 CONTINUE
COAV=COSUM/7
RHOAV=RHOSUM/7
COINC=((COAV-CO(NLAYER))/(DLEAPK-DINCR))*DINCR
RHOINC=((RHOAV-RHO(NLAYER))/(DLEAPK-DINCR))*DINCR
C
N=0
DO 128 I=NLEAPK+1,NLEAPK
N=N+1
Z(I)=DINCR
CO(I)=CO(NLAYER)+(N*COINC)
RHO(I)=RHO(NLAYER)+(N*RHOINC)
TTIME(I)=TIME
TIME=TIME+Z(I)/CO(I)
TDEPTH(I)=DEPTH
DEPTH=DEPTH+Z(I)
128 CONTINUE
DO 129 I=1,NLEAPK
129 CONTINUE

```

```

C*****
C   TO READ IN VELOCITY AND DENSITY VALUES FROM THE LOGS
C*****
      NZ1=NLEAPK
      REWIND 23
      REWIND 24
      NLAYER=NLEAPK
      NEND=NLAYER
      DO 130 J=1,(4000-NLAYER)/7
      NZ1=NZ1+7
      NBEG=NEND+1
      NEND=NBEG+6
      READ (23,11)(DDD,(TT(I),I=NBEG,NEND))
      READ (24,11)(DDD,(RHO(I),I=NBEG,NEND))
11  FORMAT(' ',8F10.3)
      L=0
      DO 131 K=NBEG,NEND
      IF (TT(K).EQ.9999.000) GO TO 135
      CO(K)=(1/TT(K))*1000000
      L=L+1
131  CONTINUE
130  CONTINUE
135  NZ1=NZ1-7+L
      NZ=NZ1-1
C*****
C   TO READ IN DEPTH VALUES TO THE END OF THE LOGS
C*****
      DO 136 I=NLAYER+1,NZ
      Z(I)=.2
      TDEPTH(I)=DEPTH
      TTIME(I)=TIME
      DEPTH=DEPTH+Z(I)
      TIME=TIME+Z(I)/CO(I)
136  CONTINUE
      Z(NZ1)=99999.
      TDEPTH(NZ1)=DEPTH
C
      DO 138 I=1,50
      WRITE(6,9) I,TDEPTH(I),TTIME(I),Z(I),CO(I),RHO(I)
138  CONTINUE
      9  FORMAT(I5,F8.2,F8.6,F8.2,F10.3,F10.3)
      WRITE (6,9) NZ1,TDEPTH(NZ1),TTIME(NZ1),Z(NZ1),CO(NZ1),RHO(NZ1)
C*****
C   CALCULATE THE STARTING POINT FOR THE BLOWUP PLOTS
C*****
      DO 220 I=1,NZ
      IF (TDEPTH(I) .LT. MANN) GO TO 220
      ISTART=I
      GO TO 221
220  CONTINUE
221  WRITE (6,27) ISTART,TDEPTH(ISTART)
      27  FORMAT('- ',I5,F10.3)
C
C*****
C   REWIND DATA FILES TO READ THE VALUES USED IN THE PLOT

```

```

C      DOCUMENTATION
C*****
      REWIND 21
      READ (21,50) LBL16(1)
50  FORMAT (2X,1X,4X,3X,2X,5X,1X,4X,5X,3X,2X,17X,2X,A5,3X,
      *2X,1X,1X,5X,1X,4X)
      WRITE (6,53) LBL14,LBL16
53  FORMAT(3A5,2A5)
C
      REWIND 31
      DO 235 I=1,NUNIT-1
      READ (31,52)
52  FORMAT(48X)
235  CONTINUE
      READ (31,51) LBL15(1)
51  FORMAT(18X,A5,25X)
      WRITE(6,53) LBL13,LBL15
C*****
C      BEGIN THE PLOT
C*****
      CALL PLOTS(0,0,5)
C
C      POSITION PEN AT THE RIGHT HAND CORNER OF THE PAPER, 2 CM. FROM
C      THE TOP OF THE PAPER, AND 1 CM FROM THE RIGHT HAND PERFORATION
C
C
      RHO(NZ+1)=1800.
      RHO(NZ+2)=200.
      CO(NZ+1)=1200.
      CO(NZ+2)=800.
      TDEPTH(NZ+1)=MANN
      TDEPTH(NZ+2)=2.4
      CALL PLOT(20.0,20.0,-3)
      CALL SYMBOL(-3.0,0.0,0.6,LABEL1(1),90.0,25)
C*****
C      DENSITY PLOT
C*****
      CALL SYMBOL(-1.5,0.5,.5,'DENSITY',90.0,7)
      CALL AXIS(0.0,0.0,'KG/CUBIC METRE',14,5.0,90.0,RHO(NZ+1),
      *RHO(NZ+2))
      CALL PLOT((TDEPTH(ISTART)-TDEPTH(NZ+1))/TDEPTH(NZ+2),(RHO(ISTART)-
      *RHO(NZ+1))/RHO(NZ+2),3)
      DO 460 I=ISTART,NZ
      CALL PLOT((TDEPTH(I)-TDEPTH(NZ+1))/TDEPTH(NZ+2),(RHO(I)-
      *RHO(NZ+1))/RHO(NZ+2),2)
460  CONTINUE
C*****
C      PLOT THE LITHOFACIES AND BED TYPE, CEMENT AND BED TYPE, AND THE
C      DEGREE OF OIL STAIN
C*****
      CALL PLOT(0.0,6.0,-3)
      CALL SYMBOL(-1.5,-.9,.5,'CORE DATA',90.0,9)
      IF (TOPBED(NUNIT) .LT. MANN) GO TO 417
      CALL SYMBOL(-1.1,0.1,.2,'OIL STAIN',90.0,10)
      CALL SYMBOL(-0.8,0.1,.2,'LITHOFACIES',90.0,12)

```

```

CALL SYMBOL(-0.5,0.1,.2,'BED, AND',90.0,8)
CALL SYMBOL(-0.2,0.1,.2,'CEMENT TYPE',90.0,11)
417 CALL AXIS(0.0,0.0,'DEPTH IN METRES',-15,50.0,0.0,TDEPTH
*(NZ+1),TDEPTH(NZ+2))
CALL PLOT(0.0,0.0,3)
CALL PLOT(0.0,2.5,2)
CALL PLOT(50.0,2.5,2)

```

C
C
C

DRAW IN THE LAYER BOUNDARIES

```

DO 420 I=1,NUNIT
CALL PLOT((TOPBED(I)-TDEPTH(NZ+1))/TDEPTH(NZ+2),0.0,3)
CALL PLOT((TOPBED(I)-TDEPTH(NZ+1))/TDEPTH(NZ+2),2.5,2)
420 CONTINUE
CALL PLOT((TOPBED(1)+THICK(1)-TDEPTH(NZ+1))/
*TDEPTH(NZ+2),0.0,3)
CALL PLOT((TOPBED(1)+THICK(1)-TDEPTH(NZ+1))/
*TDEPTH(NZ+2),2.5,2)

```

C
C
C

WRITE IN THE DEPTH OF THE TOP AND BOTTOM OF THE CORED SECTION

```

CALL SYMBOL(((TOPBED(NUNIT)-TDEPTH(NZ+1))/TDEPTH(NZ+2))- .5,
*0.1,.2,LBL13(1),90.0,15)
CALL SYMBOL(((TOPBED(NUNIT)-TDEPTH(NZ+1))/TDEPTH(NZ+2))- .2,
*0.5,.2,LBL15(1),90.0,10)
CALL SYMBOL(((TOPBED(1)+THICK(1)-TDEPTH(NZ+1))/
*TDEPTH(NZ+2))+.4,0.1,.2,LBL14(1),90.0,15)
CALL SYMBOL(((TOPBED(1)+THICK(1)-TDEPTH(NZ+1))/TDEPTH(NZ+2))
*+.7,0.5,.2,LBL16(1),90.0,10)

```

C
C
C

PLOT THE DEGREE OF OIL SATURATION

```

CALL PLOT((TOPBED(1)+THICK(1)-TDEPTH(NZ+1))/TDEPTH(NZ+2),0.1,3)
DO 422 I=1,NUNIT
XX=(TOPBED(I)-TDEPTH(NZ+1))/TDEPTH(NZ+2)
IF (OILSAT(I) .LE. 0.19) GO TO 421
CALL PLOT (XX,0.1,2)
421 CALL PLOT(XX,0.1,3)
422 CONTINUE

```

C

```

CALL PLOT((TOPBED(1)+THICK(1)-TDEPTH(NZ+1))/TDEPTH(NZ+2),0.2,3)
DO 426 I=1,NUNIT
XX=(TOPBED(I)-TDEPTH(NZ+1))/TDEPTH(NZ+2)
IF (OILSAT(I) .LE. 0.49) GO TO 425
CALL PLOT (XX,0.2,2)
425 CALL PLOT(XX,0.2,3)
426 CONTINUE

```

C

```

CALL PLOT((TOPBED(1)+THICK(1)-TDEPTH(NZ+1))/TDEPTH(NZ+2),0.3,3)
DO 430 I=1,NUNIT
XX=(TOPBED(I)-TDEPTH(NZ+1))/TDEPTH(NZ+2)
IF (OILSAT(I) .LE. 0.69) GO TO 429
CALL PLOT (XX,0.3,2)
429 CALL PLOT(XX,0.3,3)
430 CONTINUE

```

```

C
C   PLOT THE LITHOFACIES TYPE AND BED TYPE
C
DO 435 I=1,NUNIT
XX=(TOPBED(I)-TDEPTH(NZ+1))/TDEPTH(NZ+2)
CENTRE=.1+((THICK(I)-.2)/2.4)/2.
CALL SYMBOL (XX+CENTRE,0.7,.1,FAC(I),90.0,1)
CALL SYMBOL(XX+CENTRE,0.8,.1,' ',90.0,1)
CALL SYMBOL(XX+CENTRE,0.9,.1,BED(I),90.0,2)
CALL SYMBOL(XX+CENTRE,1.1,.1,' ',90.0,1)
435 CONTINUE

C
C   PLOT THE CEMENT TYPE
C
DO 440 I=1,NUNIT
XX=(TOPBED(I)-TDEPTH(NZ+1))/TDEPTH(NZ+2)
CENTRE=.1+((THICK(I)-.2)/2.4)/2.
IF (CEM(I) .EQ. 0) GO TO 440
IF (CEM(I) .EQ. 1) CALL SYMBOL(XX+CENTRE,1.7,.1,'CL',90.0,2)
IF (CEM(I) .EQ. 2) CALL SYMBOL(XX+CENTRE,1.7,.1,'PT CL',90.0,5)
IF (CEM(I) .EQ. 3) CALL SYMBOL(XX+CENTRE,1.7,.1,'CALC',90.0,4)
IF (CEM(I) .EQ. 4) CALL SYMBOL(XX+CENTRE,1.7,.1,'PT CALC',90.,7)
IF (CEM(I) .EQ. 5) CALL SYMBOL(XX+CENTRE,1.7,.1,'CALC NOD',90.,8)
IF (CEM(I) .EQ. 6) CALL SYMBOL(XX+CENTRE,1.7,.1,'CBT',90.0,3)
IF (CEM(I) .EQ. 7) CALL SYMBOL(XX+CENTRE,1.7,.1,'PT CBT',90.,6)
IF (CEM(I) .EQ. 8) CALL SYMBOL(XX+CENTRE,1.7,.1,'CBT NOD',90.,7)
IF (CEM(I) .EQ. 9) CALL SYMBOL(XX+CENTRE,1.7,.1,'MIXTURE',90.,7)
440 CONTINUE
C*****
C   PLOT THE FORMATION TOPS
C*****
XCOL=(MANN-TDEPTH(NZ+1))/TDEPTH(NZ+2)
CALL SYMBOL(XCOL+.07,2.5,.14,'-COLONY',90.0,7)
CALL SYMBOL(XCOL+.28,2.6,.14,'FM.',90.0,3)
CALL SYMBOL(XCOL+.49,2.6,.14,'(TOP OF',90.0,7)
CALL SYMBOL(XCOL+.70,2.6,.14,'MANNVILLE',90.0,9)
CALL SYMBOL(XCOL+.91,2.6,.14,'GROUP)',90.0,6)

C
XMCL=(MCLARN-TDEPTH(NZ+1))/TDEPTH(NZ+2)
CALL SYMBOL(XMCL+.07,2.5,.14,'-MCLAREN',90.0,8)
CALL SYMBOL(XMCL+.28,2.6,.14,'FM.',90.0,3)

C
XWAS=(WASECA-TDEPTH(NZ+1))/TDEPTH(NZ+2)
CALL SYMBOL(XWAS+.07,2.5,.14,'-WASECA',90.0,7)
CALL SYMBOL(XWAS+.28,2.6,.14,'FM.',90.0,3)

C
XSPAR=(SPARKY-TDEPTH(NZ+1))/TDEPTH(NZ+2)
CALL SYMBOL(XSPAR+.07,2.5,.14,'-SPARKY',90.0,7)
CALL SYMBOL(XSPAR+.28,2.6,.14,'FM.',90.0,3)

C
XGP=(GP-TDEPTH(NZ+1))/TDEPTH(NZ+2)
CALL SYMBOL(XGP+.07,2.5,.14,'-GP FM.',90.0,7)

C
IF (REX .EQ. 999.9) GO TO 449
XREX=(REX-TDEPTH(NZ+1))/TDEPTH(NZ+2)

```

```
      CALL SYMBOL(XREX+.07,2.5,.14,'-REX FM.',90.0,8)
C*****
C   VELOCITY PLOT
C*****
449 CALL PLOT(0.0,3.8,-3)
      CALL SYMBOL(-1.5,1.0,.5,'VELOCITY',90.0,8)
      CALL AXIS(0.0,0.0,'METRES/S',8,5.0,90.0,CO(NZ+1),CO(NZ+2))
      CALL PLOT((TDEPTH(ISTART)-TDEPTH(NZ+1))/TDEPTH(NZ+2),
* (CO(ISTART)-CO(NZ+1))/CO(NZ+2),3)
      DO 450 I=ISTART,NZ
      CALL PLOT((TDEPTH(I)-TDEPTH(NZ+1))/TDEPTH(NZ+2),
* (CO(I)-CO(NZ+1))/CO(NZ+2),2)
450 CONTINUE
      CALL PLOT(0.0,0.0,999)
      CLOSE(UNIT=21)
      CLOSE(UNIT=22)
      CLOSE(UNIT=23)
      CLOSE(UNIT=24)
      CLOSE(UNIT=30)
      CLOSE(UNIT=31)
      STOP
      END
```

```

C*****
C
C           S P E C A N
C
C*****
C
C PURPOSE: THIS PROGRAM PERFORMS SPECTRAL ANALYSIS
C OF A TIME SERIES. THE AMPLITUDE SPECTRUM MAY BE PLOTTED
C ON A CALCOMP PEN-PLOTTER OR A VERSATEK ELECTRO-STATIC
C PLOTTER
C
C-----
C
C PROGRAMMER: B. REILKOFF
C             DEPT. OF GEO. SCI. (GEOPHYSICS)
C             U. OF SASKATCHEWAN
C             NOV.,1979
C
C MODIFICATIONS AND PLOTTING ROUTINE:  M. LOMAS
C                                         DEPT. OF GEOL. SC.
C                                         U. OF SASKATCHEWAN
C                                         FEB., 1983
C-----
C
C DIMENSION SECTION
C
C   IA(N) N=NO. OF DATA PTS. IN THE INPUT TRACE
C   FREQ(M),GX(M) M=NO. OF FREQUENCIES ANALYZED
C
C                               INTEGER IA(5000)
C                               REAL FREQ(5000),GX(5000)
C   REAL X(5000),T(5000),S(5000)
C   DIMENSION LBL1(5),LBL2(13),LBL3(13),LBL4(4),LBL5(9),LBL6(2),
C *LBL7(12),LBL8(11),LBL9(5),LBL10(9),LBL11(9),LBL12(7),
C *LBL13(8),LBL14(10),LBL15(7)
C
C OPEN INPUT FILES
C SYNGAN.DAT IS ALSO USED AS INPUT TO SYNCEL.FOR AND
C GRFCEL.FOR
C THE FILE SYNGRF.DAT IS CREATED BY SYNCEL
C THE FILE SPECAN.DAT IS CREATED BY GRFCEL.FOR,
C OR IT MAY BE CREATED BY THE USER TO MEET SPECIAL NEEDS
C
C   OPEN(UNIT=21,DEVICE='DSK',ACCESS='SEQIN',FILE='SYNGAN.DAT'
C *,DISPOSE='SAVE',DIALOG)
C                               OPEN(UNIT=1,DEVICE='DSK',ACCESS='SEQIN',
C 1   FILE='SYNGRF.DAT',DISPOSE='SAVE',DIALOG)
C   OPEN(UNIT=32,DEVICE='DSK',ACCESS='SEQIN',
C 1   FILE='SPECAN.DAT',DISPOSE='SAVE',DIALOG)
C*****
C   READ IN LABEL DATA
C*****
C   DATA LBL4/'TYPE ', 'OF WA', 'VELET', ' :  '/,
C *LBL5/'RICKE', 'R, WI', 'TH CE', 'NTRAL', ' FREQ', 'UENCY', ' (HZ)',

```

```

*' APPR', 'OX. = '/,
*LBL6/'IMPUL', 'SE '/,
*LBL7/'BUTTE', 'RWORT', 'H ANT', 'I-ALI', 'AS FI', 'LTER ', 'INCLU',
*'DED I', 'N SYN', 'THETI', 'C TRA', 'CE '/,
*LBL8/'TIME ', 'GATE ', '(IN S', ') FOR', 'AMPL', 'ITUDE', 'SPEC',
*'TRUM ', '= ', 'TO '/,
*LBL9/'TIME ', 'GATE ', 'CORRE', 'SPOND', 'S TO: '/,
*LBL10/'SAMPL', 'E INT', 'ERVAL', 'IN T', 'IME D', 'OMAIN', ' (S) ',
*' = ', '/,
*LBL11/'SAMPL', 'E INT', 'ERVAL', 'IN F', 'REQUE', 'NCY D', 'OMAIN',
*' (HZ)', ' = ', '/,
*LBL12/'NUMBE', 'R OF ', 'FREQU', 'ENCIE', 'S ANA', 'LYSED',
*' = ', '/,
*LBL13/'HANNI', 'NG SM', 'OOTH', 'NG AP', 'PLIED', ' TO S', 'PECTR',
*'UM '/,
*LBL14/'PERCE', 'NT OF', ' TRAC', 'E ELE', 'MENTS', ' TAPE', 'RED A',
*'T EAC', 'H END', ' = ', '/,
*LBL15/'SOURC', 'E BUR', 'IED A', 'T A D', 'EPH ', ' (M) ',
*' = ', '/

```

C
C
C
C
C
C
C
C
C
C
C
C
C
C
C
C
C
C
C

READ IN INPUT PARAMETERS

NTS=NO. OF TRACES TO BE SKIPPED BEFORE ANALYSIS

NIT=NO. OF INPUT TRACES

ST=STARTING TIME OF DESIRED WINDOW

N=NO. OF POINTS IN TIME WINDOW

NPTS=NO. OF POINTS IN INPUT TIME SERIES

DELTA F=SAMPLING INTERVAL IN FREQUENCY DOMAIN

DT=DIGITAL INTERVAL IN SECONDS

NF=NO. OF FREQUENCIES ANALYZED

```

10 READ(32,10)NTS,NIT,ST,N
   FORMAT(14,2X,12,2X,F5.3,2X,14)
   READ(32,20)DT,NPTS
20  FORMAT(F5.4,2X,14)
   READ(32,30)LBL1
30  FORMAT(5A5)
   READ(32,40)LBL2
40  FORMAT(13A5)
   WRITE(6,30)LBL1
   WRITE(6,40)LBL2
   END=ST+DT*N

```

C

C*****

C IBF=5 MEANS TO INCLUDE THE BUTTERWORTH ANTI-ALIAS

C FILTER

C SDEPTH=DEPTH OF SOURCE; THIS DEPTH CAN BE ZERO

C IPULS=1,2,3,OR 4 DEPENDING ON THE TYPE OF RICKER WAVELET
C DESIRED. IF IPULS=0 NO WAVELET IS CONVOLVED (IE-AN
C IMPULSE SOURCE.

C PERIOD=THE APPROXIMATE PERIOD (IN SECONDS) OF THE INPUT
C PULSE FOR THE SYNTHETIC SEISMOGRAM. ACTUALLY, THE
C CENTRAL FREQUENCY IS ABOUT 20% LESS THAN (1/PERIOD)

C*****

```

C
  READ(21,50) IBF,SDEPTH,IPULS,PERIOD
50  FORMAT(2X,5X,5X,I5,F5.1,5X,5X,I5,F7.4)
  WRITE(6,50) IBF,SDEPTH,IPULS,PERIOD
C
  CFREQ=.8*(1/PERIOD)
C
C*****
C  REWIND DATA FILE SPECAN TO READ THE VALUES TO BE USED IN
C  THE PLOT LABELS
C*****
  REWIND 32
  READ (32,55) LBL8(10)
55  FORMAT(4X,2X,2X,2X,A5,2X,4X)
  READ (32,60) LBL10(9)
60  FORMAT (A5,2X,4X)
C
C*****
C  COMPUTE PARAMETERS
C*****
C
  D091 J=1,13
  NRP=2**J
                                     IF(NRP.GT.N.OR.NRP.EQ.N)GO TO 92
91  CONTINUE
92  CONTINUE
  DELTAF=1.0/(NRP*DT)
  NRP1=NRP+2
  N1=NRP1/2-1
  NF=(.5*(1/DT)/DELTAF)+1
  XNF=NF+0.0
C
  WRITE(6,500)
500  FORMAT(' ',15X,'INPUT PARAMETERS')
  WRITE(6,510)NIT
510  FORMAT('0','NO. INPUT TRACES= ',I7)
  FT=ST+(N*DT)
  WRITE(6,520)ST,FT
520  FORMAT('0','TIME GATE= ',F6.3,' TO ',F6.3,' SEC.')
  WRITE(6,530)DELTAF
530  FORMAT('0','SAMPLING INTERVAL IN FREQUENCY DOMAIN= ',F6.3,' HZ.')
  WRITE(6,535)NF
535  FORMAT(' ', 'NO. OF FREQUENCIES ANALYZED = ',I7)
C
C  -----
C
C  FIND DESIRED TRACES
C
  IF(NTS.EQ.0)GOTO109
  DO 100 I=1,NTS
  100 READ(1,1000)IA
  1000 FORMAT(250I6,250I6,250I6,250I6)
  109  CONTINUE
C
C  READ IN DATA AND COMPUTE AMPLITUDE SPECTRA

```

```

C
  WRITE(6,1010)
  DO 110 I=1,NIT
  READ(1,3)(IA(J),J=1,NPTS)
  3  FORMAT(8F10.3)
  READ (1,4) LBL3
  4  FORMAT(13A5)
  WRITE(6,4)LBL3
  WRITE(6,120)I
120  FORMAT('1','SPECTRAL ANALYSIS NO. ',I4)
      IADJ=(ST/DT+.5)-1

      DO 135 J=1,NRP1
135   X(J)=0.0
      DO 140 J=1,N
140   X(J)=IA(J+IADJ)
C
  WRITE (6,1010)
1010 FORMAT(' ',130(' '))
C
C
C CORRECT DATA FOR INPUT TO FFT
C
C :DETREND DATA AND REMOVE DC BIAS
C
  CALL DETR(N,X,A1,B1)
  WRITE(6,145)A1
145  FORMAT(' ',5X,'TRACE AVERAGE = ',E14.7)
C
C TAPER BOTH ENDS OF TRACE WITH HALF A COSINE BELL
C SEE SPROG LISTING FOR REQUIRED INPUTS
C
C
C
C
C SPECIFY % OF TRACE TO BE TAPERED
C
C IPCT=10
C
C XPCT=10+0.0
C
C
C CALL TAPR(X,N,1,IPCT)
  WRITE(6,146)IPCT
146  FORMAT(' ','TRACE TAPERED ',I4,' %')
C
C ADD ZEROES TO FRONT AND BACK OF TRACE SO TOTAL LENGTH =2**INTEGER
C
C
C IF (N .EQ. NRP) GO TO 150
  CALL ADZE(X,NRP,1,N,NRP,0)
  WRITE(6,147)
147  FORMAT(' ','ZEROES ADDED TO TRACE')
C
C
C COMPUTE TRANSFORM
C
C 150 CALL SING(X,NRP1,S,T,N1,-1,IFER)
C
C DEMULTIPLEX SPECTRA
C

```

```

DO 160 J=1,NF
JJ=J*2-1
FREQ(J)=DELTA*F*(J-1)
GX(J)=SQRT(X(JJ)**2+X(JJ+1)**2)
160 CONTINUE
JJL=NF
C
WRITE(6,170)
170 FORMAT(1H ,50X,'AMPLITUDE SPECTRUM')
C
C
C USE HANNING SMOOTHING TO SMOOTH THE PLOT VALUES
C
GX(1)=.5*GX(1)+.5*GX(2)
DO 180 K=2,NF-1
GX(I)=(.25*GX(I-1))+.5*GX(I)+(.25*GX(I+1))
180 CONTINUE
GX(NF)=(.5*GX(NF-1))+.5*GX(NF)
C
C*****
C CALCULATE PLOTTING PARAMETERS
C*****
TMAX=0.0
TMIN=0.0
DO 190 J=1,NF
IF(GX(J).GE.TMAX) TMAX=GX(J)
IF(GX(J).LE.TMIN) TMIN=GX(J)
190 CONTINUE
WRITE (6,192)
WRITE(6,194) TMAX,TMIN
192 FORMAT(1H-)
194 FORMAT(' ',3X,'TMAX=',E10.4,3X,'TMIN=',E10.4)
DX=(TMAX-TMIN)/100
K=-TMIN/DX
IF (TMIN.EQ.0.0) K=1
IF (TMAX.EQ.0.0) K=100
WRITE(6,196)DX,K
196 FORMAT (' ',3X,'DELTA X=',F20.10,3X,'K=',I3)
C
C NORMALIZE TO 100
C
DO 210 K=1,NF
GX(I)=(GX(I)/TMAX)*100.
210 CONTINUE
C
C*****
C CALCOMP PLOTTING ROUTINE
C*****
C
CALL PLOTS(0,0,5)
CALL PLOT(4.0,3.0,-3)
C*****
C TITLE
C*****
CALL NEWPEN(2)

```

```

      CALL SYMBOL(-1.0,19.0,1.0,LBL1(1),0.0,25)
C*****
C   LABELS SHOWING INPUT DATA
C*****
      CALL NEWPEN(1)
      CALL SYMBOL(0.0,18.0,.3,LBL3(1),0.0,65)
      CALL SYMBOL(0.0,17.5,.3,LBL15(1),0.0,35)
      CALL NUMBER(10.0,17.5,.3,SDEPTH,0.0,1)
      CALL SYMBOL(0.0,17.0,.3,LBL4(1),0.0,20)
      IF (IPULS .NE. 0) GO TO 250
      CALL SYMBOL(5.5,17.0,.3,LBL6(1),0.0,10)
      GO TO 253
250 CALL SYMBOL(5.5,17.0,.3,LBL5(1),0.0,45)
      CALL NUMBER(19.2,17.0,.3,CFREQ,0.0,0)
253 IF (IBF .NE. 5) GO TO 256
      CALL SYMBOL(0.0,16.5,.3,LBL7(1),0.0,60)
256 CALL SYMBOL(0.0,16.0,.3,LBL8(1),0.0,55)
      CALL NUMBER(16.5,16.0,.3,END,0.0,3)
      CALL SYMBOL(0.0,15.5,.3,LBL9(1),0.0,25)
      CALL SYMBOL(0.0,15.0,.3,LBL2(1),0.0,65)
      CALL SYMBOL(0.0,14.5,.3,LBL10(1),0.0,45)
      CALL SYMBOL(0.0,14.0,.3,LBL11(1),0.0,45)
      CALL NUMBER(13.0,14.0,.3,DELTA F,0.0,3)
      CALL SYMBOL(0.0,13.5,.3,LBL12(1),0.0,35)
      CALL NUMBER (10.0,13.5,.3,XNF,0.0,0)
      CALL SYMBOL(0.0,13.0,.3,LBL13(1),0.0,40)
      CALL SYMBOL(0.0,12.5,.3,LBL14(1),0.0,50)
      CALL NUMBER(14.5,12.5,.3,XPCT,0.0,0)
C*****
C   BEGIN PLOTTING AMPLITUDE SPECTRUM
C*****
      CALL SYMBOL(-1.0,11.0,0.5,'AMPLITUDE SPECTRUM OF SYNTHETIC
*SEISMOGRAM',0.0,42)
      FREQ(NF+1)=0.
      FREQ(NF+2)=FREQ(NF)/20.
      GX(NF+1)=0.
      GX(NF+2)=10.
      CALL AXIS(0.0,0.0,'FREQUENCY IN HERTZ',-18,20.0,0.0,0.0,
.FREQ(NF+2))
      CALL AXIS(0.0,0.0,'NORMALIZED AMPLITUDE',20,10.0,90.0,GX(NF+1),
.GX(NF+2))
      CALL LINE(FREQ,GX,NF,1,0,1)
      CALL PLOT(0.,0.,999)
C
110 CONTINUE
C
C
C CLOSE ALL FILES
C
      CLOSE(UNIT=21,DISPOSE='SAVE')
      CLOSE(UNIT=1,DISPOSE='SAVE')
      CLOSE(UNIT=32,DISPOSE='SAVE')
      STOP
      END
C

```

.....

SUBROUTINE CUST

PURPOSE

COMPUTE A HALF WAVELENGTH COSINE TABLE

USAGE

CALL CUST(T,M)

DESCRIPTION OF PARAMETERS

T - VECTOR CONTAINING GENERATED COSINE TABLE

M -NUMBER OF ELEMENTS IN TABLE

REMARKS

LANGUAGE - SYSTEM/360 FORTRAN IV CODING - EBCDIC C

.....

SUBROUTINE CUST(T,M)

DIMENSION T(M)

FM=3.1415927/M

L=M-1

DO 10 I=1,L

10 T(I)=COS(I*FM)

T(M)=-1.0

RETURN

END

.....

SUBROUTINE SUNT

PURPOSE

COMPUTE A HALF WAVELENGTH SINE TABLE

USAGE

CALL SUNT(S,M)

DESCRIPTION OF PARAMETERS

S - VECTOR CONTAINING GENERATED SINE TABLE

M -NUMBER OF ELEMENTS IN TABLE

REMARKS

LANGUAGE - SYSTEM/360 FORTRAN IV CODING - EBCDIC

.....

SUBROUTINE SUNT(S,M)

DIMENSION S(M)

FM=3.1415927/M

L=M-1

DO 10 I=1,L


```

FI=I
13 X(I)=X(I)-A-B*FI
RETURN
END

```

```

C .....
C
C SUBROUTINE ADZE
C

```

```

C PURPOSE
C

```

```

C   MODIFY A MULTI-CHANNEL TRACE-MODE DATA SEQUENCE SO THAT THE
C   NUMBER OF ELEMENTS IN EACH TRACE IS EQUAL TO A POWER OF TWO.
C   FRONT AND BACK TAPERING MAY BE APPLIED TO EACH TRACE IF DE-
C   Sired.
C

```

```

C USAGE
C

```

```

C   CALL ADZE(X,NDM,NC,LX,LS,IFT)
C

```

```

C DESCRIPTION OF PARAMETERS
C

```

```

C   X   MULTI-CHANNEL TRACE-MODE DATA SEQUENCE (INPUT/OUTPUT).
C   NDM MAXIMUM NUMBER OF ELEMENTS IN X.
C   NC  NUMBER OF CHANNELS IN X.
C   LX  NUMBER OF ELEMENTS IN ANY INPUT CHANNEL OF X.
C   LS  NUMBER OF ELEMENTS IN ANY OUTPUT CHANNEL OF X.
C   IFT PERCENTAGE OF TRACE ELEMENTS THAT ARE TO BE TAPERED AT
C       BOTH FRONT AND BACK.
C

```

```

C REMARKS
C

```

```

C   LANGUAGE - FORTRAN IV           CODING - EBCDIC
C   IF NUMBER OF ELEMENTS IN AN INPUT TRACE IS LESS THAN 16 OR
C   GREATER THAN 8192, THE SUBROUTINE RETURNS.
C   DATA SEQUENCE X MAY HAVE "NON-ACTIVE" ELEMENTS IN EITHER OR
C   BOTH INPUT AND OUTPUT. THESE ELEMENTS (IF THEY EXIST) FILL
C   THE BACK LOCATIONS OF A.
C   IF (LS-LX).LE.(LX/10),ZEROS ARE ADDED TO THE BACK OF EACH
C   TRACE SO THAT EACH TRACE HAS LS ELEMENTS.
C   IF (LS-LX).GT.(LX/10),BACK ELEMENTS ARE TRUNCATED SO THAT
C   EACH TRACE HAS LS/2 ELEMENTS.THE LS "OUTPUT" IN THIS CASE
C   IS LS/2.
C

```

```

C SUBROUTINES AND FUNCTION SUBPROGRAMS REQUIRED
C

```

```

C   NONE
C
C .....
C

```

```

C SUBROUTINE ADZE(X,NDM,NC,LX,LS,IFT)
C DIMENSION X(NDM)
C IF(LX-16) 22,22,4
4  LS=32
  DO 5 LM2=5,13
    IF(LS-LX) 5,6,7
5  LS=LS+LS
  GO TO 22
6  CALL TAPR(X,NDM,NC,IFT)
  RETURN

```

```

7  NZ=LS-LX
   NDN=NC*LX
   IF(FLOAT(NZ)/FLOAT(LX)-.1) 8,8,11
8  CALL TAPR(X,NDN,NC,IFT)
   DO 10 J=1,NC
   NCJ=NC-J
   NJ1=NCJ+1
   NLC=NJ1*LS+1
   NLX=NJ1*LX+1
   LNZ=NCJ*LS+LX+1
   DO 9 I=1,NZ
   INC=NLC-I
9  X(INC)=0.0
   DO 10 I=1,LX
   IND=NLX-I
   INC=LNZ-I
10 X(INC)=X(IND)
   RETURN
11 LS=LS/2
   IF(NC.EQ.1)GO TO 13
   NLP=NC-1
   DO 12 J=1,NLP
   NLC=J*LS
   NLX=J*LX
   DO 12 I=1,LS
   INC=NLC+I
   IND=NLX+I
12 X(INC)=X(IND)
13 NZ=NC*LS
   CALL TAPR(X,NZ,NC,IFT)
   RETURN
22 WRITE(6,101)

```

```

C .....
C
101 FORMAT(1H0,'NUMBER OF ELEMENTS IN TRACE NOT BETWEEN 16 AND 8192.')
```

```

C .....
C
C
```

```

C SUBROUTINE TAPR
```

```

C PURPOSE
```

```

C APPLY A HALF-COSINE BELL TO BOTH ENDS OF A DATA VECTOR
C MULTI-CHANNEL CAPABILITY(SEE"DESCRIPTION OF PARAMETERS")
```

```

C USAGE
```

```

C CALL TAPR(A,NDM,NC,IFT)
```

```

C DESCRIPTION OF PARAMETERS
```

```

C A MULTICHANNEL TRACE MODE DATA SEQUENCE (INPUT/OUTPUT).
```

```

C NDM TOTAL NUMBER OF ELEMENTS IN A.
```

```

C NC NUMBER OF CHANNELS IN A.
```

```

C IFT PERCENTAGE OF TRACE ELEMENTS THAT ARE TAPERED BOTH
```

```

C          FRONT AND BACK.
C
C          REMARKS
C          LANGUAGE - SYSTEM/360 FORTRAN IV          CODING - EBCDIC
C
C          SUBROUTINES AND FUNCTION SUBPROGRAMS REQUIRED
C          NONE
C
C          .....
C
C          SUBROUTINE TAPR(A,NDM,NC,IFT)
C          DIMENSION A(NDM)
C          IF(IFT-50) 2,2,6
C          IF(IFT) 7,7,3
C          N=NDM/NC
C          LEN=IFT*N/100
C          FN=3.141593/(FLOAT(LEN))
C          DO 5 J=1,NC
C          JN=J*N
C          JIN=JN+1
C          JIL=JN-N
C          DO 5 I=1,LEN
C          CK=.5*(1-COS((FLOAT(I-1))*FN))
C          INC=JIL+I
C          IND=JIN-I
C          A(INC)=CK*A(INC)
C          A(IND)=CK*A(IND)
C          RETURN
C          WRITE(6,100)
C
C          .....
C          100 FORMAT(1H0,'FRONT AND BACK TAPERS EQUAL TO OR GREATER THAN
C          150% ATTEMPTED. SUBROUTINE INOPERATIVE!')
C          .....
C          7  RETURN
C          END
C
C          SUBROUTINE SING
C
C          PURPOSE
C          EVALUATE DISCRETE FOURIER TRANSFORM SEQUENCE CORRESPONDING
C          TO A PHYSICAL DATA SEQUENCE USING THE FAST FOURIER TRANS-
C          FORM SUBROUTINE FORT.
C
C          USAGE
C          CALL SING(X,NDM,S,T,N,IFS,IFER)
C
C          DESCRIPTION OF PARAMETERS
C          X  INPUT PHYSICAL DATA SEQUENCE. ALSO OUTPUT FOURIER
C          TRANSFORM SEQUENCE WITH REAL ELEMENTS IN EVEN-NUMBERED
C          POSITIONS AND IMAGINARY ELEMENTS IN ODD-NUMBERED PO-
C          SITIONS.
C          NDM NUMBER OF ELEMENTS IN THE FOURIER TRANSFORM SEQUENCE

```

C S COLUMN VECTOR FOR STORING SINE TABLE.
 C T COLUMN VECTOR FOR STORING COSINE TABLE.
 C N NUMBER OF ELEMENTS IN THE SINE TABLE.
 C IFS PARAMETER TO BE SET BY USER
 C IFS=0, SET UP SINE TABLE.
 C IFS=1, SET UP SINE TABLE AND PERFORM FOURIER SYNTHESIS
 C IFS=-1, SET UP SINE TABLE AND PERFORM FOURIER ANALYSIS.
 C IFS=2, PERFORM FOURIER SYNTHESIS WITH PRE-COMPUTED S.
 C IFS=-2, PERFORM FOURIER ANALYSIS WITH PRE-COMPUTED S.
 C IFER ERROR PARAMETER SET BY SUBROUTINE FORT
 C IFER=0 NO ERROR DETECTED
 C IFER=1 $ND1.GT.16384$, OR, WHEN $IFS=+2,-2$, THE PRE-COM-
 C PUTED SINE TABLE IS TOO SMALL.
 C IFER=-1 WHEN $IFS=+1,-1$, THE SINE TABLE WAS UNNECES-
 C SARILY RE-COMPUTED.

REMARKS

LANGUAGE - FORTRAN IV CODING - EBCDIC
 THERE ARE NDM-2 ELEMENTS IN THE PHYSICAL DATA SEQUENCE AND
 THIS MUST BE A POWER OF TWO. NYQUIST PARAMETER IS $(NDM/2)-1$.
 REFERENCE - PAULSON, RESEARCH MEMORANDUM CL-72- .
 - DOCUMENTATION OF SUBROUTINE FORT.

SUBROUTINES AND SYSTEM SUBPROGRAMS REQUIRED
 CUST, FORT, SUNT

.....
 SUBROUTINE SING(X,NDM,S,T,N,IFS,IFER)
 DIMENSION X(NDM),S(N),T(N)
 ND1=NDM-2
 N2=N/2
 ND3=N/4-1
 CALL CUST(T,N)
 CALL FORT(X,ND1,S,ND3,IFS,IFER)
 CALL SUNT(S,N)
 X(NDM-1)=X(1)-X(2)
 X(NDM)=0.0
 X(1)=X(1)+X(2)
 X(2)=0.0
 DO 10 J=2,N2
 J2=2*J
 J1=J2-1
 J3=ND1-J2+3
 J4=J3+1
 J0=J-1
 A=.5*(X(J1)+X(J3))
 B=.5*(X(J2)-X(J4))
 C=.5*(X(J2)+X(J4))
 D=.5*(X(J3)-X(J1))
 E=C*T(J0)+D*S(J0)
 F=D*T(J0)-C*S(J0)
 X(J1)=A+E
 X(J2)=B+F
 X(J3)=A-E

```

10 X(J4)=-B+F
X(N+2)=-X(N+2)
RETURN
END

```

```

C      FORT      ONE-DIMENSIONAL FINITE COMPLEX FOURIER TRANSFORM.
C      BASED ON PROGRAM WRITTEN BY J.W.COOLEY, IBM.

```

```

C      FOURIER TRANSFORM SUBROUTINE, PROGRAMMED IN SYSTEM/360,
C      BASIC PROGRAMMING SUPPORT, FORTRAN IV. FORM C28-6504
C      THIS DECK SET UP FOR IBSYS ON IBM 7094.

```

```

C      DOES EITHER FOURIER SYNTHESIS, I.E., COMPUTES COMPLEX FOURIER SERIES
C      GIVEN A VECTOR OF N COMPLEX FOURIER AMPLITUDES, OR, GIVEN A VECTOR
C      OF COMPLEX DATA X DOES FOURIER ANALYSIS, COMPUTING AMPLITUDES.
C      A IS A COMPLEX VECTOR OF LENGTH  $N=2^{**}M$  COMPLEX NOS. OR  $2*N$  REAL
C      NUMBERS. A IS TO BE SET BY USER.

```

```

C      M IS AN INTEGER 0.LT.M.LE.13, SET BY USER.

```

```

C      ND1= $2^{**}(M+1)$ 

```

```

C      ND2= $2^{**}(M-2)-1$ 

```

```

C      S IS A VECTOR  $S(J) = \sin(2*PI*J/NP)$ ,  $J=1,2,\dots,NP/4-1$ ,
C      COMPUTED BY PROGRAM.

```

```

C      IFS IS A PARAMETER TO BE SET BY USER AS FOLLOWS-

```

```

C      IFS=0 TO SET  $NP=2^{**}M$  AND SET UP SINE TABLE.

```

```

C      IFS=1 TO SET  $N=NP=2^{**}M$ , SET UP SIN TABLE, AND DO FOURIER
C      SYNTHESIS, REPLACING THE VECTOR A BY

```

```

C       $X(J) = \text{SUM OVER } K=0,N-1 \text{ OF } A(K)*\exp(2*PI*I/N)^{**}(J*K)$ ,
C       $J=0,N-1$ , WHERE  $I=\sqrt{-1}$ 

```

```

C      THE X'S ARE STORED WITH RE  $X(J)$  IN CELL  $2*J+1$ 
C      AND IM  $X(J)$  IN CELL  $2*J+2$  FOR  $J=0,1,2,\dots,N-1$ .
C      THE A'S ARE STORED IN THE SAME MANNER.

```

```

C      IFS=-1 TO SET  $N=NP=2^{**}M$ , SET UP SIN TABLE, AND DO FOURIER
C      ANALYSIS, TAKING THE INPUT VECTOR A AS X AND

```

```

C      REPLACING IT BY THE A SATISFYING THE ABOVE FOURIER SERIES.

```

```

C      IFS=+2 TO DO FOURIER SYNTHESIS ONLY, WITH A PRE-COMPUTED S.

```

```

C      IFS=-2 TO DO FOURIER ANALYSIS ONLY, WITH A PRE-COMPUTED S.

```

```

C      IFERR IS SET BY PROGRAM TO-

```

```

C      =0 IF NO ERROR DETECTED.

```

```

C      =1 IF M IS OUT OF RANGE., OR, WHEN IFS=+2,-2, THE

```

```

C      PRE-COMPUTED S TABLE IS NOT LARGE ENOUGH.

```

```

C      =-1 WHEN IFS =+1,-1, MEANS ONE IS RECOMPUTING S TABLE

```

```

C      UNNECESSARILY.

```

```

C      NOTE- AS STATED ABOVE, THE MAXIMUM VALUE OF M FOR THIS PROGRAM
C      ON THE IBM 7094 IS 13. FOR 360 MACHINES HAVING GREATER STORAGE
C      CAPACITY, ONE MAY INCREASE THIS LIMIT BY REPLACING 13 IN
C      STATEMENT 3 BELOW BY  $\log_2 N$ , WHERE N IS THE MAX. NO. OF
C      COMPLEX NUMBERS ONE CAN STORE IN HIGH-SPEED CORE. ONE MUST
C      ALSO ADD MORE DO STATEMENTS TO THE BINARY SORT ROUTINE
C      FOLLOWING STATEMENT 24 AND CHANGE THE EQUIVALENCE STATEMENTS
C      FOR THE K'S.

```

```

SUBROUTINE FORT(A,ND1,S,ND2,IFS,IFERR)
DIMENSION A(ND1),S(ND2),K(14)
EQUIVALENCE (K(13),K1),(K(12),K2),(K(11),K3),(K(10),K4)
EQUIVALENCE (K( 9),K5),(K( 8),K6),(K(7),K7),(K( 6),K8)
EQUIVALENCE (K( 5),K9),(K( 4),K10),(K( 3),K11),(K( 2),K12)
EQUIVALENCE (K( 1),K13),( K(1),N2)
ND3=ND2+1
DO 77 I=1,13
IF(ND3-1) 2,78,77
78 M=I+1
GO TO 79
77 ND3=ND3/2
GO TO 2
79 CONTINUE
IF(M)2,2,3
3 IF(M-13) 5,5,2
2 IFERR=1
1 RETURN
5 IFERR=0
N=2**M
IF( IABS(IFS) - 1 ) 200,200,10
C   E ARE DOING TRANSFORM ONLY. SEE IF PRE-COMPUTED
C   S TABLE IS SUFFICIENTLY LARGE
10 IF( N-NP )20,20,12
12 IFERR=1
GO TO 200
C   SCRAMBLE A, BY SANDE'S METHOD
20 K(1)=2*N
DO 22 L=2,M
22 K(L)=K(L-1)/2
DO 24 L=M,12
L1=L+1
24 K(L1)=2
C   NOTE EQUIVALENCE OF KL AND K(14-L)
C   BINARY SORT-
IJ=2
DO 30 J1=2,K1,2
DO 30 J2=J1,K2,K1
DO 30 J3=J2,K3,K2
DO 30 J4=J3,K4,K3
DO 30 J5=J4,K5,K4
DO 30 J6=J5,K6,K5
DO 30 J7=J6,K7,K6
DO 30 J8=J7,K8,K7
DO 30 J9=J8,K9,K8
DO 30 J10=J9,K10,K9
DO 30 J11=J10,K11,K10
DO 30 J12=J11,K12,K11
DO 30 JI=J12,K13,K12
IF(IJ-JI)28,30,30
28 L1=IJ-1
T=A(L1)
L2=JI-1
A(L1)=A(L2)
A(L2)=T

```

```

T=A(IJ)
A(IJ)=A(JI)
A(JI)=T
30 IJ=IJ+2
IF(IFS)32,2,36
C DOING FOURIER ANALYSIS,SO DIV. BY N AND CONJUGATE.
32 FN = N
DO 34 I=1,N
L1=2*I-1
L2=2*I
A(L1)=A(L1)/FN
34 A(L2)=-A(L2)/FN
C SPECIAL CASE- L=1
36 DO 40 I=1,N,2
J1=2*I
L1=J1-1
L2=L1+2
T=A(L1)
A(L1)=T+A(L2)
A(L2)=T-A(L2)
J2=L2+1
T=A(J1)
A(J1)=T+A(J2)
40 A(J2)=T-A(J2)
IF(M-1) 2,1 ,50
C SET FOR L=2
50 LEXP1=2
C LEXP1=2**(L-1)
LEXP=8
C LEXP=2**(L+1)
NPL= 2**MT
C NPL = NP* 2**-L
60 DO 130 L=2,M
C SPECIAL CASE- J=0
DO 80 I=2,N2,LEXP
I1=I + LEXP1
I2=I1+ LEXP1
I3 =I2+LEXP1
J1=I-1
J2=I2-1
T=A(J1)
A(J1)=T+A(J2)
A(J2)=T-A(J2)
T =A(I)
A(I) = T+A(I2)
A(I2) = T-A(I2)
T= -A(I3)
I4=I3-1
TI=A(I4)
I5=I1-1
A(I4)=A(I5)-T
A(I3 ) = A(I1 ) - TI
A(I5)=A(I5)+T
80 A(I1) = A(I1 ) +TI
IF(L-2) 120,120,90

```

```

90 KLAST=N2-LEXP
   JJ=NPL
   DO 110 J=4,LEXP1,2
   NPJJ=NT-JJ
   UR=S(NPJJ)
   UI=S(JJ)
   ILAST=J+KLAST
   DO 100 I= J,ILAST,LEXP
   I1=I+LEXP1
   I2=I1+LEXP1
   I3=I2+LEXP1
   J1=I2-1
   J2=I-1
   T=A(J1)*UR-A(I2)*UI
   TI=A(J1)*UI+A(I2)*UR
   A(J1)=A(J2)-T
   A(I2 )=A(I  ) - TI
   A(J2)=A(J2)+T
   A(I  )=A(I)+TI
   J3=I3-1
   T=-A(J3)*UI-A(I3)*UR
   TI=A(J3)*UR-A(I3)*UI
   I5=I1-1
   A(J3)=A(I5)-T
   A(I3 )=A(I1 )-TI
   A(I5)=A(I5)+T
100 A(I1 )=A(I1)  +TI
C   END OF I LOOP
110 JJ=JJ+NPL
C   END OF J LOOP
120 LEXP1=2*LEXP1
   LEXP = 2*LEXP
130 NPL=NPL/2
C   END OF L LOOP
140 IF(IFS)145,2,1
C   DOING FOURIER ANALYSIS. REPLACE A BY CONJUGATE.
145 DO 150 I=1,N
150 A(2*I) =-A(2*I)
160 GO TO 1
C   RETURN
C   MAKE TABLE OF S(J)=SIN(2*PI*J/NP),J=1,2,...NT-1,NT=NP/4
200 NP=N
   MP=M
   NT=N/4
   MT=M-2
   IF(MT) 260,260,205
205 THETA=.7853981634
C   THETA=PI/2**(L+1)   FOR L=1
210 JSTEP = NT
C   JSTEP = 2**( MT-L+1 ) FOR L=1
   JDIF = NT/2
C   JDIF = 2**(MT-L) FOR L=1
   S(JDIF) = SIN(THETA)
   IF (MT-2)260,220,220
220 DO 250 L=2,MT

```

```
THETA = THETA/2.  
JSTEP2 = JSTEP  
JSTEP = JDIF  
JDIF = JDIF/2  
S(JDIF)=SIN(THETA)  
JC1=NT-JDIF  
S(JC1)=COS(THETA)  
JLAST=NT-JSTEP2  
IF(JLAST-JSTEP)250,230,230  
230 DO 240 J=JSTEP,JLAST,JSTEP  
JC=NT-J  
JD=J+JDIF  
240 S(JD)=S(J)*S(JC1)+S(JDIF)*S(JC)  
250 CONTINUE  
260 IF(IFS)20,1,20  
END
```


C

```

INTEGER PO,LABEL1(5)
REAL NR,NI,LCOLO,MANN,MONTAN,LEAPK,MCLARN
COMPLEX RAT,ZP,NUM,DEN,R,T,ZN,M11,M12,M21,M22,TSBM,A11,A12,A21,A22
.,FW(10000),XWC(10000)
DIMENSION XW(10000),XT(10000),Z(4001),CO(4001),QO(4001),RHO(4001)
.,XWRE(5000),XWIM(5000),XWAMP(5000),WAVPH(5000)
DIMENSION U1(10000),TT(4001),CCO(100),RRHO(100)
EQUIVALENCE (U1(1),XW(1),XT(1))
OPEN(UNIT=21,DEVICE='DSK',ACCESS='SEQIN',FILE='SYNGAN.DAT',
.DIALOG)
OPEN(UNIT=22,DEVICE='DSK',ACCESS='SEQIN',FILE='GANCEL.DAT',
.DIALOG)
OPEN(UNIT=23,DEVICE='DSK',ACCESS='SEQIN',FILE='AU.DAT',DIALOG)
OPEN(UNIT=24,DEVICE='DSK',ACCESS='SEQIN',FILE='DEN.DAT',DIALOG)
OPEN(UNIT=25,DEVICE='DSK',ACCESS='SEQOUT',FILE='WAVE.DAT',DIALOG)
OPEN(UNIT=26,DEVICE='DSK',ACCESS='SEQOUT',FILE='WAVAMP.DAT',
.DIALOG)
OPEN(UNIT=27,DEVICE='DSK',ACCESS='SEQOUT',FILE='XWAMP.DAT',
.DIALOG)
OPEN(UNIT=28,DEVICE='DSK',ACCESS='SEQOUT',FILE='COQO.DAT',DIALOG)
OPEN(UNIT=30,DEVICE='DSK',ACCESS='SEQIN',FILE='PIX.DAT',DIALOG)
OPEN(UNIT=31,DEVICE='DSK',ACCESS='SEQOUT',FILE='WAVPH.DAT',
.DIALOG)
OPEN(UNIT=1,DEVICE='DSK',ACCESS='SEQOUT',FILE='SYNGRF.DAT',
.DIALOG)
DATA TWOPI/6.283185/,PI/3.141593/,WO/.01190808/,FO/.0017810724/
WLNFAC=.18373345-ALOG(WO)/PI
RO=-1.0
TOP=1.0-RO
CALL ERRSET(100)

```

C*****

C RO IS THE REFLECTION COEFFICIENT OFF THE TOP SURFACE OF THE MODEL

C*****

```

READ (21,1) NPTS,DT,IBF,SDEPTH,FC,NLAYER,IPULS,PERIOD,PO,
.DEPCAS

```

C*****

```

C NPTS = NUMBER OF POINTS DESIRED IN SYNTHETIC TRACE
C MAXIMUM IS 8192 AND NPTS SHOULD BE POWER OF 2
C DT = SAMPLE INTERVAL IN MILLISECONDS
C IBF = 5 MEANS TO INCLUDE THE BUTTERWORTH ANTI-ALIAS FILTER
C SDEPTH = DEPTH OF SOURCE. THIS DEPTH CAN BE ZERO.
C FC = FREQUENCY AT WHICH VELOCITY AND Q ARE INPUT
C NLAYER=NUMBER OF LAYERS IN THE CASED SECTION OF THE WELL
C IPULS=1,2,3, OR 4 DEPENDING ON THE TYPE OF RICKER WAVELET DESIRED
C IF IPULS=0, NO WAVELET IS CONVOLVED
C PERIOD=PERIOD OF THE DESIRED RICKER WAVELET (IN SECONDS)
C PO=1 MEANS THAT THE LIMITING VALUES OF PHASE VELOCITY AND Q AS
C FREQUENCY APPROACHES ZERO ARE WRITTEN INTO THE OUTPUT FILE
C CO QO.DAT.
C DEPCAS=DEPTH OF THE FIRST DIGITIZED WELL LOG VALUES

```

C*****

```

1 FORMAT (2X,I5,F5.0,I5,F5.1,F5.0,I5,I5,F7.4,I5,7X,3X,3X,F6.1)
WRITE (6,3) NPTS,DT,SDEPTH
3 FORMAT ('-NUMBER OF POINTS REQUESTED IN SYNTHETIC TRACE = ',I4,/'0

```

```

.SAMPLE INTERVAL = ',F5.2,' MILLISECONDS',/'DEPTH OF SOURCE = ',F7
..2)
IF (IBF.EQ.5) WRITE (6,4)
4 FORMAT ('BUTTERWORTH ANTI-ALIAS FILTER INCLUDED IN SYNTHETIC TRAC
.E')
IF (NPTS.GT.8192) GO TO 901
C*****
C   CALCULATE LOG2N = LOG OF N TO THE BASE 2
C*****
LOG2N=0
MPTS=NPTS
DO 105 I=1,14
NPTS=NPTS/2
IF (NPTS.EQ.0) GO TO 110
105 LOG2N=LOG2N+1
GO TO 901
110 NPTS=2**LOG2N
IF (NPTS.NE.MPTS) GO TO 902
NBY2=NPTS/2
C*****
C   CALCULATE:
C   MPTS = NUMBER OF FREQUENCY POINTS FROM 0 TO FN
C   DW = ANGULAR FREQUENCY SPACING
C*****
MPTS=NBY2+1
DW=TWOPI*1000.0/(NPTS*DT)
C*****
C   READ IN MODEL
C*****
WRITE (6,5) FC
5 FORMAT ('-INPUT VALUES READ IN',10X,'(INPUT AT A
.FREQUENCY OF ',
.F8.2,' HERTZ)',//,' DEPTH      1-WAY TIME      THICKNESS      PHASE
.VELLOCITY      DENSITY      Q VALUE',/)
DEPTH=0.0
TIME=0.0
C*****
C   READ IN THE DEPTHS TO TOP OF THE VARIOUS MARKER HORIZONS
C*****
READ (30,23) LABEL 1
23 FORMAT(5A5)
WRITE(6,23) LABEL1
READ (30,12) DRIFTU,DRIFTM,DRIFTL,LEAPK,UCOLO,SWHSP,LCOLO,TWAL,
.BWAL,MANN,MCLARN,WASECA,SPARKY,GP,REX
C*****
C   DRIFTU = UPPER DRIFT LAYER (BATTLEFORD FM.?)
C   DRIFTM = MIDDLE DRIFT LAYER (FLORAL FM.?)
C   DRIFTL = LOWER DRIFT LAYER (SANDS AND GRAVELS)
C   LEAPK = LEA PARK FM. (ALSO TOP OF THE MONTANA GROUP)
C   UCOLO = UPPER COLORADO GROUP (ALSO THE TOP OF THE FIRST WHITE
C           SPECKLED SHALE)
C   SWHSP = SECOND WHITE SPECKLED SHALE
C   TWAL = TOP OF THE ST. WALBURG SANDSTONE (WITHIN THE LOWER
C           COLORADO GROUP)
C   BWAL = BASE OF THE ST. WALBURG SANDSTONE

```

```

C      MANN = MANNVILLE GROUP (ALSO THE TOP OF THE COLONY FM.)
C      MCLARN = MCLAREN FM. (OF THE MANNVILLE GROUP)
C      WASECA = WASECA FM. (OF THE MANNVILLE GROUP)
C      SPARKY = SPARKY FM. (MANNVILLE GROUP)
C      GP = GENERAL PETROLEUM FM. (MANNVILLE GROUP)
C      REX = REX FM. (MANNVILLE GROUP)
C*****
      12 FORMAT (10(F7.1),/,5(F7.1))
C*****
C      READ IN VALUES TO THE BOTTOM OF THE CASING
C*****
      DEPTH=0.0
      DO 112 I=1,NLAYER
      NZ1=I
      READ (22,2) Z(I),CO(I),RHO(I),QO(I)
      2 FORMAT (5X,4F7.1)
      IF (I.EQ.LAYBEG) DEPDEL=DEPTH
      DEPTH=DEPTH+Z(I)
      112 CONTINUE
C*****
C      DEVIDE THE PORTION OF THE LEA PARK FM. THAT IS WITHIN THE CASED
C      SECTION OF THE WELL INTO AN ARBITRARY NUMBER OF DEPTH INTERVALS
C      (IE - 10), TO ALLOW A STEP LIKE CHANGE IN Q, VELOCITY, AND
C      DENSITY VALUES FROM THE TOP OF THE LEA PARK FM. TO THE START
C      OF THE GEOPHYSICAL LOGS.
C*****
      114 DLEAPK=DEPCAS-LEAPK
      DINCR=DLEAPK/10.
      NLEAPK=NLAYER+9
      Z(NLAYER)=DINCR

C
C      THE FIRST 7 DIGITIZED VELOCITY AND DENSITY VALUES ARE
C      USED TO COMPUTE AN AVERAGE AND THEN AN
C      INCREMENT, WHICH IS THEN ADDED WITHIN EACH DEPTH INTERVAL
C      THE VALUE OF Q FOR EACH DEPTH INTERVAL IS ALSO CALCULATED
C
      READ (23,11) (DDD,(TT(I),I=1,7))
      READ (24,11) (DDD,(RRHO(I),I=1,7))
      COSUM=0.0
      RHOSUM=0.0
      DO 116 K=1,7
      CCO(K)=(1/TT(K))*1000000
      COSUM=COSUM+CCO(K)
      RHOSUM=RHOSUM+RRHO(K)
      116 CONTINUE
      COAV=COSUM/7
      RHOAV=RHOSUM/7
      QOINC=((100.-50.)/(MANN-LEAPK-DINCR))*DINCR
      COINC=((COAV-CO(NLAYER))/(DLEAPK-DINCR))*DINCR
      RHOINC=((RHOAV-RHO(NLAYER))/(DLEAPK-DINCR))*DINCR
C
      N=0
      DO 118 I=NLAYER+1,NLEAPK
      N=N+1
      Z(I)=DINCR

```

```

      QO(I)=QO(NLAYER)+(N*QOINC)
      CO(I)=CO(NLAYER)+(N*COINC)
      RHO(I)=RHO(NLAYER)+(N*RHOINC)
118 CONTINUE
      DO 119 I=1,NLEAPK
119 CONTINUE
C*****
C      Z(I) = THICKNESS OF I'TH LAYER
C          NOTE: Z(NLAYER) IS CALCULATED IN THE PROGRAM
C          =99999. FOR LAST LAYER
C      CO(I) = PHASE VELOCITY IN I'TH LAYER
C      RHO(I)=DENSITY IN I'TH LAYER
C      QO(I) = SPECIFIC ATTENUATION FACTOR IN I'TH LAYER
C      MAXIMUM NUMBER OF LAYERS IN THE MODEL IS 4000
C*****
C
C      CALCULATE THE DEPTH AND TRAVEL TIME FOR THE LAYERS IN THE
C      CASED SECTION
C
      NLAYER=NLEAPK
      NZ1=NLAYER
123 DEPTH=0.0
      DO 125 I=1,NLAYER
      WRITE (6,6) DEPTH,TIME,Z(I),CO(I),RHO(I),QO(I)
      6 FORMAT(F8.2,5X,F8.6,6X,F8.2,8X,F8.3,8X,F8.3,6X,F6.1)
      TIME=TIME+Z(I)/CO(I)
      DEPTH=DEPTH+Z(I)
125 CONTINUE
C*****
C      TO READ IN VELOCITY AND DENSITY VALUES FROM THE LOGS
C*****
      REWIND 23
      REWIND 24
      NEND=NLAYER
      DO 130 J=1,(4000-NLAYER)/7
      NZ1=NZ1+7
      NBEG=NEND+1
      NEND=NBEG+6
      READ (23,11)(DDD,(TT(I),I=NBEG,NEND))
      READ (24,11)(DDD,(RHO(I),I=NBEG,NEND))
11 FORMAT(' ',8F10.3)
      L=0
      DO 131 K=NBEG,NEND
      IF (TT(K).EQ.9999.000) GO TO 135
      CO(K)=(1/TT(K))*1000000
      L=L+1
131 CONTINUE
130 CONTINUE
      GO TO 903
135 NZ1=NZ1-7+L
      NZ=NZ1-1
C*****
C      TO CALCULATE IN Q AND DEPTH VALUES TO THE END OF THE LOGS
C      IN ORDER TO CHANGE THE INPUT Q VALUES, MODIFICATIONS
C      MUST BE MADE TO GANCEL.DAT, TO THE PART OF THE PROGRAM

```

```

C     CALCULATING Q FOR THE CASED SECTION OF THE WELL, AND TO
C     THIS PART OF THE PROGRAM
C*****
      QOINC=((100.-50.)/(MANN-LEAPK-DINCR))* .2
      QUAL=QO(NLAYER)
      KOUNT=0
      DO 136 I=NLAYER+1,NZ
      Z(I)=.2
      QUAL=QUAL+QOINC
      IF (DEPTH.GE.(MANN-DEPDEL)) QUAL=35.
      QO(I)=QUAL
      IF(KOUNT .EQ. 0) WRITE(6,6)DEPTH,TIME,Z(I),CO(I),RHO(I),QO(I)
      KOUNT=KOUNT+1
      IF(KOUNT .EQ. 20) KOUNT=0
      IF (I .EQ. NZ) WRITE(6,6)DEPTH,TIME,Z(I),CO(I),RHO(I),QO(I)
      DEPTH=DEPTH+Z(I)
      TIME=TIME+Z(I)/CO(I)
136  CONTINUE
      Z(NZ1)=99999.
      QO(NZ1)=QUAL
C*****
C     CALCULATE QO AND CO FROM INPUT Q AND PHASE VELOCITY VALUES
C*****
138  IF (FC.LT..02) GO TO 201
      W7=.18373345+ALOG(FC/FO)/PI
      DO 139 I=1,NZ1
      Q1=QO(I)
      QO(I)=QO(I)+W7
      CO(I)=Q1*CO(I)/QO(I)
139  CONTINUE
      IF (PO.NE.1) GO TO 201
      WRITE (6,7)
7     FORMAT ('-LIMITING VALUES OF PHASE VELOCITY AND Q AS FREQ.
      .APPROACHES ZERO WRITTEN TO DISK')
      WRITE(28,15) NZ1
15    FORMAT(I5)
      WRITE (28,8) (CO(I),I=1,NZ1)
      WRITE (28,8) (QO(I),I=1,NZ1)
8     FORMAT (8F10.3)
C
C*****
C
C     THIS SECTION OF CODE CONTAINS TWO LOOPS (ONE ON I AND ONE
C     ON J).  THE PURPOSE OF THESE TWO LOOPS IS TO CALCULATE RAT(1)
C     WHICH IS THE RATIO OF THE UPGOING WAVE TO THE DOWNGOING WAVE IN
C     LAYER 1 AS A FUNCTION OF FREQUENCY.  THE FIRST LOOP IS FOR THE
C     DIFFERENT FREQUENCIES.  THE SECOND LOOP IS OVER THE NUMBER OF
C     LAYERS.
C
C     THE ALGORITHM CONSISTS OF THE FOLLOWING EQUATION:
C
C           RAT(K) = AT*AT*ZP*ZP*(R+RAT(K+1)) / (1+R*RAT(K+1))
C
C     WHERE RAT(K) IS THE RATIO OF THE SPECTRUM OF THE UPGOING RAY
C     TO THAT OF THE DOWNGOING RAY IN THE K'TH LAYER

```

C R IS THE REFLECTION COEFFICIENT AT BOUNDARY BETWEEN LAYERS
 C K AND K+1
 C $ZP = \exp(-I*W*Z(K)/VP)$
 C $AT = \exp(-W*Z(K)/(2*VP*Q))$
 C I IS ROOT OF -1
 C W = ANGULAR FREQUENCY
 C Q = SPECIFIC ATTENUATION FACTOR AT ANGULAR FREQUENCY W
 C VP = PHASE VELOCITY IN LAYER K AT ANGULAR FREQUENCY W
 C
 C R IS DEFINED BY THE EQUATION
 C
 C
$$R = (NR + I*NI) / (DR + I*DI)$$
 C
 C WHERE NR = $VR(K)*RHO(K) - VR(K+1)*RHO(K+1)$
 C NI = $VI(K)*RHO(K) - VI(K+1)*RHO(K+1)$
 C DR = $VR(K)*RHO(K) + VR(K+1)*RHO(K+1)$
 C DI = $VI(K)*RHO(K) + VI(K+1)*RHO(K+1)$
 C
 C VR AND VI ARE REAL AND IMAGINARY PARTS OF THE COMPLEX VELOCITY
 C $VI = VR/2Q$
 C $VR = VP*(4*Q**2)/(4*Q**2+1)$
 C
 C VP AND Q ARE FUNCTIONS OF FREQUENCY AS DEFINED BY:
 C
 C $Q = Q0 - (.57721566 + \ln(W/W0))/PI$
 C $VP = Q0*CO/Q$
 C
 C W0 IS A LOW FREQUENCY CUTOFF FOR THE ATTENUATION-DISPERSION MODEL.
 C CO IS THE NON-DISPERSIVE LIMIT OF THE PHASE VELOCITY AS $W \rightarrow 0$.
 C Q0 IS THE SPECIFIC ATTENUATION FACTOR AS $W \rightarrow 0$. FOR THIS PROGRAM
 C $W0 = .011190808$. THIS IS A LINEAR FREQUENCY OF .0017810724 HZ.
 C
 C THE EQUATION FOR RAT IS ITERATED FROM THE BOTTOM LAYER UP TO
 C THE TOP. THE BOTTOM LAYER IS A HALF SPACE SO THERE IS NO UPGOING
 C WAVE AND RAT IS ZERO.
 C
 C WHEN RAT(1) HAS BEEN CALCULATED IT IS THEN POSSIBLE TO
 C CALCULATE THE FOURIER TRANSFORM OF THE SURFACE SYNTHETIC
 C SEISMOGRAM. THIS IS XW AND EQUALS $U1 + D1$ WHERE U1 IS THE
 C UPGOING WAVE IN LAYER 1 AND D1 IS THE DOWNGOING WAVE IN LAYER 1.
 C FOR A DOWNGOING SPIKE INPUT AT THE SURFACE AT TIME ZERO THEN
 C $D1 = 1 - RO*U1$. FOR A SPIKE AT THE SURFACE THEN
 C
 C
$$RAT(1) = U1/(1 - RO*U1)$$
 C
 C OR $U1 = RAT(1)/(1 + RO*RAT(1))$
 C
 C AND $XW = U1*(1 - RO) + 1$
 C
 C IF THE SOURCE DEPTH IS NOT ZERO U1 IS MODIFIED TO SIMULATE
 C A SPIKE SOURCE AT THE REQUESTED DEPTH. THE FIRST STEP IS TO
 C REMOVE THE REFLECTION OFF THE LAYERS ABOVE THE SOURCE FROM U1.
 C THIS IS DONE BY SUBTRACTING RS FROM U1. RS IS THE REFLECTION
 C COEFFICIENT OF THE LAYERS ABOVE THE SOURCE AS SEEN FROM ABOVE.
 C THE NEXT STEP IS TO REPLACE THE SPIKE AT THE SURFACE BY A SOURCE

WHICH SIMULATES A SPIKE AT THE REQUESTED DEPTH. THIS IS DONE BY MULTIPLYING $U1-RS$ BY $(1-RSB)/TS$ WHERE RSB IS THE REFLECTION COEFFICIENT OF THE LAYERS ABOVE THE SOURCE AS SEEN FROM THE SOURCE AND TS IS THE TRANSMISSION COEFFICIENT OF THESE LAYERS AS SEEN FROM THE SURFACE. THE FINAL STEP IS TO INCLUDE THE DIRECT WAVE FROM THE SOURCE IN $U1$. THIS IS DONE BY SUBTRACTING TSB FROM $U1$ WHERE TSB IS THE TRANSMISSION COEFFICIENT OF THE LAYERS ABOVE THE SOURCE AS SEEN FROM THE SOURCE. RS , TS , RSB AND TSB ARE ALL FUNCTIONS OF FREQUENCY. FOR A BURIED SOURCE $U1$ IS REPLACED BY:

$$U1 = (U1-RS)*(1-RSB)/TS - TSB$$

ALSO FOR A BURIED SOURCE $D1=-R0*U1$ AND THUS

$$XW = U1*(1-R0)$$

WHERE $U1$ HAS BEEN MODIFIED ACCORDING TO THE ABOVE.

IF THE BUTTERWORTH FILTER IS TO BE INCLUDED THEN XW IS MULTIPLIED BY ITS RESPONSE AFTER THE SOURCE CALCULATION HAS BEEN PERFORMED.

WHEN XW HAS BEEN CALCULATED, THEN XT IS CALCULATED BY TAKING THE FOURIER TRANSFORM OF XW . THE CORRECT SYMMETRY REQUIREMENTS ARE IMPOSED ON XW AND THUS XT IS REAL. XT WILL BE THE SYNTHETIC SEISMOGRAM THAT WOULD BE RECORDED IF THE SOURCE WAS A SPIKE AT THE REQUESTED DEPTH. IF THE BUTTERWORTH FILTER OPTION IS USED THEN XT IS THE SYNTHETIC SEISMOGRAM THAT WOULD BE RECORDED THROUGH THE BUTTERWORTH FILTER.

```

201 DO 399 I=1,MPTS
      W=DW*(I-1)
      RAT=CMPLX(0.0,0.0)
      K=NZ
      IF (I.EQ.1) GO TO 305
      QFACT=WLNFACT+ALOG(W)/PI
      Q2=QO(K+1)-QFACT
      VP2=CO(K+1)*QO(K+1)/Q2
      Q42=4.0*Q2*Q2
      RHOVR2=RHO(K+1)*VP2*Q42/(Q42+1.0)
      GO TO 310
305 Q2=QO(K+1)
      VP2=CO(K+1)
      RHOVR2=RHO(K+1)*VP2
310 DO 299 J=1,NZ
      IF (I.EQ.1) GO TO 205
      Q1=QO(K)-QFACT
      VP1=CO(K)*QO(K)/Q1
      Q42=4.0*Q1*Q1
      RHOVR1=RHO(K)*VP1*Q42/(Q42+1.0)
      ARG=2.0*W*Z(K)/VP1
      AT=EXP(-ARG/(2.0*Q1))

```


AFTER MULTIPLYING ALL THE 2 X 2 MATRICES THE EQUATION IS

$$\begin{pmatrix} 1-RO*RS & \\ & RS \end{pmatrix} = \begin{pmatrix} A11 & A12 \\ A21 & A22 \end{pmatrix} \begin{pmatrix} TS \\ 0 \end{pmatrix}$$

OR $TS = 1/(A11+RO*A21)$
 $RS = A21*TS$

IN ORDER TO CALCULATE TSB AND RSB THE MATRIX EQUATION ABOVE CAN BE REWRITTEN IN TERMS OF TSB AND RSB.

$$\begin{pmatrix} -RO*TSB & \\ & TSB \end{pmatrix} = \begin{pmatrix} A11 & A12 \\ A21 & A22 \end{pmatrix} \begin{pmatrix} RSB \\ 1 \end{pmatrix}$$

OR $RSB = (-A12-RO*A22)/RO*A21+A11)$
 $TSB = A21*RSB+A22$

WHEN RS, TS, RSB AND TSB HAVE BEEN CALCULATED, THEN U1 IS MODIFIED ACCORDING TO THE FOLLOWING EQUATION.

$$U1 = U1*DO-TSBM$$

WHERE

$$DO = A11 + A12 + RO*(A21+A22)$$

$$TSBM = A21 + A22$$

```

IF (SDEPTH.EQ.0.0) GO TO 460
DEPTH=0.0
NZA=0
DO 409 I=1,NZ1
WRITE (6,16)
16 FORMAT('-BEG 409')
IF (DEPTH.GE.SDEPTH) GO TO 410
DEPTH=DEPTH+Z(I)
NZA=NZA+1
409 CONTINUE
DEPTH=DEPTH-Z(NZ1)
Z(NZ1)=SDEPTH-DEPTH
Z(NZ1+1)=99999.0
CO(NZ1+1)=CO(NZ1)
RHO(NZ1+1)=RHO(NZ1)
QO(NZ1+1)=QO(NZ1)
GO TO 415
410 IF ((DEPTH-SDEPTH).LT..00001) GO TO 415
Z(NZA)=SDEPTH+Z(NZA)-DEPTH
RHO(NZA+1)=RHO(NZA)
CO(NZA+1)=CO(NZA)
QO(NZA+1)=QO(NZA)
415 DO 449 I=1,MPTS
W=DW*(I-1)
M11=CMPLX(1.0,0.0)
M12=CMPLX(0.0,0.0)

```

```

M21=M12
M22=M11
IF (I.EQ.1) GO TO 420
QFACT=WLNFACT+ALOG(W)/PI
Q1=QO(1)-QFACT
VP1=CO(1)*QO(1)/Q1
Q42=4.0*Q1*Q1
RHOVR1=RHO(1)*VP1*Q42/(1.0+Q42)
GO TO 425
420 Q1=QO(1)
VP1=CO(1)
RHOVR1=RHO(1)*VP1
425 DO 439 J=1,NZA
IF (I.EQ.1) GO TO 430
Q2=QO(J+1)-QFACT
VP2=CO(J+1)*QO(J+1)/Q2
Q42=4.0*Q2*Q2
RHOVR2=RHO(J+1)*VP2*Q42/(Q42+1.0)
ARG=W*Z(J)/VP1
AT=EXP(-ARG/(2.0*Q1))
C=COS(ARG)
S=SIN(ARG)
ZP=CMPLX(C,-S)
NR=RHOVR1-RHOVR2
DR=RHOVR1/(2.0*Q1)
DI=RHOVR2/(2.0*Q2)
NI=DR-DI
DI=DR+DI
DR=RHOVR1+RHOVR2
NUM=CMPLX(NR,NI)
DEN=CMPLX(DR,DI)
R=NUM/DEN
GO TO 435
430 Q2=QO(J+1)
VP2=CO(J+1)
RHOVR2=RHO(J+1)*VP2
ZP=CMPLX(1.0,0.0)
AT=1.0
NR=(RHOVR1-RHOVR2)/(RHOVR1+RHOVR2)
R=CMPLX(NR,0.0)
435 T=1.0+R
ZP=AT*ZP
ZN=1.0/ZP
A11=M11*ZN+M12*R*ZP
A12=M11*R*ZN+M12*ZP
A21=M21*ZN+M22*R*ZP
A22=M21*R*ZN+M22*ZP
M11=A11/T
M12=A12/T
M21=A21/T
M22=A22/T
Q1=Q2
VP1=VP2
439 RHOVR1=RHOVR2
TSBM=M21+M22

```

```

DEN=CMPLX(U1(I),U1(I+NBY2))
IF (I.EQ.1) DEN=CMPLX(U1(I),0.0)
NUM=DEN*(M11+M12+RO*TSBM)-TSBM
U1(I)=REAL(NUM)
IF (I.EQ.1) GO TO 449
U1(I+NBY2)=AIMAG(NUM)
449 CONTINUE
GO TO 470
C*****
C   MODIFY U1 TO ALLOW FOR DOWNGOING SPIKE IF SOURCE DEPTH IS ZERO.
C*****
460 TOPI=1.0/TOP
DO 469 I=1,MPTS
469 U1(I)=U1(I)+TOPI
C*****
C   IF THE BUTTERWORTH FILTER IS TO BE INCLUDED CALCULATE AND APPLY
C   IT HERE. THIS FILTER IS THE FREQUENCY DOMAIN VERSION OF A
C   12 POLE BUTTERWORTH LO-PASS FILTER WITH 3 DB DOWN POINT AT FN/2.
C   IT IS USED TO SIMULATE AN ANTI-ALIAS FILTER AND IS 72 DB DOWN
C   AT FN. FN IS THE NYQUIST FREQUENCY.
C*****
470 IF (IBF.NE.5) GO TO 480
DO 479 I=2,MPTS
W=(I-1)*4.0/NPTS
W2=W*W
W3=W2*W
W4=W2*W2
W5=W3*W2
W6=W3*W3
W7=W4*W3
W8=W4*W4
W9=W5*W4
WA=W5*W5
WB=W6*W5
WC=W6*W6
BR=1.0-29.34779*(W2+WA)+136.8752*(W4+W8)-218.4690*W6+WC
BI=7.661320*(W-WB)-74.07633*(W3-W9)+194.7190*(W5-W7)
DEN=CMPLX(BR,BI)
NUM=CMPLX(U1(I),U1(I+NBY2))
NUM=NUM/DEN
U1(I)=REAL(NUM)
479 U1(I+NBY2)=AIMAG(NUM)
C*****
C   CALCULATE XW FROM U1
C*****
480 DO 484 I=1,NPTS
484 XW(I)=XW(I)*TOP
C*****
C   IF A WAVELET OTHER THAN THE SPIKE IS DESIRED, THIS WAVELET IS
C   NOW CALCULATED. THE F.T. OF THE SURFACE SYNTHETIC IS THEN
C   MULTIPLIED BY THE F.T. OF THE DESIRED WAVELET.
C*****
IF (IPULS.EQ.0) GO TO 500
CALL PULSE (LOG2N,PERIOD,DT,IPULS,FW)
C*****

```

```

C      PUT XW IN A FORM TO ALLOW THE MULTIPLICATION
C*****
      CALL RECOV(LOG2N,XW,XWRE,XWIM)
      DO 486 I=1,MPTS
      XWC(I)=CMPLX(XWRE(I),XWIM(I))
486 CONTINUE
C*****
C      MULTIPLY
C*****
      DO 488 I=2,MPTS
      XWC(I)=XWC(I)*FW(I)
488 CONTINUE
      XWC(1)=CMPLX(0.,0.)
C*****
C      PUT XWC IN A FORM TO USE THE FOURIER TRANSFORM
C*****
      DO 490 I=1,NBY2+1
      XW(I)=REAL(XWC(I))
490 CONTINUE
      DO 495 I=NBY2+2,NPTS
      J=I-NBY2
      XW(I)=AIMAG(XWC(J))
495 CONTINUE
C*****
C      COMPUTE THE AMPLITUDE SPECTRUM OF XW
C*****
500 CALL RECOV(LOG2N,XW,XWRE,XWIM)
      DO 520 I=1,MPTS
      XWAMP(I)=SQRT(XWRE(I)**2+XWIM(I)**2)
520 CONTINUE
      WRITE(27,21) (XWAMP(I),I=1,MPTS)
21 FORMAT(8F10.3)
C*****
C      PERFORM FOURIER TRANSFORM ON XW TO GET XT THE SYNTHETIC TRACE
C*****
      CALL FFTCX1(LOG2N,XW)
      WRITE (1,10) (XT(I),I=1,NPTS)
10 FORMAT(8F10.3)
      WRITE (6,9)
9 FORMAT ('-SURFACE SYNTHETIC SEISMOGRAM WRITTEN TO OUTPUT FILE.')
      GO TO 999
C*****
C      ERROR MESSAGES
C*****
901 WRITE (6,951)
      GO TO 999
902 WRITE (6,952)
      GO TO 999
903 WRITE (6,953)
951 FORMAT ('1 MAXIMUM NUMBER OF POINTS ALLOWED IN SYNTHETIC TRACE IS
.8192')
952 FORMAT ('1NUMBER OF POINTS IN SYNTHETIC MUST BE A POWER OF 2')
953 FORMAT ('1 MAXIMUM NUMBER OF LAYERS ALLOWED IS 4000')
      CLOSE(UNIT=21)
      CLOSE(UNIT=22)

```

```

CLOSE(UNIT=1)
CLOSE(UNIT=23)
CLOSE(UNIT=24)
CLOSE(UNIT=25)
CLOSE(UNIT=26)
CLOSE(UNIT=27)
CLOSE(UNIT=28)
CLOSE(UNIT=30)
CLOSE(UNIT=31)
999 STOP
END

C
C
C
SUBROUTINE PULSE(LOG2N,PERIOD,DT,IPULS,FW)
C*****
C
C WRITTEN BY MARGARET LOMAS, JULY 1982
C
C THIS SUBROUTINE CALCULATES AN INPUT PULSE FOR THE SYNTHETIC
C SEISMOGRAM AND TAKES ITS FOURIER TRANSFORM UTILIZING THE FFT.
C THE AMPLITUDES SPECTRUM OF THE PULSE IS ALSO CALCULATED.
C
C PULSE ALLOWS A CHOICE OF FOUR TYPES OF RICKER WAVELET
C SOURCES.
C
C*****
C DIMENSION WAVAMP(4098),SS(8193),SRE(4098),SIM(4098),A(5000)
C .,WAVPH(5000)
C COMPLEX FW(8200)
C
C NPTS=2**LOG2N
C NBY2=NPTS/2.
C MPTS=NBY2+1
C TAU=1./(2.*(1./(2.*DT*.001)))
C F=1./PERIOD
C DO 5 I=1,4098
5 SS(I)=0.0
C NSAMP=IFIX(6.*PERIOD/TAU)+1
C M=0
C S=DT
C GO TO (10,20,30,40),IPULS
C*****
C A VELOCITY TYPE RICKER WAVELET, AT R=INFINITY. ZERO PHASE.
C*****
10 DX=(3.4641*F*S)/1000.
C L=0
11 DO 15 K=1,NSAMP
C L=K-1
C X=L*DX-3.75
C D=(X**2.-1.)
C E=EXP((X**2)/2.)
C A(K)=-D/E
C IF (X.GT.13.) A(K)=0.
15 CONTINUE

```

```

      GO TO 50
C*****
C      A DISPLACEMENT TYPE RICKER WAVELET, MINIMUM PHASE
C*****
      20 DX=(3.650*F*S)/1000.
          L=0
          DO 25 K=1, NSAMP
              L=K-1
              X=L*DX-3.85
              A(K)=(X**2-X-1.)/EXP((X**2)/2.)
              IF (X.GT.13.) A(K)=0.
      25 CONTINUE
          GO TO 50
C*****
C      AN ACCELERATION TYPE RICKER WAVELET, MINIMUM PHASE
C*****
      30 DX=(2.90*F*S)/1000.
          L=0
          DO 35 K=1, NSAMP
              L=K-1
              X=L*DX-3.85
              A(K)=(-X**3+3.*X)/EXP((X**2)/2.)
              IF (X.GT.13.) A(K)=0.
      35 CONTINUE
          GO TO 50
C*****
C      AN ACCELERATION TYPE RICKER WAVELET, MINIMUM PHASE
C*****
      40 DX=2.35*F*S/1000.
          L=0
          DO 45 K=1, NSAMP
              L=K-1
              X=L*DX-3.20
              B=(-X**6+X**5+15.*X**4-10.*X**3-45.*X**2+15.*X+15.)
              C=EXP((X**2)/2.)
              A(K)=B/C
              IF (X.GT.13.) A(K)=0.
      45 CONTINUE
C
      50 DO 60 I=1, NSAMP
          SS(I)=A(I)
      60 CONTINUE
C*****
C      WRITE PARAMETERS FOR PLOTTING THE WAVELET SHAPE TO OUTPUT FILE
C      WAVE.DAT
C*****
          WRITE (25,72) NSAMP, LOG2N
          WRITE (25,70) (SS(I), I=1, NSAMP)
      70 FORMAT (8F10.3)
      72 FORMAT (2I5)
C*****
C      FOURIER TRANSFORM THE WAVELET AMPLITUDES
C*****
          CALL FFTR1(LOG2N, SS)
C*****

```

```

C      SS NOW CONTAINS THE REAL AND IMAGINARY COEFFICIENTS FOR THE
C      TRANSFORM POINTS OF THE INPUT PULSE
C*****
      CALL RECOV(LOG2N,SS,SRE,SIM)
C*****
C      THE REAL PART OF THE F.T. IS NOW IN SRE; THE IMAGINARY PART IS IN
C      SIM. COMPUTE THE AMPLITUDE AND PHASE SPECTRA OF THE WAVELET
C      AND WRITE THESE TO DISK.
C*****
      DO 80 I=1,MPTS
      FW(I)=CMPLX(SRE(I),SIM(I))
      WAVAMP(I)=CABS(FW(I))
      WAVPH(I)=ATAN(-SIM(I)/SRE(I))
      WAVPH(I)=WAVPH(I)*180./3.1415927
      80 CONTINUE
      WRITE(31,82) (WAVPH(I),I=1,MPTS)
      82 FORMAT(8F10.3)
C*****
C      WRITE PARAMETERS FOR PLOTTING THE AMPLITUDE SPECTRUM OF THE
C      WAVELET TO THE OUTPUT FILE WAVAMP.
C*****
      WRITE(26,85) (WAVAMP(I),I=1,MPTS)
      85 FORMAT(8F10.3)
      RETURN
      END

C
C
C
C*****
C*****
C
      SUBROUTINE FFTCX1(LOG2N,X)
C*****
C
C      WRITTEN BY DAVE GANLEY ON MAY 1, 1972.
C
C      THIS SUBROUTINE ACCEPTS AS INPUT ONE COMPLEX FUNCTION
C       $R(W) + I*J(W)$ . IT WILL CALCULATE THE INVERSE FOURIER TRANSFORM
C      OF THIS FUNCTION AND OUTPUT A REAL FUNCTION X. THE LENGTH OF X
C      IS  $N=2**LOG2N$ . THE FIRST  $N/2+1$  TERMS OF X ARE THE  $P(W)$  AND THE
C      NEXT  $N/2-1$  TERMS ARE THE  $J(W)$ .  $J(0)$  AND  $J(N)$  ARE ASSUMED TO BE 0.
C       $W=0$  IS ZERO FREQUENCY AND  $W=N/2$  IS NYQUIST FREQUENCY. THE OUTPUT
C      IS STORED IN X AND IS OF LENGTH N.
C
C      EXAMPLE:
C      INPUT A FREQUENCY FUNCTION WITH  $N=8$ . TERMS 1 TO 5
C      ARE REAL COEFFICIENTS OF FREQUENCIES 0, 125, 250, 375, AND
C      500 HERTZ. TERMS 5 TO 8 ARE IMAGINARY COEFFICIENTS OF
C      FREQUENCIES 125, 250, AND 375 HERTZ. THE OUTPUT FUNCTION
C      X IS A TIME FUNCTION AT 1 MILLISECOND SAMPLE RATE WITH 8
C      TERMS.
C
C      IF THIS ROUTINE IS USED SEVERAL TIMES IN A ROW IT WOULD BE
C      SPEEDED UP BY INCLUDING TABLES OF SINE AND COSINE FUNCTIONS AND

```

```

C AN ARRAY OF INDICES IN BIT REVERSED ORDER.
C
C FFTCX1 AND FFTR1 FORM A TRANSFORM PAIR
C
C SUBROUTINES CALLED:
C 1. MR1DFT
C 2. SW1RBO
C
C*****
C
C DIMENSION X(1)
C IF (LOG2N.LT.1) RETURN
C M=2**(LOG2N-1)
C N=2*M
C MP1=M+1
C
C*****
C
C PRIOR TO CALLING MR1DFT, MANIPULATE TERMS AS FOLLOWS:
C
C M=N/2
C
C XE(W) = X(W) + X$(M-W)
C
C XO(W) = (X(W)-X$(M-W))*EXP(2PI*I*W/2M)
C
C W GOES FROM 0 TO M/2 AND XE(W) AND XO(W) ARE COMPLEX
C ($ DENOTES COMPLEX CONJUGATE AND I IS ROOT OF -1)
C
C THE FOLLOWING 2 EQUATIONS ARE THEN USED TO CALCULATE F(W)
C FOR W = 0 TO M-1. ACTUALLY THE COMPLEX CONJUGATE OF F(W)
C IS CALCULATED.
C
C F(W) = XE(W) + I*XO(W)
C
C F$(M-W) = XE(W) - I*XO(W)
C
C F$(W) IS NOW COMPLEX AND OF LENGTH M. THE REAL COEFFICIENTS
C OF F(W) ARE STORED IN THE FIRST HALF OF X AND THE IMAGINARY
C COEFFICIENTS IN THE SECOND HALF.
C WE INPUT F$(W) TO MR1DFT. THE OUTPUT CAN BE UNSCRAMBLED
C BY CALLING SW1RBO TO PRODUCE X. PRIOR TO CALLING SW1RBO
C THE SIGNS OF THE TERMS FROM X(M+1) TO X(N) ARE REVERSED.
C
C*****
C
C IF (LOG2N.EQ.1) GO TO 30
C MBY2=M/2
C IF (LOG2N.EQ.2) GO TO 20
C MP2=M+2
C ARG=3.1415927/M
C DO 10 I=2,MBY2
C J=MP2-I
C IM=I+M

```

```

JM=J+M
XER=X(I)+X(J)
XEI=X(IM)-X(JM)
XOR=X(I)-X(J)
XOI=X(IM)+X(JM)
TARG=ARG*(I-1)
C=COS(TARG)
S=SIN(TARG)
YOR=XOR*C-XOI*S
YOI=XOI*C+XOR*S
X(I)=XER-YOI
X(IM)=-XEI-YOR
X(J)=XER+YOI
10 X(JM)=XEI-YOR
20 X(MBY2+1)=2.0*X(MBY2+1)
   X(3*MBY2+1)=2.0*X(3*MBY2+1)
30 XER=X(1)+X(MP1)
   X(MP1)=X(MP1)-X(1)
   X(1)=XER
   CALL MR1DFT(LOG2N-1,X(1),X(MP1))
   DO 39 I=MP1,N
39 X(I)=-X(I)
   CALL SW1RBO(LOG2N,X)
   RETURN
   END

```

C
C
C

SUBROUTINE MR1DFT(LOG2N,X,Y)

C*****

C

MIXED RADIX ONE DIMENSIONAL FOURIER TRANSFORM

C

WRITTEN BY DAVE GANLEY MAY 1, 1972.

C

THIS ROUTINE CALCULATES THE FOURIER TRANSFORM OF $X + I*Y$
AND OUTPUTS THE TRANSFORM IN THE ARRAYS X AND Y.

C

OUTPUT N-1 INPUT
 $X(J)+I*Y(J) = \sum_{K=0}^{N-1} (X(K)+I*Y(K)) \exp(-2*PI*I*J*K/N)$

C

WHERE I IS SQUARE ROOT OF -1 AND $N=2**LOG2N$

C

IF THIS ROUTINE IS USED SEVERAL TIMES IT MAY BE SPEEDED UP
BY SUPPLYING ARRAYS OF COSINE AND SINE VALUES.

C

AFTER USING MR1DFT ONE MUST CALL SW1RBO BECAUSE THE OUTPUT
ARRAY IS SCRAMBLED AND MUST BE UNSCRAMBLED BY STORING SUBSCRIBED
ELEMENTS AS IF THE BIT ORDER OF THE SUBSCRIPT WAS REVERSED. AN
ARRAY OF INDICES IN BIT REVERSED ORDER COULD BE SUPPLIED TO SPEED
UP THIS PROCESS IF THIS ROUTINE WAS USED MANY TIMES IN 1 JOB.

C

C*****

C

C

```

DIMENSION X(1),Y(1)
N=2**LOG2N
IF (LOG2N.LE.1) GO TO 50
DO 40 I=2,LOG2N,2
MM=2**(LOG2N-I)
M4=4*MM
DO 30 J=1,MM
IF (J.EQ.1) GO TO 6
ARG=6.2831853*(J-1)/M4
C1=COS(ARG)
S1=SIN(ARG)
C2=C1*C1-S1*S1
S2=2.0*C1*S1
C3=C2*C1-S2*S1
S3=C2*S1+S2*C1
GO TO 8
6 C1=1.0
C2=1.0
C3=1.0
S1=0.0
S2=0.0
S3=0.0
8 DO 20 K=M4,N,M4
I1=K+J-M4
I2=I1+MM
I3=I2+MM
I4=I3+MM
X1=X(I1)+X(I3)
X2=X(I1)-X(I3)
X3=X(I2)+X(I4)
X4=X(I2)-X(I4)
Y1=Y(I1)+Y(I3)
Y2=Y(I1)-Y(I3)
Y3=Y(I2)+Y(I4)
Y4=Y(I2)-Y(I4)
X(I1)=X1+X3
Y(I1)=Y1+Y3
IF (J.EQ.1) GO TO 10
X(I2)=(X1-X3)*C2+(Y1-Y3)*S2
Y(I2)=(Y1-Y3)*C2-(X1-X3)*S2
X(I3)=(X2+Y4)*C1+(Y2-X4)*S1
Y(I3)=(Y2-X4)*C1-(X2+Y4)*S1
X(I4)=(X2-Y4)*C3+(Y2+X4)*S3
Y(I4)=(Y2+X4)*C3-(X2-Y4)*S3
GO TO 20
10 X(I2)=X1-X3
Y(I2)=Y1-Y3
X(I3)=X2+Y4
Y(I3)=Y2-X4
X(I4)=X2-Y4
Y(I4)=Y2+X4
20 CONTINUE
30 CONTINUE
40 CONTINUE

```

```

50 IF (LOG2N.EQ.LOG2N/2*2) GO TO 70
   DO 60 I=1,N,2
   X1=X(I)+X(I+1)
   X2=X(I)-X(I+1)
   Y1=Y(I)+Y(I+1)
   Y2=Y(I)-Y(I+1)
   X(I)=X1
   Y(I)=Y1
   X(I+1)=X2
60 Y(I+1)=Y2
70 RETURN
   END

```

```

C
C
C
C
SUBROUTINE SW1RBO(LOG2N,X)

```

```

C
C*****

```

```

C
C   WRITTEN BY DAVE GANLEY ON MAY 1, 1972.

```

```

C
C   THIS ROUTINE SWITCHES POSITIONS OF ELEMENTS IN THE INPUT
C   ARRAY. THIS IS DONE BY REVERSING THE BIT ORDER OF THE SUBSCRIPT
C   OF THE INPUT ELEMENT TO CALCULATE THE SUBSCRIPT OF THE OUTPUT
C   ELEMENT OF THE ARRAY. THE ARRAY LENGTH IS 2**LOG2N. LOG2N
C   CAN'T EXCEED 14.

```

```

C
C   FOR EXAMPLE:

```

```

C   IF LOG2N IS 3 THEN THE SUBSCRIPTS ARE THOUGHT TO GO FROM 0
C   TO 7. CONSIDER THE TERM WHICH IS IN POSITION 2 ON INPUT. ITS
C   SUBSCRIPT WOULD BE 001 IN BINARY. REVERSING THIS GIVES 100
C   WHICH IS THE SUBSCRIPT OF POSITION 5. THUS THE TERM IN POSITION
C   2 IS OUTPUT IN POSITION 5 AND VICE VERSA.

```

```

C   IF SW1RBO WILL BE USED SEVERAL TIMES, TIME COULD BE SAVED
C   BY STORING THE REVERSED BIT ORDER INDICES IN AN ARRAY AND
C   SWITCHING TERMS ACCORDING TO THIS ARRAY.

```

```

C
C*****

```

```

C
C   DIMENSION X(1),IS(13),ID(13)
C   EQUIVALENC (IS1,IS(1)),(IS2,IS(2)),(IS3,IS(3)),(IS4,IS(4)),(IS5,I
C   *S(5)),(IS6,IS(6)),(IS7,IS(7)),(IS8,IS(8)),(IS9,IS(9)),(IS10,IS(10)
C   *), (IS11,IS(11)),(IS12,IS(12)),(ID1,ID(1)),(ID2,ID(2)),(ID3,ID(3)),
C   *(ID4,ID(4)),(ID5,ID(5)),(ID6,ID(6)),(ID7,ID(7)),(ID8,ID(8)),(ID9,I
C   *D(9)),(ID10,ID(10)),(ID11,ID(11)),(ID12,ID(12)),(ID13,ID(13)),(IS1
C   *3,IS(13))
C   IF (LOG2N.GT.14) GO TO 25
C   IF (LOG2N.LE.1) RETURN
C   ID13=2**(LOG2N-1)
C   IS13=2*ID13
C   DO 10 I=2,13
C   J=14-I
C   IS(J)=ID(J+1)

```

```

ID(J)=1
IF (ID(J+1).GT.1) ID(J)=ID(J+1)/2
10 CONTINUE
J=0
DO 20 I1=1, ID1
DO 20 I2=I1, IS1, ID1
DO 20 I3=I2, IS2, ID2
DO 20 I4=I3, IS3, ID3
DO 20 I5=I4, IS4, ID4
DO 20 I6=I5, IS5, ID5
DO 20 I7=I6, IS6, ID6
DO 20 I8=I7, IS7, ID7
DO 20 I9=I8, IS8, ID8
DO 20 I10=I9, IS9, ID9
DO 20 I11=I10, IS10, ID10
DO 20 I12=I11, IS11, ID11
DO 20 I13=I12, IS12, ID12
DO 20 I14=I13, IS13, ID13
J=J+1
IF (J.LE.I14) GO TO 20
T=X(J)
X(J)=X(I14)
X(I14)=T
20 CONTINUE
RETURN
25 WRITE (6,26)
26 FORMAT ('1 LOG2N IS TOO LARGE IN SW1RBO')
STOP
END

C
C
C*****
C*****
C
C      SUBROUTINE FFTR1(LOG2N,X)
C
C*****
C
C      WRITTEN BY DAVE GANLEY ON MAY 1,1972.
C
C      THIS SUBROUTINE ACCEPTS AS INPUT ONE REAL FUNCTION (TIME
C      DOMAIN) AND CALCULATES ITS FOURIER TRANSFORM. THE INPUT ARRAY
C      X IS OF LENGTH N=2**LOG2N. ON OUTPUT THE REAL COEFFICIENTS FOR
C      N/2+1 TRANSFORM POINTS FOR FREQUENCIES ZERO TO NYQUIST FREQUENCY
C      ARE STORED IN POSITIONS 1 TO N/2+1 OF X. THE IMAGINARY
C      COEFFICIENTS ARE STORED IN POSITIONS N/2+2 TO N AND APPLY TO
C      FREQUENCIES FROM ONE ABOVE ZERO TO ONE LESS THAN THE NYQUIST
C      FREQUENCY. THE IMAGINARY COEFFICIENTS OF ZERO AND NYQUIST
C      FREQUENCY WOULD BE ZERO.
C
C      FOR EXAMPLE:
C      INPUT 8 POINTS AT 1 MILLISECOND SPACING. ON OUTPUT THE
C      REAL COEFFICIENTS OF THE SPECTRUM ARE IN POSITIONS 1 TO 5
C      AND APPLY TO FREQUENCIES 0,125,250,375, AND 500 HERTZ.
C      THE IMAGINARY COEFFICIENTS ARE IN POSITIONS 6 TO 8 AND APPLY

```

```

C      TO FREQUENCIES OF 125, 250, AND 375 HZ.
C
C      THIS SUBROUTINE WOULD BE SPEEDED UP IF IT WAS USED SEVERAL
C      TIMES BY SUPPLYING ARRAYS OF SINE AND COSINE VALUES AND AN
C      ARRAY OF INDICES IN BIT REVERSED ORDER.
C
C      FFTR1 AND FFTCX1 FORM A FOURIER TRANSFORM PAIR.
C
C      SUBROUTINES CALLED:
C      1. MR1DFT
C      2. SW1RBO
C      3. SW2RBO
C
C*****
C
C      DIMENSION X(1)
C      IF (LOG2N.LT.1) RETURN
C      LOG2M=LOG2N-1
C      M=2**LOG2M
C      N=2*M
C      MP1=M+1
C      IF (LOG2N.EQ.1) GO TO 30
C      MBY2=M/2
C      WRITE(6,2) LOG2M,M,N,MP1,MBY2
C 2  FORMAT(5I6)
C
C      SPLIT X INTO TWO ARRAYS, ONE CONTAINING EVEN TERMS, XE, AND
C      ONE CONTAINING ODD TERMS, XO.  THE EVEN ARRAY CONTAINS THE
C      1ST,3RD ETC TERMS OF X CORRESPONDING TO TIMES 0, 2 ETC.  THE ODD
C      ARRAY CONTAINS THE 2ND, 4TH ETC TERMS AND IS STORED IN THE SECOND
C      HALF OF X WHILE THE EVEN ARRAY IS STORED IN THE FIRST HALF OF X.
C      THIS SPLITTING IS ACCOMPLISHED BY CALLS TO SW1RBO AND SW2RBO.
C      MR1DFT IS THEN CALLED ON THE ARRAY XE + I*XO (I=ROOT OF -1).
C
C      CALL SW1RBO(LOG2N,X)
C      WRITE(6,3)
C 3  FORMAT('-END SW1RBO')
C      CALL SW2RBO(LOG2M,X(1),X(MP1))
C      WRITE(6,4)
C 4  FORMAT('-END SW2RBO')
C      CALL MR1DFT(LOG2M,X(1),X(MP1))
C      WRITE(6,5)
C 5  FORMAT('-END MR1DFT')
C      CALL SW2RBO(LOG2M,X(1),X(MP1))
C      WRITE(6,6)
C 6  FORMAT('-END SW2RBO')
C      IF (LOG2N.EQ.2) GO TO 20
C
C      SW2RBO WAS CALLED AFTER MR1DFT TO ARANGE THE OUTPUT TERMS
C      IN THE CORRECT ORDER.
C      FOLLOWING THE FOURIER TRANSFORM ON XE + I*XO ABOVE, X(W)
C      (FOURIER TRANSFORM OF X) IS CONSTRUCTED BY USING THE FOLLOWING
C      RELATIONS.  F(W) = A(W) + I*B(W) IS THE OUTPUT FROM SW2RBO WHERE
C      A IS IN THE FIRST M POSITIONS OF X AND B IS IN THE REST.  M=N/2.

```

```

C      F(W) IS THE TRANSFORM OF XE + I*XO FOR W=0 TO M-1.
C
C      CALCULATE THE TRANSFORMS OF XE AND XO AS FOLLOWS, WHERE
C      W GOES FROM 0 TO M/2.
C
C      XE(W) = (A(W)+A(M-W) + I*(B(W)-B(M-W)))/2
C
C      XO(W) = (B(W)+B(M-W) + I*(A(M-W)-A(W)))/2
C
C      WHERE NOW XE(W) AND XO(W) ARE COMPLEX
C      ( _ DENOTES COMPLEX CONJUGATE)
C
C      NOW
C      X(W) = .5*(XE(W) +XO(W)*EXP(-2PI*I*W/2M))
C
C      X(W+M) = .5*(XE(W) - XO(W)*EXP(-2PI*I*W/2M))
C
C      ONLY THE TERMS OF X(W) FOR W=0 TO M ARE CALCULATED AND
C      OUTPUT BECAUSE OF THE SYMMETRY INVOLVED. THE RELATION
C      X(W+M) = X(M-W) IS USED.
C
MP2=M+2
FOURM=4*M
ARG=3.1415927/M
WRITE(6,7) MP2,FOURM,ARG
7  FORMAT(I6,F8.2,F10.7)
DO 10 I=2,MBY2
J=MP2-I
IM=I+M
JM=J+M
XER=X(I)+X(J)
XEI=X(IM)-X(JM)
XOR=X(IM)+X(JM)
XOI=X(J)-X(I)
TARG=ARG*(I-1)
C=COS(TARG)
S=SIN(TARG)
YOR=XOR*C+XOI*S
YOI=XOI*C-XOR*S
X(I)=(XER+YOR)/FOURM
X(IM)=(XEI+YOI)/FOURM
X(J)=(XER-YOR)/FOURM
10 X(JM)=(YOI-XEI)/FOURM
WRITE(6,11)
11 FORMAT('-END 10')
20 X(M+MBY2+1)=-X(M+MBY2+1)/N
X(MBY2+1)=X(MBY2+1)/N
30 XER=(X(1)+X(MP1))/N
X(MP1)=(X(1)-X(MP1))/N
IF(LOG2N.NE.1) X(MP1)=X(MP1)*2.0
X(1)=XER
DO 40 I=1,N
X(I)=N*X(I)
40 CONTINUE
RETURN

```

END

SUBROUTINE SW2RBO(LOG2M,X,Y)

WRITTEN BY DAVE GANLEY ON MAY 1,1972.

THIS ROUTINE SWITCHES POSITIONS OF ELEMENTS IN THE INPUT ARRAYS. THIS IS DONE BY REVERSING THE BIT ORDER OF THE SUBSCRIPTS OF THE INPUT ELEMENT TO CALCULATE THE SUBSCRIPT OF THE OUTPUT ELEMENT OF THE ARRAY. THE ELEMENTS IN BOTH ARRAYS ARE STORED IN BIT REVERSED ORDER. THE ARRAYS ARE OF LENGTH 2**LOG2M. LOG2M CAN'T EXCEED 13.

FOR EXAMPLE:

IF LOG2M IS 3 THEN THE SUBSCRIPTS ARE THOUGHT TO GO FROM 0 TO 7. CONSIDER THE TERM WHICH IS IN POSITION 2 ON INPUT. ITS SUBSCRIPT WOULD BE 001 IN BINARY. REVERSING THIS GIVES 100 WHICH IS THE SUBSCRIPT OF POSITION 5. THUS THE TERM IN POSITION 2 IS OUTPUT IN POSITION 5 AND VICE VERSA.

IF SW2RBO WILL BE USED SEVERAL TIMES, TIME COULD BE SAVED BY STORING THE REVERSED BIT ORDER INDICES IN AN ARRAY AND SWITCHING TERMS ACCORDING TO THIS ARRAY.

```

DIMENSION X(1),Y(1),IS(12),ID(12)
EQUIVALENCE (IS1,IS(1)),(IS2,IS(2)),(IS3,IS(3)),(IS4,IS(4)),(IS5,I
*S(5)),(IS6,IS(6)),(IS7,IS(7)),(IS8,IS(8)),(IS9,IS(9)),(IS10,IS(10)
*), (IS11,IS(11)),(IS12,IS(12)),(ID1,ID(1)),(ID2,ID(2)),(ID3,ID(3)),
*(ID4,ID(4)),(ID5,ID(5)),(ID6,ID(6)),(ID7,ID(7)),(ID8,ID(8)),(ID9,I
*D(9)),(ID10,ID(10)),(ID11,ID(11)),(ID12,ID(12))
IF (LOG2M.GT.13) GO TO 25
IF (LOG2M.LE.1) RETURN
ID12=2**(LOG2M-1)
IS12=2*ID12
DO 10 I=2,12
J=13-I
IS(J)=ID(J+1)
ID(J)=1
IF (ID(J+1).GT.1) ID(J)=ID(J+1)/2
10 CONTINUE
J=0
DO 20 I1=1, ID1
DO 20 I2=I1, IS1, ID1
DO 20 I3=I2, IS2, ID2
DO 20 I4=I3, IS3, ID3
DO 20 I5=I4, IS4, ID4
DO 20 I6=I5, IS5, ID5
DO 20 I7=I6, IS6, ID6
DO 20 I8=I7, IS7, ID7

```

```

DO 20 I9=I8,IS8,ID8
DO 20 I10=I9,IS9,ID9
DO 20 I11=I10,IS10,ID10
DO 20 I12=I11,IS11,ID11
DO 20 I13=I12,IS12,ID12
J=J+1
IF (J.LE.I13) GO TO 20
T=X(J)
X(J)=X(I13)
X(I13)=T
T=Y(J)
Y(J)=Y(I13)
Y(I13)=T
20 CONTINUE
RETURN
25 WRITE (6,26)
26 FORMAT ('1 LOG2M IS TOO LARGE IN SW2RBO')
STOP
END

```

C
C

```

SUBROUTINE RECOV(LOG2N,X,XRE,XIM)

```

C
C

```

C*****

```

C
C

```

WRITTEN BY MARGARET LOMAS, NOVEMBER, 1982

```

C
C

```

THIS ROUTINE SEPARATES THE REAL AND IMAGINARY PARTS OF THE
FOURIER TRANSFORM WHICH HAVE BEEN STORED AS OUTLINED IN SUBROUTINE
FFTR1.

```

C
C

```

THE REAL COEFFICIENTS FOR FREQUENCIES ZERO TO NYQUIST FREQ.
WILL BE STORED IN XRE( ) AND ARE TAKEN FROM THE FIRST N/2+1
POSITIONS OF X.

```

C
C

```

THE IMAGINARY PART WILL BE STORED IN IM( ). THE IMAGINARY
COEFFICIENTS FOR FREQUENCIES OF ZERO AND THE NYQUIST FREQUENCY ARE
SET TO ZERO, WHILE THOSE FROM ONE ABOVE ZERO TO ONE LESS THAN THE
NYQUIST FREQUENCY ARE RECOVERED FROM POSITIONS N/2+2 TO N OF X.

```

C
C

```

C*****

```

C
C

```

REAL X(8193),XRE(4098),XIM(4098)
NPTS=2**LOG2N
NBY2=NPTS/2
MPTS=NBY2+1
DO 10 I=1,NBY2+1
XRE(I)=X(I)
10 CONTINUE

```

C
C

```

XIM(1)=0.0
DO 20 I=2,NBY2
J=NBY2+I
XIM(I)=X(J)
20 CONTINUE

```

C XIM(NBY2+1)=0.0
RETURN
END